Dissertation zur Erlangung des Doktorgrades
der Fakultät für Chemie und Pharmazie
der Ludwig-Maximilians-Universität München

Role of the transcriptional coactivators Megakaryoblastic Leukemia Proteins 1 and 2 in tumorigenesis

Veronika Liane Hampl

aus

Rosenheim

2014

Erklärung:

Diese Dissertation wurde im Sinne von § 7 der Promotionsordnung vom 28. November 2011 von Herrn Prof. Dr. Thomas Gudermann betreut und von Frau Univ.-Prof. Dr. Angelika M. Vollmar von der Fakultät für Chemie und Pharmazie vertreten.

Eidesstattliche Versicherung

Diese Dissertation wurde eigenständig und ohne unerlaubte Hilfe erarbeitet.

München, den 31.01.2014

_____

Veronika Hampl

Dissertation eingereicht am:	31.01.2014
1. Gutachterin:	Frau Prof. Dr. Angelika M. Vollmar
2. Gutachter:	Herr Prof. Dr. Thomas Gudermann
Mündliche Prüfung am:	04.04.2014

Table of content

1 Summary

The Megakaryoblastic Leukemia proteins 1 and 2 (MKL1/2) are transcriptional coactivators of the nuclear transcription factor serum response factor (SRF) that controls fundamental processes like cell growth, cell migration, differentiation and organization of the cytoskeleton. Deleted in Liver Cancer 1 (DLC1), encoding a RhoGAP protein, was identified as a tumor suppressor whose allele is lost in 50 % of liver, breast, lung and 70 % of colon cancers. Despite its significance, the molecular mechanism which drive cancerous transformation remained so far unknown. Preliminary data indicated a direct correlation between the subcellular localization of MKL1 and the endogenous expression levels of DLC1. In this work, we found that loss of DLC1 expression in hepatocellular and breast carcinoma cells caused the nuclear translocation of MKL2. We demonstrated that the nuclear MKL1/2 localization in hepatocellular and breast carcinoma cells lacking endogenous DLC1 expression was accomplished by the constitutive activation of RhoA/actin signaling and simultaneous impairment of MKL1 phosphorylation resulting in the constitutive activation of the tumor-relevant MKL/SRF dependent target genes CTGF and Cyr61. In the context of hepatocarcinogenesis, we found that RNAi-mediated silencing of nuclear, active MKL1/2 expression suppressed tumor cell proliferation of human hepatocellular carcinoma cells characterized by a DLC1-deficient background. Loss of DLC1 and the subsequent RhoA activation were prerequisites for the MKL1/2 knockdown-mediated growth arrest. We identified oncogene-induced senescence as the underlying molecular mechanism of the observed anti-proliferative effect of MKL1/2 knockdown. Depletion of MKL1/2 caused the activation of oncogenic Ras signaling that resulted in elevated $p16^{Ink4a}$ expression and hypophosphorylation of the retinoblastoma protein (Rb) in DLC1-deficient HCC cells. Furthermore, senescent DLC1-deficient HCC cells depleted of MKL1/2 were marked by a DNA damage response documented by elevated phosphorylation of p53 on serine 15 and revealed an upregulation of the chemokine (C-S-C) motif ligand 10 and tumor necrosis factor (ligand) superfamily 10, both components of the senescence-messaging secretome. Notably, reconstitution of DLC1-expression in HuH7 HCC cells also provoked the induction of a senescence response. Evaluation of the therapeutic efficacy of MKL1/2 knockdown *in vivo* demonstrated that systemic treatment of nude mice bearing subcutaneous DLC1-deficient HuH7 cells derived tumor xenografts with siRNAs targeting MKL1 and MKL2 complexed with polyethylenimine (PEI) significantly suppressed the tumor growth due to the induction of a senescence response *in vivo*. Of note, PEI-complexed MKL1 siRNA alone was sufficient to completely abolish HCC xenograft growth. A DNA-microarray based transcriptome analysis of MKL1/2 depleted DLC1-deficient HuH7 cells highlighted myoferlin as a novel, hitherto unnoticed MKL1/2 and SRF dependent target gene.

We characterized myoferlin as a novel regulator of EGFR activity in DLC1-deficient HCC cells and its downregulation enabled sustained EGFR signaling thereby triggering the tumor suppressive oncogene-induced senescence response. Our study highlights MKL1/2 as promising novel pharmacological targets for the anti-tumor therapy of HCC characterized by loss of the tumor suppressor DLC1.

2 Introduction

2.1 The transcription factor serum response factor (SRF)

Transcription is a well-controlled and coordinated process that requires the cooperation between transcription factors and co-regulators. Transcription factors mediate the execution of genetic programs in response to extra- and intracellular signals. SRF is a founding member of the MADS-box family of transcription factors and constitutes one of the best understood DNA-binding proteins in the human genome (Shore & Sharrocks, 1995). The MADS box (MCM1, Agamous, Deficiens, SRF) constitutes a modular, conserved DNA binding domain composed of 56 amino acids (Pellegrini et al, 1995). SRF binds DNA at the palindromic $CC(A/T)_6GG$ consensus sequence, designated as CArG box or serum response element (SRE) which is found in numerous promoters of actin cytoskeleton and immediate early genes (IEG) (Miano et al, 2007; Treisman, 1995a). SRF binds to the CArG boxes as a homodimer. Meanwhile, approximately 160 different target genes have been found to be directly regulated by SRF signaling and about half of these have been experimentally proven (Sun et al, 2006a). The majority of SRF target genes is implicated in cell growth, migration, cytoskeletal organization and myogenesis (Johansen & Prywes, 1995; Takeda et al, 1992; Treisman, 1986). The first prototypical described SRF target gene involved in cell growth, c-fos, is controlled by a single CArG-box (Norman et al, 1988). SRF-dependent enhancers of muscle gene expression were initially described as duplicated CArG-boxes activating transcription (Chow & Schwartz, 1990; Miwa & Kedes, 1987). It has been hypothesized that SRF-dependent target genes involved in cell growth are controlled by a single CArG-box whereas SRF-dependent muscle genes are controlled by duplicated CArG-boxes. However, it has been shown that most SRF target genes are controlled by duplicated CArG-boxes (Sun et al, 2006a). In vitro experiments using downregulation of SRF expression or the expression of dominant-negative SRF mutants documented that SRF signaling is functionally required for cell growth and skeletal muscle differentiation (Kaplan-Albuquerque et al, 2005; Soulez et al, 1996; Wei et al, 1998). Moreover, dominant-negative SRF mutants disrupted skeletal as well as cardiac muscle differentiation in transgenic mice (Zhang et al, 2001). SRF-null embryos failed to develop mesoderm resulting in lethality at gastrulation (Arsenian et al, 1998). The involvement of SRF in cell migration and adhesion was substantiated by the findings that embryonic stem cells (ES) lacking SRF revealed defects in spreading, adhesion and migration that correlated well with the abnormalities of actin stress fibers and loss of the expression of genes encoding the actin cytoskeleton such as vinculin and talin (Schratt et al, 2002). Studies with tissue specific knockout mice highlighted the importance of SRF expression in the cardiovascular system (Parlakian et al, 2004), skin development (Verdoni et al, 2010), skeletal muscle cells (Li et al, 2005b), liver development (Sun et al, 2009) and central nervous system (Alberti et al, 2005).

Transcription factors are relatively weak transcriptional activators and function through the recruitment of transcriptional coactivators or corepressors that do not directly bind to DNA but regulate transcription through the association with DNA-bound factors like SRF (Spiegelman & Heinrich, 2004).

2.1.1 The ternary complex factor (TCF)-dependent signaling pathway of SRF activation

Historically, Shaw and colleagues showed that SRF bound to the SRE element of the c-fos promoter formed a ternary complex with p62 which has been shown to be homologous to Elk-1 (Ets-like transcription factor 1) (Hipskind et al, 1991; Shaw et al, 1989). The ternary complex factors act as transcriptional coactivators and are composed of Elk-1, SAP-1 (SRF accessory protein 1) and Net (Erp/Sap-2/Elk-3) which belong to the Ets group of transcription factors, one of the largest family of transcription factors (Sharrocks, 2001).

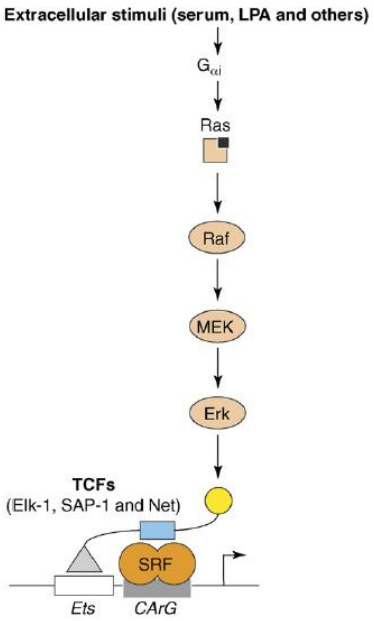

Figure 1: The TCF-dependent signaling pathway of SRF activation.
Activation of the MAPK signaling cascade contributes to the phosphorylation of TCFs which binds via their own Ets DNA recognition site near the CArG box of immediate early genes thereby activating SRF-mediated transcription. Picture is taken from (Posern & Treisman, 2006).

Extracellular stimuli which activate MAPK signaling contribute to the phosphorylation of TCFs. Phosphorylated TCFs bind to a core sequence GGA(A/T), termed as EBS (Ets binding sequence) which is located in the direct proximity of CArG boxes and is required for the ternary complex formation between TCFs and SRF (Treisman, 1994; Treisman, 1995b). Upon extracellular stimuli, the TCF-factor Elk-1 has been shown to be activated by all three key MAP kinases, ERK, JNK and p38, Net by p38 and JNK and SAP-1 by ERK and p38 ((Buchwalter et al, 2004). Besides activation through MAPK signaling, SAP-1 has been shown to be activated by the colony stimulating factor 1 (CSF-1) (Hipskind et al, 1994). Immediate early

genes like c-fos, egr-1, pip92 and JunB are regulated by TCFs, as IEGs containing SREs are the best characterized targets of TCFs (Treisman, 1990; Treisman, 1992). IEGs are rapidly induced upon extracellular stimuli and do not require *de novo* protein synthesis for their induction. Despite the large number of studies investigating the physiological roles of TCFs, their implication *in vivo* is not well understood. For example, homozygous mutant Net mice developed a specific defect in thoracic lymphatic vessels which was manifested by the accumulation of chyle in lungs and these mice died from respiratory failure (Ayadi et al, 2001). Net expression has been reported to be required for angiogenesis in normal adult tissue (Zheng et al, 2003). By contrast, Elk-1 and Sap-1 null mice revealed few, less severe abnormalities suggesting that the members of the TCF family may act redundantly. Consequently, further *in vivo* studies using combinatorial and tissue specific knockouts are required to elucidate the exact physiological roles of the TCFs.

2.1.2 Rho-actin signaling dependent activation of SRF

First evidence for a secondary, TCF-independent activation of SRF was documented by the findings that the mutation of the TCF-binding site within the c-fos promoter did not completely abolish the serum-induced activation of the c-fos promoter. These findings led to the suggestion that at least two independent pathways activate SRF: the TCF-dependent and TCF-independent pathway (Hill & Treisman, 1995). The TCF-independent activation of SRF was blocked by Rho inhibition and activated upon expression of active RhoA indicating that Rho activation was required for the transcriptional response to serum (Hill et al, 1995). Many mechanistic studies linked Rho signaling to the activation of SRF, finally it has been realized that cytoskeletal actin dynamics is closely involved in this process. It has been clarified that Rho signaling promoted F-actin polymerization and the concomitant reduction of G-actin stimulated SRF signaling (Sotiropoulos et al, 1999). Actin polymerization is controlled by mDia, a downstream mediator of RhoA which promotes F-actin polymerization (Copeland & Treisman, 2002). ROCK stabilizes F-actin via phosphorylation of the Lim-kinase which in turn phosphorylates and inactivates the actin depolymerization factor cofilin (Sotiropoulos et al, 1999). Moreover it has been shown that the Lim-kinase cooperated with mDia to regulate SRF activation (Geneste et al, 2002). Furthermore, Posern and colleagues demonstrated that the overexpression of non-polymerizable actin mutants failed to activate SRF reporters (Posern et al, 2002). So far, no direct interaction between G-actin and SRF could be detected suggesting that an unknown cofactor may sense cellular F and G-actin levels and controls thereby SRF activity.

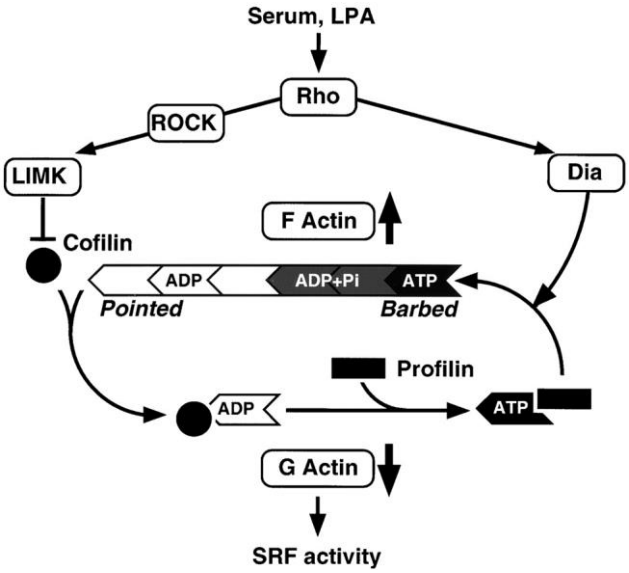

Figure 2: SRF activity is controlled via actin dynamics.
Rho signaling promotes F-actin polymerization via the ROCK- Lim-kinase and mDia pathway and the concomitant G-actin depletion contributes to the activation of SRF. Picture is taken from (Geneste et al, 2002).

2.1.3 The family of myocardin-related transcription factors

In 2002, Wang and colleagues identified a new group of transcriptional coactivators activating SRF (Wang et al, 2002) which were designated as the family of myocardin-related transcription factors (MRTFs). The founding member of this group, myocardin, was initially identified by an in silico screen and described to specifically expressed in cardiac and smooth muscle cells, where it functioned as a potent transcriptional coactivator of SRF (Wang et al, 2001). By contrast, the two other members of the MRTF family, MRTF-A alternatively termed MAL, MKL1 (megakaryoblastic leukemia protein 1) or BSAC and MRTF-B, designated as MKL2 (megakaryoblastic leukemia protein 2) or MAL16 were shown to be ubiquitously expressed in a broad spectrum of embryonic and adult tissues including embryonic stem cells (Du et al, 2004; Wang et al, 2002).

2.1.3.1 Structure of the members of the myocardin-related transcription factors

The members of the myocardin family feature high sequence similarity and share a series of conserved domains. The amino-termini of myocardin and MKLs contain three Arg-Pro-X-X-X-Glu-Leu (RPEL) domains which form a stable complex with monomeric G-actin (Guettler et al, 2008; Miralles et al, 2003; Mouilleron et al, 2008). The transcriptional coactivators associate with SRF through a basic region and an adjacent glutamin-rich domain (Wang et al, 2001; Wang et al, 2002). One of the notable features of the members of the myocardin family represents the SAP domain, named after SAF-A/B, Acinus and PIAS which in other proteins is well established to be implicated in the regulation of nuclear organization, chromosomal dynamics and apoptosis (Aravind & Koonin, 2000). The SAP domain is predicted to be composed of two amphipathic α-helices which function as weak DNA-binding sites (Gohring et al, 1997; Kipp et al, 2000). Deletion of the SAP domain of either MKL1 or myocardin does

not interfere with their transcriptional activity and the ability to form a complex with SRF (Cen et al, 2003; Miralles et al, 2003; Wang et al, 2001). The highly conserved coiled-coil-leucine zipper-like domain is required for the homo- and heterodimerization among the members of the myocardin family. The heterodimerization between myocardin and the other two members of the myocardin family has been proposed to support the cooperativity between CArG boxes and SRF controlled muscle genes (Wang et al, 2001). Moreover, for MKL1 it has been shown that the deletion of the leucin zipper domain exerted only a modest effect on the MKL1 mediated activation of SRF-reporter genes (Cen et al, 2003). The C-termini of the members of the myocardin family share low sequence identity and function as transcription activation domains (TADs). Deletion of the TAD domains contributes to the generation of dominant-negative mutants (Cen et al, 2003).

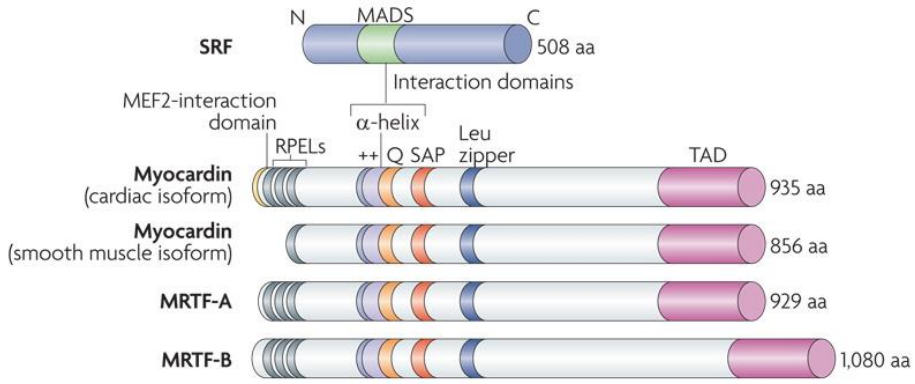

Figure 3: Modular structure of the members of the myocardin family.
The basic (++) and glutamin-rich (Q) domains are required for the direct interaction of SRF. RPEL domains are binding sites for G-actin; SAP domain constitutes a putative DNA-binding element. The Leucine zipper motif is required for homo and heterodimerization among the members of the myocardin family. TAD-transactivation domain. MEF2 is an interaction domain exclusively found in the cardiac form of myocardin. Picture is taken from (Olson & Nordheim, 2010).

2.1.4 Regulation of the subcellular localization and transcriptional activity of MKL1 and MKL2

In 2003, Miralles and colleagues found that the subcellular localization of MKL1 is regulated by Rho-actin signaling and MKL1 was characterized as the cofactor which mediates actin-sensitivity of SRF (Miralles et al, 2003). In unstimulated NIH3T3 fibroblasts, MKLs are sequestered in the cytoplasm by binding via their N-terminal RPEL-motifs to monomeric G-actin (Miralles et al, 2003; Posern et al, 2004). Serum or LPA induced Rho activation stimulates F-actin polymerization in the cytoplasm and the concomitant depletion of G-actin induces the release of MKLs from the inhibitory complex (Miralles et al, 2003; Posern et al, 2004). Dissociation of MKLs from G-actin unmasks a nuclear localization sequence within the RPEL domain which is required for the importin α/β mediated nuclear import of MKLs (Pawlowski et al, 2010). Upon accumulation in the nucleus, MKLs have to dissociate from nuclear G-actin, bind to SRF as a dimer and activate the transcription of target genes (Miralles et al, 2003;

Vartiainen et al, 2007). Recently, Baarlink and colleagues showed that serum stimulation promoted nuclear actin polymerization which triggered MKL1 mediated SRF activation (Baarlink et al, 2013). Nevertheless, how nuclear actin polymerization is recognized and transduced into MKL/SRF signaling remains unknown so far. Complex formation between nuclear G-actin and MKLs promotes the Crm1-dependent nuclear export of MKLs back into the cytoplasm (Vartiainen et al, 2007). Serum or TPA stimulation (phorbol ester 12-O-tetradecanoyl-13-acetate) promotes not only the nuclear accumulation of MKLs but also induces ERK1/2 dependent phosphorylation of MKL1 at serine 454 (Muehlich et al, 2008). MKL1 phosphorylation functions as a switch-off stimulus for MKL1/SRF signaling since it supports binding between MKL1 and nuclear G-actin thereby facilitating nuclear the export of MKL1 (Muehlich et al, 2008). Moreover, it was supposed that the nuclear export rate is the determining factor for the subcellular localization of MKL1 (Vartiainen et al, 2007). The described nuclear-cytoplasmic shuttling mechanism of MKLs is well established for fibroblasts and muscle cells whereas myocardin is constitutively nuclear and specifically expressed in cardiac and smooth muscle cells.

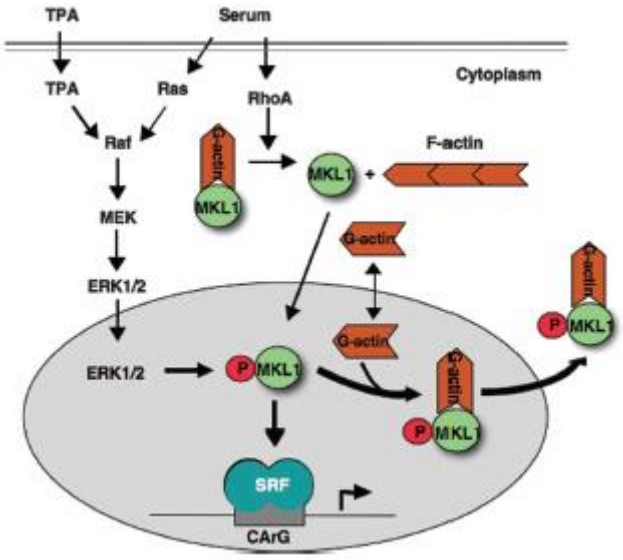

Figure 4: Regulation of the subcellular localization and transcriptional activity of MKLs.
Serum induced Rho activation induces F-actin polymerization and the concomitant G-actin depletion induces the dissociation of MKLs from G-actin. MKLs translocate into the nucleus, bind to the homodimer of SRF and activate the transcription of target genes. ERK1/2 mediated phosphorylation of MKL1 at serine 454 facilitates binding between MKL1 and nuclear G-actin thereby promoting the nuclear export of MKL1. Picture is taken from (Muehlich et al, 2008).

By contrast, in striated muscle cells, expression of STARS proteins drove MKLs into the nucleus and triggered their constitutive nuclear localization (Kuwahara et al, 2007). A constitutive nuclear accumulation of MKL1 without any stimuli was observed in neurons (Kalita et al, 2006; Stern et al, 2009). Therefore it is supposed that the subcellular localization of MKLs is a cell-type dependent feature.

2.1.5 Biological function of the transcriptional coactivators MKL1 and MKL2

Overexpression of MKL1 and MKL2 in fibroblasts activated smooth muscle gene expression (Du et al, 2004; Selvaraj & Prywes, 2004; Wang et al, 2002). Moreover, MKL1 expression was required for skeletal muscle differentiation and expression of dominant negative mutants of MKL1 *in vivo* caused thin muscle fibers suggesting that MKL1 expression is required for muscle growth (Li et al, 2005b; Selvaraj & Prywes, 2003). Despite the numerous physiological processes in which MKL1 takes part, the majority of MKL1 knockout mice are viable and fertile, presumably due to the functional redundancy between MKL1 and the other members of the myocardin family. This suggestion is supported by the fact that a single MKL1 or MKL2 knockout phenotype do not phenocopy SRF knockout. A small subset of MKL1 null embryos died from cardiac abnormalities (Sun et al, 2006b). Furthermore, female MKL1 knockout mice failed to nurse their offspring due to specific defects in the mammary gland myoepithelial cell differentiation that affected ejection of milk from the mammary gland during lactation (Li et al, 2006; Sun et al, 2006b). MKL1 knockout mice displayed a reduced number of platelets in the peripheral blood and a diminished quantity of mature megakaryocytes suggesting that MKL1 expression plays a crucial role in the differentiation and maturation of megakaryocytes (Cheng et al, 2009). A similar effect on megakaryocyte maturation and platelet formation was reported for double knockout mice lacking both MKL1 and MKL2 (Smith et al, 2012). Mice with global MKL2 knockout revealed a defect in the smooth muscle differentiation and a failure of the cardiovascular development leading to death between embryonic day 17.5 and postnatal day 1 (Oh et al, 2005). The observed phenotype arose presumably from the cell autonomous flaw in differentiation of smooth muscle cells from the cardiac neural crest (Li et al, 2005a). Conditional knockout of MKL1 and MKL2 in the brain caused morphological abnormalities in the hippocampus, cerebral cortex and subventricular zone. The defects were due to a failure of actin polymerization and dysfunctional cytoskeletal organization resulting in impaired neuronal migration and neurite outgrowth (Mokalled et al, 2010). In acute megakaryoblastic leukemia, MKL1 was found to be translocated and fused with RBM15 (RNA-binding motif protein 15) also known as OTT (Mercher et al, 2009). The RBM1-MKL1 fusion protein was functionally deregulated and caused the constitutive activation of SRF dependent target gene expression thereby promoting tumor progression (Cen et al, 2003; Descot et al, 2008). Besides the involvement of MKL1 in acute megakaryoblastic leukemia, MKL1 and MKL2 expression was required for tumor cell invasion and experimental metastasis (Medjkane et al, 2009). RNAi mediated downregulation of MKL1/2 expression abolished cell adhesion, spreading, motility and invasion of human breast carcinoma and mouse melanoma cells. Moreover reduced MKL1/2 expression abolished the capability of breast carcinoma cells to form lung metastases upon intravenous injection into the mouse tail vein. This study documented that the observed phenotypes were mediated by the two MKL/SRF dependent target genes MYH9 and MYL9,

both encoding cytoskeletal associated proteins (Medjkane et al, 2009). SCAI (suppressor of cancer cell invasion) was characterized as a novel binding partner of nuclear MKL1 (Brandt et al, 2009). SCAI expression antagonized ß1-integrin driven tumor cell invasion which was activated by MKL1/SRF signaling. Interestingly, the epithelial protein in Neoplasma α (Eplin α), acting as a cytoskeletal associated tumor suppressor, whose expression correlates inversely with tumor progression, was identified as an actin-MKL1 regulated target gene (Leitner et al, 2010). In contrast to tumor cells where MKL1/2 expression augmented the migratory behavior of the cells, Leitner and colleagues found that in non-invasive cells activation of G-actin-MKL signaling reduced cell migration via upregulation of cytoskeletal-associated proteins such as integrin alpha 5 (Itgα5), plakophilin (Pkp2) and FHL1 (Leitner et al, 2011). Furthermore, overexpression of MKL1 in NIH 3T3 fibroblasts induced a strong anti-proliferative effect through the upregulation of anti-proliferative target genes such as mig6, functioning as a negative regulator of the EGFR-MAPK signaling pathway (Descot et al, 2009). By contrast, RNAi mediated silencing of MKL1 and MKL2 expression in the same cell line caused a modest anti-proliferative effect (Shaposhnikov et al, 2013). Consequently it seems that the expression levels and activation status of MKLs determine the expression of specific clusters of target genes through which MKLs exert various, often opposing effects on cell migration and proliferation, depending on the cellular context.

2.2 Rho GTPases

The small GTPases of the Rho family form a distinct group within the Ras superfamily of monomeric GTP-binding proteins of which RhoA, Rac1 and cdc42 are well characterized. Rho GTPases have been described to be involved in a plethora of cellular processes such as cytoskeleton organization, gene transcription, cell proliferation, migration, growth and cell survival (Jaffe & Hall, 2005). Rho proteins can act as molecular switches by connecting changes from the external environment to intracellular signaling pathways. Activation of growth factors as well as tyrosine kinase receptors, G protein coupled receptors and integrins results in the activation of Rho GTPases which subsequently interact with their effector molecules and modulate their activity and subcellular localization.

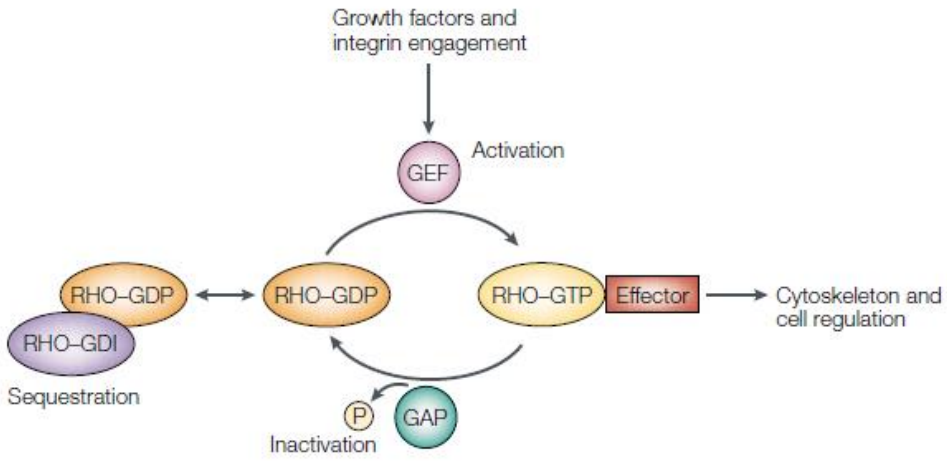

Figure 5: Rho GTPases are complexly regulated molecular switches.
Rho GTPases cycle between an inactive, GDP-bound and an active, GTP bound state. GDIs sequester GDP-bound GTPases in the cytoplasm. The exchange of GDP to GTP is promoted by GEFs which is often associated with the translocation of Rho proteins to the cell membrane. GAPs promote the hydrolysis of GTP to GDP thereby returning activated Rho GTPases in their inactive state. Activated GTP-bound Rho proteins bind to effector molecules which mediate downstream signaling. This picture is taken from (Sahai & Marshall, 2002).

Rho proteins shuttle between an active, GTP-bound and an inactive, GDP-bound state which is controlled by three classes of regulatory proteins (Figure 5). GEFs (guanine nucleotide exchange factors) promote the activation of Rho proteins by catalyzing the exchange of GDP to GTP (Rossman et al, 2005). On the other hand, GAPs (GTPase activating proteins) accelerate the intrinsic catalytic activity of Rho GTPases to hydrolyze bound GTP. Thus, the activity of Rho GAPs promotes the return of Rho GTPases in their inactive, GDP bound state (Bos et al, 2007). A third class of Rho GTPase inhibitors constitute GDIs (guanine nucleotide-dissociation inhibitors) which bind to GTPases and sequester them in their inactive, GDP-bound state in the cytoplasm (Dransart et al, 2005).

2.2.1 Rho GTPases and their role in cancer

Besides the involvement of Rho GTPase signaling in physiological processes, there is emerging evidence that deregulated Rho GTPase signaling contributes to cancer initiation,

tumor progression, unlimited proliferation potential, survival, evasion from apoptosis, invasion and the establishment of metastasis (Vega & Ridley, 2008). In contrast to the small GTPase Ras, no gain or loss-of-function mutations have been reported for Rho GTPases in human tumors, instead Rho proteins were found to be frequently overexpressed (Sahai & Marshall, 2002). In addition to unlimited cell proliferation, tumor cells adopt typical morphological characteristics which are necessary for invasion and metastasis. RhoA induces stress fiber assembly which are required as contractile structures, whereas cdc42 is essential for the formation of filopodia and Rac1 promotes lamellipodia formation.

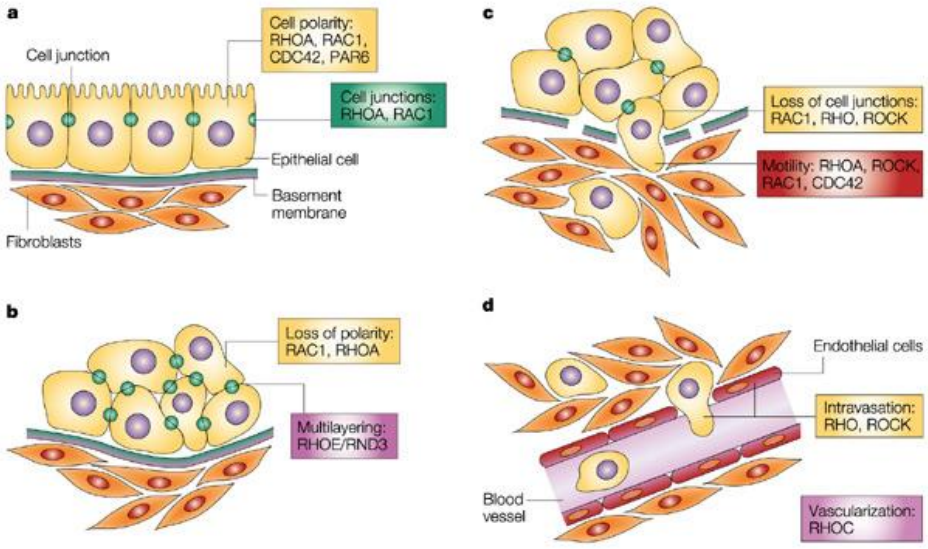

Figure 6: Requirement of Rho protein signaling at different stages during tumor progression.
(A) Normal epithelial polarity is maintained by RhoA, Rac1 and cdc42 whereas RhoA and Rac1 are required for the formation of cell junctions. (B) Loss of cell polarity is caused by RhoA and Rac1 signaling. (C) Augmented RhoA, ROCK, Rac1 and cdc42 signaling increases the motility of tumor cells thereby favoring the local invasion of tumor cells. (D) Metastasis to distinct sites is facilitated by Rho and ROCK signaling promoting transendothelial migration. Rho signaling increases the expression of pro-angiogenetic factors. Picture is taken from (Sahai & Marshall, 2002).

The polarity of normal epithelial cells is maintained by RhoA, Rac1 and cdc42. Loss of epithelial cell polarity is an important step during the process of epithelial-mesenchymal transition where cells render a more motile phenotype. Activation of RhoA signaling is able to trigger the loss of cell polarity. Loss of cell polarity and cell-cell junctions, increased migratory behavior and remodeling of the extracellular matrix (ECM) are required for tumor cells to become locally invasive. Modulation of Rac1 and Rho/ROCK activation can promote the loss of polarity whereas increased RhoA, ROCK, Rac1 and cdc42 activity increase the cell motility. Moreover RhoA and Rac1 regulate the expression of MMPs (matrix metalloproteinases) which affect remodeling of the basement membrane and other extracellular matrix compounds thereby promoting tumor cell invasion. For metastasis to distant sites, tumor cells have to enter the blood and lymphatic vasculature. It has been shown that the activity of RhoA and ROCK was required for the transendothelial migration of tumor cells (Adamson et al, 1999; Worthylake et

al, 2001). Moreover, tumor cells are not able to grow without the appropriate blood vessel support, hence angiogenesis is essential for the tumor formation *in vivo*. Increased Rho GTPase expression promoted the expression of pro-angiogenetic factors which facilitated vascularization of the tumors (Turcotte et al, 2003; van Golen et al, 2000). Alternative mechanism for increased Rho GTPase signaling in cancer can be envisaged such as the constitutive activation of a GEF, deletion of a GAP or altered expression of GDIs. A subset of GEFs were found to be mutated or aberrantly expressed in malignancies thereby functioning as oncogenes. For example, the RhoA specific GEF LARG (leukemia associated Rho GEF) was found in a fused version with the mixed lineage leukemia gene (MLL) in acute myeloid leukemia (AML) thereby promoting tumor progression (Kourlas et al, 2000; Reuther et al, 2001). Furthermore the Vav family of Rho GEF proteins was described to play a crucial role in human cancers (Lazer & Katzav, 2011). By contrast, the human genome encodes about 70 members of the RhoGAP family and their downregulation was found in different types of cancers like ArhGAP8 in colorectal and breast cancer, ArhGAP20 in leukemia and PIK3R1 in prostate cancer (Hellwinkel et al, 2008; Herold et al, 2011; Johnstone et al, 2004; Tcherkezian & Lamarche-Vane, 2007). Nevertheless, the family of Deleted in Liver Cancer proteins constitutes the best characterized group of RhoGAP proteins in the context of tumorigenesis.

2.2.2 The Deleted in Liver Cancer proteins

Three genes of the human genome encode for a RhoGAP subfamily termed “deleted in liver cancer “(DLC) proteins. The first member of this group, DLC1 also termed as ArhGAP7 or StarD12 was originally identified by Yuan and colleagues in 1998 by a representational difference analysis (a PCR-based subtractive hybridization technique) as a gene frequently deleted in primary human hepatocellular carcinoma (HCC) which shared high homology with the rat p122 RhoGAP gene (Yuan et al, 1998). The gene locus of DLC1 was mapped to chromosome 8p22, a region that recurrently shows LOH or heterozygous deletions in numerous solid tumors and hematological malignancies. Consequently, it was proposed that DLC1 is a candidate tumor suppressor (Yuan et al, 1998). DLC1 was found to be widespread expressed in normal tissues like brain, heart, kidney, liver, lung and spleen (Durkin et al, 2002). Since DLC1 has been characterized as a tumor suppressor, its expression was analyzed in various types of human cancers and was found to be downregulated or lost in many human cancers including breast, lung, colon, ovarian, stomach and brain (Guan et al, 2006; Kim et al, 2003; Plaumann et al, 2003; Seng et al, 2007; Ullmannova & Popescu, 2006; Xue et al, 2008; Yuan et al, 1998). The principle mechanism for DLC1 inactivation can be attributed to the frequent chromosomal deletions of its gene locus. Moreover the promoter region of the DLC1 gene is GC-rich with typical CpG islands that function as methylation sites. Thus, aberrant promoter methylation is thought to be the second mechanism that contributes to the silence of DLC1 expression in various types of human cancers (Wong et al, 2003; Yuan et al, 2003a). In

addition, transcriptional silencing has been linked to histone hypoacetylation due to the recruitment of histone deacetylases to chromatin (Marks et al, 2001). As DLC1 expression could be restored after the treatment with a histone deacetylase inhibitor in different human cancer cell lines, it was supposed that alterations in histone modifications could constitute the third mechanism accounting for the frequently observed suppression of DLC1 expression (Guan et al, 2006; Kim et al, 2003). Somatic mutations in the coding region of DLC1 were thought to be rare since it has been reported to occur in prostate and colon cancers (Liao et al, 2008). The other two members of the deleted in liver cancer family feature high similarity to DLC1. DLC2 also termed STARD13 is located on chromosome 13q12 and seems to be underexpressed in hepatocellular carcinoma. DLC3, also known as STARD8, was mapped to chromosome Xq13 and reduced DLC3 mRNA expression levels were detected in many human cancer tissues like prostate, kidney, lung, breast, uterus and ovary (Durkin et al, 2007a). Recently, the DLC1 isoform 4 (DLC1-i4) was discovered and reported to be absent in a large number of nasopharyngeal, esophageal, gastric, breast, colorectal, cervical and lung carcinoma cell lines as well as in primary tumors due to its epigenetic silencing (Low et al, 2011).

2.2.2.1 **Structure of the Deleted in Liver Cancer proteins**

DLC1-3 are multidomain proteins that are structurally composed of three functional domains. The N-terminal sterile alpha motif (SAM) features a five-helical structure and is a common protein-protein interaction motif, found in a variety of human signaling proteins (Kim & Bowie, 2003). Unlike this common feature, it has been reported that the SAM motifs of DLC1 and DLC2 adopt a four-alpha helical structure (Kwan & Donaldson, 2007; Li et al, 2007). SAM domains can form homo-and hetero-oligomers with other SAM-domain containing proteins or bind to other proteins, RNA and DNA (Qiao & Bowie, 2005). However the general role of the SAM-domain for the DLC1 function remains largely unknown. One study to the structure related function of the SAM domain pointed out that it seems to be autoinhibitory for the catalytic function of the RhoGAP domain (Kim et al, 2008). Using protein precipitation and mass spectrometry, the eukaryotic elongation factor 1A1 (EF1A1) was identified as a novel interaction partner of the SAM domain of DLC1, but not of DLC2. Zhong and colleagues showed that the interaction facilitated the distribution of EF1A1 to the membrane periphery and ruffles and suppressed significantly cell migration (Zhong et al, 2009).

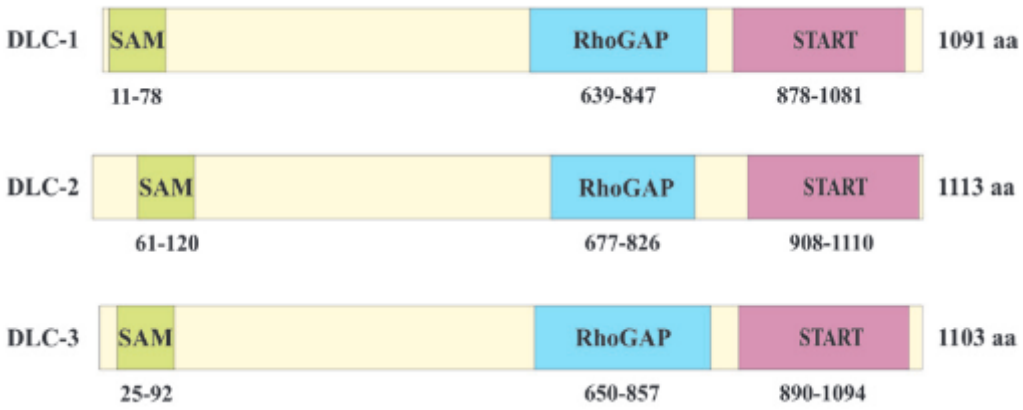

Figure 7: The modular structure of the DLC protein family, representing three major functional domains. Picture taken from (Lukasik et al, 2011).

Next to the SAM domain, there follows a region lacking a secondary structure which shows hardly any sequence identity to known conserved protein motifs. This unstructured middle part is an important feature since the open and extended conformation enables the interaction with other proteins and the attachment of post-translational modifications like phosphorylation (Tompa, 2003). Multiple serine threonine kinase phosphorylation sites were identified for DLC1, most of them are located in the middle region (Durkin et al, 2007b). For example, it has been shown that DLC1 is phosphorylated by protein kinase D (PKD) at serines 327 and 431 and this phosphorylation is required for the interaction with 14-3-3 proteins (Scholz et al, 2009). This phosphorylation prevented DLC1-mediated hydrolysis of GTP-bound Rho. In addition, Kawai and colleagues found in this unstructured region a focal adhesion targeting (FAT) domain which is responsible for the focal adhesion localization of DLCs (Kawai et al, 2009). Several studies reported that DLCs were targeted to focal adhesion sites via binding to the Src Homology 2 (SH2) domain of tensin proteins (Kawai et al, 2010; Liao et al, 2007; Qian et al, 2007). The focal adhesion localization seems to be critical for the tumor suppressive properties of DLCs. Moreover it has been shown that the family of DLC proteins interact with the phosphotyrosine binding (PTB) domain of tensin 2 proteins (Chan et al, 2009; Chen et al, 2012; Kawai et al, 2010; Yam et al, 2006). However, the best characterized domain of the DLC protein family constitutes the around 200 amino acid long RhoGAP domain, the most highly conserved region among the three proteins. The GAP domain catalyzes the conversion of active GTP-bound Rho proteins to their inactive GDP-bound form. The conserved arginine residue of all three DLC proteins is essential for their RhoGAP activity (Fidyk & Cerione, 2002). DLC1-3 exert a strong GAP activity towards RhoA and to a lesser extent towards cdc42 whereas they have almost no effect on the GTPase activity of Rac1 (Ching et al, 2003; Durkin et al, 2007a; Qian et al, 2007; Sekimata et al, 1999; Wong et al, 2003). The carboxyterminal START (steroidogenic acute regulatory protein (StAR)-related lipid transfer) domain is described to bind to lipids and sterols (Iyer et al, 2001). Altogether, fifteen human proteins

containing a START domain have been discovered which are implicated in different physiological processes like transfer between intracellular compartments, lipid metabolism and regulation of cell signaling (Alpy & Tomasetto, 2005; Ponting & Aravind, 1999). The exact physiological function as well as the interaction partners of the DLC1-3 START domains are not well characterized. In the case of DLC2, Ng and colleagues found that the DLC2 START domain colocalizes with mitochondria (Ng et al, 2006). Moreover, recently an interaction between the START domain of DLC1 and the tumor suppressor caveolin was identified affecting the tumor suppressive functions of DLC1 in a RhoGAP independent manner (Du et al, 2012).

2.2.2.2 **The biological function of DLC1 and its pivotal role in cancer**

As a RhoGAP protein with a proven activity towards the small GTPases of the Rho family, a major function of DLC1 constitutes certainly its involvement in the regulation of the cytoskeletal organization. Overexpression of DLC1 caused a rounded morphology of adherent cells accompanied by the disruption of actin stress fibers and focal adhesions, cellular processes which are well established to be reversely controlled by RhoA signaling (Kim et al, 2007; Sekimata et al, 1999; Wong et al, 2005). Knockout studies evidenced a crucial role of DLC1 expression for the embryonic development as homozygous mutant embryos died before 10.5 day postcoitus due to defects in the neural tube, brain, heart and placenta (Durkin et al, 2005). Analysis of fibroblasts isolated from DLC1 mutant embryos revealed disruption of the actin cytoskeleton thereby confirming the pivotal role of DLC1 for the cytoskeletal organization (Durkin et al, 2005). Moreover this study provided evidence that DLC2 and DLC3 were not able to compensate for the DLC1 deficiency during embryonic development suggesting that the different DLC isoforms may not act redundantly. First evidence for the tumor suppressive function of DLC1 derived from experiments where ecotopic DLC1 was expressed in different human cancer cell lines who have lost endogenous DLC1 expression. Restoration of DLC1 expression suppressed cell proliferation, colony formation and anchorage-independent growth of hepatocellular, breast and lung carcinoma cell lines (Ng et al, 2000; Plaumann et al, 2003; Qian et al, 2007; Wong et al, 2005; Yuan et al, 2003b; Zhou et al, 2004). The limitation of cell proliferation of HCC and renal carcinoma cells originated from the induction of apoptosis (Zhang et al, 2009; Zhou et al, 2004). Besides, overexpression of DLC1 in human breast, non-small lung and hepatocellular carcinoma cells suppressed tumorigenicity *in vivo* (Wong et al, 2005; Yuan et al, 2004; Yuan et al, 2003b; Zhou et al, 2004). Underexpression of DLC1 consistently correlated with the invasive and metastatic potential of cancer cell lines. In line with this, DLC1 was characterized as a metastasis suppressor in breast cancer cells (Goodison et al, 2005). Consistent with this description, reconstitution studies of DLC1 expression revealed inhibition of cell motility and invasiveness of HCC, breast, ovarian and lung cancer cell lines (Goodison et al, 2005; Qian et al, 2007; Syed et al, 2005; Wong et al, 2005). RNAi

mediated silencing of DLC1 expression in breast cancer cells increased migration in a mDia1 dependent but ROCK-independent manner (Holeiter et al, 2008). Recently, Tripathi and colleagues found that DLC1 expression modulated the invasiveness of metastatic prostate carcinoma cells by increasing E-cadherin expression which functioned as suppressor of cancer cell invasion (Tripathi et al, 2013). Using a novel mouse model of liver cancer, which allowed to identify and characterize new oncogenes and tumor suppressors in their appropriate genetic context, highlighted DLC1 as a bona fide tumor suppressor in HCC *in vivo* (Xue et al, 2008; Zender et al, 2006). ShRNA mediated DLC1 knockdown promoted in the context of Myc overexpression and p53 deficiency the formation of liver tumors (Xue et al, 2008). Many studies support the assumption that the tumor suppressive properties of DLC1 are attributed to its functional GAP activity as it has been shown that mutants lacking GAP activity were incapable to inhibit tumor cell growth (Wong et al, 2005). Mutational analysis of tumor samples of patients with prostate carcinoma revealed two missense mutations within the FAT region resulting in a significant reduction of RhoGAP activity thereby abrogating the tumor suppressive activity of DLC1 (Liao et al, 2008). Nonetheless, there is given evidence for GAP independent tumor suppressive activities of DLC1. Indeed, expression of a GAP-defective mutant abolished colony formation of small lung cancer cells and partially blocked the cell migration of NIH3T3 fibroblasts (Healy et al, 2008; Zhong et al, 2009). It is likely that DLC1 makes use of both GAP-dependent and GAP-independent mechanism for its tumor suppressive functions, however future investigations are required to figure out the underlying mechanism.

2.3 Cellular senescence and cancer

Cancer cells acquire the capability of sustained proliferative signaling and are characterized by the bypass of restriction points normally limiting their uncontrolled expansion (Hanahan & Weinberg, 2000). Excessive proliferation is counteracted by so called cellular “failsafe programs” which constitute stress-responsive, genetically encoded programs with the task to eliminate damaged, inappropriately proliferating cells from the cell cycle to maintain cellular integrity (Schmitt, 2003). Apoptosis is regarded as the most prominent and best-studied failsafe mechanism (Lowe & Lin, 2000). It has become clear that additional programs are presumably involved in controlling the proliferative capacity of tumor cells. Cellular stress or active oncogenic signaling does not necessarily result in programmed cell death but can force cells to escape the cell cycle in order to enter a permanent cell cycle arrest state which reminds on cellular senescence.

2.3.1 Cellular senescence

Four decades ago, Hayflick and colleagues established the term “cellular senescence” as a stable proliferation arrest of human diploid fibroblasts in culture when cells lost their ability to divide due to the accumulation of cell doublings (Hayflick & Moorhead, 1961). Some years

later, excessive telomere shortening was found to be the initial event contributing to the irreversible growth arrest that was designated as “replicative senescence” (Harley et al, 1990; Hayflick & Moorhead, 1961). Senescent cells were detected to accumulate in aging skin, fibroblasts and primates as well as in other tissues like liver or retina implying that senescence is tightly linked to the process of aging (Dimri et al, 1995; Herbig et al, 2006; Mishima et al, 1999; Paradis et al, 2001). In the past years, it has been established that the irreversible growth arrest can be additionally caused by various stress stimuli such as excessive mitogenic signaling, oxidative stress, DNA damage, chemotherapeutic agents as well as genetic defects, referred to as “premature senescence” which seemed to be independent on progressive telomere shortening (Collado & Serrano, 2006).

2.3.2 Common features of cellular senescence

The typical hallmark of senescence is an irreversible growth arrest by blocking the cell in the G1-phase although cells are viable and remain metabolically active (Sherwood et al, 1988). Cells can enter a reversibly arrested state, termed quiescence, where they survive for extensive periods of time. Quiescent cells can resume proliferation upon physiological stimuli whereas senescent cells are insensitive to mitogenic signals and are incapable to re-enter the cell cycle (Campisi & d'Adda di Fagagna, 2007). Senescent cells undergo typical structural and morphological changes, adopting an enlarged, flattened morphology and displaying a vacuole enriched cytoplasm (Dimri et al, 1995). Most senescent cells are resistant to apoptosis and reveal an altered gene expression pattern compared to normal cycling or quiescent cells (Hampel et al, 2004; Shelton et al, 1999).

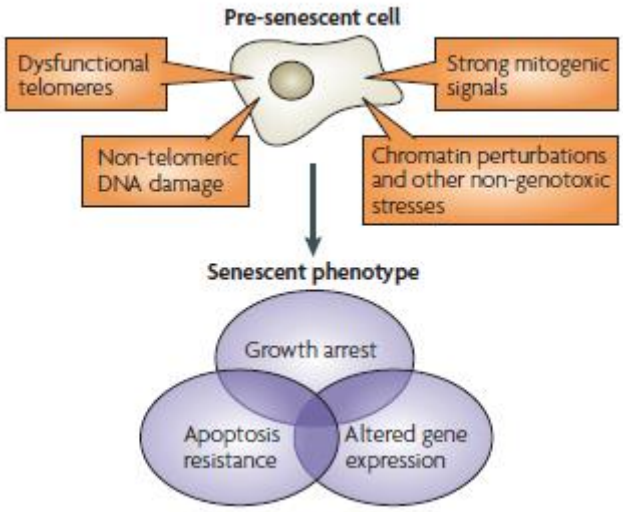

Figure 8: Different stimuli induce the senescent phenotype.
DNA damage, excessive mitogenic signals, dysfunctional telomeres and cytotoxic agents can induce the cellular senescence response. The senescent phenotype is defined by an irreversible growth arrest, resistance to apoptosis and altered gene expression pattern. Picture is taken from (Campisi & d'Adda di Fagagna, 2007).

Typically, senescent cells are marked by increased lysosomal activity of the cytoplasmic ß-galactosidase enzyme which can be histochemically stained and is considered as the

goldstandard procedure for the detection of senescent cells in vitro and *in vivo* (Dimri et al, 1995; Lee et al, 2006). A further characteristic feature of most senescent cells is the upregulation of proteins such as $p16^{Ink4a}$, p53, alternate-reading-frame protein (ARF) or product of the promyelocytic leukemia gene (PML) (Dimri et al, 2000; Ferbeyre et al, 2000; Kamijo et al, 1997; Pearson et al, 2000; Serrano et al, 1997).

2.3.3 Oncogene-induced senescence

Besides a variety of cellular stimuli, numerous lines of evidence indicate that the overexpression of active forms of oncogenes is able to provoke a senescence like cell cycle arrest designated as “oncogene-induced senescence” (OIS). The story started in 1997 when Serrano and colleagues overexpressed an active oncogenic version of H-Ras (H-Ras^{GV12}) in rodent and human fibroblasts and observed a senescent like growth arrest accompanied by the upregulation of proteins such as $p16^{Ink4a}$, p53 and $p21^{CIP/WAF1}$ (Serrano et al, 1997). Following studies demonstrated that overexpression of oncogenic versions of the members of the Ras signaling pathway like Raf, Mek or Braf caused the oncogene-induced senescence response (Lin et al, 1998; Michaloglou et al, 2005; Zhu et al, 1998). Oncogene-induced senescence has become a central issue of investigations and constitutes a multifaceted process depending on different effector mechanism.

2.3.3.1 Signaling pathways of the oncogene-induced senescence response

As senescence is characterized as a permanent cell cycle arrest, significant attention has been placed on proteins involved in controlling cell cycle progression. In fact, several cell cycle regulators and their signaling pathways are closely related with the induction of a senescence response. It has already been shown that upon accumulation of cell doublings and certain stress stimuli, the transcriptional activity of the tumor suppressor p53 is increased (Serrano et al, 1997). The Arf/p53/$p21^{CIP1/WAF1}$ pathway plays a crucial role in the mediation of the senescence response upon certain stress stimuli like oncogenic signaling (Levine & Oren, 2009; Vousden & Lane, 2007). The steady state levels of p53 are controlled by the E3 ubiquitin ligase HDM2 which promotes the degradation of p53. Senescence inducing signals activate the INK4aArf locus (ARF) which blocks the HDM2 mediated degradation of p53 (Levine & Oren, 2009). Subsequently, p53 activates its transcriptional target $p21^{CIP1/WAF1}$, a cyclin dependent kinase inhibitor which executes the senescence response (Brown et al, 1997). On the other hand there exists the well-established $p16^{Ink4a}$/Rb tumor suppressor pathway which is critically implicated in the regulation of the G1 to S-phase transition. $P16^{Ink4a}$, a principal member of the Ink4a family of Cdk inhibitors, was found to be transcriptionally overexpressed during replicative as well as premature senescence (Alcorta et al, 1996; Hara et al, 1996; Serrano et al, 1997). $P16^{Ink4a}$ binds to CDK4/6 thereby inhibiting their kinase activity that prevents the phosphorylation of Rb and contributes to the maintenance of the Rb protein in its

active, hypophosphorylated state. In its active form, Rb associates with the transcription factors of the E2F family and silences the transcription of E2F target genes like cyclin E or A which are required for the G1/S phase transition (Burkhart & Sage, 2008; Serrano et al, 1997). Both pathways can interact mechanistically with each other at different stages, however they possess the ability to halt independently the cell-cycle progression. Additionally which tumor suppressor pathway is mainly engaged depends on both cell-type-specific and species-specific differences.

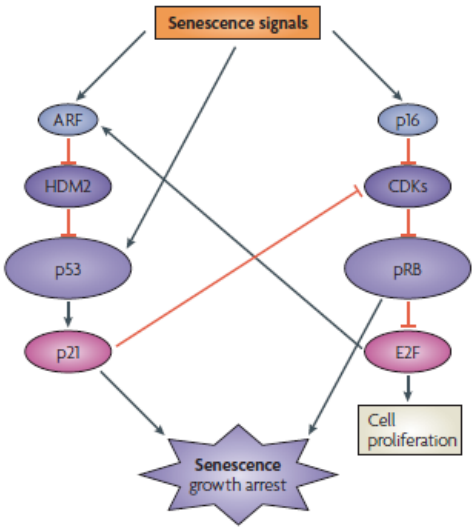

Figure 9: Senescence response is mediated by the ARF/p53/p21 $^{CIP1/WAF1}$ and p16^{Ink4a}/Rb signaling pathway.
Normally, the tumor suppressor p53 is degraded by the E3-ubiquitin ligase HDM2 which is negatively regulated by ARF. Senescence stimulating signals activate ARF which consequently inhibits HDM2 thereby activating p53. Active p53 induces the expression of p21 $^{CIP1/WAF1}$, a cyclin dependent inhibitor which executes the senescence response. Senescence triggers engage the p16^{Ink4a}/Rb tumor suppressor pathway by primarily inducing the expression of the Cdk inhibitor p16^{Ink4a} which inhibits cyclin D/Cdk4/6 thereby abrogating the phosphorylation of Rb and its inactivation. Rb controls the senescence induction by repression of the transcription factors of the E2F family which stimulate the expression of genes required for cell-cycle progression. It is thought that the ARF/p53/p21 $^{CIP1/WAF1}$ and p16^{Ink4a}/Rb pathway can influence themselves reciprocally and can interact at different stages depending on the cellular context. Picture is taken from (Campisi & d'Adda di Fagagna, 2007).

2.3.3.2 **DNA damage response (DDR*)***

The involvement of the DNA damage response in the induction of a replicative senescence response due to dysfunctional telomeres has already been well established (d'Adda di Fagagna, 2008). DNA damage response is activated by single or double strand breaks or other DNA discontinuities which are sensed by the MRE11-RAD50-NBS1 complex. Detection of DNA damage leads to the activation of the downstream protein kinases such as ataxia telangiectasia mutated (ATM) and ataxia telangiectasia and Rad-3 related (ATR) which trigger immediate events such as phosphorylation of the histone variant H2AX. The modified chromatin structure recruits multiple proteins and some of these proteins enhance signaling by the kinases, participate in transducing the damage signals and optimize repair activities by other proteins. ATR and ATM activate the downstream kinases checkpoint-1 (CHK1) and CHK2 which activate and phosphorylate the tumor suppressor p53. Activated p53 induces the

cell cycle arrest through activation of p21$^{CIP/WAF1}$ which governs the senescence response (d'Adda di Fagagna, 2008).

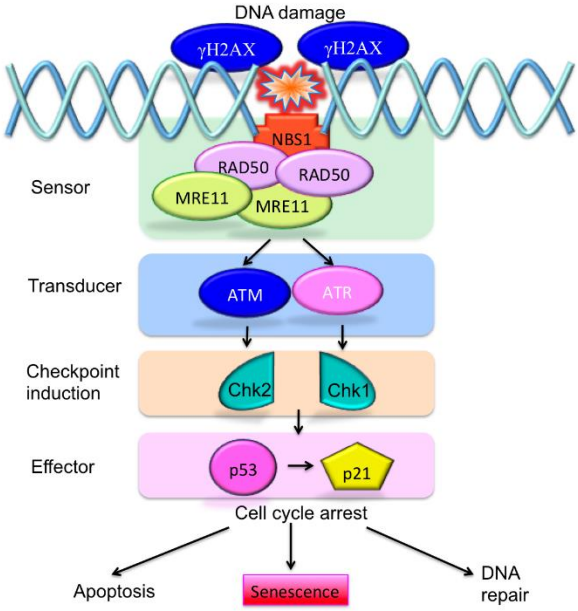

Figure 10: DNA damage response triggers senescence induction.
DDR is activated through DNA damage which is sensed by the MRE-RAD50-NBS1 complex. The kinases ATM, ATR, CHK1 and CHK2 are activated upon DNA damage. CHK1 and CHK2 activate and phosphorylate p53 which induces the senescence response via activation of p21$^{CIP/WAF1}$. Picture is taken from (Becker et al, 2013).

In the case of oncogene-induced senescence it has been shown that activated oncogenes enforce uncontrolled, constitutive replication cycles which lead to DNA replication stress thereby causing DNA damage (Bartkova et al, 2006; Di Micco et al, 2006). For example, inactivation of CHK2 abrogates oncogenic H-Ras induced senescence thereby highlighting the importance of a DDR for the induction of the oncogene-induced senescence (Di Micco et al, 2006). Of note, DDR activation seems not to be a universal requirement for oncogene-induced senescence, as several studies reported the occurrence of oncogene-induced senescence without the induction of a DDR and despite the lack of DDR effector proteins (Efeyan et al, 2009; Kuilman et al, 2008; Olsen et al, 2002). Consequently, DDR seems to participate in the establishment of oncogene-induced senescence, however depending on the setting of oncogene-induced senescence induction.

2.3.3.3 **Senescence-associated heterochromatin foci (SAHF)**

Senescent cells undergo profound changes of the chromatin structure which are thought to be important mediators of the senescence response. Their manifestation is caused by the formation of facultative heterochromatin structures termed as senescence-associated heterochromatin foci which were initially found microscopically when senescent cells were stained with 4`,6-diamidino-2-phenylindole (DAPI) (Narita et al, 2003). SAHFs reveal a specific enrichment of histone 3 lysine 9 trimethylation (H3K9me3) and are devoid of euchromatin structures such as histone H3 lysine 9 acetylation or histone H4 lysine 4 methylation. Moreover, histone H2A variant macroH2A, heterochromatin protein 1 (HP1) and high mobility

group A (HMGA) were found as heterochromatin structures of SAHFs (Narita et al, 2006; Narita et al, 2003; Zhang et al, 2007). Functionally, the heterochromatin structures of SAHFs contribute to the silencing of proliferation-promoting genes such as E2F target genes like cyclin A. Moreover it has been well documented that oncogenic signaling caused the formation of SAHFs (Martin et al, 2010; Michaloglou et al, 2005; Narita et al, 2003). Recent investigations from Di Micco and colleagues led to the suggestion that SAHFs could damper the extent of DNA damage signaling which may prevent senescent cells from undergoing apoptosis induced by high DNA damage signaling thereby preserving the viability of senescent cells (Di Micco et al, 2011). Thus, chromatin remodeling contributes to the maintenance of the irreversible growth arrest and reinforces the senescence response.

2.3.3.4 **Senescence-messaging secretome (SMS)**

A further characteristic of cells undergoing the oncogene-induced senescence response constitutes the secretion of a broad spectrum of soluble and insoluble as well as other factors which is collectively termed as “senescence-messaging secretome” (SMS) or alternatively called “senescence-associated secretory phenotype” (SASP) (Coppe et al, 2010; Kuilman & Peeper, 2009). The SMS factors can be classified into different categories such as interleukins, chemokines, other inflammatory factors, proteases and regulators, growth factors, receptors and their ligands as well as extracellular components (Coppe et al, 2010). Moreover it has been shown that a persistent DNA damage response was required for the expression of SMS factors (Rodier et al, 2009).

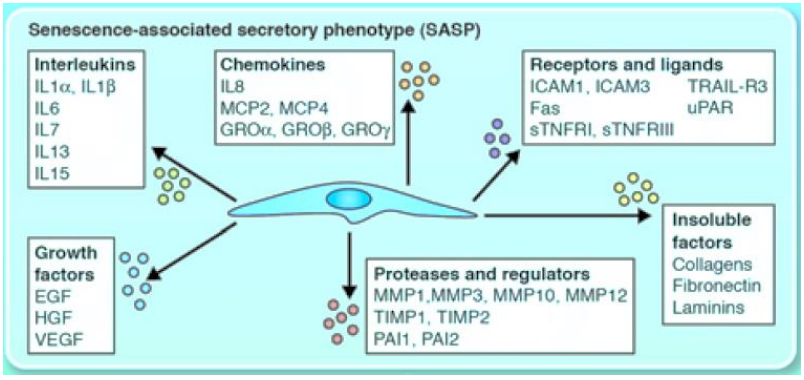

Figure 11: Senescent cells are characterized by the induction of a senescence-messaging secretome. Senescent cells secrete a plethora of different soluble and insoluble factors, depending on the individual cell type. SMS factors contributes to the maintenance of the stable cell cycle arrest and can feature both tumor-suppressive as well as pro-tumorigenic properties. Picture is taken from (Pawlikowski et al, 2013).

In addition, signaling of SMS factors like interleukin 6 or 8 (IL-6/IL-8) was shown to reinforce the stable proliferation arrest upon oncogenic signaling thereby suggesting that SMS induction is an essential effector mechanism for the establishment of a senescence response (Acosta et al, 2008b; Kuilman et al, 2008). Functionally, the SMS creates a complex signaling network which affects not only senescent cells but also allows them to communicate with their

microenvironment in a paracrine fashion to promote their senescence response, for example via IL-1 and TGF-ß signaling (Acosta et al, 2013). In some cases, SMS factors feature tumor suppressive properties by attracting the innate immune system for the clearance of senescent cells in vitro and *in vivo* (Kang et al, 2011; Krizhanovsky et al, 2008; Xue et al, 2007). By contrast, secretion of SMS factors can also promote tumorigenesis of neighboring, premalignant cells by stimulating their cell growth, enhancing their migratory and invasiveness properties and promoting EMT (Coppe et al, 2010; Krtolica et al, 2001). Thus, SMS reflects a defined and essential feature for the senescence response that can both limit and boost tumor progression depending on the cellular context.

2.3.3.5 Oncogene-induced senescence – its role in tumorigenesis

Tumor cells are characterized by an unlimited lifespan and are exposed to many cellular stress stimuli, therefore induction of a senescence response would represent an important tumor suppressive mechanism counteracting unrestrained proliferation. Several studies have demonstrated that the occurrence of the oncogene-induced senescence response in premalignant stages of murine and human tumors and its absence in malignant types (Braig et al, 2005; Chen et al, 2005; Collado et al, 2005; Michaloglou et al, 2005). For example, using an *in vivo* mouse model, endogenous expression of oncogenic K-Ras (K-*Ras*^{G12V}) was able to trigger oncogene-induced senescence during premalignant stages of lung and pancreatic tumors (Collado et al, 2005). The first evidence for oncogene-induced senescence in human tumors was brought by investigations of Michaloglou and colleagues showing that melanocytes expressing oncogenic BRAF^{V600E} underwent oncogene-induced senescence (Michaloglou et al, 2005). Moreover, Braig and colleagues described oncogene-induced senescence as an initial barrier in lymphoma development (Braig et al, 2005). Thus, oncogenic signaling causes an early senescent growth arrest in premalignant lesions.

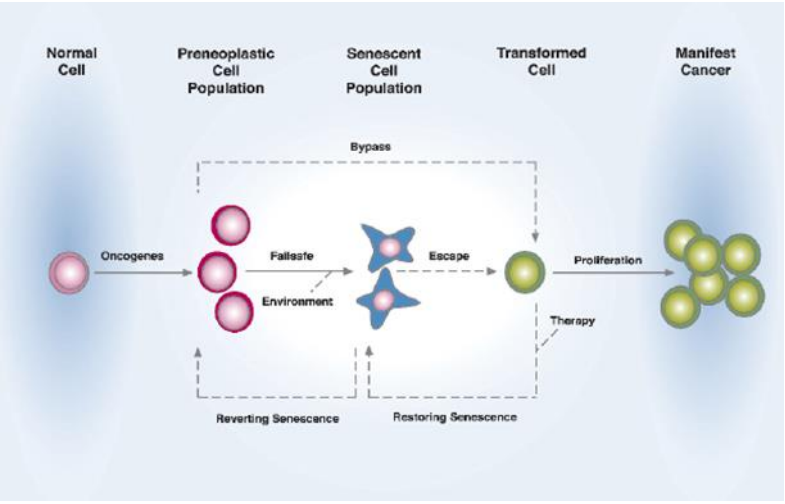

Figure 12: Model for oncogene-induced senescence during tumorigenesis.
Oncogenic driven cells can enter the senescence state or bypass senescence and develop an oncogenic transformed, malignant phenotype. Moreover it is supposed that genetic defects in the senescence effector molecules can facilitate the establishment of malignant cells. Therapeutic approaches might aim for reverting malignant cells into a senescent state. Picture is taken from (Braig & Schmitt, 2006).

Nevertheless, it remains unresolved whether transformed, fully malignant cells directly originate from an oncogenic driven cell that bypassed senescence or secondary lesions like mutations in crucial senescence effector molecules are required. However, it is supposed that genetic defects inactivating senescence effectors are not directly sufficient to transform cells harboring the initiate oncogene (Braig & Schmitt, 2006). In a therapeutic setting, specific markers for oncogene-induced senescence could be used as indicators for premalignant tumor lesions. Detection of oncogene-induced senescence will facilitate staging tumor lesions and to monitor the therapeutic efficacy of anti-tumor strategies (Collado & Serrano, 2006). Of note, DNA-damaging agents like anti-cancer drugs have already been reported to induce oncogene-induced senescence in tumor cells, therefore it might be conceivable that induction of oncogene-induced senescence in malignancies could be viewed as a novel, pharmacological approach (Chang et al, 1999; Schmitt et al, 2002; te Poele et al, 2002). A future goal might be to identify and characterize novel oncogene-induced senescence inducing molecules as well as drugs to understand and improve the outcome of the senescence response in the context of tumor progression.

2.4 Myoferlin

Myoferlin, also named Fer-1-like protein 3, belongs to the family of ferlin proteins which consists of dysferlin (DYSF), myoferlin (MYOF) and otoferlin (OTOF). Recently, three further members of the ferlin family, Fer1L-4, Fer1L-5 and Fer1L-6 has been identified but their function remains so far unknown. All members share structural similarity, consisting of several cytosolic C2 domains and a single-pass transmembrane domain at their C-termini (Bansal & Campbell, 2004). A common feature of C2 domains is the capability to bind phospholipids and other proteins in a calcium dependent manner (Nalefski & Falke, 1996).

Figure 13: Structure of myoferlin.
The structure of myoferlin contains several cytosolic C2 domains and a C-terminal single-pass transmembrane domain. Picture is taken from (McNeil & Kirchhausen, 2005).

Initially, myoferlin expression was found to be restricted to cardiac and skeletal muscle cells and it was supposed as a potential modifier of muscular dystrophy and cardiomyopathy (Davis et al, 1996). However several studies were able to report myoferlin expression in other cell tissues and cell types, such as endothelial and breast carcinoma cells (Bernatchez et al, 2007; Eisenberg et al, 2011). Myoferlin has been reported to play a role in a variety of processes, such as endocytosis, endothelial membrane repair and vesicular transport (Bernatchez et al, 2009; Cipta & Patel, 2009; Sharma et al, 2010). Interestingly, numerous studies reported an

influence of myoferlin on growth factor stability. In endothelial cells, myoferlin was found to control the biological activity of the vascular endothelial growth factor receptor 2 (VEGFR2) via inhibition of its polyubiquitination and proteasomal degradation (Bernatchez et al, 2007). Loss of myoferlin expression thereby reduced cell proliferation, migration and release of nitric oxide (NO) in response to VEGF (Bernatchez et al, 2007). Moreover in the same cell type, downregulation of myoferlin expression reduced the expression of angiopoietin-1 receptor (TIE2), another receptor tyrosine kinase, mainly expressed in the vascular endothelium (Yu et al, 2011). Additionally, Demonbreu and colleagues described that myoferlin deficiency caused defective insulin growth factor-like (IGFR1) trafficking as well as decreased IGFR1 signaling (Demonbreun et al, 2010). So far, there exists only little knowledge about the role of myoferlin expression in tumor cells. Silencing of myoferlin expression diminished the invasiveness of human breast carcinoma cells and decreased the tumor growth of mouse Lewis lung carcinoma cells *in vivo* (Eisenberg et al, 2011; Leung et al, 2013; Li et al, 2012a). Recently, Turtoi and colleagues characterized myoferlin as a specific regulator of the epidermal growth factor (EGF) receptor in human breast carcinoma cells (Turtoi et al, 2013). Downregulation of myoferlin blocked the degradation of phosphorylated EGF receptor and inhibited simultaneously EGF-induced cell migration and epithelial-to-mesenchymal transition (EMT) (Turtoi et al, 2013). Thus, the discovery of the role of myoferlin in the context of tumorigenesis has just started and the evaluation of the underlying molecular mechanism will help to better understand the complexity of tumor progression.

3 Aim of the thesis

The subcellular localization of MKL1 and MKL2 is tightly linked to their transcriptional activity. In fibroblasts and muscle cells, a nuclear-cytoplasmic shuttling mechanism is well described for MKL1/2, nevertheless their subcellular localization seems to be a cell-type specific feature. Preliminary studies of our group illustrated a correlation between the subcellular localization of MKL1 and the endogenous expression levels of the tumor suppressor DLC1.

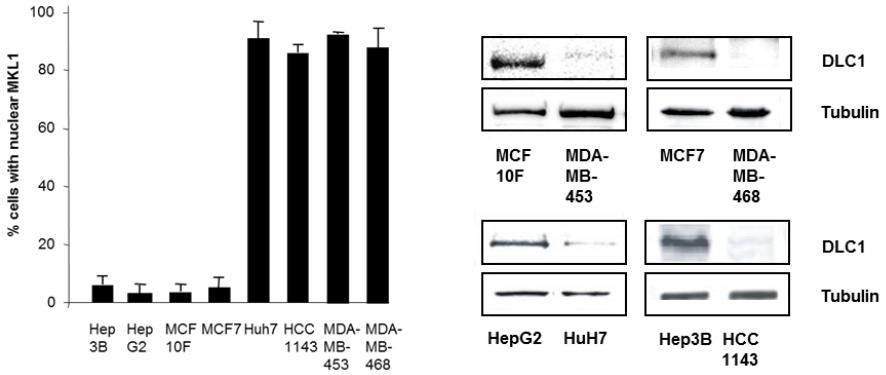

Figure 14: Nuclear accumulation of MKL1 in DLC1-deficient hepatocellular and breast carcinoma cell lines (Muehlich et al, 2012).

Our data demonstrate a predominantly nuclear MKL1 localization in hepatocellular and breast carcinoma cell lines lacking endogenous DLC1 expression. Originally, DLC1 was identified as a tumor suppressor in hepatocellular carcinoma, but a representative oligonucleotide microarray analysis (ROMA) illustrated a heterozygous deletion of DLC1 in about 50 % of liver, breast and lung and 70 % of colon cancers, almost as frequently as p53 in these cancers (Xue et al, 2008). DLC1 encodes a RhoGAP protein which modulates the activity of RhoGTPases. Interestingly, the subcellular localization of MKL1/2 is well known to be regulated by Rho-actin signaling. In addition, a landmark publication by the group of Richard Treisman highlighted that MKL1/2 signaling is required for tumor cell invasion and experimental metastasis of human breast carcinoma cells (Medjkane et al, 2009). Consequently, we hypothesize a direct functional relationship between DLC1 expression and MKL1/2 signaling in the context of tumorigenesis.

Thus three main issues will be addressed within this thesis:

I. Molecular mechanism which drive nuclear MKL1/2 signaling in human cancer cells upon loss of DLC1 expression
II. Does nuclear MKL1/2 signaling influence the tumor growth of human hepatocellular carcinoma cells characterized by a DLC1-deficient background in vitro and in *vivo*
III. Identification and characterization of novel MKL1/2 dependent target genes which expression influence the tumor growth of DLC1-deficient hepatocellular carcinoma cells

4 Materials

4.1 Cell culture

4.1.1 Cell lines

Cell line	Organism/ Cell Type	Culture conditions	Provider/ Origin
HEK293T	Human embryonic kidney	DMEM	Kind gift of Anna-Lena Forst, Ludwig-Maximilians-University Munich
HuH7	Human hepatocellular carcinoma	DMEM	Kind gift of Stephan Singer, University of Heidelberg
HuH6	Human hepatoblastoma	DMEM	Kind gift of Stephan Singer, University of Heidelberg
Amphotropic Phoenix cells	Modified HEK293T cells expressing gag-pol and envelop proteins	DMEM	Kind gift of Antonio Sarikas, Technical University of Munich
HepG2	Human hepatoma	RPMI	Kind gift of Stephan Singer, University of Heidelberg
HLF	Human hepatocellular carcinoma	RPMI	Kind gift of Stephan Singer, University of Heidelberg
MCF7	Human breast carcinoma	DMEM	Kind gift of Dr. Ramon Parsons, Mount Sinai Hospital, New York, USA
MDA-MB-468	Human breast carcinoma	DMEM	Kind gift of Dr. Ramon Parsons, Mount Sinai Hospital, New York, USA
HepG2 MLC	Human hepatoma cells stably expressing control shRNA	RPMI	Kind gift of Scott Lowe, Memorial Sloan-Kettering Cancer Center, New York, USA
HepG2 shRNA DLC1	Human hepatoma cells stably expressing DLC1 shRNA	RPMI	Kind gift of Scott Lowe, Memorial Sloan-Kettering Cancer Center, New York, USA
Murine hepatocytes control shRNA	Embryonic liver progenitor cells expressing control shRNA	DMEM	*(Xue et al, 2008)*
Murine hepatocytes DLC1 shRNA	Embryonic liver progenitor cells expressing DLC1 shRNA	DMEM	*(Xue et al, 2008)*

HepG2 Tet off	Human hepatoma cells expressing Tet-responsive trans-activator (tTA)	RPMI	*(Sun & Nassal, 2006)*
HuH7 Tet off	Human hepatocellular carcinoma cells expressing Tet-responsive trans-activator (tTA)	DMEM	*(Sun & Nassal, 2006)*

4.1.2 Cell culture media and solutions

Reagent	Provider
Dulbecco`s Modified Eagle Medium (DMEM)	Sigma-Aldrich, Taufkirchen, Germany
RPMI 1640 Medium	Sigma-Aldrich, Taufkirchen, Germany
Opti-MEM®	Gibco® Invitrogen, Karlsruhe, Germany
Fetal Bovine Serum	Gibco® Invitrogen, Karlsruhe, Germany
Penicillin-Streptomycin (5000 U/mL)	Gibco® Invitrogen, Karlsruhe, Germany

4.1.3 Transfection Reagents

Reagent	Provider
Lipofectamine® 2000	Invitrogen, Karlsruhe
Lipofectamine® RNAiMAX	Invitrogen, Karlsruhe
GenJet™ DNA In Vitro Transfection Reagent	SignaGen Laboratories, Rochville, USA

4.1.4 Plasmid constructs

Plasmid construct	Vector	Provider
Wildtype human Flag-DLC1	Flag-pEFrPGKpuro	Kind gift of Prof. Monilola Olayioye, University Stuttgart
Flag-RhoA-V14	pRevTRE	Kind gift of Prof. Ron Prywes, Columbia University
Flag-MKL1 mutant N100	pCin4	Kind gift of Prof. Ron Prywes, Columbia University
Wildtype human GFP-DLC1	pcDNA5/FRT/TO-GFP-DLC1	Kind gift of Prof. Monilola Olayioye, University Stuttgart

4.1.5 Lentiviral and retroviral expression constructs

Construct	Vector	Provider
H-RasV12	pBabe-puro	Kind gift of Dr. Antonio Sarikas, Technical University of Munich
nontarget shRNA vector, SHC002	pLKO.1-puro	Sigma-Aldrich, Taufkirchen, Germany
shRNA MKL1/2	pLKO.1-puro	*(Lee et al, 2010b)*
shRNA Myoferlin (TRCN0000010628)	pLKO.1-puro	Sigma-Aldrich, Taufkirchen, Germany
pD8.9	pCMV	Kind gift of Prof. Ron Prywes, Columbia University
pVSVG	pCMV	Kind gift of Prof. Ron Prywes, Columbia University

4.1.6 siRNA sequences

All siRNA oligonucleotides were custom synthesized by Sigma-Aldrich, Taufkirchen, Germany. Lyophilized siRNA oligonucleotides were dissolved in water to a concentration of 50 µM and stored in aliquots at -20°C.

target	Sequence [5`- 3`]
siRNA hDLC1	UUA AGA ACC UGG AGG ACU A [dT] [dT]
siRNA hMKL1	GAA UGU GCU ACA GUU GAA A [dT] [dT]
siRNA hMKL1/2	AUG GAG CUG GUG GAG AAG AA [dT] [dT]
siRNA hMKL2	GUA ACA GUG GGA AUU CAG C [dT] [dT]
siRNA hMYOF	CCC UGU CUG GAA UGA GA [dT] [dT]
siRNA Neg. ctrl	CGU ACG CGG AAU ACU UCG A [dT] [dT]
siRNA hp16^{Ink4a}	CGC ACC GAA UAG UUA CGG U [dT] [dT]
siRNA hSRF	GAU GGA GUU CAU CGA CAA CAA [dT] [dT]

4.1.7 Selection antibiotics for cell culture

Antibiotic	Stock solution	Final concentration	Provider
Doxycycline hyclate	1 mg/mL	0.5 µg/mL	Sigma Aldrich, Taufkirchen, Germany
Geneticin (G418 Sulfate)	50 mg/mL	200 µg/mL	Carl Roth, Karlsruhe, Germany
Hygromycin B solution Cellpure®	50 mg/mL	200 µg/mL	Carl Roth, Karlsruhe, Germany
Puromycin Dihydrochloride	1 mg/mL	1-10 µg/mL	Calbiochem, Darmstadt, Germany

4.1.8 Inhibitors and stimulants

Inhibitor	Final concentration	Provider
UO126 1,4-diamino-2,3-dicyano-1,4- bis (2-aminophenylthio) butadiene	10 mM	Tocris Bioscience, Germany
Lysophosphatidic acid (LPA)	10 µM	Sigma-Aldrich, Taufkirchen, Germany
Human recombinant epidermal growth factor EGF	10 nM	Sigma-Aldrich, Taufkirchen, Germany

4.2 Antibodies

4.2.1 Primary antibodies

Primary antibody	Dilution	Provider
Active caspase 3 (rabbit polyclonal)	1:500	Promega, Mannheim
Active Ras (mouse monoclonal)	1:500	NewEast Bioscience, Malvern, USA
Active RhoA (mouse monoclonal)	1:500	NewEast Bioscience, Malvern, USA
Alexa Fluor® Phalloidin	1:500	Invitrogen, Karlsruhe
CTGF (L-20) (polyclonal goat)	1:250	Santa Cruz Biotechnology, CA, USA
DLC1 (mouse monoclonal)	1:500	BD Bioscience, Heidelberg, Germany
DLC1 H-260 (rabbit polyclonal)	1:500	Santa Cruz Biotechnology, CA, USA
EGFR antibody (mouse monoclonal)	1:250	Spring Bioscience, USA

ERK (C14) (rabbit polyclonal)	1:10000	Santa Cruz Biotechnology, CA, USA
Flag M2 (mouse monoclonal)	1:500	Sigma-Aldrich, Taufkirchen, Germany
GAPDH (mouse, monoclonal)	1:500	Sigma-Aldrich, Taufkirchen, Germany
HA (3F10) (goat monoclonal)	1:500	Roche Applied Science, Germany
H3K9me3 (rabbit polyclonal)	1:500	Actif Motif, Carlsbad, USA
HSP90 (mouse monoclonal)	1:500	Santa Cruz Biotechnology, CA, USA
MKL1 (rabbit polyclonal)	1:500	*(Cen et al, 2003)*
MKL2 (rabbit polyclonal)	1:500	*(Cen et al, 2003)*
MRTF-A (C-19) (goat polyconal)	1:100	Santa Cruz Biotechnology, CA, USA
Myoferlin (D-11) (mouse monoclonal)	1:500	Santa Cruz Biotechnology, CA, USA
$p16^{Ink4a}$ (mouse monoclonal)	1:500	MTM Laboratories, Heidelberg, Germany
p53 Clone DO1 (mouse monoclonal)	1:1000	Actif Motif, Carlsbad, USA
Phospho EGF receptor (Tyr1173) (rabbit monoclonal)	1:1000	Cell Signaling Technology, Danvers, USA)
Phospho MKL1 Serine 454 (rabbit, polyclonal)	1:500	*(Muehlich et al, 2008)*
Phospho p44/42 MAPK (ERK1/2) (Thr202/Tyr204) (rabbit polyclonal)	1:1000	Cell Signaling Technology, Danvers, USA
Phospho p53 Serine 15 (rabbit, polyclonal)	1:1000	Santa Cruz Biotechnology, CA, USA
Ras (rabbit polyclonal)	1:500	NewEast Bioscience, Malvern, USA
Retinoblastoma protein Clone EP44 (rabbit polyclonal)	1:1000	Epitomics, Burlingame, USA
RhoA (rabbit polyclonal)	1:500	NewEast Bioscience, Malvern, USA
Smooth muscle actin (SMA) Clone 1A4 (mouse monoclonal)	1:500	Dako, Hamburg, Germany

4.2.2 Secondary antibodies

Secondary antibody	Target	Dilution	Provider
Alexa Fluor® 488	mouse	1:1000	Invitrogen, Karlsruhe
Alexa Fluor® 488	rabbit	1:1000	Invitrogen, Karlsruhe
Alexa Fluor® 555	goat	1:1000	Invitrogen, Karlsruhe
Anti-rabbit IgG HRP-conj	rabbit	1:10000	Cell Signaling Technology, USA
Anti-mouse IgG HRP-conj	mouse	1:10000	Cell Signaling Technology, USA
Anti-goat IgG HRP-conj	goat	1:50000	Santa Cruz Biotechnology, CA, USA

4.3 Nucleotides

4.3.1 Random Hexamers

Nucleotide	Sequence [5'-3']	Provider
Random Hexamers	NNN NNN	Metabion International AG, Martinsried, Germany

4.3.2 Real-time PCR primers

Target gene specific primers were designed with the software Universal Probe Library from Roche (https://www.roche-applied-science.com). Custom-synthesized primers were purchased by Metabion International AG, Martinsried, Germany. The real-time PCR primers were diluted to a concentration of 100 µM and stored at -20°C.

h=human; F=forward; R=reverse

Name	Sequence [5`- 3`]
h18S rRNA F	TCG AGG CCC TGT AAT TGG AAT
h18S rRNA R	CCC TCC AAT GGA TCC TCG TTA
hc-fos F	AAC CAC AGG GAA AGG AGA CC
hc-fos R	ATG GTG CCT GCG TGA TAC T
hCNN1 F	GCT GTC AGC CGA GGT TAA GA
hCNN1 R	CCC TCG ATC CAC TCT CTC AG
hCTGF F	TTG GCA GGC TGA TTT CTA GG
hCTGF R	GGT GCA AAC ATG TAA CTT TTG G
hCXCL10 F	GAA AGC AGT TAG CAA GGA AAG GT
hCXCL10 R	GAC ATA TAC TCC ATG TAG GGA AGT GA
hCyr61 F	AAG AAA CCC GGA TTT GTG AG
hCyr61 R	GCT GCA TTT CTT GCC CTT T
hDLC1 F	GCG AAT GAG TTC TGT CAT TTC A
hDLC1 R	GAG CAG TGT CAT GCC TTG G
hGLIPR1 F	TCT TTC CAA TGG AGC ACA TTT
hGLIPR1 R	TCT TAT ATG GCC AAG TTG GGT AA
hKi-67 F	TCA AGG AAC TGA TTC AGG AGA AG
hKi-67 R	GTG CAC TGA AGA ACA CAT TTC C
hMAP1B F	GAC GCT TTG TTG GAA GGA AA
hMAP1B R	CTG AGT CAT GAG TTG GGA TCA G
hMKL1 F	CCC AAT TTG CCT CCA CTT AG
hMKL1 R	CCT TGG CTC ACC AGT TCT TC
hMKL2 F	CTT ACC CCC TCT GAA CGA
hMKL2 R	CTC TCG TCC TCC TTT GTTGC
hMYH9 F	GGT TGG TGG TGA ACT CAG CTA
hMYH9 R	TGG AGG ACC AGA ACT GCA A
hMYOF F	CCA TTA CTG GCT TCT AAG CTG AC
hMYOF R	TTC CCC TGA GGA AGC ATA AA
hSM22 F	GGC CAA GGC TCT ACT GTC TG
hSM22 R	CCC TTG TTG GCC ATG TCT
hSRF F	AGC ACA GAC CTC ACG CAG A
hSRF R	GTT GTG GGC ACG GAT GAC
hTGFß1 F	ACT ACT ACG CCA AGG AGG TCA C
hTGFß1 R	TGC TTG AAC TTG TCA TAG ATT TCG
hTNFSF10 F	CCT CAG AGA GTA GCA GCT CAC A
hTNFSF10 R	CAG AGC CTT TTC ATT CTT GGA
hVGLL3 F	TCC CAG TAT CTG CCC AAC C
hVGLL3 R	CTG CAT CTT GCT GAA TAC CG

4.4 Bacterial strains and media

Bacterial strain	Provider
E.coli DH5α	Takara BIO

LB agar
1 % sodium chloride
1 % bacto tryptone
0.5 % yeast extract
1.5 % bacto agar

LB liquid medium
1 % sodium chloride
0.5 % yeast extract
1 % bacto tryptone
adjustment to pH 7.5 with 10 N NaOH

4.5 Kits

Reagent	Provider
RhoA Activation Assay Kit	NewEast Biosciences, Malvern, USA
Ras Activation Assay Kit	NewEast Bioscience, Malvern, USA
G-LISA RhoA Activation Assay Biochem Kit	Cytoskeleton, Denver, CO
Ambion® WT Expression Kit	Affymetrix, CA, USA
GeneChip® WT Terminal Labeling and Control Kit	Affymetrix, CA, USA
GeneChip® Hybridzation, Wash and Stain Kit	Affymetrix, CA, USA
GenElute™ HP Plasmid Midiprep Kit	Sigma-Aldrich, Taufkirchen, Germany
Senescence ß-Galactosidase Staining Kit	Cell Signaling Technology, Danvers, USA

4.6 Reagents

Reagent	Provider
Horse serum	Sigma-Aldrich, Taufkirchen, Germany
Protease Inhibitor, Cocktail Set III, Animal Free	Calbiochem, Darmstadt, Germany
Spectra™ Multicolor Broad Range Protein Ladder	Fermentas, St. Leon-Rot, Germany
Rec-Protein G-Sepharose® 4B conjugate	Invitrogen, Karlsruhe, Germany
Roti®-Quant	Carl Roth, Karlsruhe, Germany
Roti®-Lumin 1; Roti®-Lumin 2	Carl Roth, Karlsruhe, Germany
Super Signal West Femto Trialkit (Enhancer peroxide solution)	Thermo Scientific, Schwerte, Germany
Trizol® LS Reagent	Invitrogen, Karlsruhe, Germany

4.7 DNA Chips

GeneChip® Human Gene 1.0 ST Array	Affymetrix, CA, USA

4.8 Enzymes

SuperScript II Reverse Transcriptase	Invitrogen, Karlsruhe, Germany
RNaseA	Fermentas, St. Leon-Rot, Germany
Trypsin-EDTA 0.05 %	Sigma-Aldrich, Taufkirchen, Germany

4.9 Athymic nude mice

CD-1® Nude Mouse	Crl:CD1-Foxn1^{nu}	Charles River Laboratories, Sulzfeld, Germany

4.10 Buffers and solutions

2.5 M $CaCl_2$ solution
87.6 g $CaCl_2$*$6H_2O$
ad 200 mL with distilled water, sterilfiltration

2 x HBS
8.0 g NaCl
0.2 g Na_2HPO_4*$7H_2O$
6.5 g HEPES
adjustment of pH to 7.0
ad 500 mL with distilled water

Kralewski cell lysis buffer
50 mM HEPES (pH 7.4)
150 mM NaCl
1 % Triton X-100
1 mM EDTA
10 % Glycerol

4 x Laemmli Sample Buffer (4xLSB)
1 M TRIS/HCl (pH 8.8)
0.01 % (w/v) Bromphenolblau
20 % (w/v) SDS
2 % (v/v) Glycerol
0.5 M ETDA
5 % (v/v) ß-mercaptoethanol

10 x PBS pH 7.4
140 mM NaCl
2.7 mM KCl
10 mM Na_2HPO_4
1.8 mM KH_2PO_4

10 x Gel running buffer (pH 8.3)
0.25 M TRIS
2 M Glycin
1 % (w/v) SDS
H_2O ad 1000 ml

10 x TBS
0.2 M TRIS
1.4 M NaCl
H_2O ad 5000 mL

10 x TBST
0.2 M TRIS
1.4 M NaCl
1 % Tween 20
H_2O ad 5000 mL

10 x Blotting buffer
0.25 M TRIS
2 M Glycine

1.5 M TRIS (pH 6.8)
121.1 g TRIS
adjustment of pH with 1 N HCl to 6.8
H_2O ad 1000 ml

1.5 M TRIS (pH 8.8)
121.1 g TRIS
adjustment of pH with 1 N HCl to 8.8
H_2O ad 1000 ml

FACS staining solution 1
10 mM Sodium chloride
3.8 mM Trisodium citrate
0.3 mL /L Nonidet P-40
0.5 % (v/v) Propidium iodide

FACS staining solution 2
70 mM Citric acid
0.25 M Saccharose
0.5 % (v/v) Propidium iodide

Enhanced Chemiluminescence solution (ECL) S1 and S2

S1 solution	
80 mL	H_2O
10 mL	1M TRIS/HCl pH 8.5
1 mL	250 mM 3-Aminophthalhydrazide
0.44 mL	90 mM p-Coumaric acid
ad 100 mL with H_2O	

S2 solution	
80 mL	H_2O
10 mL	1M TRIS/HCl pH 8.5
60 µL	30% H_2O_2
ad 100 mL with H_2O	

Both solution were stored at -20°C and thawed prior to use. Both solutions were mixed at a ratio of 1:1 to yield the ready-to-use assay solution.

1 % Toluidine staining solution
0.1 g toluidine blue dye
0.1 g Sodium tetraborate decahydrate
dissolved in 100 mL distilled water

4.11 Chemicals

Chemicals	Provider
2-Propanol	Carl Roth, Karlsruhe, Germany
4,6`Diamidino-2-phenylindole (DAPI)	Sigma Aldrich, Taufkirchen, Germany
Agarose	PEQLAB, Erlangen, Germany
Ammonium peroxodisulfate	Carl Roth, Karlsruhe, Germany
Ampicillin	Gibco® Invitrogen, Karlsruhe, Germany
Bovine serum albumin	Carl Roth, Karlsruhe, Germany
Bromphenol blue	Carl Roth, Karlsruhe, Germany
Calcium chloride	Carl Roth, Karlsruhe, Germany
Chloroform	VWR, Ismaning, Germany
Citric acid	Carl Roth, Karlsruhe, Germany
Desoxynucleosid triphosphates (dATP, dCTP, dGTP, dTTP)	Invitrogen, Karlsruhe, Germany
Dimethyl sulfoxide (DMSO)	Carl Roth, Karlsruhe, Germany
Dithiothreitol (DTT)	Carl Roth, Karlsruhe, Germany
DMF (N,N-Dimethylformamide)	Sigma Aldrich, Taufkirchen, Germany
ECM gel from Engelbert-Holm-Swarm mouse sarcoma	Sigma-Aldrich, Taufkirchen, Germany
Ethylenediaminetetraacetic acid	Carl Roth, Karlsruhe, Germany
Ethanol	Carl Roth, Karlsruhe, Germany
Glycine	Carl Roth, Karlsruhe, Germany
Glycerol	Carl Roth, Karlsruhe, Germany
HEPES	Carl Roth, Karlsruhe, Germany
Immersion Oil (TM) 518F	Zeiss, Oberkochen, Germany
Low fat milk powder	Vitalia, Bruckmühl, Germany
Methanol	Carl Roth, Karlsruhe, Germany
Mounting Fluoromount	Sigma Aldrich, Taufkirchen, Germany
Nonidet™ P-40	Sigma-Aldrich, Taufkirchen, Germany
Paraformaldehyd	Carl Roth, Karlsruhe, Germany
Phenylmethylsulfonylfluorid (PMSF)	Calbiochem, Darmstadt, Germany
Potassium dihydrogen phosphate	Carl Roth, Karlsruhe, Germany
Propidium iodide	Sigma-Aldrich, Taufkirchen, Germany
Protease Inhibitor, Cocktail Set III, Animal Free	Calbiochem, Darmstadt, Germany
Saccharose	Carl Roth, Karlsruhe, Germany
Sodium chloride	Carl Roth, Karlsruhe, Germany
Sodium dodecyl sulfate (SDS)	Carl Roth, Karlsruhe, Germany
Sodium hydrogen phosphate	Carl Roth, Karlsruhe, Germany
Sodium tetraborate decahydrate	Carl Roth, Karlsruhe, Germany
ß-Mercaptoethanol	Serva, Heidelberg, Germany
TEMED	Carl Roth, Karlsruhe, Germany
TRIS tris(hydroxymethyl)aminomethane	Carl Roth, Karlsruhe, Germany
Trisodium citrate	Carl Roth, Karlsruhe, Germany
Triton X-100	Carl Roth, Karlsruhe, Germany
Tryptone	Carl Roth, Karlsruhe, Germany
Toluidine blue dye	Carl Roth, Karlsruhe, Germany
Tween® 20	Carl Roth, Karlsruhe, Germany

4.12 Technical devices and other equipment

24-well Transwell® inserts 8 µM	Milllipore, Germany
BioPhotometer	Eppendorf, Hamburg, Germany
Blotting equipment Mini PROTEAN® Tetra Cell	BIORAD, Munich
Cell culture dishes	Sarstedt, Nümbrecht, Germany
Centrifuge 5424R	Eppendorf, Hamburg
Centrifuge 5804R	Eppendorf, Hamburg
Centrifuge Heraeus Biofuge Stratos	Thermo Scientific, Freiburg, Germany
Chemiluminescent imager Chemismart 5100	PEQLAB, Erlangen, Deutschland
Confocal microscope LSM 510	Zeiss, Jena, Germany
Cryo vials CryoPure 1.6 mL	Sarstedt, Nümbrecht, Germany
Eppendorf tubes	Eppendorf, Hamburg
Falcon tubes	Sarstedt, Germany
Flow cytometer BD FACS Calibur Flow Cytometer	BD Bioscience, New Jersey, USA
Incubator for Bacteria	Thermo Scientific, Germany
Incubator for Mammalian Cell Culture	Thermo Scientific, Germany
Laminar Flow HERACell 150i	Thermo Scientific, Germany
LightCycler® 480	Roche Applied Biosystems, Germany
Microscope Axiovert 135M	Zeiss, Göttingen
Neubauer cell counting chamber	Marienfeld, Lauda-Königshofen, Deutschland
PCR machine	Biometra GmbH, Göttingen
pH meter Lab850	Schott Instruments, SI Analytics, Mainz, Germany
Power supply PeqPower 300	PEQLAB, Erlangen, Germany
Precision balance	Acculab, Sartorius, Göttingen, Germany
PVDF-membrane	Millipore, Billerica, MA
SDS-PAGE equipment	BIORAD, Munich
Thermoblock	Eppendorf, Germany
UV-transparent cuvettes	Sarstedt, Nümbrecht, Germany
Water bath	Memmert, Schwabach, Germany
Whatman Paper 0.8 mm	Optilab, Munich, Germany

5 Methods

5.1 Cell culture methods

5.1.1 Culturing and maintenance of mammalian cell lines

Cells were cultured as monolayers in the appropriate medium, containing 10 % (v/v) heat-inactivated fetal calf serum and 5 % (v/v) penicillin/streptomycin. All mammalian cell lines were cultured in 60 cm^2 cell culture dishes and maintained at 37°C in a humidified atmosphere containing 5 % CO_2. Passaging of cells was performed twice per week. Culture medium was aspirated and the adherent cells were washed with 10 mL sterile phosphate buffered saline (PBS). The cells were detached with 2 mL prewarmed trypsin and carefully resuspended in 8 mL culture medium. An appropriate amount of cell the suspension (dilution typically ranging from 1:3 to 1:40) was added to a fresh cell culture dish containing 10 mL of medium.

For cryoconservation and long-term storage, cells were trypsinized and resuspended in fresh medium to inactivate the trypsin. Cells were pelleted by centrifugation at 1000 rpm for 5 minutes and resuspended in ice-cold freezing medium (fetal bovine serum with 10 % DMSO). Cell suspensions were aliquoted in 2 mL cryogenic vials and placed in an isopropanol cryofreezing container which allows freezing of the cells at a cooling rate of 1°C/min. Thereafter the vials were stored in liquid nitrogen.

5.1.2 Liposome-mediated transient transfection

Mammalian cells were plated 24 h prior to transfection. At about 60 to 70 % confluency, cells were transfected using Lipofectamine 2000 reagent according to the manufacturer's instructions. The transfection mix was prepared in OptiMEM and added to the cells for 6 hours. Thereafter, the medium was replaced by fresh medium and cells were incubated for at least 24 hours prior further treatment or cell analysis.

For liposome-mediated transfection of the human hepatocellular carcinoma cell line HepG2, the GenJet transfection reagent was used according to the manufacturer’s instructions. Therefore, 4.5 x 10^5 HepG2 cells were seeded onto 6-wells 24 hours prior transfection and thereafter transfected with DNA-plasmid diluted with the GenJet transfection reagent at a ratio of 1:3. 18 hours posttransfection, medium was replaced by fresh medium supplemented with serum and antibiotics and cells were incubated for at least 24 hours.

5.1.3 Transient silencing of target genes using siRNA

Knockdown of target genes by RNA interference (RNAi) results in a transient gene-specific reduction in gene expression. For RNA interference, cells were transfected with either 50 nM gene-specific small interfering RNA (siRNA) or 50 nM of negative control siRNA using

Lipofectamine RNAiMAX according to the manufacturer's instructions. Reverse transfection showed the highest transfection efficiency. This method worked as follows: 5 µL Lipofectamine RNAiMAX were directly incubated with the appropriate amount of siRNA in 500 µL OptiMEM for 20 minutes at room temperature in a 6-well dish. Meanwhile cells were detached, pooled and resuspended in OptiMEM and 4.5 x 10^5 HepG2 or 2.5 x 10^5 HuH7 cells in 1.5 mL OptiMEM were added to the prepared reaction mix. Cells were incubated at 37°C and 5 % CO_2 overnight and on the next day medium was replaced by 2 mL fresh medium supplemented with serum and antibiotics. Depending on the gene of interest, either at 48 or 96 hours posttransfection, knockdown efficiencies were assessed by quantitative real-time PCR and immunoblotting.

5.1.4 Calcium-phosphate transfection method

Cells were transiently transfected by the calcium DNA-precipitation method. Therefore 1 x 10^6 HEK293T or amphotrophic Phoenix cells were seeded onto 6-well plates the day before transfection. 2 hours prior to transfection, medium was replaced by 2 mL fresh medium supplemented with 10 % serum but without antibiotics. The following table illustrates the required volumes for a single transfection experiment in a 3.5 cm dish.

Solution A	Amount
Plasmid DNA	2 to 4 µg
2 M $CaCl_2$	3.5 µL
dd H_2O	ad 62.5 µL

Solution B	Amount
2 x HBS buffer	62.5 µL

Table 1: Required volumes for a single transfection experiment in a 3.5 cm dish.

The DNA-$CaPO_4$ cocktail was added drop by drop while vortexing in HBS. Thereafter the transfection mix was incubated at room temperature for 5 minutes and subsequently added dropwise to the cells. 16 hours after transfection the medium was replaced by 2 mL fresh medium, supplemented with 10 % serum and antibiotics.

5.1.5 Establishment of stables cell lines via lentiviral transduction

Cell lines with a stable, gene-specific knockdown were generated by lentiviral transduction. Lentiviral particles were produced by transient cotransfection of HEK293T cells with the plasmids VSVG (0.25 µg), pD8.9 (0.75 µg) and shRNA (1.0 µg) by the calcium phosphate DNA precipitation method. The medium was replaced by 2 mL fresh medium supplemented with 10 % serum and antibiotics one day after transfection. Overnight conditioned medium was pooled and filtered through a 0.45 µm sterile filter and supplemented with 4 µg/mL polybrene. 4 mL of the lentiviral supernatant were directly added to the target cells which had been plated the day before in 6 cm dishes. After 3 hours incubation, 4 mL fresh medium and after additional 5 hours incubation 8 mL fresh medium were directly added to the target cells. One day after

transduction, infected cells were detached, resuspended in fresh medium and transferred in 1:5 dilutions to new 10 cm cell culture dishes containing 10 mL of medium. The selection antibiotic puromyin was added to the medium and cells expressing the shRNA vectors were selected with puromycin for 7 days. Concentration of puromycin was dependent on the cell type. Cells were analyzed for gene-specific knockdown by immunoblotting and quantitative real-time PCR one week after lentiviral transduction.

5.1.6 Retroviral transduction

Expression of the constitutively active H-RasV12 allele in HuH7 and HuH6 cells was done by retroviral transduction. Generation of retroviral particles was performed by transient transfection of the amphotrophic Phoenix packaging cells, a specific producer cell line for the generation of helper-free amphotropic retroviruses, with the pBabe-puro H-RasV12 plasmid (2 µg) or the pBabe-puro control vector using the calcium phosphate DNA precipitation method. One day after transfection, medium was replaced by 2 mL fresh medium with 10 % serum. Overnight conditioned medium was sterile-filtered through a 0.45 µm filter and 4 mL of the retroviral supernatant were pipetted on the target cells which had been plated in 6 cm dishes before. 24 hours after infection, medium was replaced by fresh medium. 5 days after post-transduction, cells were processed for immunoblot analysis.

5.1.7 Serum starvation

Cells were serum-starved by washing twice with PBS followed by incubation in culture medium supplemented with 0.2 % serum for 16 hours overnight.

5.1.8 Serum stimulation

After serum starvation, cells were stimulated with 20 % fetal bovine serum for the indicated time intervals. The serum was directly added to the growth medium used for starvation.

5.1.9 Drug treatment

Stock solutions of drugs were diluted to the required working concentration with medium. For drug treatment, seeded or transfected cells were washed with medium and exposed to the drug at 37°C and 5 % CO_2 atmosphere.

5.1.10 Cell harvest and lysis

During harvest and lysis, the cells were kept on ice to avoid degradation of proteins. The cell culture medium was aspirated and monolayers of cells were washed twice with cold PBS. A selected volume of lysis buffer supplemented with protease inhibitor cocktail 1:100, phenylmethanesulfonylfluoride (PMSF) 1:500 and dithiothreitol (DTT) 1:250 was added to the cells which were scrapped off and transferred to an Eppendorf tube. The samples were incubated on ice for 10 minutes and pelleted by centrifugation at 12,700 rpm for 10 minutes at 4°C. The supernatant containing the extracted proteins was transferred into a new Eppendorf

tube, supplemented with 4 x Laemmli buffer and boiled at 95°C for 10 minutes. The protein lysates were stored at -20°C or directly used for immunoblot analysis. If applicable, total protein concentration was measured prior to addition of Laemmli buffer using the Bradford method.

5.2 Protein biochemistry

5.2.1 Measurement of total protein content

For determination of total protein concentration in cell lysates prior to immunoblot analysis, Roti®-Quant Bradford reagent was used according to the manufacturer's instructions. 2 µL lysis buffer served as blank and 2 µL of each sample were diluted with 1000 µL Roti®- Quant Bradford Reagent (Coomassie Brilliant Blue G-250 was diluted 1:5 with H_2O) and incubated at room temperature for 5 minutes. The protein concentration was analyzed by measuring the absorbance at 595 nm with the BioPhotometer. Typically, 10 to 40 µg of total protein were subjected to immunoblot analysis.

5.2.2 RhoA Activation Assay

Active, GTP-bound RhoA levels were determined using the RhoA Activation Assay kit based on immunoprecipitation of the GTP-bound form of RhoA. Cells were plated the day before in 10 cm dishes to reach about 80 % to 90 % confluency. For activation of RhoA, cells were serum-starved for 16 hours overnight and stimulated with 10 µM lysophosphatidic acid (LPA) for exactly 2 minutes. Subsequently, cells were washed twice with ice-cold PBS and lysed in 500 µL lysis buffer (50 mM TRIS-HCl pH 8, 150 mM NaCl, 1 % TritonX-100 and 10 % glycerol). After incubation for 45 minutes on ice, lysates were cleared by centrifugation at 12,000 rpm for 10 minutes at 4°C. For determination of total cellular RhoA levels, 20 µL were taken from the supernatant and mixed with 4 x Laemmli sample buffer. The remaining supernatant was incubated with 1 µL of the anti-active RhoA monoclonal mouse antibody by rotating head-over-end overnight at 4°C. For the negative beads-only control, the supernatant was incubated without the antibody. For immunoprecipitation, 50 µL ProteinG-Sepharose beads were mixed with 50 µL washing buffer (50 mM TRIS-HCl, 150 mM NaCl, 10 mM $MgCl_2$, 1 mM EDTA, 1 % TritonX-100) and added to the probe. All probes were incubated by slowly rotating head-over-end at 4°C for at least 3 hours. For washing, the beads were settled by centrifugation at 12,700 rpm for 30 seconds and washed four times with 500 µL washing buffer. All washing steps were carried out on ice. Finally the supernatant was discarded and the beads were incubated with 15 µL 4 x Laemmli buffer and heated at 95°C for 3 minutes to dissolve the proteins from the beads. For the subsequent immunoblot analysis, the beads were sedimented and the supernatant was subjected together with the lysates for total cellular RhoA levels to immunoblot analysis using the anti-RhoA rabbit polyclonal antibody.

5.2.3 Ras Activation Assay

The GTP bound form of Ras was determined by using the Ras Activation Assay kit according to the manufacturer's protocol. HuH7 cells were plated the day before in 10 cm dishes to reach about 80 % confluency. On the next day, cells were washed twice with ice-cold PBS, lysed in 500 µL lysis buffer (50 mM TRIS-HCl, pH 8, 150 mM NaCl, 10 mM $MgCl_2$, 1 mM EDTA, 1 % TritonX-100) and incubated on ice for 10 minutes. Subsequently lysates were cleared by centrifugation at 12,000 rpm for 10 minutes at 4°C. For determination of total cellular Ras levels, 20 µL were taken from the supernatant and mixed with 4 x Laemmli buffer. The remaining supernatant was incubated with 1 µL of the anti-active Ras monoclonal mouse antibody by rotating head-over-end for 60 minutes at 4°C. Thereafter 20 µL of protein A/G agarose beads were added and incubated by rotating head-over-end for additional 60 minutes at 4°C. For washing, the beads were centrifuged at 12,700 rpm for 30 seconds and washed four times with cold lysis buffer. All washing steps were carried out on ice. Finally, the supernatant was discarded and the beads were incubated with 15 µL 4 x Laemmli buffer and heated at 95°C for 3 minutes to dissolve the proteins from the beads. For the subsequent immunoblot analysis, the beads were sedimented and the supernatant was subjected together with the lysates for total cellular Ras levels to immunoblot analysis using the anti-Ras rabbit polyclonal antibody.

5.2.4 Sodium dodecyl sulfate polyacrylamide gel electrophoresis (SDS-PAGE)

The SDS-PAGE method was used to separate proteins according to their molecular weight (Laemmli, 1970). Table 2 below illustrates the required volumes for a single 1.5 mm polyacrylamide gel.

Separating gel	**5 %**	**10 %**	**12 %**	**15 %**
H_2O [mL]	4.25	1.99	2.4	1.65
30 % polyacrylamide [mL]	1.25	1.67	3	3.75
1.5 M TRIS (pH 8.8) [mL]	1.875	1.25	1.95	1.95
10 % SDS [µL]	75	50	75	75
10 % APS [µL]	100	50	75	75
TEMED [µL]	6	2	3	3

Stacking gel	
H_2O [mL]	2.7
30 % polyacrylamide [mL]	0.67
1.5 M TRIS (pH 6.8) [mL]	1
10 % SDS [µL]	40
10 % APS [µL]	40
TEMED [µL]	4

Table 2: Composition of a 1.5 mm polyacrylamide gel.

Water, acrylamide and the corresponding TRIS buffer were pre-mixed. To start the polymerization reaction, APS and TEMED were added. The polymerized gel was clamped in the gel electrophoresis apparatus (BioRad) and then filled with gel running buffer. The gel was loaded with the protein lysate probes dissolved in Laemmli buffer. As molecular weight marker, the Spectra Multicolor Broad Range protein standard was used. The gel electrophoresis ran at a constant current of 100 V.

5.2.5 Immunoblotting

After gel electrophoresis, proteins were transferred from the SDS-gel onto an activated polyvinylidene fluoride (PVDF) membrane using the minigel system (BIORAD) (Towbin et al, 1979). Using the wet blotting method, the proteins were blotted at a constant current of 350 mA for 75 minutes. Membranes were blocked directly in 5 % nonfat dry milk in TBS containing 0.1 % Tween-20 (TBS-T) for 1 hour at room temperature and then probed with the primary antibody in TBS-T with 5 % milk or 5 % BSA overnight at 4°C with gentle agitation. Next day, membrane was washed three times with TBS-T for 15 minutes and thereafter probed with the horseradish peroxidase-conjugated secondary antibody in TBS-T for 1 hour at room temperature. Final washing was done three times for 5 minutes with TBS-T. Protein bands were visualized via the enhanced chemiluminescence detection method at a luminescent imager.

5.2.6 RhoA GLISA Assay

RhoA activity was quantitatively measured using the RhoA G-LISA Activation assay Biochem kit according to the manufacturer's instructions. Therefore, cells were plated in 10 cm dishes and grown to a confluency of about 70 %. For RhoA activation, cells were serum-starved for 16 hours overnight and stimulated with 10 µM lysophosphatidic acid (LPA) for exactly 2 minutes. Subsequently cells were washed twice with ice cold PBS and lysed in 250 µL cold lysis buffer. Lysates were immediately cleared by centrifugation at 10,000 rpm for 2 minutes at 4°C. 20 µL lysate were saved for protein quantification and the remaining lysate was snap frozen with liquid nitrogen. Thawed probes were equalized to a total cellular protein

concentration of 1.5 mg/mL with cold lysis buffer. Thereafter, the 96-well plate coated with a GTP-binding domain of RhoA where specifically the active GTP-bound form of RhoA can bind was incubated with the probes for 30 minutes at 4°C while shaking at 400 rpm. After several washing steps for removal of inactive GDP-bound RhoA, detection of the bound active RhoA was done by incubation with a specific primary RhoA antibody followed by the incubation with a secondary-HRP conjugated antibody. Absorbance was measured at λ=490 nm using an ELISA reader.

5.2.7 Indirect immunofluorescence

Cells were grown on glass coverslips placed in cell culture dishes. Prior to fixation, cells were washed with PBS. Cells were fixed in 4 % aqueous formaldehyde solution for 10 minutes at room temperature and permeabilized with 0.2 % Triton X-100 in PBS for 7 minutes. Blocking of unspecific binding sites was performed by incubation in 1 % bovine serum albumin in PBS for 60 minutes at room temperature. Afterwards the cells were incubated with the primary antibody (dilution dependent on antibody, range 1:100 to 1:500 in PBS) for at least 1 hour at room temperature. Thereafter cells were washed two times each with PBS, PBS-T and PBS and incubated with fluorescently labelled ALEXA conjugated secondary antibodies (1:1000 in PBS) for 1 hour at room temperature. In the final washing step, cells were washed two times each with PBS, PBS-T and PBS. Finally, cells were embedded in the mounting medium (Fluoromount®), supplemented with 1 µg/mL 4`6-diamidion-2-phenylindole (DAPI) to visualize nuclei. Images were obtained on a Zeiss LSM 510 microscope.

5.3 Cell proliferation assay

10^5 mammalian cells were seeded in 6 wells. In 24 hours intervals, cells were washed with 2 mL PBS, detached with 500 µL trypsin and resuspended in 500 µL medium. The cell number was counted using the hematocytometer method.

5.4 Flow cytometry analysis

Cells were harvested, washed with PBS and resuspended in 1 mL staining solution I supplemented with propidium iodide. To avoid unspecific binding of propidium iodide to RNA, cells were treated with 5 µL RNaseA (10 mg/mL). After 60 minutes incubation at room temperature, 1 mL of the second staining solution supplemented with propidium iodide was added. After further 30 minutes incubation, stained cells were analyzed by flow cytometry.

5.5 Senescence-associated ß-galactosidase activity assay

Cellular senescence was determined by using the senescence ß-galactosidase staining kit according to the manufacturer's protocol. In 0.5 % glutaraldehyde-fixed cells were stained with a freshly prepared senescence-associated ß-galactosidase staining solution containing 1

mg/mL of 5-bromo-4-chloro-3-indolyl-ß-galactopyranoside and incubated at 37°C overnight. By counting the number of blue colored cells and the total cells per field (0.5 x 0.5 cm^2) using a Zeiss inverted microscope, the percentage of the SA-ß-gal positive cells was calculated. More than 1000 cells were counted from four fields of vision.

5.6 Invasion assay

The invasive capacity of tumor cells was measured using 6.5 mm diameter tissue culture-treated polycarbonate membranes with 8 µm pores. Membranes were coated with 100 µL ECM gel, diluted 1:2 in cold DMEM medium according to the manufacturer's instructions. 4 x 10^4 HuH7 cells in 200 µL medium supplemented with 1 % serum were placed in the upper chamber of the Transwell® insert whereas the lower chamber was filled with 600 µL medium containing 10 % serum as a chemoattractant. HuH7 cells were allowed to invade for 24 hours at 37°C. Invaded cells were visualized by toluidine staining. Non-invading cells were removed from the top of the ECM gel with a cotton swap. For fixation of invaded cells, inserts were incubated in 100 % methanol for 2 minutes and subsequently stained in 1 % toluidine blue solution for 2 minutes. Excess dye was removed by washing the inserts in distilled water. The inserts were allowed to air dry. Cells were quantified by counting the cell number of invaded, purple-colored cells using a Zeiss inverted microscope.

5.7 Nucleic acid biochemistry

5.7.1 RNA preparation

For RNA preparation, cells were washed twice with PBS and 1 mL TRIzol® reagent per 6 cm dish was directly added to the cells. Cells were scrapped off and transferred into an Eppendorf tube and incubated for 5 minutes at room temperature. Thereafter 0.2 mL chloroform per 1 mL TRIzol® Reagent was added and the tube was shaken vigorously for 15 seconds, followed by an incubation for 3 minutes at room temperature. For phase separation, the sample was centrifuged at 12,700 rpm for 15 minutes at 4°C. The aqueous phase, containing the RNA was removed and placed in a new tube.

For precipitation of the RNA, 0.5 mL isopropanol was added to the aqueous phase followed by incubation at room temperature for 10 minutes. To collect the RNA precipitate, the sample was centrifuged at 12,000 rpm for 10 minutes at 4°C and the supernatant was carefully removed. The RNA pellet was washed with 1 mL 75 % ethanol and then centrifuged at 12,000 rpm for 10 minutes at 4°C. The supernatant was discarded and the RNA was allowed to air dry. The RNA was resuspended in nuclease-free water and completely dissolved by incubation at 55°C for 10 minutes. RNA concentration and purity were determined by photometric measurement of the absorbance at 260 nm and 280 nm, respectively. A ratio of about 2.0 was accepted as pure RNA.

5.7.2 cDNA synthesis

1 µg of total RNA was primed with 1 µL of Random Hexamers (50 µM) in reaction volume of 5 µL and heated in a thermo cycler at 70°C for 5 minutes to denaturate the template followed by incubation at 4°C for 5 minutes. To this mixture, 4 µL 5 x Frist Strand buffer, 2 µL DTT, 1 µL dNTPs (10 µM), 1 µL Superscript Reverse Transcriptase II and 7 µL H_2O were added to a final volume of 20 µL. The mixture was kept in a thermocycler at 25°C for 5 minutes and then at 42°C for 60 minutes. Thereafter the reverse transcriptase was inactivated by heating to 70°C for 15 minutes and the reaction was stopped by placing the tube on ice. The prepared cDNA was stored at -20°C or directly used for qPCR.

5.7.3 Real-time PCR

Each quantitative PCR (final reaction volume 20 µl) included 6 µL cDNA (1:10 diluted with H_2O, for 18S rRNA diluted 1:100), 10 µL LightCycler®480 SyBr Green Master I Mix, 2 µL nuclease-free H_2O and 1 µL of forward and reverse primer (10 µM). Quantification was performed with the LightCycler 480 Real-Time PCR system using the program listed below.

Step	Temperature profile	Time	Function	
1	95°C	5 min	preincubation	
2	95°C	10 sec	amplification	
	55°C	10 sec	amplification	↓ 50 cycles
	72°C	10 sec	elongation	
3	95°C	10 sec	melting curve	
	60°C	1 min	melting curve	
	95°C	10 sec	melting curve	
4	40°C	30 sec	cooling	

Table 3: Times and temperatures for a quantitative real-time PCR reaction.

The mid-linear range was used to establish the threshold of each oligonucleotide set. Gene expression was normalized with respect to the endogenous housekeeping gene 18S rRNA, which was determined not to significantly change under different conditions. Relative expression of each gene was calculated using the $\Delta\Delta C_T$ method.

5.7.4 Microarray analysis

For DNA GeneChip Array analysis, total cellular RNA from HuH7 cells stably expressing control shRNA or MKL1/2 shRNA was isolated using RNaesy Mini Kit according to the manufacturer's instructions. Sensestrand cDNA from total cellular RNA was synthesized using the Ambion WT Expression Kit according to the manufacturer's protocol which allows to prime specifically non-ribosomal RNA. Subsequently, the sense-strand cDNA was fragmented and

biotin-labeled using the Affymetrix GeneChip® WT Terminal Labeling Kit according to the manufacturer's protocol. Hybridization was performed with fragmented cRNA on the Human Gene 1.0 ST array at 45°C for 17 hours. Washing and staining by streptavidin-phycoerythrin was performed on a microfluide workstation (Affymetrix) and arrays were scanned by a laser scanner (Affymetrix). Gene expression analysis was done by using the Partek Microarray Analysis software.

5.7.5 Transformation into chemically competent *E.coli* DH5alpha bacteria cells

Aliquots of competent *E.coli* DH5alpha bacterial cells, prepared in our lab, were stored at –80°C. For each transformation, one aliquot was thawed for 15 minutes. DNA was carefully added to the bacterial cells and incubated on ice for 30 minutes. Subsequently, DNA uptake was carried out at 42°C for exactly 90 seconds and cells were chilled on ice for 2 minutes. 900 µL prewarmed LB medium (without antibiotics) were added and the suspension was shaken at 150 rpm at 37°C for one hour. 150 µL of the bacterial suspension were plated on prewarmed agar plates containing the selection antibiotic and incubated overnight at 37°C. Until further processing, the agar plate was sealed with Parafilm and stored at 4°C.

5.7.6 Midi scale plasmid preparation

A single bacterial clone was picked up with a sterile pipette tip and transferred in 50 mL LB medium containing the selection antibiotic and thereafter incubated for 16 hours overnight while shaking at 300 rpm at 37°C. Next day, bacterial cells were centrifuged at 3500 rpm for 10 minutes at 4°C and the supernatant was discarded. DNA was extracted using the GenElute HP Plasmid Midiprep Kit. Thereafter DNA concentration and purity were determined by photometric measurement of the absorbance at 260 or 280 nm, respectively.

5.8 Subcutaneous tumor xenograft mouse model

Effects of RNAi mediated knockdown of MKL1 and MKL2 on HuH7 tumor xenograft growth *in vivo* were determined by systemic injection of siRNA complexed with polyethylenimine as described previously (Hobel et al, 2010). Athymic nude mice were held under pathogen-free conditions with ad-libitum access to food and water. Experiments were approved by the government of Upper Bavaria and performed according to legal terms for animal experiments of the local administration. 2 x 10^6 HuH7 cells were injected subcutaneously into both flanks of 6 week old female athymic nude mice (Crl:CD1-Foxn1nu). After 7 days, when solid tumors were established, mice were randomized into control and treatment groups with 6 animals per group. Mice were intraperitoneally injected three times per week with 15 µg nonspecific or specific siRNAs, each complexed with PEI F25-LMW. For the siRNA MKL1+2 treatment group, 7.5 µg siRNA MKL1 and 7.5 µg siRNA MKL2 were mixed and complexed with PEI L25-LMW. Untreated mice or mice treated with nonspecific siRNA served as negative control. Tumor

volume was measured three times per week and calculated according the formula length x width x width/2. Mice bearing subcutaneous tumors were sacrificed on day 22 after therapy start, tumors excised and shock-frozen in liquid nitrogen for subsequent RNA and protein preparation. For RNA isolation from tumor samples, in TRIzol® reagent shock-frozen xenografts were thawed at room temperature and homogenized with the TissueRuptor. Thereafter, 0.2 mL chloroform per 1 mL TRIzol® reagent was added to the probe and RNA was prepared according to chapter 5.7. For protein cell lysate preparation, HuH7 cells derived xenografts were homogenized with the TissueRuptor in ice-cold lysis buffer, supplemented with protease inhibitor, phenylmethanesulfonylfluoride and dithiotreitol. Subsequently, samples were shortly sonicated and incubated on ice for 10 minutes. Thereafter samples were centrifuged at 12,700 rpm for 10 minutes at 4°C. The supernatant containing the extracted proteins was transferred to an Eppendorf tube and stored at -20°C or prepared for immunoblot analysis as described in chapter 5.2.

5.9 Statistical analysis

Unless otherwise indicated, data were expressed as mean ± standard deviation (SD). Statistical analysis among two groups was carried out using the Student's unpaired t-test. P-values are *p≤0.05, **p≤0.01, ***p≤0.001.

5.10 Software and databases

GraphPad Prism® (GraphPad Software, La Jolla, CA, USA) was used for calculations and statistical analysis. Research publications were obtained from the online database NCBI PubMed (http://www.ncbi.mlm.nih.gov/pubmed) and managed with EndNote X7. DNA sequences were obtained from NCBI (http://www.ncbi.nlm.nih.gov/nuccore). Gene array data were managed using the Partek Microarray Analysis software. Blots and microscopic images were processed with ImageJ (Wayne Rasband, National Institute of Health, Bethesda, MD, USA) and Adobe Photoshop.

6 Results

6.1 Role of the transcriptional coactivators MKL1 and MKL2 in human hepatocellular and breast carcinoma cells

Preliminary studies of our group pointed out a direct correlation between the subcellular localization of MKL1 and the endogenous expression levels of the tumor suppressor DLC1. A prevalent nuclear localization of MKL1 was found in hepatocellular and breast carcinoma cells lacking endogenous DLC1 expression. Therefore in the first part of this work, we aimed to investigate the functional role of DLC1 expression on the subcellular localization and the transcriptional activity of MKL1 and MKL2.

6.1.1 Nuclear MKL2 localization in DLC1-deficient human cancer cell lines

We found a changed subcellular localization of MKL1 in different human hepatocellular and breast carcinoma cell lines with loss of endogenous DLC1 expression. Consequently, we addressed the subcellular localization of MKL2 in these cell lines. We analyzed the subcellular distribution of MKL2 by indirect immunofluorescence analysis in human hepatoma HepG2 cells, breast epithelial MCF7 cells, hepatocellular carcinoma HuH7 cells and breast carcinoma MDA-MB-468 cells.

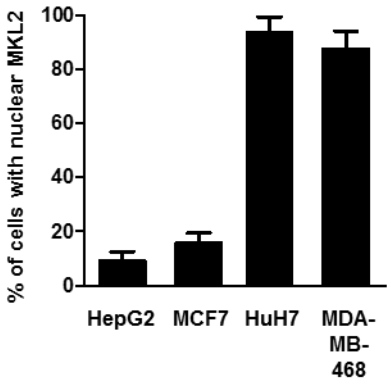

Figure 15: Nuclear localization of MKL2 in human hepatocellular and breast carcinoma cells with DLC1 loss.
HepG2, MCF7, HuH7 and MDA-MB-468 cells were fixed and immunostained by the anti-MKL2 antibody. In each cell line, the subcellular localization of MKL2 was scored as predominantly cytoplasmic, evenly distributed or predominantly nuclear. Represented is the percentage of cells with predominantly nuclear localized MKL2. Quantifications were based on at least three independent experiments where at least one hundred cells were analyzed. Values are represented as mean ± SD.

The results of the quantitative analysis of the subcellular distribution of MKL2 illustrated that HepG2 and MCF7 cells, both characterized by the expression of endogenous DLC1, showed a prevalent cytoplasmic localization of MKL2 (Figure 15). By contrast, 94 % of HuH7 cells and 87.6 % of MDA-MD-468 cells, both characterized by the lack of endogenous DLC1 expression, displayed a predominantly nuclear localization of MKL2 (Figure 15). Our data illustrated a correlation between the subcellular distribution of both, MKL1 and MKL2, and the endogenous expression levels of the tumor suppressor DLC1. These data indicate that human

hepatocellular and breast carcinoma cell lines with loss of endogenous DLC1 expression display a common nuclear localization of both MKL1 and MKL2.

6.1.2 Downregulation of DLC1 expression in murine hepatocytes induces the nuclear translocation of MKL2

As we reported a nuclear localization of MKL1 and MKL2 in DLC1-deficient cancer cells it raised the question if loss of DLC1 expression is able to trigger the nuclear translocation of MKL2. To address this question, we used established murine hepatocytes stably expressing shRNA targeting the tumor suppressor DLC1 (Xue et al, 2008). The subcellular localization of MKL2 was analyzed by indirect immunofluorescence analysis and downregulation of DLC1 expression was analyzed by immunoblotting.

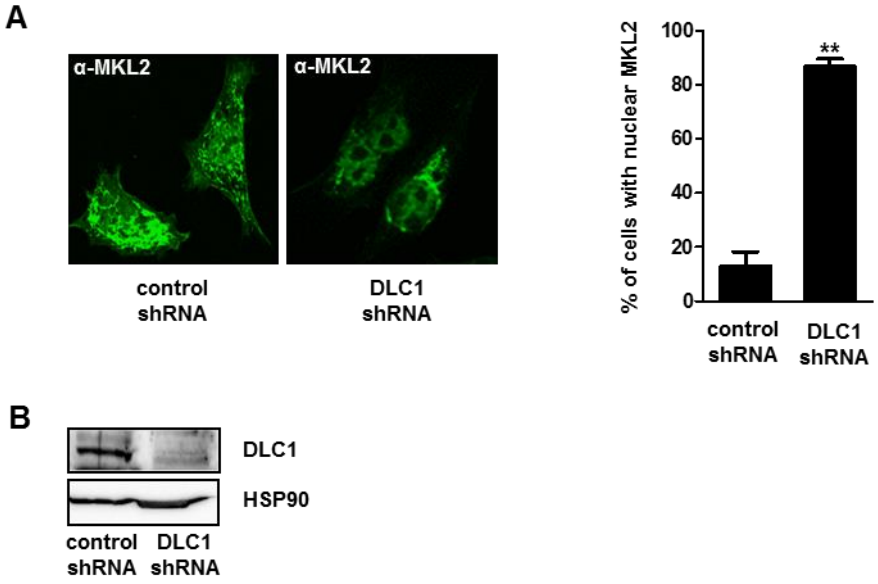

Figure 16: Downregulation of DLC1 expression triggers the nuclear translocation of MKL2.
(A) Murine hepatocytes stably expressing either control shRNA or DLC1 shRNA were immunostained by the anti-MKL2 antibody. Using indirect immunofluorescence analysis, the percentage of cells with predominantly nuclear MKL2 localization was determined. Representative images are shown. Quantifications were based on three independent experiments where at least one hundred cells were analyzed. Values are given as mean ± SD.
(B) Lysates of cells as described in (A) were prepared and equal amounts of total cellular protein were subjected to immunoblotting using anti-DLC1 antibody. Loading was controlled by re-probing the blot for HSP90.

Indirect immunofluorescence analysis illustrated that murine hepatocytes expressing control shRNA showed a clearly cytoplasmic MKL2 staining. By contrast, RNA interference mediated downregulation of DLC1 expression in murine hepatocytes induced nuclear translocation of MKL2 as shown by immunostaining (Figure 16a). These observations were confirmed by quantification of the number of hepatocytes with nuclear MKL2 staining. The results demonstrated that 88.5 % of murine hepatocytes expressing DLC1 shRNA revealed a predominantly nuclear MKL2 distribution in contrast to the murine hepatocytes expressing control shRNA where only 13 % of the analyzed cells exhibited a nuclear localization of MKL2 (Figure 16a). Downregulation of DLC1 expression on protein level was confirmed by

immunoblotting (Figure 16b). These data indicate that the endogenous expression levels of the tumor suppressor DLC1 have an influence on the subcellular distribution of MKL2. Additionally our observations in the murine hepatocytes with stable DLC1 knockdown are in agreement with the reported nuclear localization of MKL1 and MKL2 in human hepatocellular and breast carcinoma cells lacking endogenous DLC1 expression.

6.1.3 Reconstitution of DLC1 expression induces cytoplasmic relocalization of MKL1 and MKL2

Next we investigated if the reconstitution of DLC1 expression in the DLC1-deficient hepatocellular carcinoma cells HuH7 is able to induce a relocalization of MKL1 and MKL2 from the nucleus back to the cytoplasm. HuH7 cells were transiently transfected with human wildtype Flag-tagged DLC1 or with the corresponding control expression vector. The subcellular localization of MKL1 and MKL2 was determined by indirect immunofluorescence analysis.

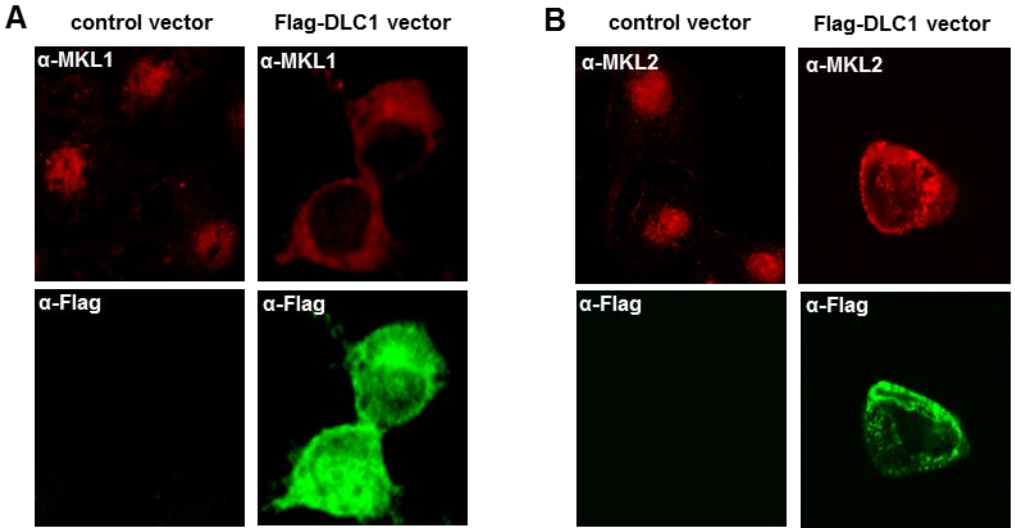

Figure 17: Reconstitution of DLC1 expression induces the relocalization of MKL1 and MKL2 from the nucleus back to the cytoplasm.
HuH7 cells were transiently transfected with human wildtype Flag-tagged DLC1 or with the corresponding control expression vector. 24 hours after transfection, cells were immunostained with (A) anti-MKL1, (B) anti-MKL2 and anti-Flag antibodies. Shown are representative images for the subcellular localization of (A) MKL1 and (B) MKL2.

Indirect immunofluorescence analysis illustrated that HuH7 cells expressing Flag-tagged DLC1 revealed a cytoplasmic redistribution of both MKL1 and MKL2 opposed to HuH7 control cells depicting the nuclear localization of MKL1 and MKL2 (Figure 17a and b). These observations indicated that the restoration of DLC1 expression in HuH7 cells was able to induce the cytoplasmic redistribution of MKL1 and MKL2. These findings led to the assumption that expression of the tumor suppressor DLC1 played a critical role in the regulation of the subcellular localization of the transcriptional coactivators MKL1 and MKL2.

6.1.4 DLC1-deficiency increases RhoA activity in human cancer cells

It is well established that the subcellular localization of MKL1/2 is regulated by the Rho/actin signaling pathway (Miralles et al, 2003). As DLC1 encodes a RhoGAP protein, we were interested if the DLC1 expression levels affected the RhoA activation state of hepatocellular and breast carcinoma cells, thereby influencing the subcellular distribution of MKL1/2. We compared the active GTP-bound RhoA levels between DLC1-expressing MCF7 cells versus DLC1-deficient MDA-MB-468 cells by immunoprecipitation using an antibody that specifically recognized the active GTP-bound form of RhoA. Simultaneously, the active GTP-bound RhoA levels were quantified by a RhoA G-LISA assay.

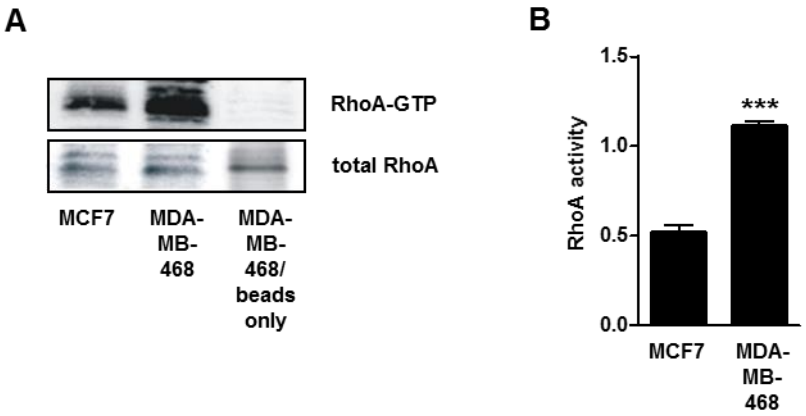

Figure 18: Increased active GTP-bound RhoA levels in DLC1-deficient MDA-MB-468 cells.
(A) MCF7 and MDA-MB-468 cells were immunoprecipitated with anti-active RhoA antibody and immunoblotted with anti-RhoA antibody. Equal amounts of lysates were directly immunoblotted with anti-RhoA antibody. For the beads only control, no antibody was added to the immunoprecipitation. (B) Active GTP-bound RhoA levels of MCF7 and MDA-MB-468 cells were quantitatively analyzed by an ELISA-assay. Absorbance was measured at 490 nm. Values are represented as mean ± SD of three independent experiments.

Immunoprecipitation illustrated that the amount of active GTP-bound RhoA was considerably increased in the DLC1-deficient MDA-MB-468 cells compared to the DLC1-expressing MCF7 cells (Figure 18a). By contrast, total cellular RhoA expression levels of both MCF7 and MDA-MB-468 cells were similar (Figure 18a). The results of quantitative measurement demonstrated that the level of active GTP-bound RhoA was elevated two-fold in MDA-MB-468 cells as compared to MCF7 cells (Figure 18b).

As we found that DLC1-deficiency augmented RhoA activity, we looked whether the absence of DLC1 expression was able to cause constitutive activation of RhoA. To test this, HepG2, HuH7, MCF7 and MDA-MB-468 cells were serum-starved and stimulated with lysophosphatidic acid (LPA) which activates RhoA via the $G_{alpha\ 12/13}$ pathway (Kranenburg et al, 1999). For the HepG2 and HuH7 cells, active RhoA levels were analyzed by immunoprecipitation using a specific antibody that binds to the GTP-bound form of RhoA. Active RhoA levels of MCF7 and MDA-MB-468 cells were measured by a RhoA G-LISA assay.

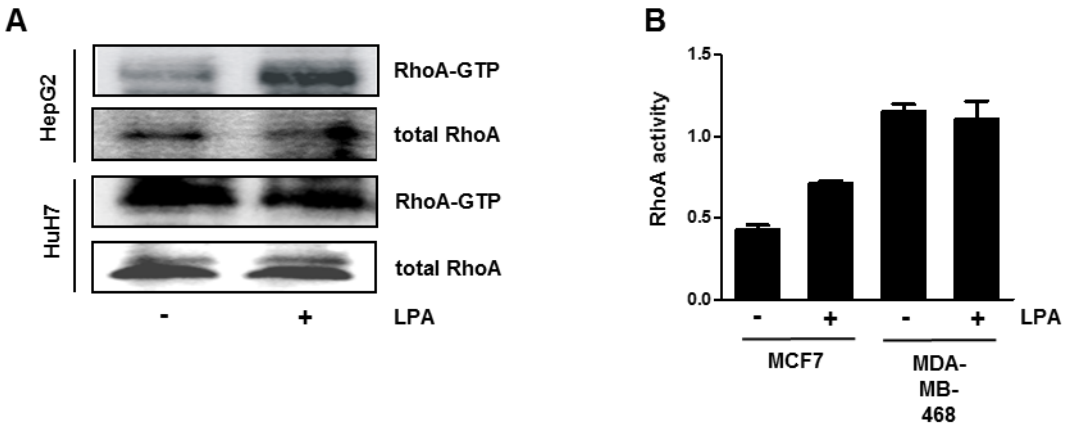

Figure 19: Constitutive activation of RhoA in hepatocellular and breast carcinoma cells with DLC1 deficiency.
(A) HepG2 and HuH7 cells were serum-starved for 16 hours, stimulated with 10 µM lysophosphatidic acid (LPA) for 2 minutes and subsequently lysed. Analysis of GTP-bound RhoA was done by immunoprecipitation with anti-active RhoA antibody and afterwards subjected to immunoblotting using total anti-RhoA antibody. Equal amounts of lysates were directly immunoblotted with anti-RhoA antibody. The blot is representative for three independent experiments. (B) MCF7 and MDA-MB-468 cells were serum-starved for 16 hours, stimulated with 10 µM lysophosphatidic acid (LPA) for 2 minutes and subsequently lysed. Active GTP-bound RhoA was quantitatively measured by an ELISA assay. Values are mean ± SD of two individual experiments.

The results from immunoprecipitation demonstrated that unstimulated, serum-starved HuH7 cells contained higher basal GTP-bound RhoA levels than HepG2 cells. The amount of active RhoA in HepG2 cells was strongly increased upon stimulation with LPA. In contrast, no further RhoA activation upon LPA stimulation was detectable in HuH7 cells concluding that RhoA was constitutively activated (Figure 19a). However, total cellular expression levels of RhoA were not affected by LPA treatment. The same effects were observed by quantitative analysis of the active RhoA levels in MCF7 and MDA-MB-468 cells. LPA stimulation of MCF7 cells increased the amount of GTP-bound RhoA whereas the RhoA activation status in MDA-MB-468 cells remained unchanged (Figure 19b). Our data illustrate that the lack of endogenous DLC1 expression in hepatocellular and breast carcinoma cells leads to the constitutive activation of RhoA.

6.1.5 Analysis of the actin cytoskeleton of DLC1-deficient cancer cells

Increased RhoA signaling causes the polymerization of F-actin and the formation of stress fibers (Ridley & Hall, 1992). Thus, we were interested if cytoskeletal alterations in the DLC1-deficient cancer cells could account for the nuclear localization of MKL1/2. The actin cytoskeleton of HepG2, HuH7, MCF7 and MDA-MB-468 cells was visualized by F-actin staining, using phalloidin, a bicyclic peptide which belongs to the family of toxins isolated from *Amanita phalloides* and specifically binds to F-actin (Dancker et al, 1975).

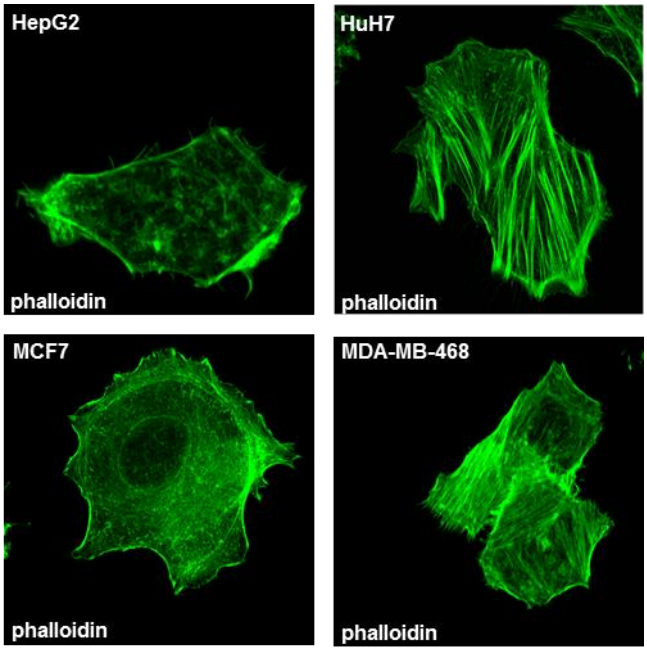

Figure 20: Increased F-actin formation in DLC1-deficient cancer cells.
The actin cytoskeleton of HepG2, HuH7, MCF7 and MDA-MB-468 cells was visualized by F-actin staining using ALEXA Fluor 488 phalloidin. Cells were analyzed by indirect immunofluorescence analysis and representative images are shown.

Immunofluorescence analysis illustrated hardly any F-actin staining in the endogenous DLC1-expressing HepG2 and MCF7 cells (Figure 20). By contrast, the DLC1-deficient HuH7 and MDA-MB-468 cells revealed a strong increase in the amount and intensity of F-actin staining (Figure 20). These data suggest an elevation of F-actin amount in DLC1-deficient cancer cells that contributes to the nuclear accumulation of MKL1/2.

6.1.6 Impaired nuclear export mechanism of MKL1 in DLC1-deficient cancer cells

Besides the importance of RhoA/actin signaling for the nuclear import of MKL1/2, it is established that nuclear export is the critical mechanism for the subcellular localization of MKL1 (Vartiainen et al, 2007). It was found that serum-inducible phosphorylation of MKL1 at serine 454 enhances G-actin binding and facilitates the nuclear export of MKL1 (Muehlich et al, 2008; Vartiainen et al, 2007). We investigated the nuclear export mechanism of MKL1 in DLC1-deficient cancer cells. At first, the phosphorylation status of MKL1 at serine 454 was determined in hepatocellular and breast carcinoma cell lines with different endogenous DLC1 expression levels.

As phosphorylation of MKL1 at serine 454 is serum-inducible (Muehlich et al, 2008), HepG2, HuH7, MCF7 and MDA-MB-468 cells were serum starved and stimulated with serum for 30 minutes. The phosphorylation status of MKL1 was analyzed by immunoblotting using an antibody that specifically recognizes MKL1 phosphorylated at serine 454.

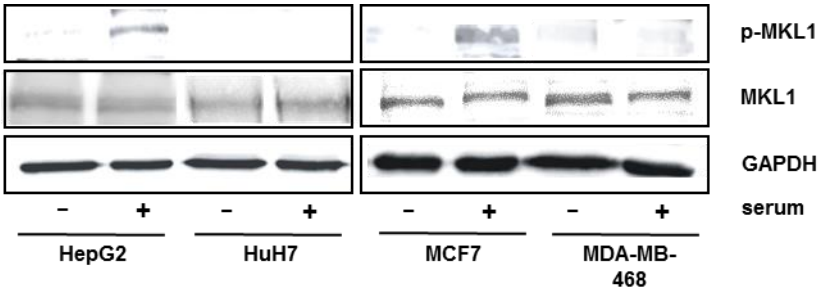

Figure 21: Impaired phosphorylation of MKL1 at serine 454 in DLC1-deficient cancer cells.
HepG2, HuH7, MCF7 and MDA-MB-468 cells were serum-starved for 16 hours overnight and afterwards stimulated with 20 % serum for 30 minutes. Equal amounts of total protein were analyzed by immunoblotting using the specific anti-phospho-MKL1 serine 454 and total anti-MKL1 antibody. Loading was controlled by re-probing the blot for GAPDH. The blots are representative for three individual experiments.

Unstimulated, serum-starved hepatocellular and breast carcinoma cells showed barely any phosphorylation level of MKL1 at serine 454. By contrast, upon serum stimulation, phosphorylation of MKL1 was strongly induced in the endogenous DLC1-expressing HepG2 and MCF-7 cells (Figure 21). On the contrary, in the DLC1-deficient HuH7 and MDA-MB-468 cells no serum-inducible phosphorylation of MKL1 was detectable. All probed cell lines showed similar expression levels of endogenous total MKL1 that were not affected by serum stimulation (Figure 21). Remarkably, serum-inducible phosphorylation of MKL1 at serine 454 occurred exclusively in hepatocellular and breast carcinoma cells expressing endogenous DLC1 whereas it was completely absent in the DLC1-deficient cancer cells.

Extracellular signal-regulated kinase 1/2 (ERK1/2) was identified as the serum-inducible kinase mediating the phosphorylation of MKL1 at serine 454 (Muehlich et al, 2008). Consequently, it raised the question if the lack of MKL1 phosphorylation in the DLC1-deficient cancer cells reflects the absence of activated ERK1/2.

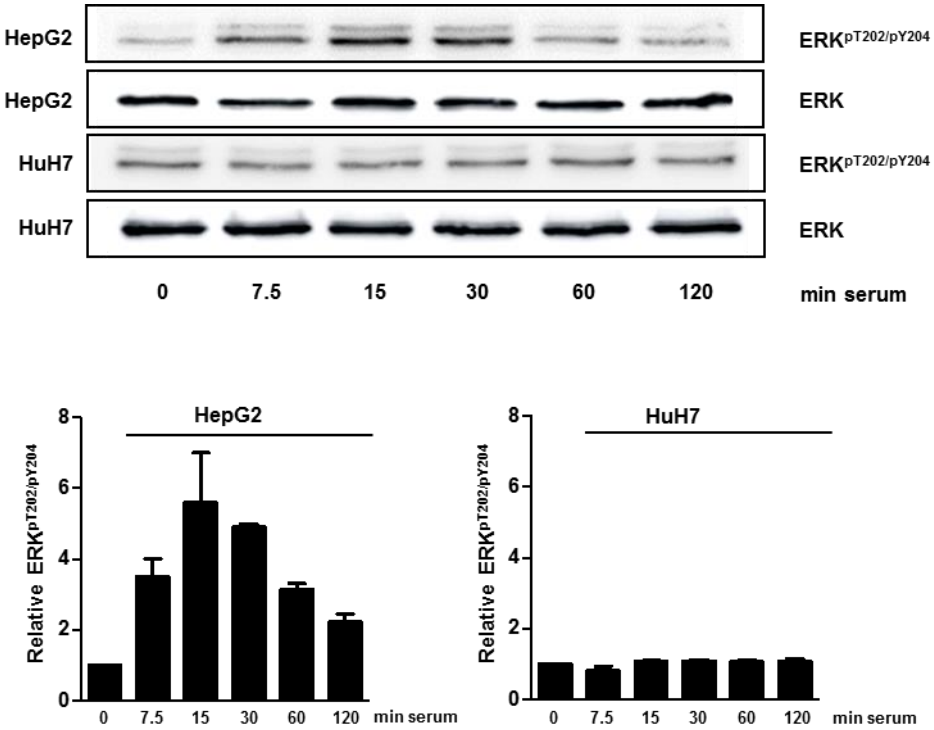

Figure 22: Inhibition of serum-inducible ERK1/2 kinase activation in DLC1-deficient cancer cells.
HepG2 and HuH7 cells were serum-starved for 16 hours and subsequently stimulated with 20 % serum for the indicated time points. Equal amounts of total protein were immunoblotted with anti-ERK$^{pT202/pY204}$ and total anti-ERK antibodies. The shown blots are representative of three individual experiments. Relative levels of ERK$^{pT202/pY204}$ to total ERK were calculated from three independent experiments and graphically depicted as the mean ± SD. Shown is the fold induction of ERK1/2 phosphorylation upon serum stimulation in comparison to unstimulated cells.

Serum stimulation of HepG2 cells resulted in increased phosphorylation level of ERK1/2 (Figure 22). Quantification demonstrated a 6-fold induction of ERK1/2 activation upon serum stimulation. ERK1/2 phosphorylation reached a maximum after 15 minutes of serum stimulation. By further stimulation a decline of serum-inducible ERK1/2 activation was observed. However, serum stimulation of HuH7 cells was not able to induce ERK1/2 phosphorylation. This observation was confirmed by quantification clearly pointing the absence of ERK1/2 phosphorylation upon serum stimulation. Our data imply that ERK1/2 activation is suppressed in carcinoma cells lacking endogenous DLC1 expression and accounts presumably for the impaired phosphorylation of MKL1 at serine 454.

6.1.7 Activation of MKL/SRF-dependent target gene expression in DLC1-deficient cancer cells

The transcriptional activities of MKL1 and MKL2 are tightly linked with their nuclear localization. As DLC1 was characterized as a tumor suppressor whose loss contributes to HCC, we addressed the question if the nuclear accumulation of MKL1 and MKL2 in human carcinoma cells contributes to the activation of tumor-relevant SRF target gene expression.

The Connective Tissue Growth Factor (CTGF, CCN2) and the cysteine-rich protein 61 (Cyr61, CCN1) belong to the CCN protein family. CCN proteins play a key role in biological processes such as cell differentiation, proliferation, adhesion, migration and angiogenesis (Leask & Abraham, 2006). CTGF was characterized as an immediate early gene which expression is regulated by SRF (Muehlich et al, 2007). It has been reported that CTGF expression is involved in tumor progression of hepatocellular and breast carcinoma cells (Mazzocca et al, 2010; Xie et al, 2001; Xiu et al, 2012). In a recently conducted microarray study, CTGF was identified as a MKL1/2-dependent target gene (Medjkane et al, 2009). Additionally, Cyr61 was classified as a MKL/SRF-dependent target gene and was described to be involved in the tumorigenic process of hepatocellular carcinoma (Li et al, 2012b; Medjkane et al, 2009; Selvaraj & Prywes, 2004). Thus, we investigated the CTGF and Cyr61 expression levels in endogenous DLC1-expressing HepG2 and MCF7 cells versus DLC1-deficient HuH7 and MDA-MB-468 cells. Cells were serum-starved and then serum-stimulated for 2 hours. Expression levels of CTGF and Cyr61 were determined by quantitative real-time PCR analysis. Serum-starved HuH7 and MDA-MB-468 cells revealed significantly enhanced CTGF mRNA expression levels in comparison to HepG2 and MCF7 cells. Serum stimulation of HepG2 and MCF7 cells strongly induced CTGF mRNA expression whereas HuH7 and MDA-MDA-MB 468 cells displayed constitutive activation of CTGF mRNA expression (Figure 23a). The same expression pattern was observed for Cyr61 mRNA expression in HepG2 and HuH7 cells (Figure 23b). Hence, the nuclear localization of MKL1/2 in DLC1-deficient hepatocellular and breast carcinoma cells was accompanied by the constitutive activation of MKL/SRF dependent CTGF and Cyr61 gene expression, both described to promote tumor progression (Li et al, 2012b; Mazzocca et al, 2010; Xiu et al, 2012).

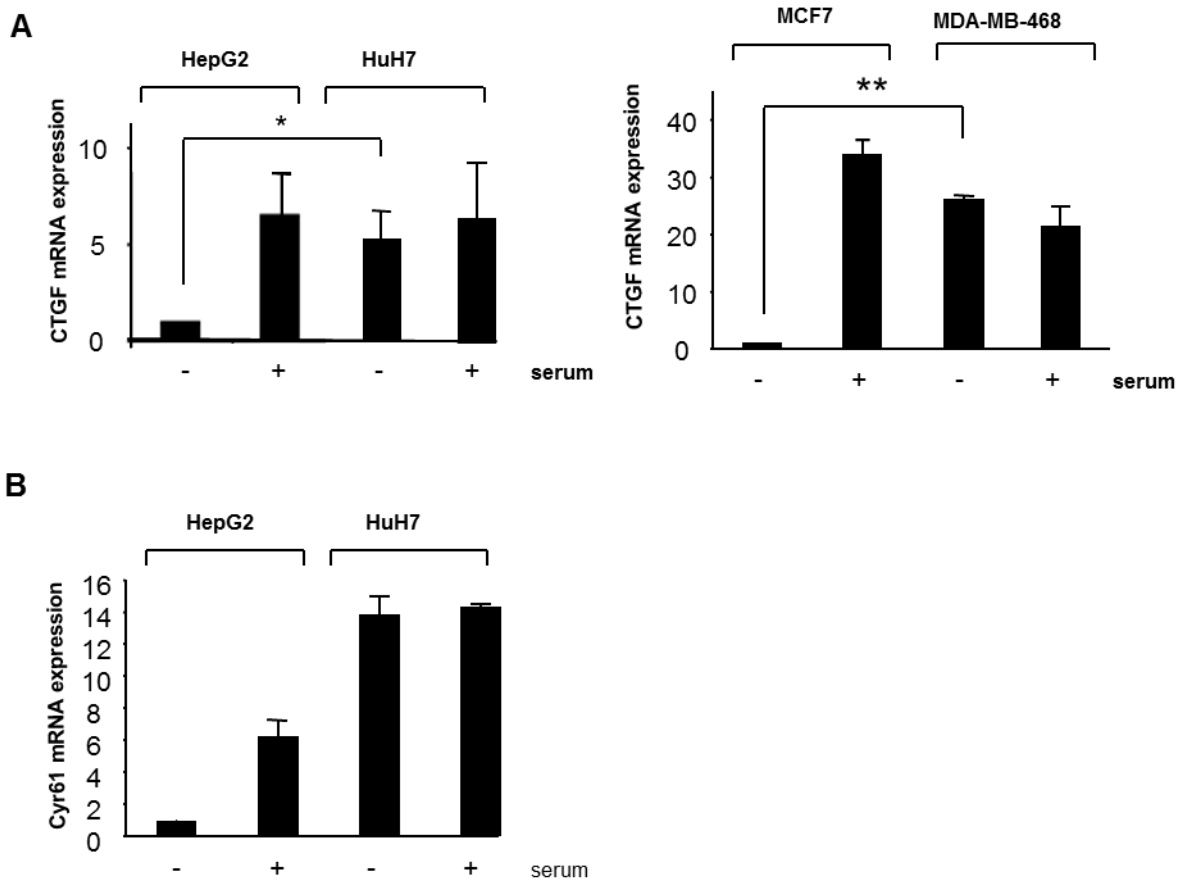

Figure 23: Upregulation of CTGF and Cyr61 mRNA expression in DLC1-deficient carcinoma cells.
(A) HepG2, HuH7, MCF7 and MDA-MB-468 cells were serum-starved for 16 hours and afterwards stimulated with 20 % serum for 120 minutes. Cells were harvested and total RNA was isolated and subjected to quantitative RT-PCR using CTGF-specific primers. The amount of RNA of each sample was normalized to the endogenous housekeeping gene 18S rRNA. Shown is the fold increase in the amount of CTGF mRNA expression in comparison to unstimulated HepG2 cells. Values are represented as mean ± SD of three independent experiments. (B) Cyr61 mRNA expression in HepG2 and HuH7 cells was measured as described in (A) using Cyr61-specific primers. Values are mean ± SD of two independent experiments.

Based on our findings we supposed a direct link between endogenous DLC1 expression levels and the activation of MKL/SRF dependent gene expression. We used an RNAi approach and examined the effects of DLC1 expression on the protein expression levels of CTGF by immunoblotting. Downregulation of DLC1 expression in HepG2 cells induced elevated CTGF expression (Figure 24a). To substantiate our observation, DLC1 expression was reconstituted in DLC1-deficient HuH7 cells by transient transfection of wildtype human DLC1. As shown by real-time PCR analysis, expression of Flag-tagged DLC1 significantly suppressed CTGF mRNA expression (Figure 24b). Therefore it is obvious that the expression levels of the tumor suppressor DLC1 significantly influence the expression of tumor-relevant MKL/SRF dependent target genes.

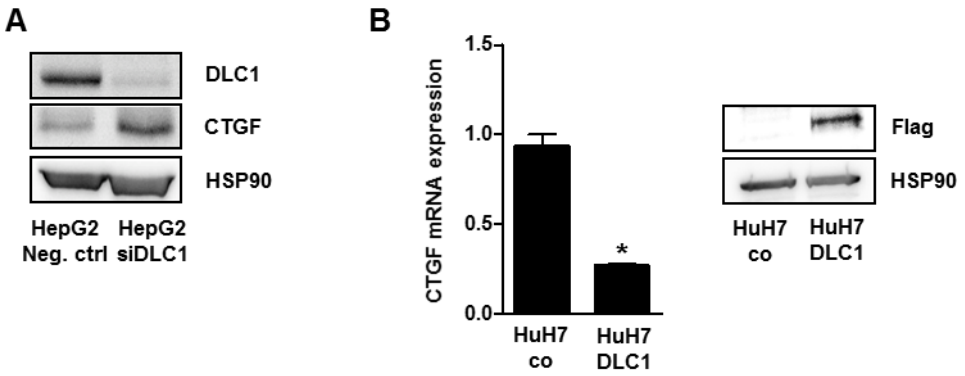

Figure 24: Activation of CTGF expression depends on the expression levels of DLC1.
(A) HepG2 cells were transfected with Neg. ctrl siRNA or DLC1-specific siRNA (50 nM). 96 hours posttransfection, cells were lysed and equal amounts of total protein were analyzed by immunoblotting using the anti-DLC1 and anti-CTGF antibodies. Loading was controlled by re-probing the blot for HSP90. (B) HuH7 cells were transiently transfected with a plasmid encoding human Flag-DLC1 or the corresponding control expression vector. 24 hours after transfection, total cellular RNA was isolated and subjected to quantitative RT-PCR using CTGF-specific primers. Shown is the fold induction of CTGF-specific mRNA expression compared to HuH7 cells expressing control vector. Values are mean ± SD of three independent experiments. Analysis of Flag-tagged DLC1 expression was done by immunoblotting using anti-Flag and anti-HSP90 antibodies.

6.1.8 MKL1/2 knockdown induces alterations of the actin cytoskeleton structure of DLC1-deficient cancer cells

Recently, it was shown that depletion of MKL1 and MKL2 in highly invasive cancer cells reduced cell adhesion, cell motility and experimental metastasis (Medjkane et al, 2009). Besides, our group demonstrated that downregulation of MKL1/2 was able to revert the pro-migratory effect caused by the loss of DLC1 (Muehlich et al, 2012). As changes in cell motility are associated with structural alterations of the actin cytoskeleton, we investigated the structure of the actin cytoskeleton of DLC1-deficient hepatocellular and breast carcinoma cells in dependence of MKL1/2 expression. Therefore, HuH7 and MDA-MB-468 cells with stable knockdown of MKL1 and MKL2, established in our laboratory, were stained with fluorescently labeled phalloidin.

Indirect immunofluorescence analysis illustrated that depletion of MKL1/2 in DLC1-deficient HuH7 and MDA-MB-468 cells provoked a disorganization of stress fibers (Figure 25). Besides, the number of stress fibers crossing the cells was remarkably decreased upon MKL1/2 downregulation. The quantity and length of protrusive structures, known as filopodia, were strongly diminished in MKL1/2 depleted HuH7 and MDA-MD-468 cells in comparison to the control cells. We tentatively assume that the effect of MKL1/2 depletion on the structure of the actin cytoskeleton is due to the influence of MKL1/2 on the transcription of genes encoding for actin dynamics (Olson & Nordheim, 2010).

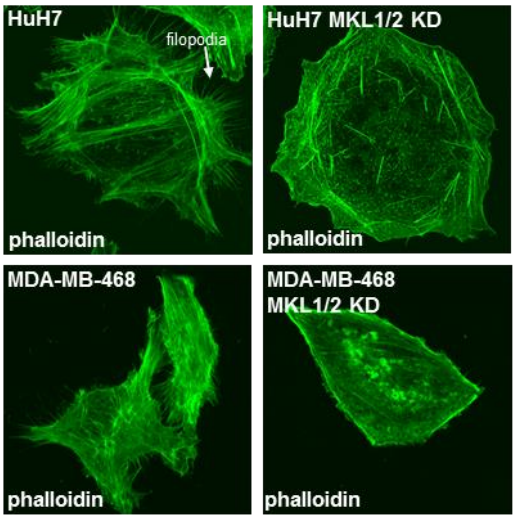

Figure 25: MKL1/2 depletion in DLC1-deficient cancer cells induces disorganization of stress fibers and reduces the amount of filopodia.
The actin cytoskeleton of HuH7 and MDA-MB-468 cells stably expressing either control shRNA or MKL1/2 shRNA was visualized by F-actin staining using ALEXA Fluor 488 phalloidin. One representative image for each cell line is shown.

6.2 Effects of MKL1 and MKL2 expression on the tumor growth of hepatocellular carcinoma cells in vitro and *in vivo*

Recently, our group reported a correlation between decreased DLC1 expression in primary human hepatocellular carcinomas (HCC) and the nuclear localization of MKL1 *in vivo* (Muehlich et al, 2012). It has been found that the nuclear accumulation of MKL1 correlated with significantly increased expression of the proliferation marker Ki-67. Expression of the human protein Ki-67 correlates directly with cell proliferation and is an established marker for the progression of hepatocellular carcinoma (Gerdes et al, 1983; King et al, 1998). As DLC1 was initially identified as a tumor suppressor with frequent deletions in human hepatocellular carcinomas (Yuan et al, 1998), we focused us in the second part of this work on the effects of MKL1/2 expression on the growth of hepatocellular carcinoma cells with a DLC1-deficient background.

6.2.1 Characterization of human hepatocellular carcinoma cell lines

We analyzed the human hepatoma cell lines HuH7, HLF, HepG2 and HuH6 for their endogenous DLC1 expression levels. As shown by immunoblotting, HLF and HepG2 cells expressed endogenous DLC1, whereas its expression was lacking in HuH7 and HuH6 cells (Figure 26a). However, all probed cell lines displayed similar expression levels of endogenous MKL1 and MKL2 (Figure 26a). In chapter 6.1.1 and 6.1.2, the subcellular distribution of MKL1/2 and the RhoA activation state was already shown for HepG2 and HuH7 cells. Consequently, HuH6 and HLF cells were analyzed. Accordingly, measurement of the RhoA activation state by a RhoA GLISA assay clearly depicted elevated active GTP-bound RhoA levels in the DLC1-deficient HuH6 cells in comparison to the DLC1-expressing HLF cells (Figure 26b). Indirect

immunofluorescence analysis demonstrated a prevalent nuclear MKL1 staining in HuH6 cells meanwhile HLF cells displayed a cytoplasmic distribution of MKL1 (Figure 26c). This observation was confirmed by quantification clearly illustrating the nuclear distribution of MKL1 in the DLC1-deficient HuH6 cells (Figure 26c). Hence, endogenous DLC1 expressing HepG2 and HLF cells are characterized by a cytoplasmic localization of MKL1/2 and low RhoA activity, whereas the DLC1-deficient HuH6 and HuH7 cells are distinguished by nuclear accumulation of MKL1/2 and high active RhoA levels.

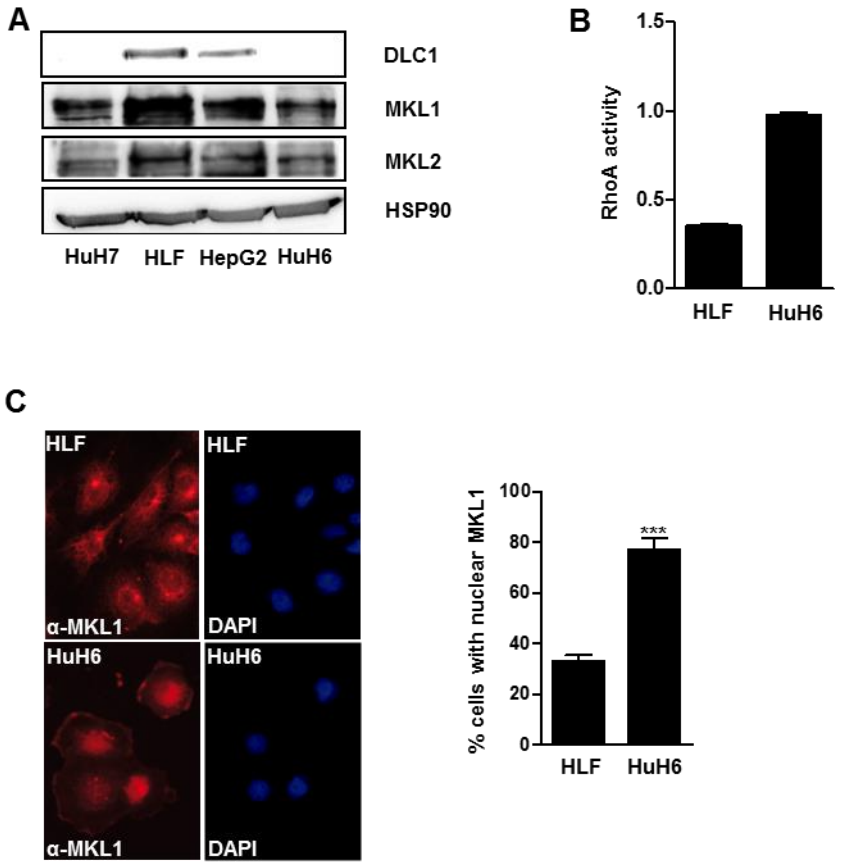

Figure 26: Characterization of hepatocellular carcinoma cell lines with different endogenous DLC1 expression levels.
(A) Lysates of HuH7, HLF, HepG2 and HuH6 cells were prepared and equal amounts of total protein were immunoblotted with anti-DLC1, anti-MKL1, anti-MKL2 and anti-HSP90 antibody as loading control.
(B) Active RhoA-GTP levels of HLF and HuH6 cells were assessed by an ELISA assay. Data are expressed as mean ± SD of two independent experiments. (C) HLF and HuH6 cells were immunostained with anti-MKL1 antibody and nuclei were counterstained with DAPI. Subcellular localization of endogenous MKL1 was predominantly scored as nuclear in 100 cells per experiment. Quantification is based on three independent experiments and data are represented as mean ± SD. Representative images for each cell line are shown.

6.2.2 Establishment of hepatocellular carcinoma cell lines with stable knockdown of MKL1 and MKL2

To investigate the effects of MKL1/2 expression on tumor cell proliferation, we generated hepatocellular carcinoma cell lines with a stable knockdown of MKL1 and MKL2 that allows long-term analysis of cell proliferation. Cells were transduced with a lentiviral shRNA vector containing one sequence that enables simultaneously targeting both MKL1 and MKL2 (Lee et al, 2010b; Medjkane et al, 2009). We choose the double-knockdown strategy as studies in fibroblasts had shown that a single knockdown of MKL1 was not sufficient to reduce immediate early gene expression (Cen et al, 2003). Control cells were transduced with a lentiviral vector harboring a sequence that does not target known genes. The shRNA expression vector co-expressed a puromycin-resistance gene that enabled selection of transduced cells within 7 days. As shown by immunoblotting, transduction of HuH7, HuH6, HepG2 and HLF cells with MKL1/2 shRNA clearly reduced the protein expression levels of both MKL1 and MKL2 (Figure 27). MRNA expression analysis of MKL1 and MKL2 revealed an overall knockdown efficiency of about 40-80 % in MKL1/2 shRNA transduced cells. For the validation of functional MKL1/2 depletion, expression of the well-established MKL/SRF dependent target gene smooth muscle actin (SMA) was analyzed in MKL1/2 depleted HuH7 and HepG2 cells (Cen et al, 2003).

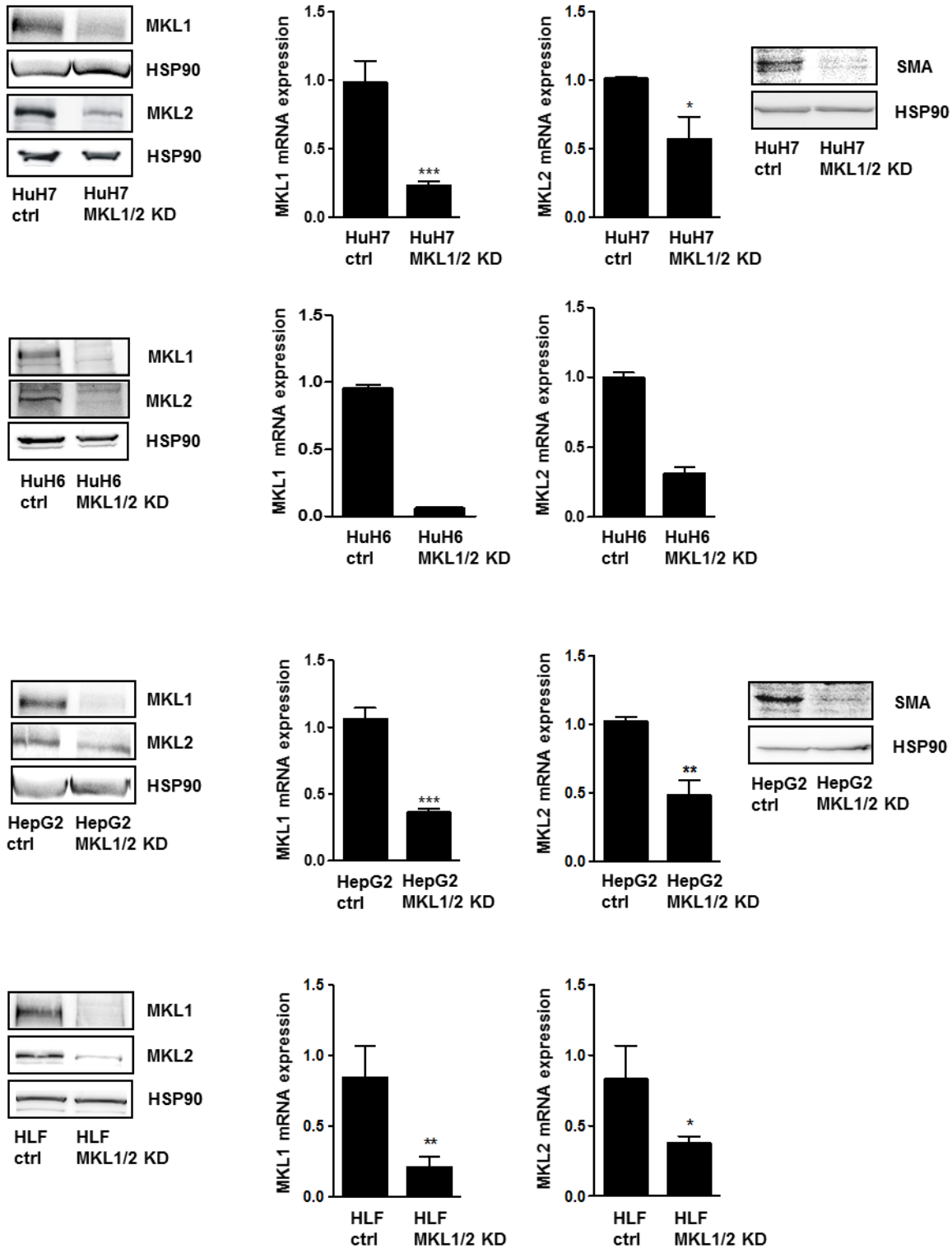

Figure 27: Establishment of hepatocellular carcinoma cell lines with a stable knockdown of MKL1 and MKL2.

HuH7, HuH6, HepG2 and HLF cells were lentivirally transduced with either control shRNA or MKL1/2 shRNA and thereafter cells were selected with puromycin for 7 days. Lysates of cells expressing control shRNA or MKL1/2 shRNA were prepared and equal amounts of total protein were immunoblotted using anti-MKL1, anti-MKL2 and anti-SMA antibodies. Loading was controlled by re-probing the blots for HSP90. Total RNA was isolated of the indicated cell lines and subjected to quantitative RT-PCR analysis using MKL1 and MKL2-specific primers. The amount of each RNA sample was normalized to the endogenous housekeeping gene 18S rRNA. Shown is the fold change of MKL1 and MKL2 specific mRNA expression in MKL1/2 shRNA transduced cells in comparison to control shRNA transduced cells. Quantifications are based on three independent experiments and data are represented as mean ± SD. For HuH6 cells, quantification of MKL1 and MKL2 mRNA expression is based on two independent experiments.

6.2.3 Inhibition of tumor cell proliferation of DLC1-deficient hepatocellular carcinoma cells upon MKL1/2 depletion

After the establishment and characterization of hepatocellular carcinoma cell lines with stable MKL1/2 knockdown, we analyzed their cellular proliferation rate for 6 days. The DLC1-deficient HuH7 and HuH6 cells stably expressing MKL1/2 shRNA displayed a significant reduction in the amount of proliferating cells in comparison to the control cells (Figure 28a). The cell number of endogenous DLC1-expressing HepG2 and HLF cells remained unchanged upon MKL1/2 depletion (Figure 28b). These data suggested that downregulation of MKL1/2 expression provoked an anti-proliferative effect in hepatocellular carcinoma cells characterized by a DLC1 loss.

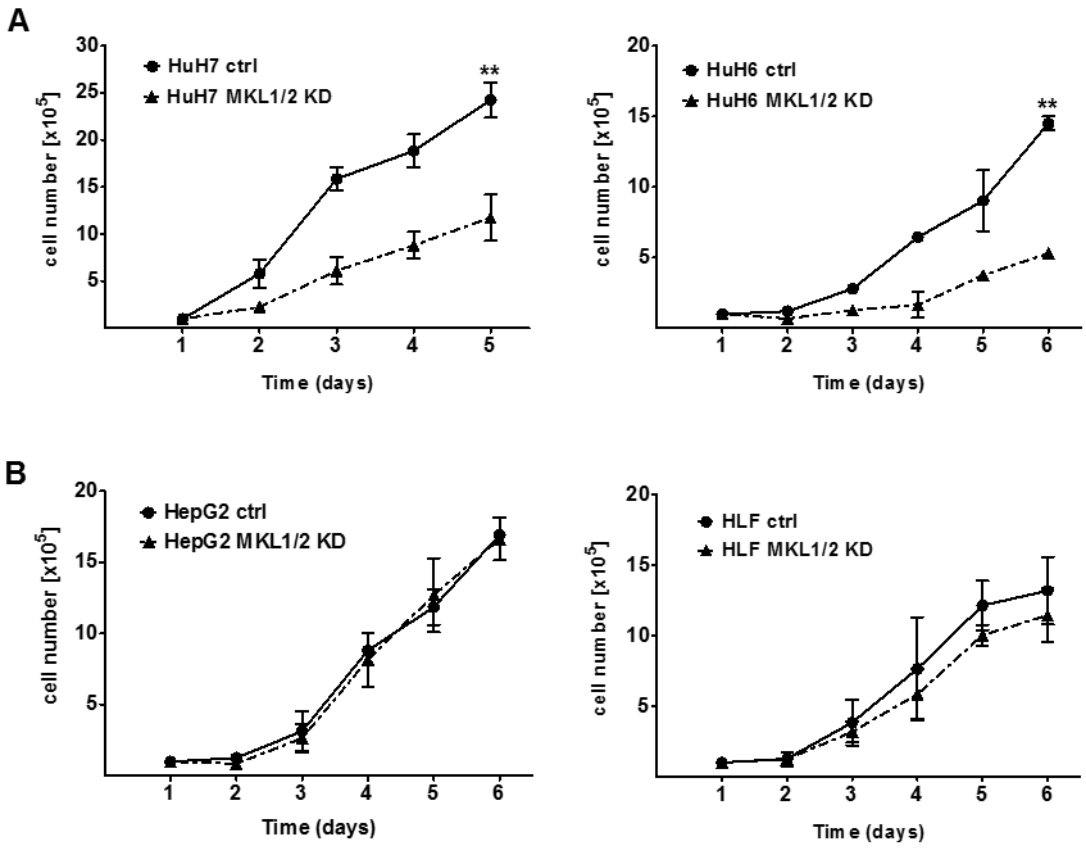

Figure 28: Downregulation of MKL1/2 expression in DLC1-deficient hepatocellular carcinoma cells provokes an anti-proliferative effect.
(A) The DLC1-deficient HuH7 and HuH6 cells stably expressing control shRNA or MKL1/2 shRNA were counted daily for 6 days. Values are mean ± SEM of three independent experiments.
(B) Endogenous DLC1-expressing HepG2 and HLF cells stably expressing control shRNA or MKL1/2 shRNA were counted daily for 6 days. Values are mean ± SEM of three independent experiments.

6.2.4 DLC1 knockdown renders cells responsive to the anti-proliferative effect of MKL1/2 depletion

The previous experiments suggested that DLC1 expression constitutes the decisive factor for the responsiveness of the anti-proliferative effect upon MKL1/2 knockdown. To test this, we used established HepG2 cells stably expressing a shRNA vector targeting human DLC1 and verified the reduction of endogenous DLC1 expression levels by immunoblotting that depicted a knockdown efficiency of 83 % on protein level (Figure 29a). MKL1 and MKL2 expression was downregulated by an RNAi approach, using a siRNA sequence that corresponded to the MKL1/2 shRNA sequence. We selected the siRNA method because we intended to analyze cell proliferation within a shorter period of 4 days. As shown by immunoblotting, transfection of HepG2 cells stably expressing DLC1 shRNA with the siRNA targeting MKL1/2 resulted in decreased expression of MKL1 and MKL2 compared to cells transfected with inert control siRNA (Neg. ctrl) (Figure 29b). Enhanced cell proliferation was observed in HepG2 cells expressing DLC1 shRNA in comparison to HepG2 cells expressing control shRNA. Downregulation of MKL1/2 expression in HepG2 cells expressing DLC1 shRNA significantly reversed the proliferative effect of DLC1 knockdown (Figure 29c). These data imply that DLC1 knockdown renders cell responsive to the anti-proliferative effect of MKL1/2 downregulation.

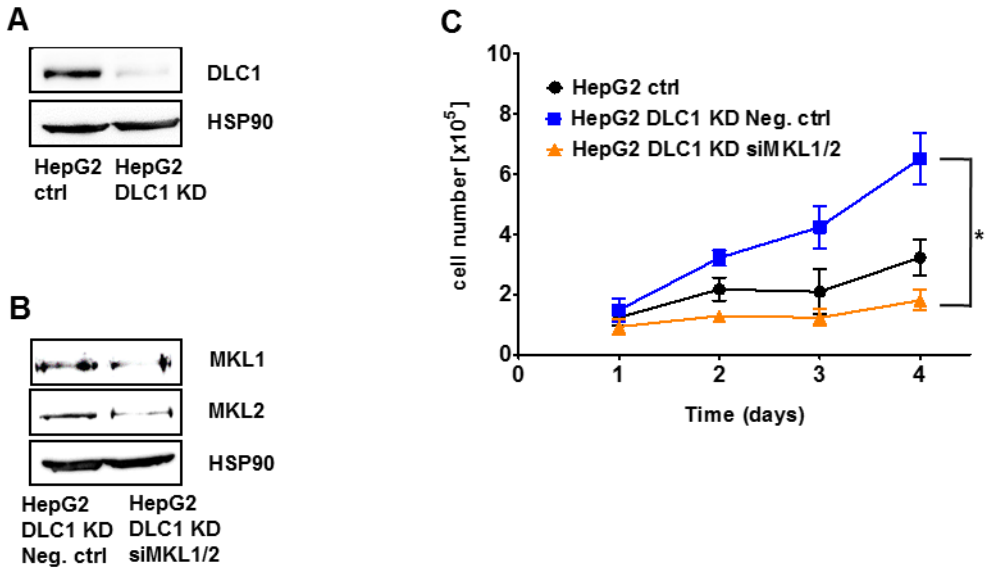

Figure 29: DLC1 knockdown renders cells responsive to the anti-proliferative effect of MKL1/2 knockdown.
(A) Protein lysates of HepG2 cells stably expressing either control shRNA or DLC1 shRNA were prepared and equal amounts of total protein were subjected to immunoblotting using anti-DLC1 antibody. Loading was controlled by re-probing the blot for HSP90. (B) HepG2 cells expressing DLC1 shRNA were transfected with either Neg. ctrl siRNA or siRNA MKL1/2 (50 nM). At day 4 posttransfection, cells were harvested and equal amounts of total protein were immunoblotted using the anti-MKL1 and anti-MKL2 antibodies. Loading was controlled by re-probing the blot for HSP90. (C) HepG2 cells expressing DLC1 shRNA were transfected with Neg. ctrl siRNA or siRNA MKL1/2 (50 nM) and counted daily for 4 days. Values are represented as mean ± SEM of three independent experiments.

6.2.5 Increased RhoA activity is required for the anti-proliferative effect upon MKL1/2 knockdown

Since lack of DLC1 expression is an essential requirement for the growth arrest upon MKL1/2 knockdown, we speculated whether the enhanced RhoA activity due to the loss of DLC1 (as described in chapter 6.1.4) constitutes a prerequisite for the observed growth arrest. We generated HepG2 cells overexpressing constitutively active RhoA (RhoAV14) the expression of which is driven by a rather weak Tet-off-regulated promoter. Established HepG2 cells, stably expressing the Tet-responsive transactivator, were transfected with the plasmid encoding the Tet-responsive promoter controlled Flag-tagged RhoAV14 or with the corresponding control expression vector. Expression of RhoAV14 was regulated by the absence or presence of doxycline in the culture medium for at least two days. Overexpression of constitutively active RhoAV14 in HepG2 cells was confirmed by immunoblotting (Figure 30a). Upon removal of doxycline, indirect immunofluorescence analysis illustrated a nuclear translocation of MKL1 in HepG2 cells expressing Flag-tagged RhoAV14 in comparison to HepG2 cells transfected with the control expression vector displaying a cytoplasmic distribution of MKL1 (Figure 30b). RhoAV14 expression was switched off by addition of doxycline and caused a cytoplasmic redistribution of MKL1. Simultaneously, downregulation of MKL1/2 expression in RhoAV14 expressing HepG2 cells significantly reduced their cell proliferation (Figure 30c). However, unmodified HepG2 cells with low RhoA activity and cytoplasmic MKL1 localization showed no changes in the cell proliferation upon MKL1/2 knockdown. These findings strongly suggest that increased RhoA activity and the concomitant nuclear localization of MKL1 are required for the growth arrest induced by MKL1/2 knockdown.

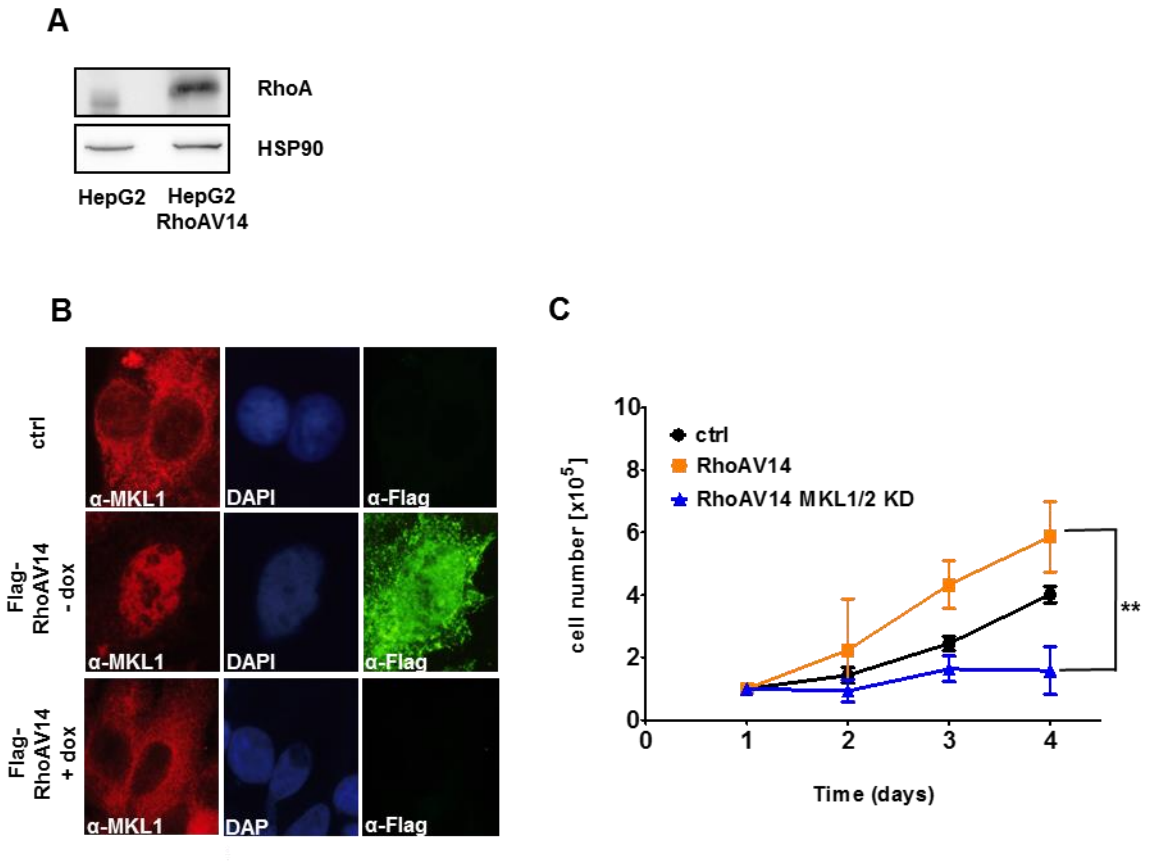

Figure 30: Increased RhoA activity is necessary for the reduction of cell prolferation upon MKL1/2 knockdown.
(A) HepG2 cells expressing the Tet-responsive transactivator (Tet-Off) were transfected with either pRevTRE control or pRevTRE Flag-RhoAV14 expression vector, lysed and equal amounts of total protein were immunoblotted with anti-RhoA and anti-HSP90 antibodies. (B) HepG2 Tet-off and HepG2 Tet-off cells transfected with pRevTRE Flag-RhoAV14 were incubated with and without 0.5 µg/mL doxycycline (dox) for at least 2 days. Thereafter cells were fixed and immunostained with anti-MKL1 and anti-FLAG antibodies. Nuclei were counterstained with DAPI. Representative images are shown. (C) HepG2 Tet off cells expressing pRevTRE RhoAV14 were transduced with either control shRNA or MKL1/2 shRNA and counted daily for 4 days. Values are represented as mean ± SEM of three independent experiments.

6.2.6 Determination of apoptosis

The reduced cell proliferation upon MKL1/2 knockdown in DLC1-deficient hepatocellular carcinoma cells prompted us to investigate the mechanism of the anti-neoplastic effect of MKL1/2 knockdown. It is well established that cell proliferation and apoptotic cell death are tightly linked to tumor progression (Kerr et al, 1994; Williams, 1991). Apoptosis, programmed cell death, is a failsafe feature in malignancies and is associated with the delay or suppression of tumor growth (Kerr et al, 1994). Therefore we analyzed the effect of MKL1/2 on apoptosis by measuring activated, caspase-3 (apoptosis-related cysteine peptidase 3) because activation of caspases are fundamental steps in the execution of apoptosis. Caspase-3 belongs to the group of cysteine-aspartic acid proteases and is required as a critical mediator for the programmed cell death in mammalian cells (Fernandes-Alnemri et al, 1994; Nicholson et al, 1995). HuH7 cells expressing either control shRNA or MKL1/2 shRNA were immunostained with an anti-active caspase-3 antibody which enables to specifically detect

apoptotic cells. Using indirect immunofluorescence analysis, no active-caspase-3 stained positive cells could be detected in either control shRNA or MKL1/2 shRNA expressing HuH7 cells (Figure 31). Therefore we supposed that apoptosis was not responsible for the observed growth arrest.

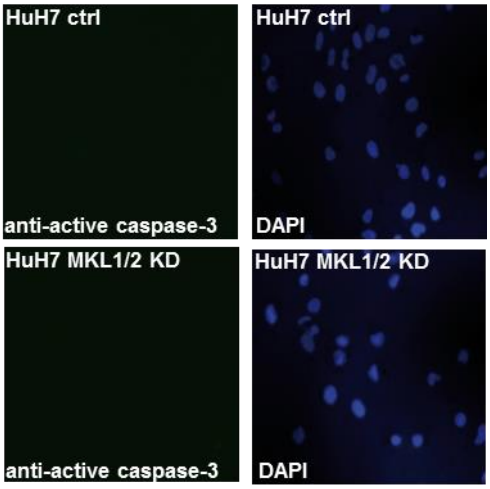

Figure 31: Analysis of apoptosis in MKL1/2 depleted HuH7 cells.
HuH7 cells expressing control shRNA or MKL1/2 shRNA were immunostained with anti-active caspase-3 antibody and DAPI for nuclear counter staining. Representative images are given.

6.2.7 Depletion of MKL1/2 induces a G1-phase cell cycle arrest in DLC1-deficient HuH7 cells

We analyzed the cell cycle phase distribution of HuH7 and HepG2 cells expressing control shRNA or MKL1/2 shRNA by flow cytometry. Cells were stained with the propidium iodide dye which binds stoichiometrically to nuclei acids. The binding of propidium iodide is proportional to the DNA content of cells (Nicoletti et al, 1991). Analysis of the cell cycle phase distribution revealed that 37.1 % of HuH7 control cells are in G1-phase. In contrast, in HuH7 MKL1/2 KD cells the percentage of cells in G1-phase was significantly increased to 48.35 %. Simultaneously, the percentage of cells in the S-phase was significantly reduced from 45.55 % in HuH7 control cells to 33.85 % in HuH7 MKL1/2 KD cells (Figure 32). The percentage of cells in the G2 phase did not differ between HuH7 control and HuH7 MKL1/2 KD cells. Analysis of HepG2 cells that did not respond to the anti-proliferative effect of MKL1/2 depletion, showed no effect of MKL1/2 knockdown on the cell cycle phase distribution (Figure 32). These data indicate that MKL1/2 depletion in DLC1-deficient hepatocellular carcinoma cells causes a G1-arrest that is in line with the observed anti-proliferative-effect.

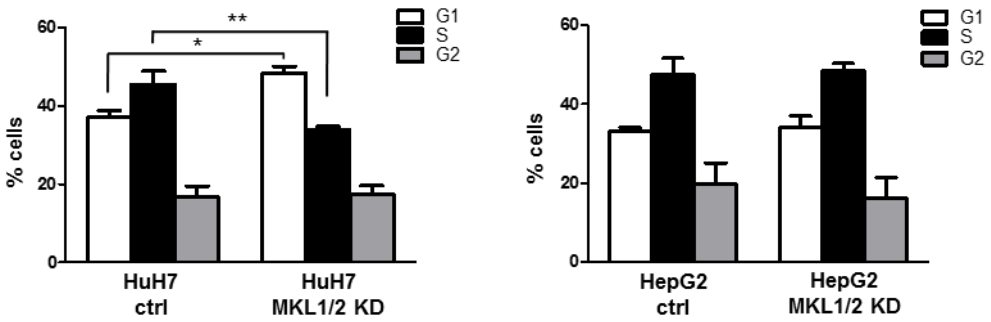

Figure 32: MKL1/2 depletion provokes a G1-arrest in DLC1-deficient HuH7 cells.
HuH7 and HepG2 cells stably expressing control shRNA or MKL1/2 shRNA were stained with propidium iodide and the cell cycle phase distribution was examined by flow cytometry analysis. *Flow cytometry analysis was kindly done by Natalie Frank.*

6.2.8 MKL1/2 depleted HuH7 cells feature a senescent cell morphology

Further we investigated the cell morphology of MKL1/2 depleted HuH7 cells undergoing the growth arrest. In contrast to the control cells, MKL1/2 depleted HuH7 cells adopted a flattened and enlarged cell shape (Figure 33). Furthermore HuH7 MKL1/2 KD cells displayed increased granularity and a vacuole-enriched cytoplasm. As already described in chapter 6.1.8, HuH7 cells with MKL1/2 knockdown displayed a reduction and disorganization of the actin stress fibers (Figure 33).

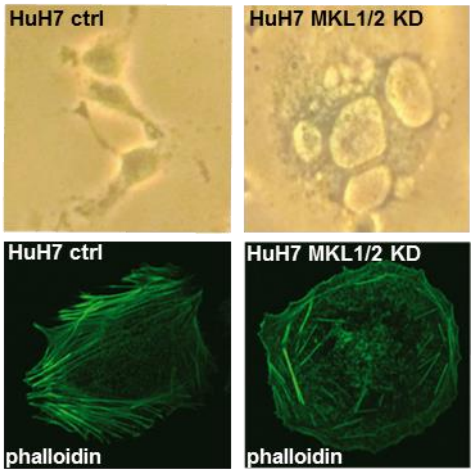

Figure 33: Structural and morphological alterations of MKL1/2 depleted HuH7 cells.
The cell morphology of HuH7 cells expressing control shRNA or MKL1/2 shRNA was analyzed by a transmitted light microscope. The actin cytoskeleton was visualized by Alexa Fluor 488 phalloidin binding. Representative images are shown.

The described morphological and structural alterations of MKL1/2 depleted HuH7 cells were reminiscent of cells undergoing senescence (Angello et al, 1989; Goldstein, 1990). Cellular senescence is characterized as an irreversible G1-phase proliferation arrest which can be triggered by numerous cellular stimuli and constitutes a multifaceted process (Rittling et al, 1986; Sherwood et al, 1988).

6.2.9 MKL1/2 depletion increases the senescence-associated ß-galactosidase activity in DLC1-deficient HCC cells

To confirm our assumption that MKL1/2 downregulation provokes the growth arrest by senescence induction, we tested hepatocellular carcinoma cell lines with stable MKL1/2 knockdown for the senescence-associated ß-galactosidase activity (SA-ß-gal). Increased lysosomal ß-galactosidase activity, detectable at pH 6.0, is a well-established marker for the determination of cellular senescence (Dimri et al, 1995). We detected a significant increase in the percentage of SA-ß-gal positive HuH7 cells upon MKL1/2 knockdown (Figure 34). The same effect was observed in DLC1-deficient HuH6 cells upon MKL1/2 knockdown, however to a lesser extent in comparison to HuH7 MKL1/2 KD cells. No induction of SA-ß-gal activity upon MKL1/2 knockdown was observed in DLC1-expressing HepG2 and HLF cells (Figure 34).

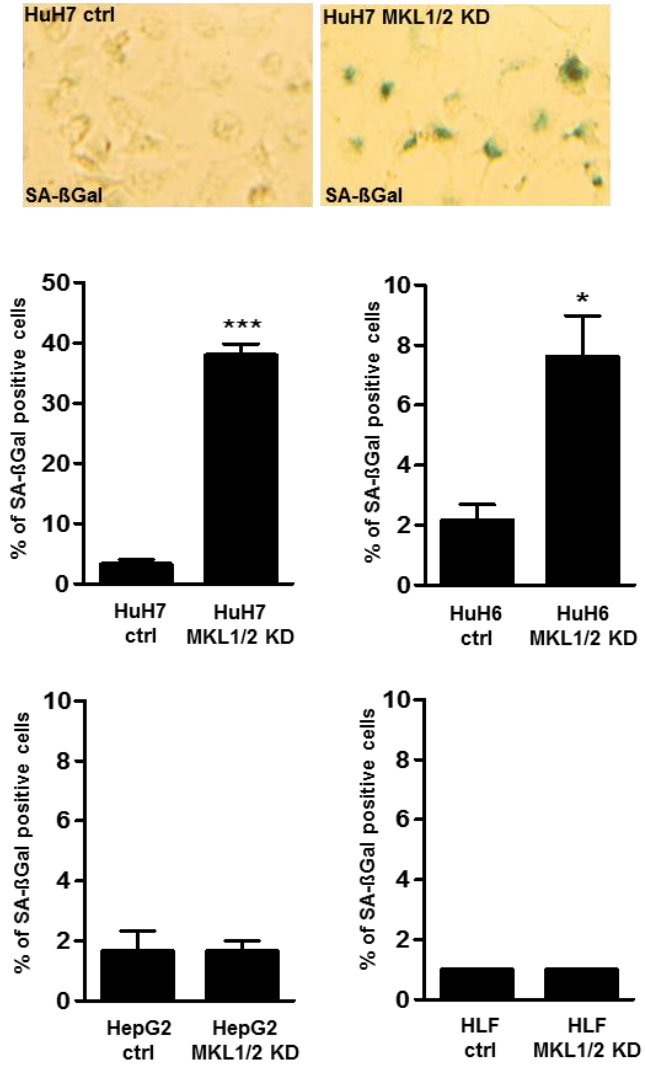

Figure 34: Increased senescence-associated ß-galactosidase activity in DLC1-deficient HCC cells upon MKL1/2 knockdown.
HuH7, HuH6, HepG2 and HLF cells were transduced with either control shRNA or MKL1/2 shRNA. At day 7 posttransduction, cells were stained for senescence-associated ß-galactosidase activity. The percentage of SA-ß-Gal positive cells was counted under an inverted microscope. Values are given as mean ± SD of three independent experiments. Representative images of SA-ß-Gal positive stained cells are shown for HuH7 and HuH7 MKL1/2 KD cells.

Is the DLC1 expression status crucial for the induction of cellular senescence upon MKL1/2 knockdown? To address this issue, we generated HepG2 cells with double knockdown of DLC1 and MKL1/2. As SA-ß-gal activity is a late senescence marker, a stable knockdown of MKL1/2 was required. HepG2 cells expressing DLC1 shRNA were lentivirally transduced with control shRNA and MKL1/2 shRNA and thereafter selected with puromycin for 7 days. As shown by immunoblotting, transduction of HepG2 DLC1 KD cells with MKL1/2 shRNA reduced the protein expression levels of both MKL1 and MKL2 (Figure 35). Downregulation of DLC1 expression in HepG2 cells led to a significant upregulation of the percentage of SA-ß-gal positive cells upon MKL1/2 depletion in contrast to the wildtype HepG2 cells which did not respond (Figure 35). The phenotype of cellular senescence due to MKL1/2 depletion was consistent with the observed proliferation arrest caused by MKL1/2 knockdown in HCC cells lacking DLC1 expression.

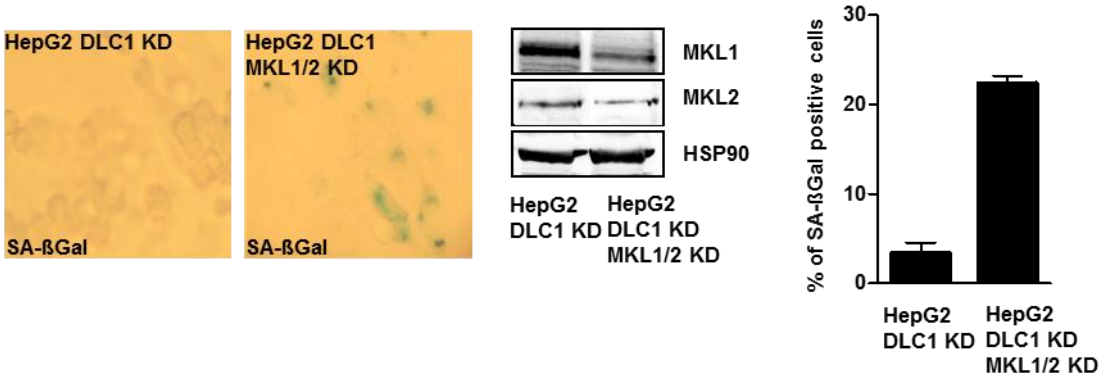

Figure 35: DLC1 depletion renders cells responsive to the induction of cellular senescence upon MKL1/2 depletion.
HepG2 cells expressing DLC1 shRNA and MKL1/2 shRNA were immunoblotted with anti-MKL1, anti-MKL2 and anti-HSP90 antibodies. Senescence-associated ß-galactosidase staining was performed and the percentage of SA-ß-gal positive cells was counted under an inverted microscope. Values are mean ± SD of two independent experiments.

6.2.10 MKL1/2 depletion in DLC1-deficient HCC cells induces oncogene-induced senescence via activation of oncogenic Ras signaling

As we found that the downregulation of MKL1/2 expression triggered the cellular senescence response in hepatocellular carcinoma cells with a DLC1-deficient background, we aimed to get mechanistic insights into the MKL1/2 knockdown mediated senescence response. First of all, we were interested if MKL1/2 depletion activates oncogenic signaling and triggers the tumor suppressive oncogene-induced senescence response. The active GTP-bound Ras levels of HuH7 and HepG2 cells expressing control shRNA or MKL1/2 shRNA were determined by immunoprecipitation using an antibody that specifically detects active GTP-bound Ras.

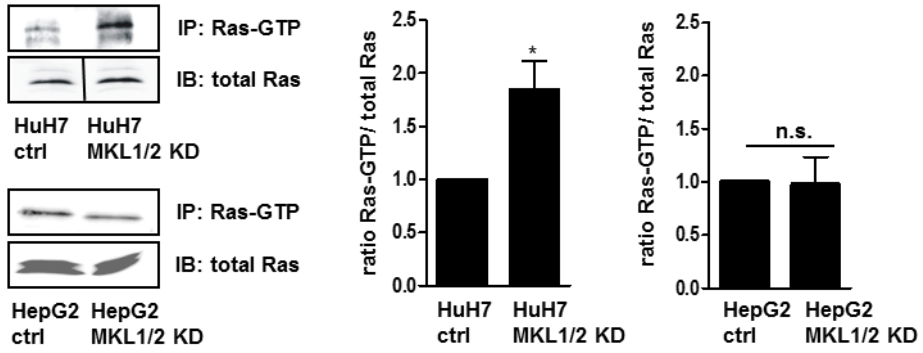

Figure 36: MKL1/2 depletion increases the amount of GTP-bound Ras in DLC1-deficient HuH7 cells.
HuH7 and HepG2 cells stably expressing either control shRNA or MKL1/2 shRNA were immunoprecipitated with anti-active Ras antibody and immunoblotted with total anti-Ras antibody. Equal amounts of lysates were directly immunoblotted with total anti-Ras antibody. The black line delineates a boundary caused by juxtaposing lanes that were non-adjacent in the same gel. The relative ratio of active Ras versus total Ras was quantitated and graphically depicted. Data are represented as mean ± SD of three independent experiments.

The results from immunoblotting demonstrated an increased amount of GTP-bound Ras in HuH7 MKL1/2 KD cells compared to HuH7 control cells both expressing equal amounts of total Ras (Figure 36). Quantification illustrated an almost twofold upregulation of the active, GTP-bound Ras levels in MKL1/2 depleted HuH7 cells. On the contrary, no effects on the amount of GTP-bound Ras levels were detected in HepG2 MKL1/2 KD cells that did not respond to the senescence induction. Our data provide evidence that MKL1/2 depletion activates oncogenic Ras signaling in HuH7 cells characterized by DLC1-deficiency. In concert with this, it is established that activation of oncogenic signaling can provoke the premature form of senescence that is termed as oncogene-induced senescence (Lin et al, 1998; Michaloglou et al, 2005; Serrano et al, 1997). As oncogenic signaling can elicit the oncogene-induced senescence response via different intrinsic pathways like the Arf/p53/$p21^{CIP/WAF1}$, DNA damage and $p16^{Ink4a}$-Rb pathway, we intended to determine their involvement in the MKL1/2 depletion mediated senescence response.

6.2.11 Activation of ERK1/2 upon MKL1/2 depletion in DLC1-deficient HCC cells

As Ras signaling activates the Raf-MEK1-ERK1/2 pathway, we tested for ERK activation by determining its phosphorylation status (Crews & Erikson, 1993). ERK1/2 phosphorylation levels were strongly increased upon MKL1/2 knockdown in the DLC1-deficient HuH7 and HuH6 cells but not in endogenous DLC1-expressing HepG2 and HLF cells (Figure 37). Moreover, ERK1/2 phosphorylation occurred to a lesser extent in HuH6 MKL1/2 KD cells in comparison to HuH7 MKL1/2 KD cells presumably due to other differences in the genetic background.

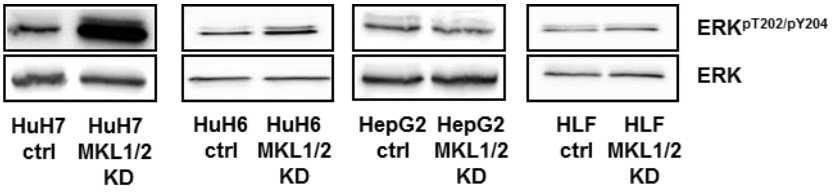

Figure 37: Increased ERK1/2 phosphorylation upon MKL1/2 knockdown in DLC1-deficient HCC cells. Protein lysates of HuH7, HuH6, HepG2 and HLF cells expressing either control shRNA or MKL1/2 shRNA were prepared. Equal amounts of total protein were subjected to immunoblotting using anti-ERK$^{pT202/pY204}$ and total anti-ERK antibodies.

6.2.12 Activation of MAPK signaling is required for the MKL1/2 knockdown mediated proliferation arrest

To demonstrate that activation of the Ras-Raf-MEK1-ERK1/2 signaling pathway triggers the MKL1/2 knockdown mediated proliferation arrest, HuH7 cells were transfected with Neg. ctrl siRNA and siRNA MKL1/2 and afterwards incubated with the MEK1 inhibitor UO126. As shown by immunoblotting, siRNA MKL1/2 transfected HuH7 cells showed reduced protein expression levels of MKL1 and MKL2. Suppression of ERK1/2 activation by UO126 treatment abrogated the anti-proliferative effect of MKL1/2 downregulation in HuH7 cells (Figure 38). Efficiency of UO126 treatment was determined by its ability to inhibit ERK1/2 phosphorylation (Figure 38). This strongly suggests that Ras-ERK signaling is involved in the anti-proliferative response caused by MKL1/2 knockdown.

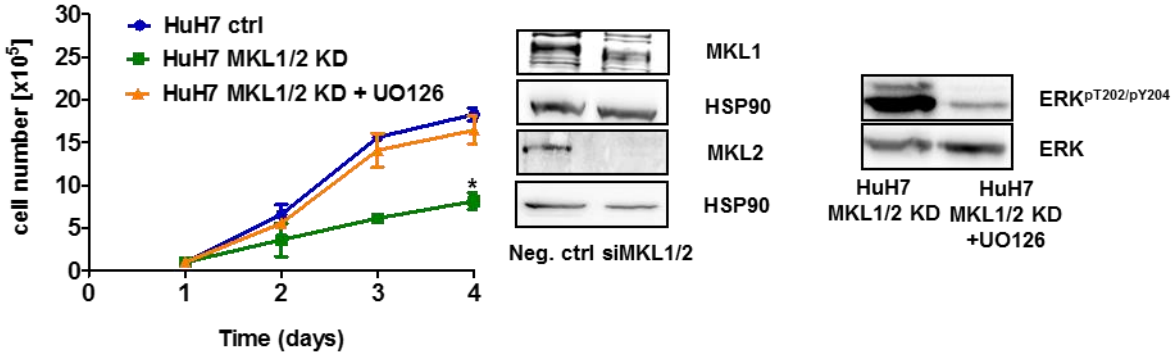

Figure 38: Inhibition of ERK1/2 activation abrogates the MKL1/2 knockdown mediated proliferation arrest. Neg. ctrl or MKL1/2 siRNA (50 nM) transfected HuH7 cells were treated with and without 10 µM UO126 and cells were daily counted for 4 days. Data are represented as mean ± SD of three independent experiments. Lysates of the transfected cells were subjected to immunoblotting using anti-MKL1, anti-MKL2, anti-HSP90, anti-ERK$^{pT202/pY204}$ and total anti-ERK antibodies.

6.2.13 Accumulation of p16^{Ink4a} expression in DLC1-deficient HCC cells upon MKL1/2 depletion

P16^{Ink4a} functions as a tumor suppressor by inhibiting the cyclin-dependent kinases 4 and 6 (CDK4 and CDK6) thereby inducing a G1-cell cycle arrest (Sherr & Roberts, 1999). It has been found that p16^{Ink4a} expression was specifically upregulated in senescent cells and its expression was sufficient to trigger the senescence response (Alcorta et al, 1996; Hara et al, 1996). As activation of mitogenic signaling promoted p16^{Ink4a} expression, we determined the

p16^{Ink4a} expression levels in the MKL1/2 depleted HCC cell lines (Lin et al, 1998; Serrano et al, 1997; Zhu et al, 1998). We found an accumulation of p16^{Ink4a} protein expression in DLC1-deficient HuH7 and HuH6 cells upon MKL1/2 depletion but not in DLC1-expressing HepG2 cells (Figure 39).

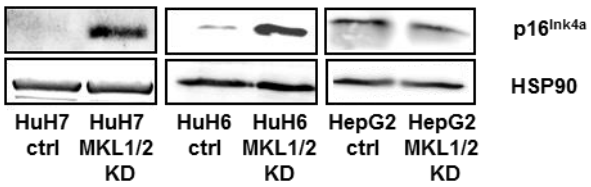

Figure 39: Accumulation of p16^{Ink4a} expression in DLC1-deficient HCC cells upon MKL1/2 depletion.
HuH7, HuH6 and HepG2 cells transduced with control shRNA or MKL1/2 shRNA were lysed and equal amounts of total protein were immunoblotted using anti-p16^{Ink4a} and anti-HSP90 antibodies.

6.2.14 Hypophosphorylation of the retinoblastoma protein upon MKL1/2 knockdown in DLC1-deficient HCC cells

The retinoblastoma protein (Rb) is a well-established downstream target of p16^{Ink4a} that functions as a tumor suppressor and constitutes a master regulator for the G1-S phase transition (Weinberg, 1995). In its active, hypophosphorylated form, the Rb protein suppresses the transcription of genes of the E2F transcription factor family that promote the transition from the G1-phase to the S-phase (Burkhart & Sage, 2008). We analyzed the activity of the Rb protein by detecting changes in the electrophoretic mobility which indicated the phosphorylation state of the Rb protein (Connell-Crowley et al, 1997). Compared to the control cells, downregulation of MKL1/2 in the DLC1-deficient HuH7 and HuH6 cells produced a faster migrating, hypophosphorylated form of the Rb protein (Figure 40). By contrast, in HepG2 MKL1/2 KD cells there were no detectable changes in the mobility of Rb.

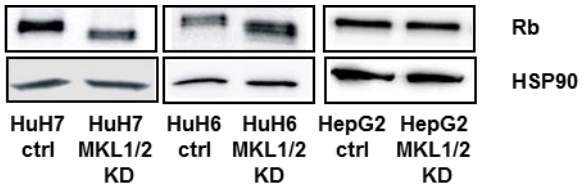

Figure 40: Downregulation of MKL1/2 induces hypophosphorylation of the Rb protein in HCC cells with DLC1-deficiency.
HuH7, HuH6 and HepG2 cells transduced with control shRNA and MKL1/2 shRNA were lysed and equal amounts of total protein were subjected to immunoblotting using anti-Rb and anti-HSP90 antibodies.

6.2.15 Requirement of the p16^{Ink4a}-Rb pathway for the MKL1/2 knockdown mediated senescence response

As the p16^{Ink4a}-Rb pathway plays a critical role in the induction of a senescence response, we intended to demonstrate that induction of p16^{Ink4a} expression upon MKL1/2 knockdown is required for the senescence response. Prior to lentiviral transduction with MKL1/2 shRNA, HuH7 cells were transfected with siRNA targeting p16^{Ink4a} and thereafter the phosphorylation

state of the Rb protein was analyzed. Due to the low endogenous expression levels of the p16^{Ink4a} protein in HuH7 cells, only a slight reduction of the p16^{Ink4a} expression was detectable in HuH7 cells transfected with p16^{Ink4a} specific siRNA. Downregulation of the p16^{Ink4a} expression abolished hypophosphorylation of the Rb protein upon MKL1/2 knockdown (Figure 41). As Rb lies at the core of the senescence response, the lack of Rb hypophosphorylation upon reduction of p16^{Ink4a} expression substantiates the importance of the p16^{Ink4a}-Rb signaling pathway for the execution of the MKL1/2 knockdown-mediated growth arrest in DLC1-deficient HCC cells.

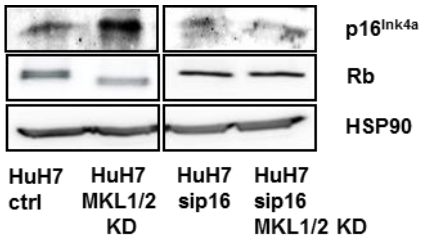

Figure 41: Activation of the p16^{Ink4a}-Rb pathway is required for the senescence induction upon MKL1/2 knockdown.
HuH7 cells were transfected with p16^{Ink4a} siRNA (50 nM) and after 24 hours, cells were transduced with control shRNA or MKL1/2 shRNA. At day 5 postinfection, cells were lysed and subjected to immunoblotting using anti-p16^{Ink4a}, anti-Rb and anti-HSP90 antibodies.

6.2.16 Depletion of MKL1/2 in DLC1-deficient HCC cells induces a DNA-damage response

Induction of a DNA damage response (DDR) is well established as a crucial effector mechanism for the induction of the oncogene-induced senescence response. Di Micco and colleagues showed that oncogene-induced senescence was caused by the activation of the DNA damage response which was characterized by increased phosphorylation of p53 on serine 15 (Di Micco et al, 2006). Therefore we evaluated the phosphorylation status of p53 on serine 15 as an indicator for the DNA damage response. The results from immunoblotting demonstrated enhanced phosphorylation levels of p53 on serine 15 upon MKL1/2 depletion in HuH7 and HuH6 cells whereas HepG2 MKL1/2 KD cells were excluded (Figure 42).

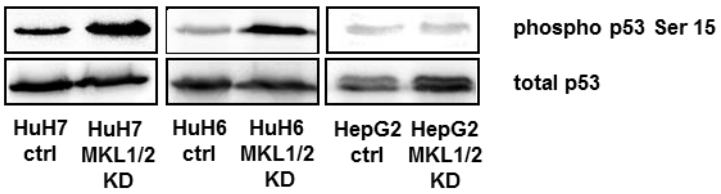

Figure 42: MKL1/2 knockdown induces a DNA damage response by increased phosphorylation levels of p53 on serine 15.
Lysates of HuH7, HuH6 and HepG2 cells expressing control shRNA or MKL1/2 shRNA were prepared and equal amounts of total protein were immunoblotted with anti-phospho p53 serine 15 and total anti-p53 antibodies.

6.2.17 Formation of senescence-associated heterochromatin foci (SAHF) in MKL1/2 depleted DLC1-deficient HCC cells

Another requirement for the induction of oncogene-induced senescence is the remodeling of chromatin structure. Cells undergoing senescence display the formation of facultative heterochromatin structures, termed senescence-associated heterochromatin foci that are specifically enriched with heterochromatin structures like histone 3 trimethylated on lysine 9 (H3K9me3) (Narita et al, 2003). Accumulation of SAHF suppresses the expression of proliferation-promoting genes like E2F target genes and induces the recruitment of Rb and other heterochromatin proteins (Adams, 2007; Narita et al, 2003). We tested whether MKL1/2 knockdown affects SAHF formation by analyzing the expression level of H3K9me3 (Di Micco et al, 2011). Expression of H3K9me3 was elevated in HuH7 and HuH6 cells upon MKL1/2 knockdown, but remained almost unchanged in HepG2 MKL1/2 KD cells (Figure 43).

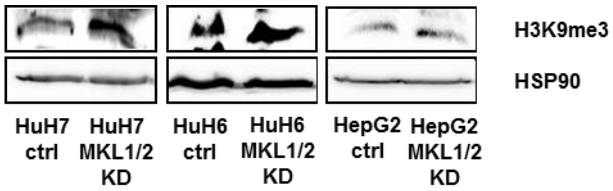

Figure 43: Formation of senescence-associated heterochromatin foci upon MKL1/2 knockdown.
Lysates of HuH7, HuH6 and HepG2 cells expressing control shRNA or MKL1/2 shRNA were prepared and equal amounts of total protein were immunoblotted with anti-H3K9me3 and total anti-HSP90 antibodies.

6.2.18 Senescence-messaging secretome – induction of CXCL10 and TNFSF10 expression in MKL1/2 depleted DLC1-deficient HCC cells

Senescent cells secrete a plethora of different interleukins, inflammatory cytokines and growth factors, collectively known as the senescence-messaging secretome (SMS) or senescence-associated secretory phenotype (SASP) (Coppe et al, 2010; Kuilman & Peeper, 2009). Induction of the SMS has multiple facets, it can feature pro-tumorigenic as well as tumor suppressive functions by reinforcing a permanent cell cycle arrest (Acosta et al, 2008a; Krtolica et al, 2001). Expression of the chemokine (C-S-C motif) ligand 10 (CXCL10) and tumor necrosis factor (ligand) superfamily member 10 (TNFSF10) promote the senescence response of human cancers (Braumuller et al, 2013). We analyzed the mRNA expression levels of CXCL10 and TNFSF10 in our HCC cell lines with a stable MKL1/2 knockdown. We found a significant upregulation of the CXCL10 mRNA expression in HuH7 MKL1/2 KD cells in comparison to the HuH7 control cells (Figure 44a). Besides, CXCL10 mRNA expression was 4-fold induced in HuH6 cells upon MKL1/2 knockdown whereas no effect was observed in HepG2 cells depleted of MKL1/2. Simultaneously, TNFSF10 mRNA expression was significantly increased in HuH7 MKL1/2 KD cells in contrast to HepG2 cells where MKL1/2 knockdown did not influence the mRNA expression levels of TNFSF10 (Figure 44b).

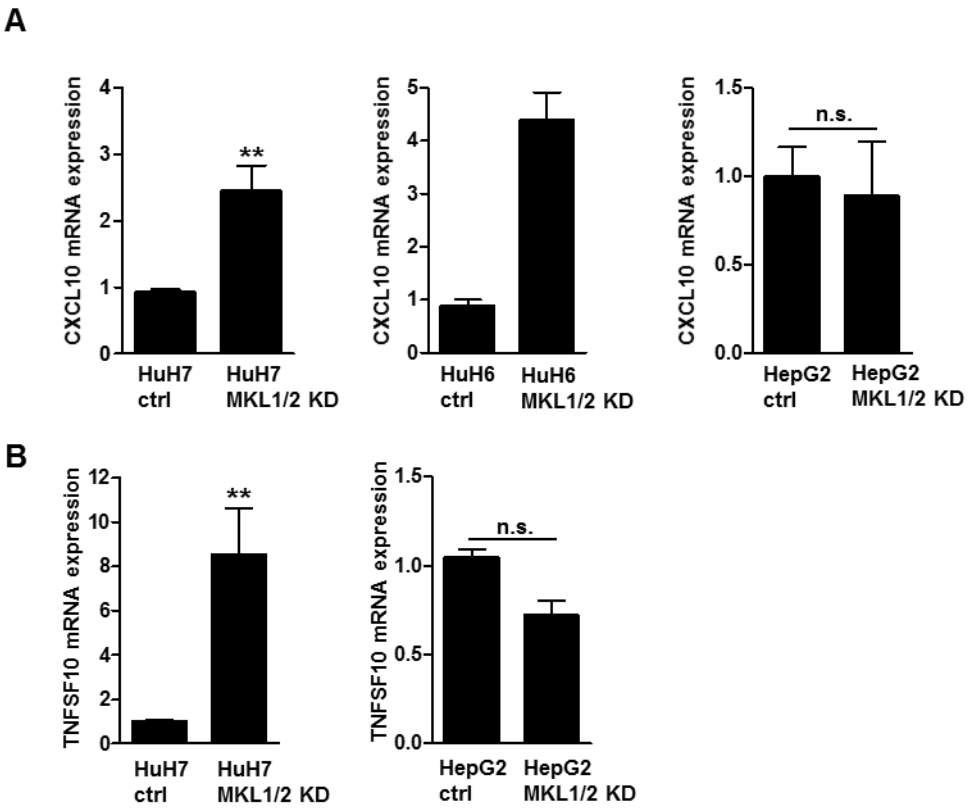

Figure 44: Upregulation of CXCL10 and TNFSF10 mRNA expression in DLC1-deficient HuH7 and HuH6 cells upon MKL1/2 depletion.
Total RNA was isolated from HuH7, HuH6 and HepG2 cells transduced with control shRNA or MKL1/2 shRNA and subjected to quantitative RT-PCR using (A) CXCL10 and (B) TNFSF10-specific primers. The amount of RNA of each sample was normalized to the endogenous housekeeping gene 18S rRNA. Shown is the fold increase of (A) CXCL10 and (B) TNFSF10 specific mRNA expression. Values are mean ± SD of three independent experiments. Quantification of HuH6 cells is based on two independent experiments.

6.2.19 Overexpression of the constitutively activated Ras allele (H-*Ras*V12) induces senescence in DLC1-deficient HCC cells

So far MKL1/2 depletion in DLC1-deficient HCC cells provokes a growth arrest. Evaluation of different senescence markers indicated that oncogene-induced senescence is the underlying mechanism of the growth arrest. Ras and its downstream targets were well established as inducers of the oncogene-induced senescence response (Michaloglou et al, 2005; Serrano et al, 1997; Zhu et al, 1998). Assuming that the increase of the Ras activity caused by MKL1/2 knockdown is the critical trigger for the induction of the oncogene-induced senescence response in DLC1-deficient HCC cells, we expressed the constitutively active ras allele (H-*ras*V12) in HuH7 and HuH6 cells. HuH7 and HuH6 cells were retrovirally transduced with a plasmid encoding human H-*Ras*V12 or with the corresponding control vector and at day 5 posttransduction the expression of the oncogene-induced senescence markers was evaluated by immunoblotting. Expression of constitutively active H-*ras*V12 in HuH7 and HuH6 cells induced increased phosphorylation of ERK1/2, accumulation of $p16^{Ink4a}$ expression, hypophosphorylation of Rb and enhanced phosphorylation of p53 on serine 15 (Figure 45). Obviously, the expression of active Ras triggered oncogene-induced senescence in human

hepatocellular carcinoma cells, deficient in DLC1. Expression of active Ras resulted in the same expression pattern of oncogene-induced senescence markers like MKL1/2 depletion. Therefore we conclude that the activation of Ras signaling upon MKL1/2 knockdown triggers the proliferation arrest caused by the oncogene-induced senescence response.

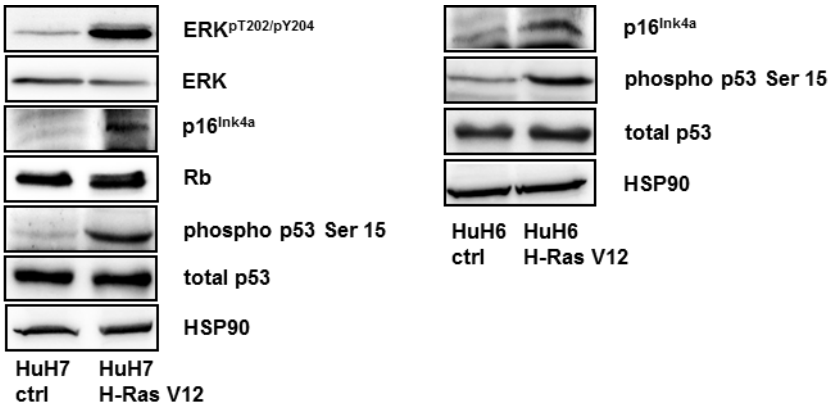

Figure 45: Expression of the constitutively active ras allel (H-*ras*V12) provokes oncogene-induced senescence in DLC1-deficient HCC cells.
HuH7 and HuH6 cells were retrovirally infected with pBabe H-RasV12 or pBabe control vector. At day 5 posttransduction, cells were harvested and lysed. Equal amounts of total protein were subjected to immunoblotting using anti-ERK$^{pT202/pY204}$, total anti-ERK, anti-p16^{Ink4a}, anti-Rb, anti-phospho p53 serine 15, total anti-p53 and anti-HSP90 antibodies.

6.2.20 Reconstitution of DLC1 expression in HuH7 cells induces cellular senescence

We recently published that MKL1/2 depletion counteracts the tumorigenic properties of loss of the tumor suppressor DLC1 in hepatocellular and breast carcinoma cells (Muehlich et al, 2012). To check whether MKL1/2 knockdown in DLC1-negative cells may substitute for the tumor suppressive function of DLC1, we generated a stable Tet-off HuH7 cell line expressing human GFP-DLC1 upon removal of doxycycline. HuH7 cells stably expressing the tet-responsive transactivator were transfected with human GFP-DLC1 which expression is regulated by a doxycycline regulated promoter. The expression vector of GFP-DLC1 coexpressed a hygromycin gene that allowed the selection of transfected cells. Removal of doxycycline induced the exogenous expression of DLC1 in HuH7 cells which featured a concomitant lower proliferation rate in comparison to HuH7 control cells lacking endogenous DLC1 expression (Figure 46a+b). Addition of doxycycline also slightly reduced the cell proliferation rate that was presumably due to the residual exogenous DLC1 as shown by immunoblotting. Flow cytometry analysis revealed that upon reconstitution of DLC1 expression HuH7 cells accumulated in the G1 phase and exhibited a concomitant reduction of the S-phase (Figure 46c).

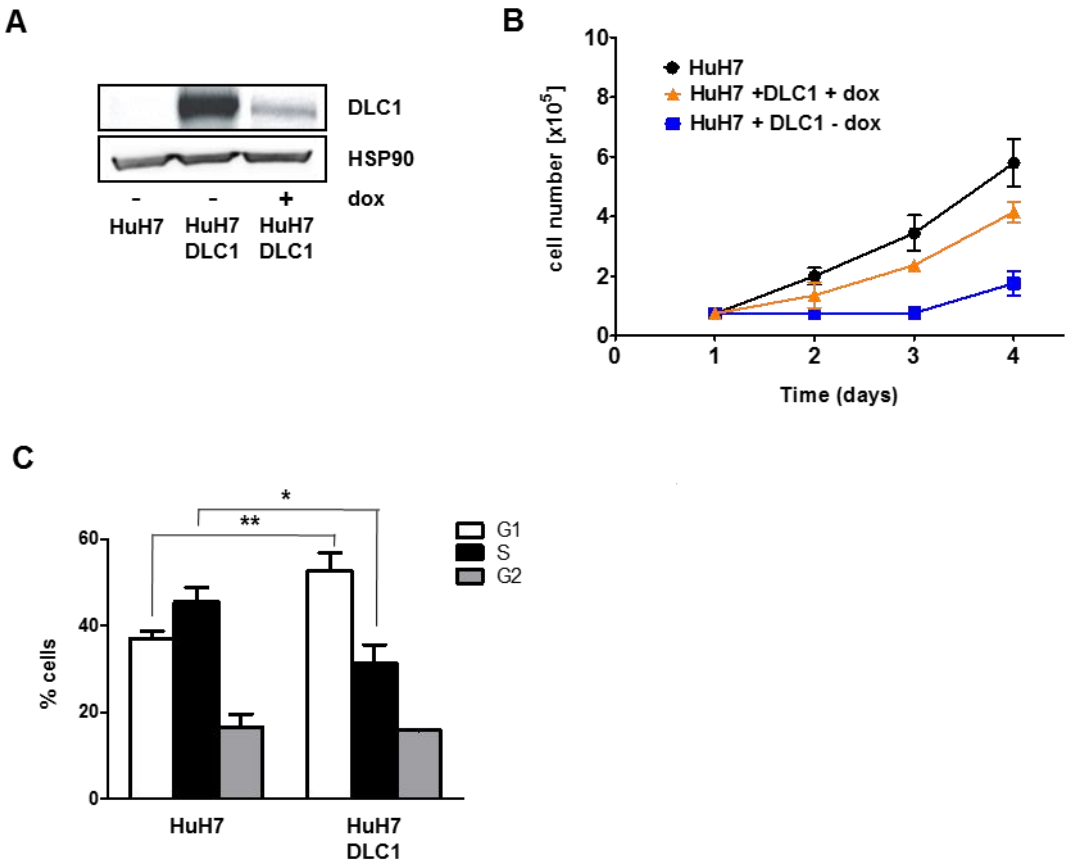

Figure 46: Reconstitution of DLC1 expression in DLC1-negative HuH7 cells reduces tumor cell proliferation.
(A) HuH7 cells stably expressing the tet-responsive transactivator (HuH7 Tet off) were transfected with a plasmid encoding human GFP-DLC1. Transfected cells were selected with hygromycin for 7 days and thereafter cells were treated with and without 0.5 µg/mL doxycycline (dox). Cells were harvested, lysed and equal amounts of total protein were subjected to immunoblotting using anti-DLC1 and anti-HSP90 antibodies. (B) The indicated cell lines were counted daily for 4 days. Values are mean ± SEM of two independent experiments. (C) Cell cycle phase distribution of HuH7 Tet-off and HuH7 Tet-off DLC1 cells in the absence of doxycycline was determined by flow cytometry analysis. Values are mean ± SD of three individual experiments. *Flow cytometry analysis was kindly done by Natalie Frank.*

As DLC1 reconstitution in HuH7 cells resembled to the effects of MKL1/2 depletion on tumor cell proliferation, we investigated if cellular senescence was the underlying mechanism. Overexpression of DLC1 significantly elevated the percentage of SA-ß-gal positive HuH7 cells (Figure 47a). DLC1-expressing HuH7 cells revealed an enlarged flat cell morphology and the cytoplasm was enriched with vacuoles (Figure 47a). Analysis of different senescence markers demonstrated that the reconstitution of DLC1 expression in HuH7 cells induced increased ERK1/2 phosphorylation, enhancement of $p16^{Ink4a}$ expression, hypophosphorylation of Rb, increased methylation of histone H3 at lysine 9 and enriched phosphorylation of p53 on serine 15 (Figure 47b). Addition of doxycycline eliminated the induction of the senescence markers. These data led to the conclusion that the induction of cellular senescence is part of the tumor suppressive properties of DLC1. In relation to our previous results we assume that downregulation of MKL1/2 expression mimics the effects of DLC1 reconstitution.

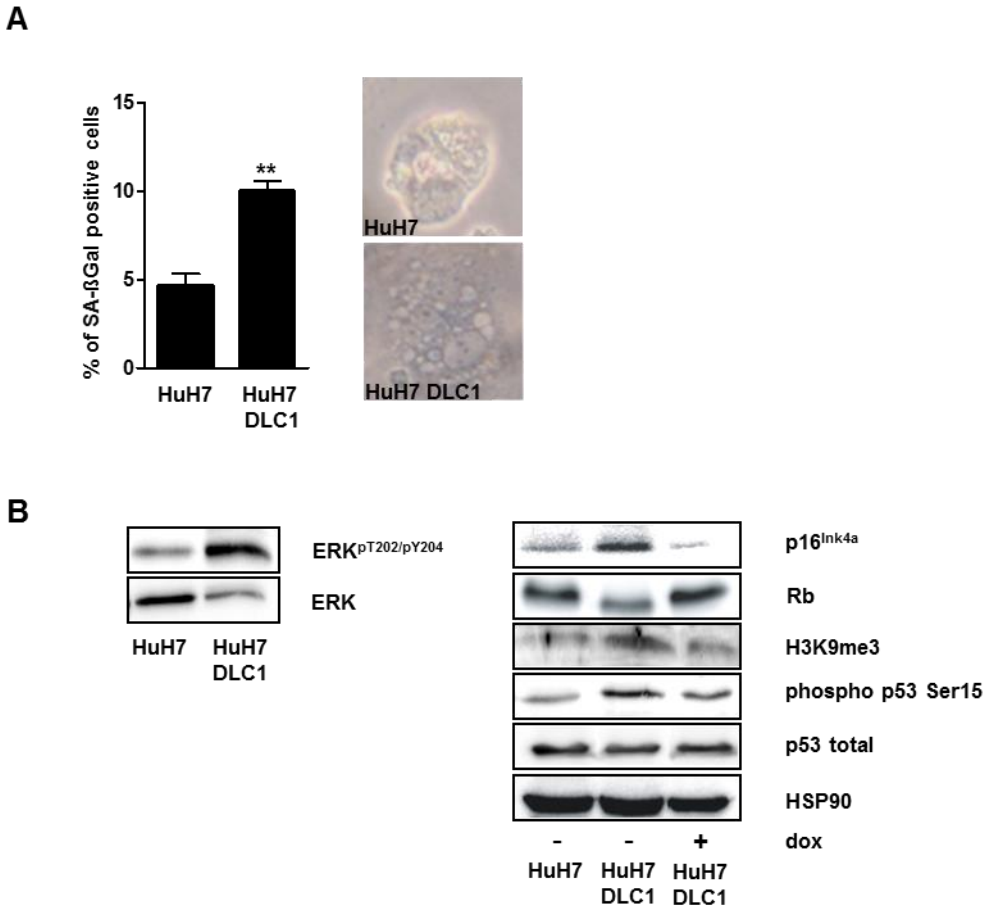

Figure 47 : Induction of cellular senescence in HuH7 cells upon DLC1 reconstitution.
(A) HuH7 Tet-off and HuH7 Tet-off DLC1 cells cultivated without doxycycline were assessed for senescence-associated ß-galactosidase activity. Values are mean ± SD of three independent experiments. Representative images of the cell morphology are shown. (B) HuH7 Tet-off and HuH7 Tet-off DLC1 cells cultivated without and with 0.5 µg/mL doxycycline (dox) were immunoblotted with anti-ERK$^{pT202/pY204}$, total anti-ERK, anti-p16^{Ink4a}, anti-Rb, anti-H3K9me3, anti-phospho p53 serine 15, total anti-p53 and anti-HSP90 antibodies. *(With experimental help of Claudia Martin)*

6.2.21 Evaluation of MKL1/2 as efficient anti-tumor targets *in vivo*

Our results obtained in vitro demonstrated that MKL1/2 represent efficient anti-tumor targets for the treatment of DLC1-deficient hepatocellular carcinoma cells by inducing the tumor suppressive oncogene-induced senescence response. A recently published study demonstrated that the injection of MKL1/2 depleted breast carcinoma cells into the mouse tail vein abolished the formation of lung metastases (Medjkane et al, 2009). However, there is little knowledge about the function role of MKL1/2 expression on tumor progression *in vivo*. One major aim of our study was to analyze the influence of MKL1/2 expression on the tumor growth of DLC1-deficient HCC cells *in vivo*. We decided to use a RNA-interference approach to evaluate the therapeutic efficacy of MKL1/2 downregulation as this method allows to explore the specific function of disease-related genes *in vivo*. The delivery of small molecules *in vivo* is very limited due to their instability, charge and low molecular weights and requires specific nanoparticle formulations for their *in vivo* application. SiRNA molecules were complexed with the low molecular weight branched polyethylenimine (PEI) F25-LMW which is well established as an efficient carrier system for the delivery of siRNA molecules *in vivo* due to its low

cytotoxicity and high biological activity (Hobel & Aigner, 2010; Hobel & Aigner, 2013). Polyethylenimine complexation protects siRNAs from nucleolytic degradation and allows the delivery of intact siRNA molecules into different organs like subcutaneous tumors, muscle, liver, kidney and to a lesser extent to lung and brain (Urban-Klein et al, 2005). Moreover, polyethylenimine complexation allows the systemic, intraperitoneal application of siRNA molecules which was preferred in our setting due to the higher relevance in a therapeutic setting (Hobel et al, 2010).

6.2.21.1 **Functional characterization of siRNAs targeting MKL1 and MKL2.**

First of all, we validated different siRNAs targeting MKL1 and MKL2 for their ability to efficiently downregulate the protein expression of MKL1 and MKL2 in HuH7 cells. We used an MKL1/2 siRNA that simultaneously targets both MKL1 and MKL2 and corresponds to the MKL1/2 shRNA sequence. Furthermore, we used a combination of MKL1 and MKL2-specific siRNAs and MKL1 siRNA alone, as we intended to examine the influence of a single knockdown. The results from immunoblotting indicated that the MKL1 and MKL2 specific siRNAs are sufficient to downregulate the protein expression of MKL1 and MKL2 in HuH7 cells (Figure 48a). Knockdown efficiency of the MKL1/2 siRNA had already been shown in chapter 6.2.12. For the evaluation of the functional depletion of MKL1 and MKL2, we examined the protein expression levels of the well-established MKL1/2 dependent target gene smooth muscle actin (Cen et al, 2003). As shown by immunoblotting, SMA protein expression was strongly suppressed in HuH7 cells transfected with MKL1/2 siRNA, MKL1+MKL2 siRNA and MKL1 siRNA (Figure 48b).

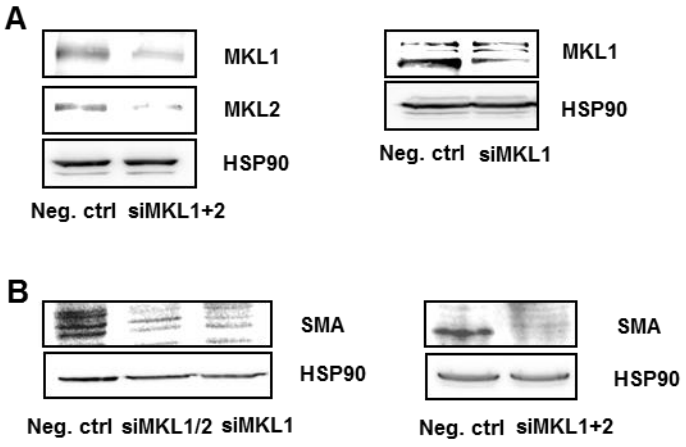

Figure 48: Validation of siRNAs targeting MKL1 and MKL2.
(A) HuH7 cells were transfected with either Neg. ctrl siRNA (50 nM), MKL1 siRNA (50 nM) or a combination of MKL1 and MKL2 siRNAs (each 25 nM). 48 hours after transfection, cells were harvested and equal amounts of total protein were immunoblotted with anti-MKL1, anti-MKL2 and anti-HSP90 antibodies. (B) Lysates of HuH7 cells transfected with Neg. ctrl siRNA, MKL1/2 siRNA, MKL1 siRNA or a combination of MKL1 and MKL2 siRNAs were prepared and equal amounts of total protein were subjected to immunoblotting using anti-SMA and anti-HSP90 antibodies.

6.2.21.2 Downregulation of MKL1/2 expression reduces tumor growth of DLC1-deficient HCC xenografts

To investigate whether MKL1/2 depletion affects the tumor growth of DLC1-deficient HCC cells *in vivo*, we aimed to treat well established tumor xenografts derived from HuH7 cells systemically by the intraperitoneal injection of PEI-complexed siRNAs targeting MKL1 and MKL2. Additionally, we were interested if MKL1 and MKL2 can act redundantly in the context of HCC tumor growth and intended therefore to evaluate the effect of the MKL1-specfic siRNA on tumor growth. For the generation of the subcutaneous tumors, HuH7 cells were implanted into the left and right flank of 6 week old female, athymic nude mice. Within 7 days solid tumors were established and mice were treated systemically by intraperitoneal injection of PEI complexed siRNAs three times a week. As control groups, we used mice which remained untreated and one control group was treated with PEI-complexed control siRNA that does not target known genes. 28 days after tumor cell implantation, the tumor growth of HuH7 derived xenografts treated with MKL1/2 and MKL1 specific siRNAs was completely suppressed (Figure 49a). By contrast, in the MKL1+2 specific treatment group, one out of six mice carried a tumor, but its tumor volume was lesser compared to the tumors of the control groups (Figure 49a). At day 28 after HuH7 cell injection, downregulation of MKL1 and MKL2 expression in the tumors was analyzed by quantitative real-time PCR. Tumors treated with MKL1+2 siRNA revealed a strong reduction of the mRNA expression levels of both MKL1 and MKL2 (Figure 49b). In addition, we found that the regression of the tumors of mice treated with MKL1+2 specific siRNA correlated with decreased mRNA expression of the proliferation marker Ki-67 (Figure 49c).

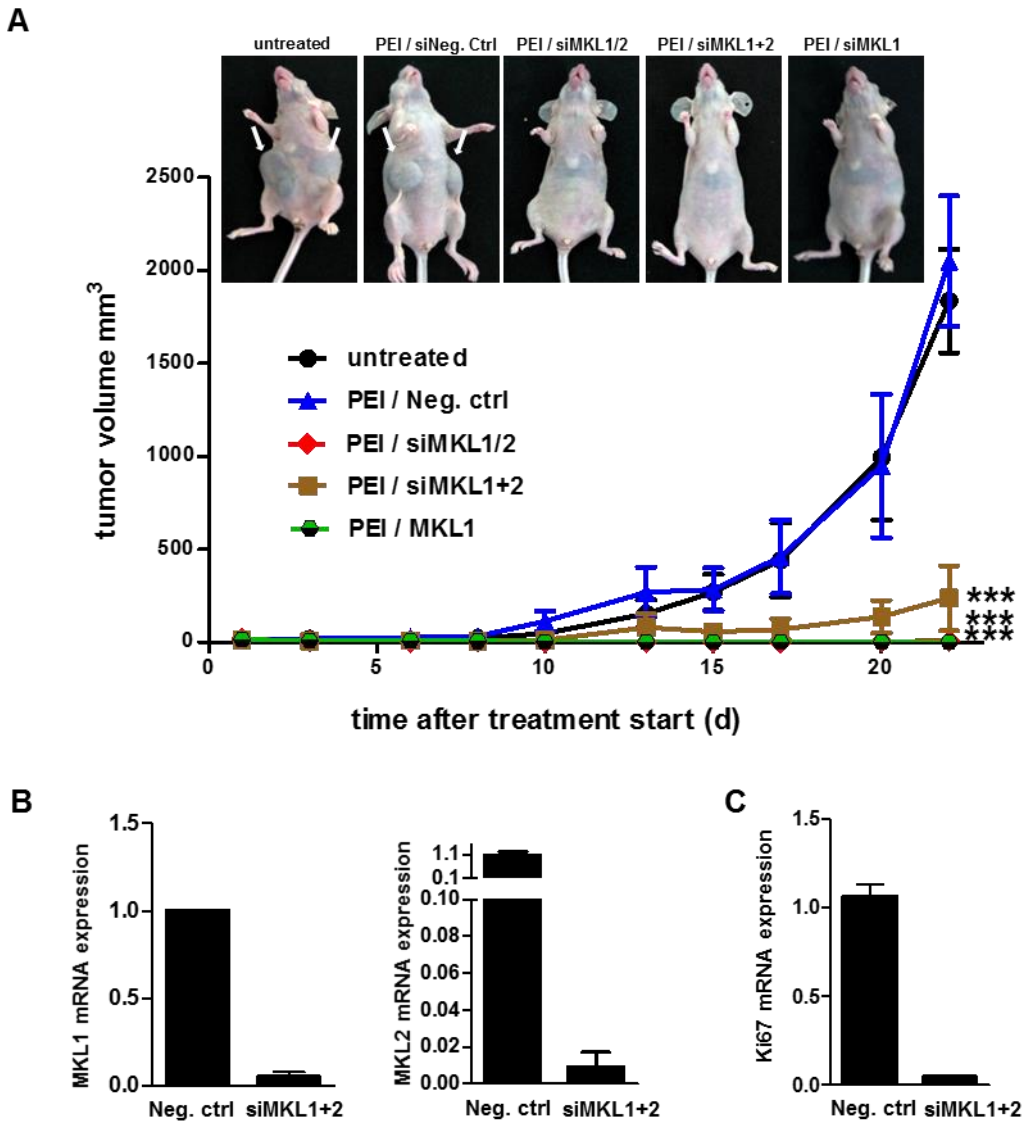

Figure 49: Anti-tumor effects of therapeutic MKL1/2 knockdown *in vivo*.
(A) HuH7 cells were subcutaneously injected into the right and left flank of 6-week old, female athymic nude mice. Upon establishment of subcutaneous HuH7 cells derived tumor xenografts, tumor-bearing mice were randomized into control and treatment groups. Three times per week, mice were systemically treated by intraperitoneal injection of 15 µg Neg. ctrl siRNA, MKL1/2 siRNA, MKL1+2 siRNA and MKL1-specific siRNA, each complexed with polyethylenimine (PEI). One control group remained untreated. Values are mean ± SEM. Upper panel represents example of mice of each treatment and control group and tumors are indicated by arrows.
(B) Total RNA from HCC xenografts treated with Neg. ctrl siRNA and MKL1+2 siRNA was isolated and subjected to quantitative RT-PCR using MKL1 and MKL2-specific primers. The RNA amount of each tumor sample was normalized to the endogenous housekeeping gene 18S rRNA. Shown is the fold decrease of MKL1 and MKL2 mRNA expression in MKL1+2 siRNA treated tumors in comparison to Neg. ctrl siRNA treated tumors. Values are expressed as mean ± SD of two independent RNA isolations from one xenograft specimen.
(C) Relative Ki-67 mRNA expression of MKL1+2 siRNA and Neg. ctrl siRNA treated tumors was determined by quantitative real-time PCR as described in (B) using Ki-67-specific gene primers. Values are represented as mean ± SD of two independent RNA isolations from one xenograft specimen.

6.2.21.3 MKL1/2 depletion in HCC xenografts induces senescence *in vivo*

Our findings demonstrated that depletion of MKL1/2 inhibited growth of DLC1-deficient HCC xenografts. These findings prompted us to investigate the underlying molecular mechanism of the observed tumor growth inhibition *in vivo*. We analyzed the HCC xenografts from mice treated with MKL1+2 specific siRNA for the different oncogene-induced senescence markers which were regulated by the MKL1/2 knockdown mediated oncogene-induced senescence

response in vitro. The results from the quantitative real-time PCR analysis showed strongly induced $p16^{Ink4a}$ mRNA expression levels in MKL1+2 siRNA treated tumors in comparison to neg. ctrl treated tumors (Figure 50a). Results from immunoblotting revealed increased expression levels of histone H3 methylated on lysine 3 (H3K9me3) and an accumulation of p53 phosphorylated on serine 15 in tumors of mice treated with MKL1+2 siRNA (Figure 50b). Additionally, we detected enhanced CXCL10 mRNA expression in MKL1+2 siRNA treated tumors that has been identified as a component of the senescence-messaging secretome upon MKL1/2 knockdown (Figure 50c). These data demonstrate that downregulation of MKL1 and MKL2 expression inhibits HCC xenograft growth by inducing senescence *in vivo*.

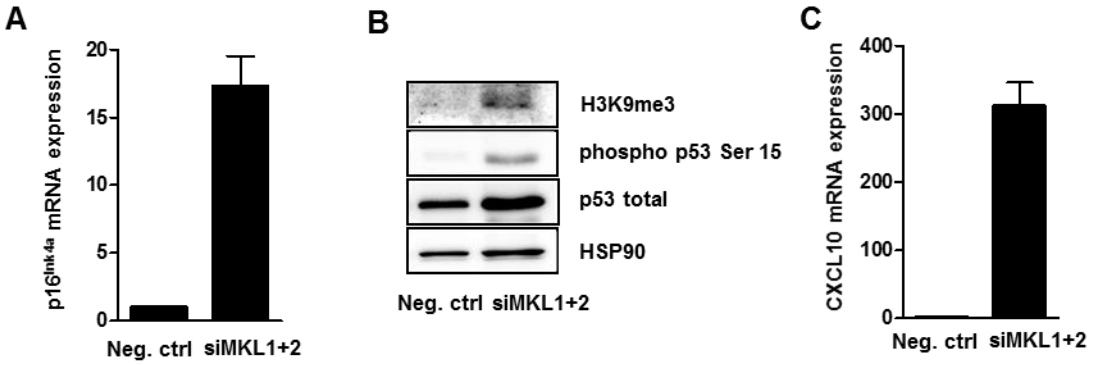

Figure 50: MKL1/2 downregulation induces senescence *in vivo*.
(A) Total RNA from HCC xenografts treated with Neg. ctrl siRNA and MKL1+2 siRNA was isolated and subjected to quantitative RT-PCR using $p16^{Ink4a}$ -specific primers. The RNA amount of each tumor sample was normalized to the endogenous housekeeping gene 18S rRNA. Shown is the fold induction of $p16^{Ink4a}$ mRNA expression in MKL1+2 siRNA treated tumors in comparison to Neg. ctrl siRNA treated tumors. Values are expressed as mean ± SD of two independent RNA isolations from one xenograft specimen. (B) Lysates from xenografts treated with either Neg. ctrl siRNA or MKL1+2 siRNA were prepared and equal amounts of total protein were analyzed by immunoblotting using anti-H3K9me3, anti-phospho p53 serine 15, total anti-p53 and anti-HSP90 antibodies. (C) Relative CXCL10 mRNA expression of Neg. ctrl siRNA and MKL1+2 siRNA treated tumors was analyzed by quantitative RT-PCR as described in (A) using CXCL10-specific gene primers. Values are expressed as mean ± SD of two independent RNA isolations from one xenograft specimen.

6.2.22 MKL1/2 knockdown does not influence the RhoA activity of DLC1-deficient HuH7 cells

Our data provided evidence that MKL1/2 depletion activated oncogenic Ras signaling in DLC1-deficient HCC cells thereby triggering the oncogene-induced senescence response. However, it remained to be clarified how MKL1/2 depletion can mechanistically induce Ras activation by enhancing the GTP-bound levels of Ras. An inverse correlation between RhoA and ERK activity was reported by Morin and colleagues who showed a reduced ERK activity in cells overexpressing constitutively active RhoA (Morin et al, 2009). As DLC1-deficient carcinoma cells are characterized by constitutive activation of RhoA, we tested whether activation of Ras-ERK signaling upon MKL1/2 depletion was due to changes in the RhoA activity. We studied the RhoA activation status in HuH7 cells expressing control shRNA and MKL1/2 shRNA by a RhoA GLISA assay. The amount of active GTP-bound RhoA was not changed upon MKL1/2

depletion in HuH7 cells (Figure 51). We concluded that MKL1/2 knockdown does not influence the RhoA activity.

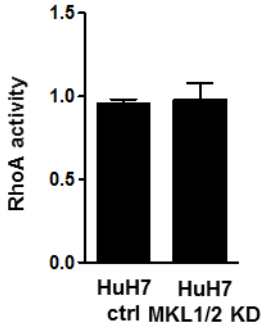

Figure 51: RhoA activation status in MKL1/2 depleted HuH7 cells.
Active RhoA-GTP levels of HuH7 cells expressing either control shRNA or MKL1/2 shRNA were assessed by an ELISA assay. Values are mean ± SD of three independent experiments.

6.2.23 MKL1/2 depletion does not affect the expression levels of mig6

We hypothesized that a target gene of MKL1/2 could mediate the effect on Ras activation. Descot and colleagues had described a negative feedback mechanism between the actin-MKL1 and the EGFR-MAPK signaling pathway via the MKL target gene mig6 (Descot et al, 2009). To learn whether mig6 has an influence on the activation of the MAPK cascade in our model, we determined the mig6 mRNA expression levels in MKL1/2 depleted HuH7 cells. Quantitative RT-PCR analysis revealed no distinctive difference in the amount of mig6 mRNA expression levels between MKL1/2 depleted HuH7 cells and the corresponding control cells (Figure 52). Obviously, mig6 expression is not addressed by MKL1/2 in DLC1-deficient hepatocellular carcinoma cells.

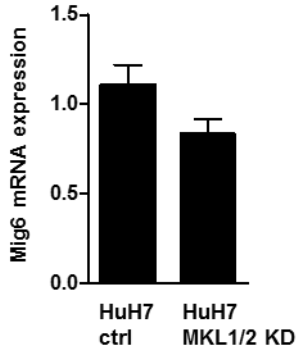

Figure 52: Mig6 mRNA expression in MKL1/2 depleted HuH7 cells.
Total RNA from HuH7 cells expressing control shRNA or MKL1/2 shRNA was isolated and subjected to quantitative RT-PCR using mig6-specific primers. The amount of RNA of each sample was normalized in respect to the endogenous housekeeping gene 18S rRNA. Shown is the fold change of mig6-specific mRNA expression. Data are represented as mean ± SD of two independent experiments.

6.3 Identification and characterization of novel MKL1/2 dependent target genes in DLC1-deficient hepatocellular carcinoma cells

6.3.1 DNA-microarray analysis of MKL1/2 depleted HuH7 cells

It appears that depletion of MKL1/2 expression abolish the tumor growth of hepatocellular carcinomas with DLC1-deficiency. We aimed to identify target genes that are regulated by MKL1/2 expression and are functionally implicated the in the regression of the tumor growth. We analyzed the transcriptome of HuH7 control cells and MKL1/2 depleted HuH7 cells by a DNA-microarray study. To identify the target genes which expression was controlled MKL1/2 signaling, we compared the datasets of both settings and found that 8 genes were downregulated more than 2.5 fold upon MKL1/2 depletion (Table 4).

gene assignment	gene symbol	fold change	p-value
NM_001152	Transgelin / smooth muscle protein 22-alpha (SM22)	6.42	0.0047
NM_006851	GLI pathogenesis – related 1 (GLIPR1)	5.68	0.0010
NM_001299	Calponin (CNN1)	5.58	0.005
NM_002473	Heavy chain 9, non – muscle MYH9	4.78	0.014
NM_000660	Transforming growth factor beta 1 (TGFß1)	3.82	0.015
NM_016206	Vestigial like 3 (VGLL3)	3.67	0.0083
NM_005909	Microtubule-associated protein 1B (MAPB1)	3.17	0.0012
NM_013451	Myoferlin (MYOF)	2.86	0.0063

Table 4: DNA-microarray based transcriptome analysis of MKL1/2 depleted HuH7 cells.
The transcriptome of HuH7 cells expressing either control shRNA or MKL1/2 shRNA was analyzed by a DNA microarray analysis. Genes are sorted according to the average fold of downregulation upon MKL1/2 depletion and the corresponding p-values are given. The threshold for MKL1/2 dependence was taken as 2.5 fold downregulation.

We validated the results obtained from DNA microarray analysis by quantitative real-time PCR analysis. Our data confirmed that MKL1/2 depletion in the DLC1-deficient HuH7 cells significantly suppressed the mRNA expression levels of transgelin (SM22), GLI-pathogenesis related 1 (GLIPR1), calponin (CNN1), heavy chain 9, non-muscle (MYH9), transforming growth factor beta 1 (TGFß1), vestigial like 3 (VGLL3), microtubule-associated protein 1B (MAPB1) and myoferlin (MYOF) (Figure 53). We concluded that the expression of these target genes are regulated by the transcriptional coactivators MKL1 and MKL2 in the DLC1-negative HuH7 cells. Numerous gene expression studies already reported that the expression of transgelin is controlled by MKL/SRF dependent signaling in different cell types like human fibroblasts or smooth muscle cells (Cen et al, 2003; Descot et al, 2009; Du et al, 2004; Wang et al, 2002). Calponin was described as a target gene which expression is regulated by actin-MKL1 signaling (Descot et al, 2009). A recent conducted gene expression analysis in human breast

carcinoma cells revealed that MYH9 and VGLL3 are target genes of MKL1/2 (Medjkane et al, 2009). Notably, MKL1/2 dependent target gene expression of GLIPR1, TGFß1, MAP1B and MYOF has not been noticed before and constitute a novel cluster of target genes which expression is regulated by MKL1/2 signaling in DLC1-deficient HuH7 cells.

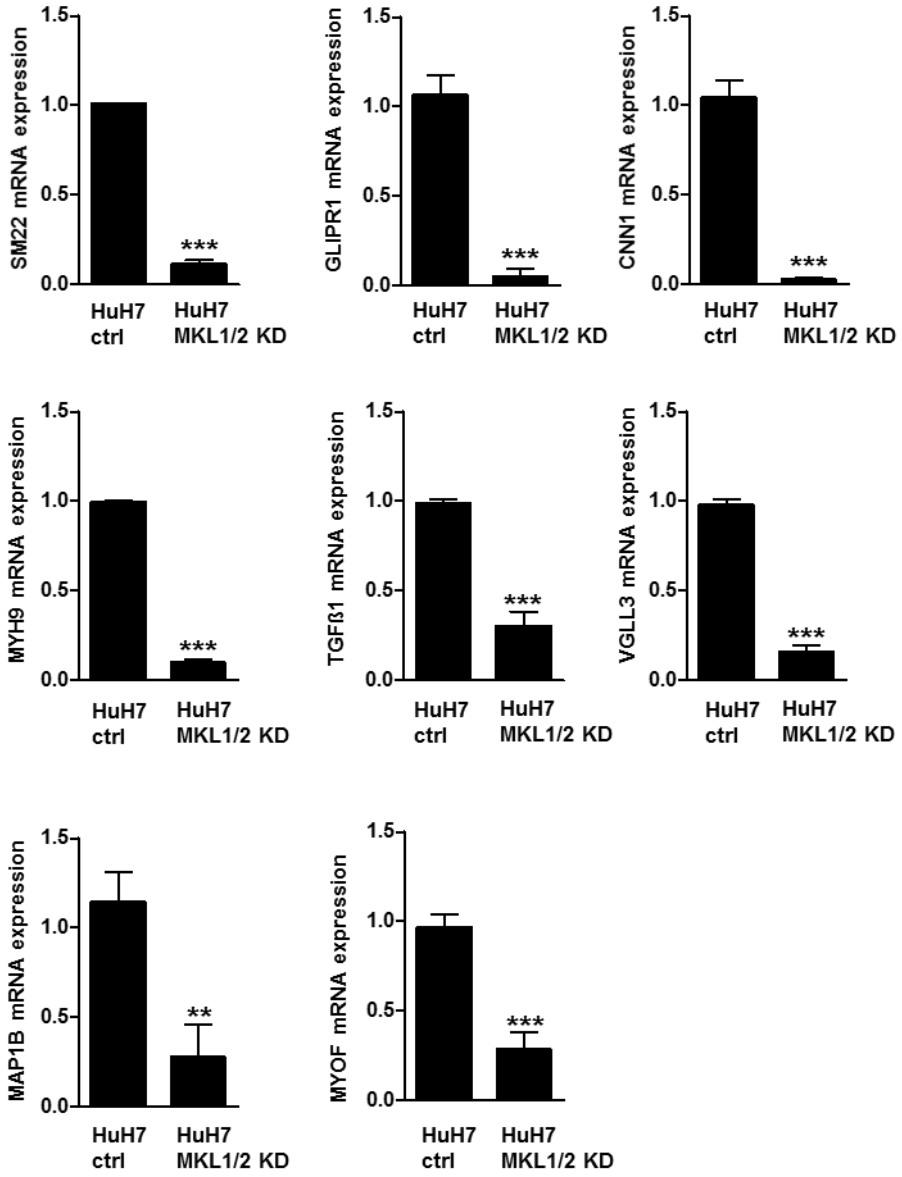

Figure 53: Validation of MKL1/2 dependent target gene expression in HuH7 cells.
HuH7 cells were lentivirally transduced with either control shRNA or MKL1/2 shRNA and total RNA was extracted. MRNA expression was measured by quantitative RT-PCR using gene specific primers for SM22, GLIPR1, CNN1, MYH9, TGFß1, VGLL3, MAPB1 and MYOF. The amount of each RNA sample was normalized to the endogenous housekeeping gene 18S rRNA. Shown is the fold decrease of gene specific mRNA expression of MKL1/2 depleted HuH7 cells in comparison to HuH7 control cells. Values are represented as mean ± SD of three independent experiments.

Next we analyzed their mRNA expression levels in HuH7 cells derived tumor xenografts that were treated with MKL1+2 specific siRNA as described in chapter 6.2.21.2.

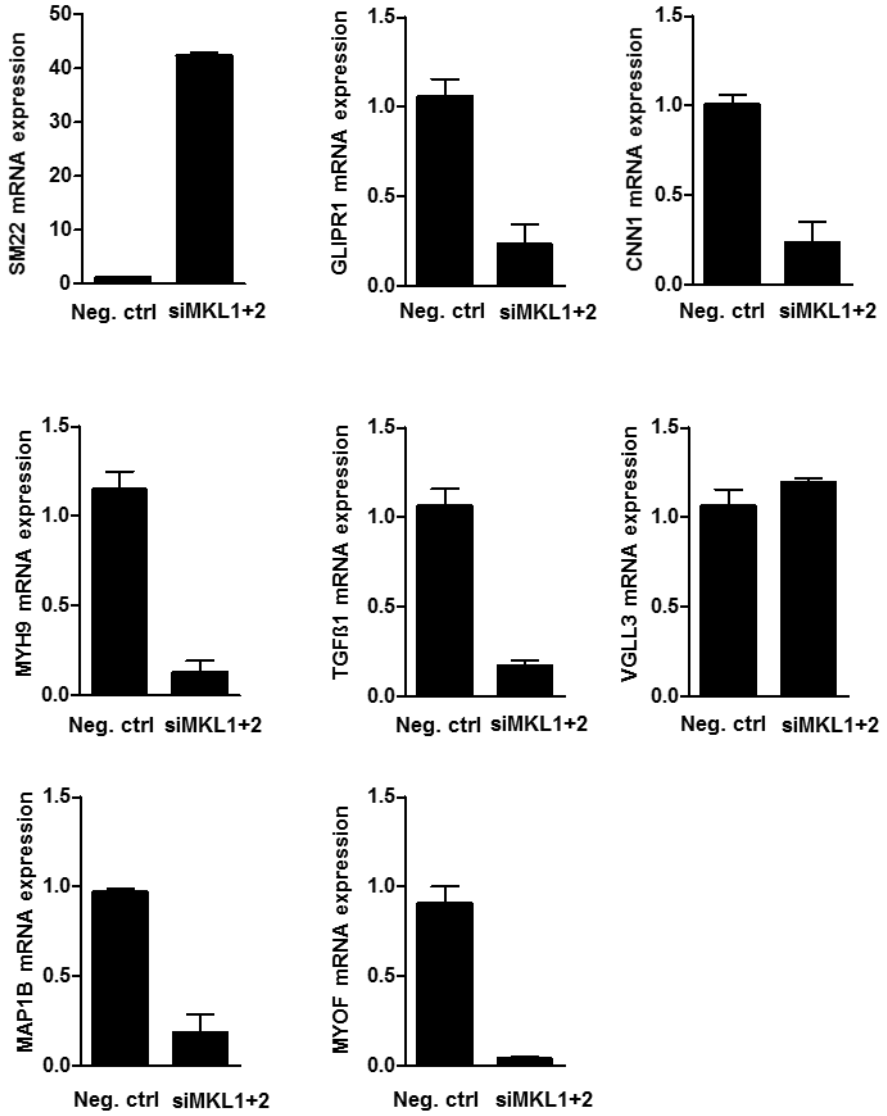

Figure 54: Analysis of the MKL1/2 dependent target gene expression in HCC xenografts *in vivo*.
Total RNA from xenografts treated with either PEI/Neg. ctrl siRNA or PEI/MKL1+2 specific siRNA was isolated and subjected to quantitative RT-PCR using gene specific primers for SM22, GLIPR1, CNN1, MYH9, TGFß1, VGLL3, MAPB1 and MYOF. The RNA amount of each tumor sample was normalized with respect to the endogenous housekeeping gene 18S rRNA. Shown is the fold change of gene specific mRNA expression in PEI/MKL1+2 siRNA treated tumors in comparison to PEI/Neg. ctrl siRNA treated tumors. Values are represented as mean ± SD of two RNA isolations from one xenograft specimen.

Results from quantitative RT-PCR analysis revealed that mRNA expression of GLIPR1, CNN1, MYH9, TGFß1, MAPB1 and MYOF was strongly reduced in tumors from mice treated with PEI/MKL1+2 siRNA in comparison to tumors treated with PEI/Neg.ctrl siRNA (Figure 54). On the contrary, SM22 mRNA expression was upregulated in xenografts treated with MKL1+2 specific siRNA. Therefore the observed upregulation of SM22 mRNA expression *in vivo* is opposite to the downregulation of SM22 expression upon MKL1/2 depletion in vitro. VGLL3 mRNA expression levels were not reduced upon MKL1/2 knockdown *in vivo* suggesting that VGLL3 expression is not influenced by MKL1/2 in HCC xenograft growth *in vivo*.

6.3.2 Regulation of MYOF expression by the transcriptional coactivators MKL1/2

In order to prove that MYOF expression is regulated by the transcriptional coactivators MKL1 and MKL2, we studied the influence of exogenous expression of MKL1 on MYOF expression. HuH7 cells were transiently transfected with MKL1+2 specific siRNA. As the MKL1-specific siRNA targets MKL1 within the first 100 N-terminal amino acids, MKL1 expression was reconstituted by the transfection of the siRNA-resistant ΔN100 MKL1 mutant lacking the first 100 N-terminal amino acids of MKL1 that contain the RPEL motifs required for actin binding. It was shown that the ΔN100 MKL1 mutant is nuclear localized and is transcriptionally constitutively activated (Miralles et al, 2003). MYOF mRNA expression analysis by quantitative real-time PCR illustrated that MYOF mRNA expression was significantly reduced upon MKL1/2 knockdown in comparison to HuH7 cells transfected with inert siRNA. In contrast, exogenous expression of the ΔN100 MKL1 mutant in MKL1/2 depleted HuH7 cells induced a 4-fold upregulation of MYOF mRNA expression compared to the control cells (Figure 55a). Expression of the ΔN100 MKL1 mutant was analyzed by immunoblotting for its expression of the Flag-tag (Figure 55b). Downregulation of MKL1 expression in MKL1+2 specific siRNA transfected HuH7 cells was confirmed by immunoblotting (Figure 55b). Reconstitution of MKL1 expression was shown by enhanced MKL1 protein expression levels. Thus, MYOF gene expression was directly controlled by transcriptional coactivators MKL1 and MKL2.

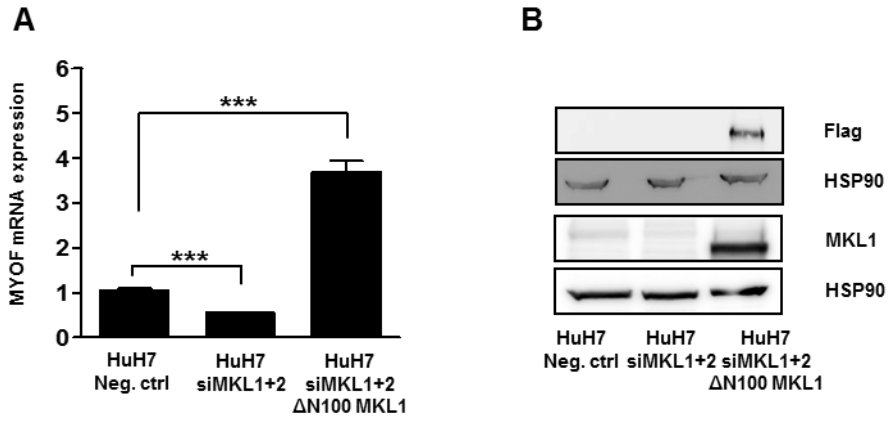

Figure 55: MYOF mRNA expression is directly regulated by the transcriptional coactivators MKL1 and MKL2.

(A) HuH7 cells were transiently transfected with Neg. ctrl siRNA (50 nM) and MKL1 and MKL2 specific siRNAs (each 25 nM). After 18 hours, cells were transfected with a DNA plasmid encoding the Flag-ΔN100 MKL1 mutant. After additional 24 hours, cells were harvested and total cellular RNA was extracted and subjected to quantitative RT-PCR using MYOF-specific gene primers. The amount of RNA each sample was normalized with respect to the endogenous housekeeping gene 18S rRNA. Shown is the fold change of MYOF mRNA expression referring to HuH7 cells transfected with Neg. ctrl siRNA. Values are mean ± SD of three independent experiments. (B) Lysates of HuH7 cells transfected as described in (A) were prepared and equal amounts of total protein were immunoblotted with anti-Flag, anti-MKL1, anti-MKL2 and anti-HSP90 antibodies.

6.3.3 Myoferlin is a SRF dependent target gene

To date, MYOF has not been functionally characterized as a SRF target gene nor has a conserved SRF binding site within the promoter of MYOF been reported. As MKL1/2 were transcriptional coactivators of the nuclear transcription factor SRF, we were interested whether MYOF expression directly depends on the expression of SRF. HuH7 cells were transfected with siRNA targeting SRF and afterwards MYOF expression was analyzed by quantitative real-time PCR. The results demonstrated that downregulation of SRF mRNA expression in HuH7 cells simultaneously reduced MYOF mRNA expression (Figure 56). This put MYOF in the position as a novel SRF target gene and we assumed that a SRF binding site resides within the transcription start site of the MYOF gene.

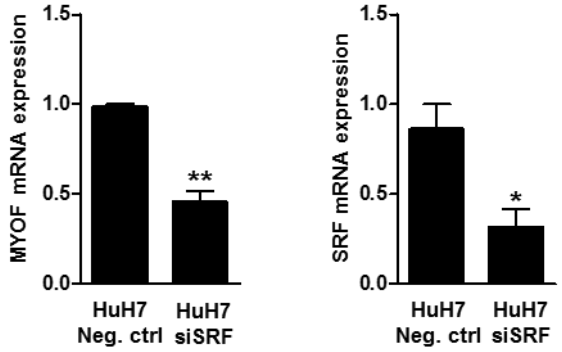

Figure 56: Myoferlin expression depends on SRF expression.
HuH7 cells were transiently transfected with Neg. ctrl siRNA and SRF-specific siRNA (50 nM). 72 hours after transfection, total RNA was extracted and subjected to quantitative RT-PCR using SRF and MYOF-specific primers. The amount of each sample was normalized to 18S rRNA expression. Shown is fold change of mRNA expression of SRF-specific siRNA transfected HuH7 cells in comparison to Neg. ctrl transfected HuH7 cells. Values are expressed as mean ± SD of three independent experiments.

6.3.4 Downregulation of DLC1 expression activates mRNA expression of myoferlin

MYOF was identified as a gene the expression of which is regulated by MKL/SRF signaling in hepatocellular carcinoma cells lacking endogenous DLC1 expression. We aimed to identify whether the expression level of DLC1 has an influence on the MKL/SRF dependent target gene expression of MYOF. DLC1 expression was downregulated in HepG2 cells via an RNAi mediated approach and the resulting MYOF mRNA expression levels were determined by quantitative real-time PCR. Transfection of endogenous DLC1-expressing HepG2 cells with DLC1-specific siRNA strongly reduced the mRNA expression levels of DLC1 compared to HepG2 cells transfected with Neg. ctrl siRNA (Figure 57). In contrast, downregulation of DLC1 expression led to a significant upregulation of MYOF mRNA expression. These findings indicate that loss of DLC1 promotes MYOF expression. We concluded that increased MYOF expression upon DLC1 downregulation was due to the nuclear localization of MKL1/2 that was linked to the activation of the transcription of MKL/SRF dependent target genes.

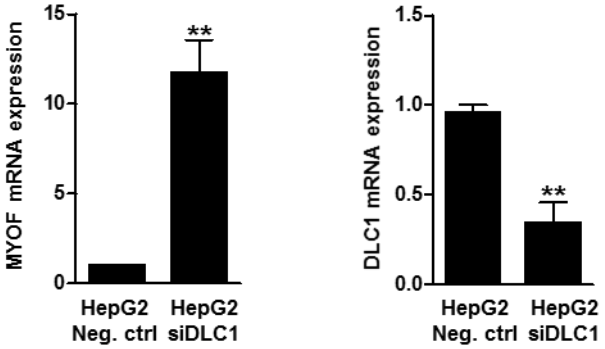

Figure 57: Downregulation of DLC1 expression increases MYOF mRNA expression.
HepG2 cells were transfected with Neg. ctrl siRNA or DLC1-specific siRNA (50 nM) and 96 hours after transfection, total RNA was isolated. MRNA expression was measured by quantitative RT-PCR analysis using gene specific primers for DLC1 and MYOF. The RNA amount of each sample was normalized with respect to 18S rRNA expression. Shown is the fold change of DLC1 and MYOF mRNA expression in HepG2 cells transfected with DLC1-specific siRNA in comparison to Neg. ctrl transfected HepG2 cells. Values are means ± SD of three independent experiments.

6.3.5 Knockdown of myoferlin reduces tumor cell invasion of HuH7 cells

To investigate the functional role of MYOF expression in DLC1-deficient hepatocellular carcinoma cells, we analyzed its effect on tumor cell invasion. MYOF expression was silenced by an RNAi approach in HuH7 cells, and we analyzed their ability to invade through inserts coated with extracellular matrix (ECM) in response to FCS stimulation as a chemoattractant for a period of 24 hours. Reduction of MYOF expression strongly diminished the number of invaded HuH7 cells compared to the control cells (Figure 58a). Downregulation of MYOF expression in HuH7 cells transfected with MYOF-specific siRNA was confirmed by immunoblotting (Figure 58b). Essentially, MYOF expression affects the invasiveness of hepatocellular carcinoma cells characterized by a DLC1-deficient background.

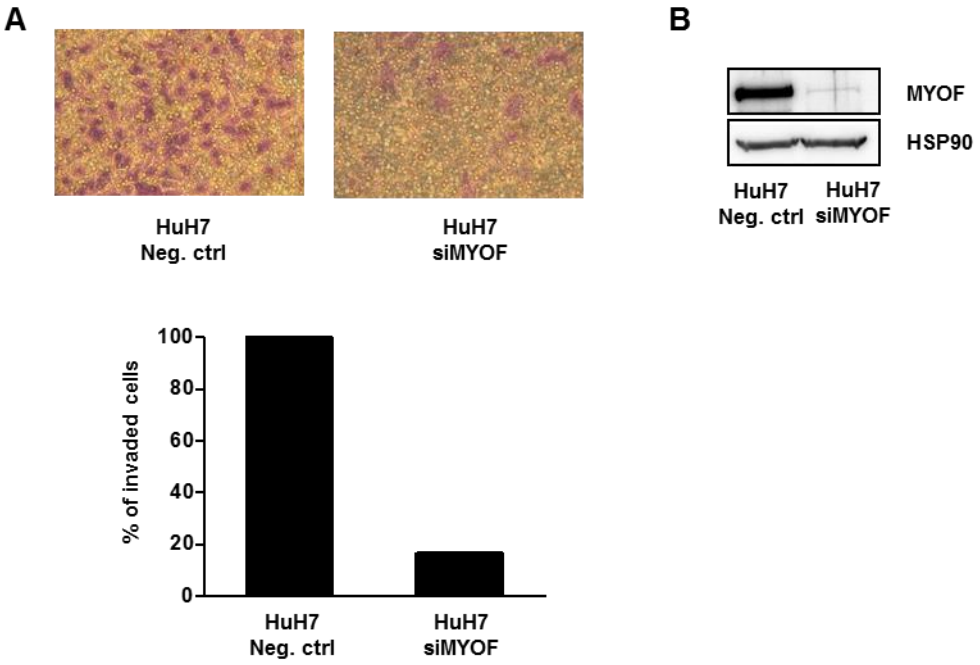

Figure 58: Myoferlin depletion inhibits tumor cell invasion of HuH7 cells.
(A) HuH7 cells were transfected with Neg. ctrl siRNA and MYOF-specific siRNA (50 nM). 48 hours after transfection, cells were seeded into the upper well of a Transwell® insert and allowed to invade through extracellular matrix towards the lower chamber containing 10 % FCS for a period of 24 hours. Invaded cells were fixed with methanol and visualized by toluidine blue staining. Representative images are shown. The graph illustrates the relative invasion of HuH7 cells with Neg. ctrl siRNA transfected HuH7 cells set to 100 %. (B) Lysates of cells transfected as described in (A) were prepared and equal amounts of total protein were subjected to immunoblotting using the anti-MYOF antibody. Loading was controlled by re-probing the blot for HSP90.

6.3.6 Depletion of myoferlin inhibits tumor cell proliferation of HuH7 cells

To study the influence of MYOF expression on tumor cell proliferation, we generated a cell line with stable knockdown of MYOF that allows long-term analysis of cell proliferation. HuH7 cells were transduced with a shRNA vector that targets specifically human MYOF. The shRNA expression vector coexpressed a puromycin-resistance gene that enabled the selection of transduced cells within 7 days. As shown by immunoblotting, lentiviral transduction of HuH7 cells with MYOF shRNA strongly reduced the protein expression levels of MYOF (Figure 59a). Analysis of the cell proliferation demonstrated that downregulation of MYOF expression significantly inhibited the proliferation rate of HuH7 cells in comparison to the control cells

(Figure 59b). These findings highlighted that MYOF expression influences the cell proliferation of DLC1-deficient hepatocellular carcinoma cells.

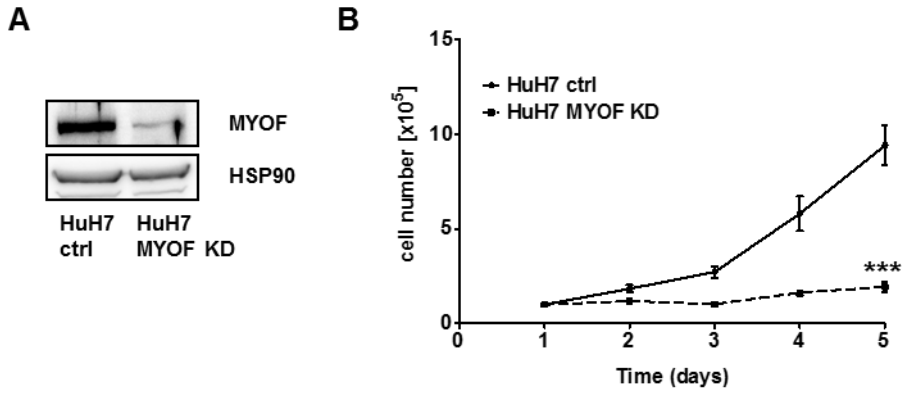

Figure 59: Myoferlin depletion inhibits tumor cell proliferation of HuH7 cells.
(A) HuH7 cells expressing control shRNA or MYOF shRNA were lysed and equal amounts of total protein were immunoblotted using anti-MYOF antibody. Loading was controlled by re-probing the blot for HSP90. (B) Indicated HuH7 cells were counted daily for 5 days. Values are expressed as mean ± SEM of three independent experiments.

6.3.7 Depletion of myoferlin augments senescence-associated ß-galactosidase activity

The effect of MYOF expression on tumor cell proliferation attracted our interest as MKL1/2 depletion caused the identical phenotype by the induction of cellular senescence. Was cellular senescence the underlying mechanism of the growth arrest upon MYOF depletion? We assessed MYOF-depleted HuH7 cells for their senescence-associated ß-galactosidase activity. Quantification demonstrated that downregulation of MYOF expression highly augmented the percentage of SA-ß-gal positive HuH7 cells (Figure 60). These findings showed that MYOF depletion triggers the phenotype of cellular senescence that is commensurate with the observed anti-proliferative effect.

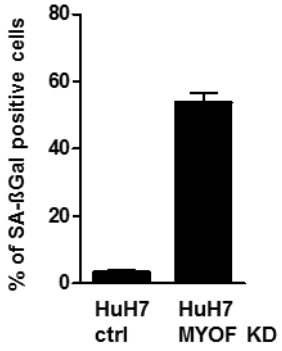

Figure 60: Increased senescence-associated ß-galactosidase activity in HuH7 cells upon MYOF depletion.
HuH7 cells expressing control shRNA or MYOF shRNA were stained for senescence-associated ß-galactosidase activity. The number of SA-ß-gal positive HuH7 cells was counted under an inverted microscope.

6.3.8 Increased ERK1/2 phosphorylation upon myoferlin depletion

Next, we intended to analyze whether MYOF depletion in HuH7 cells is able to induce the senescence response via activation of the Raf-MEK-ERK1/2 pathway that has already been shown for MKL1/2 depletion. We tested for ERK1/2 activation by determining its phosphorylation status. The results from immunoblotting revealed that ERK1/2 phosphorylation was strongly increased upon MYOF depletion in HuH7 cells. This effect was comparable to the extent of ERK1/2 phosphorylation upon MKL1/2 knockdown. Determination of the MYOF protein expression levels revealed that increased ERK1/2 phosphorylation was due to the reduction of MYOF expression upon MYOF and MKL1/2 knockdown in HuH7 cells (Figure 61). This is evidence for the MKL1/2 dependent target gene MYOF leading to the activation of MAP kinase signaling, thereby inducing the senescence response.

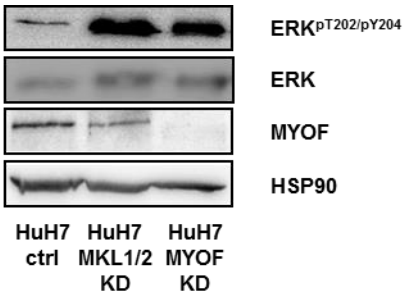

Figure 61: Increased phosphorylation of ERK1/2 upon downregulation of MYOF expression.
HuH7 cells stably expressing either control shRNA, MKL1/2 shRNA or MYOF shRNA were lysed and equal amounts of total protein were immunoblotted with anti-ERK$^{pT202/pY204}$, total anti-ERK, anti-MYOF and anti-HSP90 antibodies.

6.3.9 Myoferlin depletion induces oncogene-induced senescence in DLC1-deficient HuH7 cells

To corroborate our findings we assessed MYOF-depleted HuH7 cells for their expression of the oncogene-induced senescence markers $p16^{Ink4a}$ and the phosphorylation status of p53 on serine 15. In contrast to HuH7 control cells, MYOF depleted HuH7 cells revealed a strong accumulation of $p16^{Ink4a}$ protein expression. Phosphorylation of p53 on serine 15 was clearly enhanced upon MYOF downregulation in HuH7 cells (Figure 62). This was evidence that MYOF depletion in DLC1-deficient HuH7 cells abrogates cell proliferation via activation of the oncogene-induced senescence response.

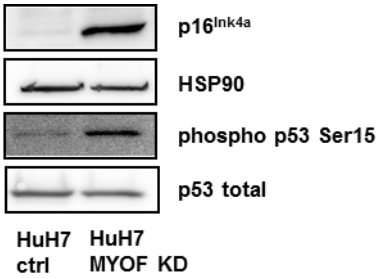

Figure 62: Induction of oncogene-induced senescence upon MYOF depletion in HuH7 cells.
HuH7 cells transduced with either control shRNA or MYOF shRNA were lysed and equal amounts of total protein were subjected to immunoblotting using anti-$p16^{Ink4a}$, anti-phospho p53 serine 15, total anti-p53 and anti-HSP90 antibodies.

6.3.10 Myoferlin depletion elevates mRNA expression levels of c-fos

As shown, MYOF depletion in DLC1-deficient HuH7 cells led to sustained ERK1/2 activation. By analyzing downstream targets of ERK1/2, we focused us on the immediate early gene c-fos encoding a transcription factor that is known to govern ERK signaling (Murphy et al 2002). ERK signaling can stimulate c-fos expression via different stimuli, however the best studied mechanism is the stimulation of c-fos transcription via the transcription cofactor Elk-1 which interacts with the serum response factor to activate the c-fos promoter (Monje et al, 2003). Consequently, the mRNA expression levels of c-fos in MYOF depleted HuH7 cells were determined by quantitative real-time PCR. The results demonstrated that the downregulation of MYOF mRNA expression in HuH7 cells caused a 20-fold upregulation of c-fos mRNA expression in comparison to HuH7 control cells (Figure 63). These findings indicated that the increase of the c-fos mRNA expression levels upon MYOF depletion reflects the activation of ERK signaling.

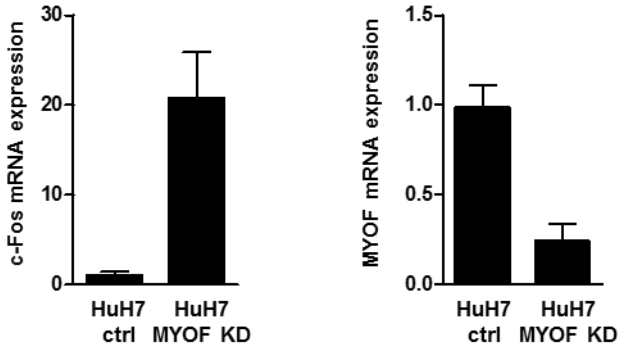

Figure 63: Induction of c-fos mRNA expression in HuH7 cells upon MYOF depletion.
Total cellular RNA from HuH7 cells transduced with control shRNA or MYOF shRNA was isolated. MRNA expression was analyzed by quantitative real-time PCR using c-fos and MYOF-specific primers. Shown is the fold change of c-fos and MYOF specific mRNA expression in MYOF depleted HuH7 cells in comparison to HuH7 control cells. Quantification is based on two independent experiments and data are expressed as mean ± SD.

6.3.11 Myoferlin depletion increases the activity of the human epidermal growth factor receptor

The underlying molecular mechanism of MYOF depletion mediated upregulation of MAPK signaling still remained to be investigated. A recently published study by Turtoi and colleagues described that MYOF downregulation increased the activity of the epidermal growth factor receptor (EGFR) in breast carcinoma cells (Turtoi et al, 2013). The EGF receptor is a key upstream effector of Ras signaling and it is well established that activation of the tyrosine kinase receptor is able to activate Ras which in turn leads to an upregulation of MAPK signaling (Gale et al, 1993). Thus, we addressed the question whether MYOF expression can directly influence the EGFR activity in DLC1-deficient hepatocellular carcinoma cells and thereby activating MAP kinase signaling that contributes to the oncogene-induced senescence response. To test whether activation of the EGF receptor is able to induce MAPK signaling in HuH7 cells, HuH7 cells were serum-starved and stimulated with human recombinant epidermal growth factor (EGF) that binds and activates the tyrosine kinase activity of the human EGF receptor. Activation of MAPK signaling was checked by the determination of the phosphorylation status of ERK1/2. The results from immunoblotting showed that EGF treatment of HuH7 cells increased the phosphorylation levels of ERK1/2 compared to untreated, serum-starved HuH7 control cells (Figure 64). However, the protein expression levels of total ERK were not affected by EGF stimulation. EGF stimulation for 5 minutes was sufficient to induce ERK1/2 phosphorylation and EGF treatment for longer time periods potentiated the phosphorylation levels of ERK1/2 (Figure 64). This indicated that activation of the EGF receptor in DLC1-deficient HuH7 cells upregulates the Raf-MEK1-ERK1/2 pathway.

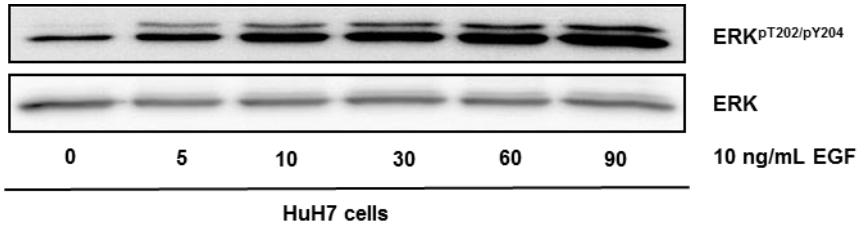

Figure 64: EGF stimulation of HuH7 cells induces phosphorylation of ERK1/2.
HuH7 cells were serum-starved for 16 hours and thereafter stimulated with 10 ng/mL EGF for the indicated time points. Afterwards cells were harvested, lysed and equal amounts of total protein were immunoblotted using anti-ERK$^{pT202/pY204}$ and total anti-ERK antibodies.

In order to learn if depletion of MKL1/2 and MYOF can directly activate the EGF receptor, activation of the EGF receptor was analyzed by the determination of its phosphorylation status at tyrosine 1173 that is considered to reflect activation of MAP kinase signaling (Hsu et al, 2011). HuH7 cells were transduced with MKL1/2 shRNA and MYOF shRNA and 24 hours after posttransduction, the phosphorylation levels of the EGF receptor at tyrosine 1173 were analyzed by immunoblotting. Compared to HuH7 control cells, HuH7 cells transduced with MKL1/2 shRNA and MYOF shRNA demonstrated increased phosphorylation levels of the EGF receptor at tyrosine 1173. The expression levels of total EGF receptor remained unchanged upon MKL1/2 and MYOF knockdown suggesting that MKL1/2 and MYOF expression influence the activation state of the EGF receptor. Determination of the MYOF expression levels by immunoblotting revealed that HuH7 cells expressing MKL1/2 shRNA and MYOF shRNA expressed reduced MYOF protein levels in comparison to HuH7 control cells. This provided evidence that reduction of MYOF expression in HuH7 cells contributes to the activation of the EGF receptor.

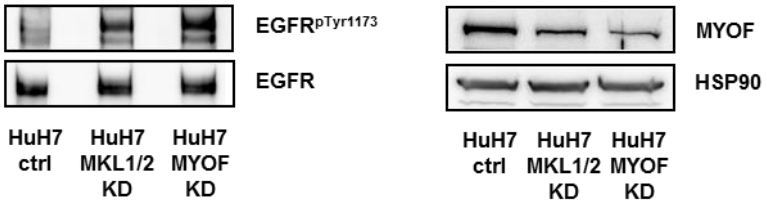

Figure 65: Downregulation of MYOF expression increases the phosphorylation levels of the EGF receptor at tyrosine 1173.
HuH7 cells were transduced with control shRNA, MKL1/2 shRNA or MYOF shRNA and 24 hours posttransduction, cells were harvested and lysed. Equal amounts of total protein were analyzed by immunoblotting using anti-EGFR^{pTyr1173}, total anti-EGFR, anti-MYOF and anti-HSP90 antibodies.

The ultimate verification that MYOF is the target gene of MKL1/2 and mediates the activation of MAPK kinase signaling, came when we reconstituted MYOF expression in MKL1/2 depleted HuH7 cells and analyzed its influence on the activation status of the EGF receptor. HuH7 cells were transfected with a plasmid encoding human HA-tagged MYOF and after 24 hours cells were transduced with MKL1/2 shRNA. Transduction of HuH7 cells with MKL1/2 shRNA reduced the protein expression level of MKL1 compared to HuH7 control cells. However, transfection of HuH7 cells with human HA-tagged MYOF was able to restore MYOF expression

in HuH7 cells expressing MKL1/2 shRNA (Figure 66). Analysis of the activation state of the EGF receptor revealed that downregulation of MYOF expression in MKL1/2 shRNA transduced HuH7 cells increased the phosphorylation of EGFR at tyrosine 1173. On the contrary, restoration of MYOF expression in MKL1/2 depleted HuH7 cells suppressed the induction of EGFR phosphorylation at tyrosine 1173. With this experimental setup, we found that the expression levels of MYOF concomitantly affected the total expression levels of the EGF receptor. Reduction of MYOF expression contributed to an increase of total EGFR levels whereas MYOF overexpression diminished total EFGR expression levels. These data are preliminary and it remains to be resolved whether MYOF depletion influences in the first instance the phosphorylation status of EGFR or the total expression levels. So our data highlight for the first time that MYOF constitutes a novel MKL1/2 dependent target gene involved in the regulation of the EGF receptor activity.

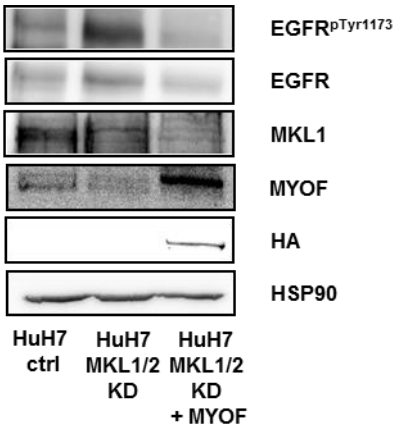

Figure 66: MYOF mediates the effects of MKL1/2 on the activation of EGFR signaling.
HuH7 cells were transfected with human HA-MYOF and after 24 hours, cells were transduced with MKL1/2 shRNA. After additional 24 hours, cells were lysed and equal amounts of total protein were subjected to immunoblotting using anti-EGFR^{pTyr1173}, total anti-EGF, anti-MKL1, anti-MYOF, anti-HA and anti-HSP90 antibodies.

7 Discussion

7.1 Molecular mechanism which drive MKL1/2 signaling in human cancer cells

7.1.1 Nuclear accumulation of MKL1 and MKL2 in human hepatocellular and breast carcinoma cells with DLC1 loss

We investigated the subcellular localization of MKL1 and MKL2 in different human hepatocellular and breast carcinoma cell lines. A correlation between the subcellular distribution of MKL1 and MKL2 and the endogenous expression levels of the tumor suppressor Deleted in Liver Cancer 1 (DLC1) in both hepatocellular and breast carcinoma cell lines was identified. Initially DLC1 was recognized as the human homolog of the rat p122RhoGAP. It was found to be frequently absent in primary human hepatocellular carcinoma (Yuan et al, 1998). DLC1 is located at chromosome 8p21.2-22, a region that is prominent for loss of hererozygosity (LOH) in a large number of different tumors (Arbieva et al, 2000; Yuan et al, 1998). A representative oligonucleotide microarray analysis (ROMA) pointed to a heterozygous deletion of DLC1 in about 50 % of liver, breast, lung and 70 % of colon cancers almost frequently as p53 in these cancers (Xue et al, 2008). DLC1 encoded a RhoGAP protein the functional role of which was to turn off Rho-mediated signaling. DLC1 showed some specificity for RhoA, B, C and to a lesser extent to cdc42 (Wong et al, 2003). Our data demonstrated a predominantly nuclear MKL1/2 localization in human hepatocellular and breast carcinoma cells who have lost endogenous DLC1 expression. By contrast, DLC1-expressing cancer cells were marked by a clear cytoplasmic localization of MKL1/2. To ascertain that the observed nuclear accumulation of MKL1/2 in DLC1-deficient cancer cell lines was not due to other functional characteristics in the genetic background of the cancer cell lines, we investigated the influence of DLC1 expression on the subcellular localization of MKL1/2 in hepatocytes by an RNAi approach. Established murine hepatocytes lacking p53 expression and coexpressing the oncogene MYC were used which resembles to the common genetic background of HCC (Zender et al, 2006). Downregulation of DLC1 expression in these murine hepatocytes led to the nuclear translocation of both MKL1 and MKL2. Restoration of DLC1 expression in HuH7 cells provoked a relocalization of both MKL1 and MKL2 back from the nucleus to the cytoplasm. These data provided evidence that DLC1 expression is directly involved in the regulation of the subcellular distribution of MKL1 and MKL2 which has not been noticed before. The first described mechanism for loss of DLC1 expression is attributed to its frequent heterozygous deletion, however aberrant hypermethylation of CpG islands within the promoter region of DLC1 also contributes to silencing of its expression (Wong et al, 2003; Yuan et al, 2003a). Somatic mutations of DLC1 were thought to be rare until it was discovered to occur in prostate and colon cancers, accompanied by the loss of the tumor-suppressive

properties of DLC1 (Liao et al, 2008). It was interesting to see whether epigenetic silencing of DLC1 expression or missense mutations also affected the subcellular localization of MKL1/2 in human cancer cells.

7.1.2 Increased RhoA signaling upon loss of DLC1 in human cancer cells

We addressed the question, how the DLC1 expression status would influence the subcellular localization of MKL1/2? As it is well established that nuclear translocation of MKL1/2 requires RhoA-actin signaling, the influence of DLC1 expression on the RhoA activation state in human hepatocellular and breast carcinoma cells was analyzed. Our data documented that the lack of endogenous DLC1 expression in HuH7 and MDA-MB-468 cells caused the constitutive activation of RhoA. This result was in line with previous studies demonstrating a significant influence of DLC1 expression on the RhoA activity (Healy et al, 2008; Wong et al, 2003; Xue et al, 2008). It was quite surprising that the deletion of DLC1, one out of 67 RhoGAPs, was sufficient to cause the constitutive activation of RhoA in human cancer cells. A similar crosstalk was reported for the tumor suppressor neurofibromin (NF1) encoding a RasGAP protein which loss contributed to the hyperactivation of Ras in human tumor cells (Basu et al, 1992; Bollag et al, 1996). RhoA overexpression was also found in numerous cancers but the underlying mechanism of RhoA activation has been not well understood (Gomez del Pulgar et al, 2005). In agreement with other studies, we identified the tumor suppressor DLC1 as a specific regulator of RhoA activity in hepatocellular and breast carcinoma cells (Xue et al, 2008). Our findings provide mechanistic insights into the underlying mechanism of RhoA activation in human tumor cells. Xue and colleagues were able to show that the increase of RhoA activation upon DLC1 loss drives hepatocarcinogenesis *in vivo* (Xue et al, 2008). As increased RhoA signaling causes the F-actin polymerization and stress fibers formation, we investigated the influence of DLC1 expression on the actin cytoskeleton of human cancer cells. The DLC1-deficient HuH7 and MDA-MD-468 cells were marked by a significant increase in the amount of actin stress fibers, which are composed of filamentous actin. Quantitative assessment of G- and F-actin levels revealed a significant elevation of the F-actin levels in DLC1-deficient cancer cells (Muehlich et al, 2012). Other groups had also shown that DLC1 expression exerted an inhibitory effect on stress fiber formation and was critically implicated in the remodeling of the actin cytoskeleton (Holeiter et al, 2008; Wong et al, 2008). These findings allowed us to interpret the nuclear localization of MKL1/2 in DLC1-deficient human cancer cells. Based on the established nuclear import mechanism of MKL1/2 in fibroblasts, we propose that DLC1 loss activates RhoA, which controls F-actin formation thereby leading to the nuclear translocation of MKL1/2. The concomitant G-actin depletion in DLC1-deficient cancer cells abrogates G-actin binding to the N-terminal RPEL domains within MKL1/2 which are required for the cytoplasmic sequestration of MKL1/2. Pawlowski and colleagues recently demonstrated that the dissociation of MKL1 from G-actin leads to the exposition of a nuclear localization

sequence within the RPEL actin binding domain, which is required for the nuclear import of MKL1 via the importin (Imp)α/β dependent pathway (Pawlowski et al, 2010). We conclude that the DLC1-deficiency in hepatocellular and breast carcinoma cells addresses different aspects of the nuclear import mechanism of MKL1/2 thereby favoring their constitutive nuclear localization.

7.1.3 Defective nuclear export mechanism of MKL1 in DLC1-deficient cancer cells

Besides the importance of RhoA/actin signaling for the nuclear import of MKL1/2, we focused us on the nuclear export mechanism of MKL1 in DLC1-deficient hepatocellular carcinoma cells. Vartiainen and colleagues showed that nuclear export, rather than import, constituted the key regulatory step of the subcellular distribution of MKL1 (Vartiainen et al, 2007). ERK1/2 mediated phosphorylation of MKL1 at serine 454 enhances binding between nuclear G-actin and MKL1 which was required for the Crm1-dependent nuclear export of MKL1 (Muehlich et al, 2008; Vartiainen et al, 2007). Our data pointed to a lack of ERK1/2 mediated phosphorylation of MKL1 at Serine 454 in HuH7 and MDA-MB-468 cells, both characterized by DLC1 deficiency. The lack of MKL1 phosphorylation was presumably due to the observed suppression of ERK1/2 activity in DLC1-deficient cancer cells. Morin and colleagues reported reduced ERK activity in cells overexpressing active RhoA and therefore the observed constitutive RhoA activation in DLC1-deficient cancer cells provides a imaginable explanation for the obtained effect (Morin et al, 2009). Our group substantiated these findings by showing that the suppression of RhoA activity by simvastatin treatment enabled phosphorylation of MKL1 in DLC1-deficient cancer cells (Muehlich et al, 2012). We analyzed the nuclear export mechanism of MKL1 due to its extensive description in the literature but we suppose the same nuclear export mechanism for MKL2 as it can be phosphorylated at the same residue like MKL1 and the phospho-specific MKL1 antibody also recognizes phosphorylated MKL2 (data are unpublished, personnel communication). However, we did not test whether the deficiency of DLC1 expression in the cancer cells directly affects the ability of MKL1 to associate with nuclear G-actin, a prerequisite for its nuclear export. Recently, a nuclear-cytoplasmic shuttle mechanism was reported for DLC1 (Chan et al, 2011; Yuan et al, 2007). The nuclear translocation of DLC1 depends on a bipartite nuclear localization sequence (NLS), but two contradictory studies, each report different residues for the NLS sequence, possibly arising from differences in the cellular context (Chan et al, 2011; Yuan et al, 2007). It was reported that the nuclear localization of DLC1 is associated with decreased tumor suppressive properties and the nuclear translocation could be viewed as a spatial regulatory mechanism (Chan et al, 2011). Scholz and colleagues found that phorbol-ester induced phosphorylation of DLC1 blocked the nuclear import by masking a nuclear localization sequence (Scholz et al, 2009). A similar mechanism was reported for MKL1 where TPA induced MKL1 phosphorylation thereby causing its cytoplasmic localization (Muehlich et al, 2008). We performed an in-silico

analysis of DLC1 and found the expected leucin-rich nuclear export signal which resembled to a mitogen-activated protein kinase phosphorylation site. As the nuclear import and export of both MKL1 and DLC1 features similarity in their mechanism we speculated that MKL1 and DLC1 can interact mechanistically, thereby influencing their subcellular distribution.

7.1.4 Activation of MKL1/2 and SRF dependent target gene expression in DLC1-deficient cancer cells

So far, our data pointed to the constitutive nuclear accumulation of MKL1/2 in human DLC1-deficient cancer cells, due to the activation of RhoA/actin signaling required for the nuclear import and impairment of the nuclear export mechanism. It is well established that nuclear localization is required but not sufficient for the association with SRF and activation of MKL/SRF dependent target gene expression because MKL1 has to dissociate from G-actin to obtain transcriptional activity (Vartiainen et al, 2007). Recently, Baarlink and colleagues demonstrated that serum stimulation promoted formin-regulated actin polymerization in the nucleus (Baarlink et al, 2013). Nuclear actin polymerization was sufficient to drive MKL1-mediated SRF signaling, so this study described initially that nuclear F-actin structures regulate the transcriptional activity of MKLs. It has been reported that the group of ternary complex factors, acting as transcriptional coactivators of SRF, repress the transcription of some MKL1/2 target genes (Lee et al, 2010b). We were interested whether the constitutive nuclear accumulation of MKL1/2 is sufficient to activate their target gene expression. We analyzed the expression levels of the immediate early gene CTGF, a member of the CCN family classified as a MKL/SRF dependent target gene (Medjkane et al, 2009; Muehlich et al, 2007). CTGF expression was constitutively activated in DLC1-deficient HuH7 and MDA-MB-468 cells whereas endogenous DLC1-expressing HepG2 and MCF7 cells displayed low basal expression levels of CTGF which were strongly upregulated by serum-stimulation. Silencing of DLC1 expression in HepG2 cells enhanced the expression of CTGF, while restoration of DLC1 expression in HuH7 cells reverted this effect by suppressing CTGF expression. We investigated the expression levels of Cyr61, a further member of the CCN family which expression has been described to be dependent on SRF and MKL1/2 (Lee et al, 2010b; Medjkane et al, 2009). Cyr61 revealed the same expression pattern like CTGF, defined by low basal expression levels in DLC1-expressing HepG2 cells and constitutively activated Cyr61 expression in DLC1-deficient HuH7 cells. These findings suggest that DLC1 loss caused nuclear translocation of MKL1/2 directly contributes to the constitutive activation of MKL/SRF dependent target gene expression. Both CTGF and Cyr61 are aberrantly expressed in hepatocellular and breast carcinoma cells, thereby promoting tumor progression (Li et al, 2012b; Mazzocca et al, 2010; Tsai et al, 2002; Xie et al, 2001; Xiu et al, 2012). Our data provide evidence that activation of MKL/SRF signaling in tumor cells features oncogenic properties by promoting the expression of tumor-relevant target genes. We concluded that loss of DLC1

expression promotes tumorigenesis via direct activation of MKL/SRF dependent target gene signaling. A similar effect was obtained for MKL1 fused with the RBM15 gene in megakaryoblastic leukemia cells (Ma et al, 2001). The RBM15-MKL1 fusion protein revealed a constitutive nuclear localization and activation of SRF and its target genes thereby promoting megakaryoblastic leukemia (Cen et al, 2003; Descot et al, 2008; Mercher et al, 2009). These results led to the conclusion that the nuclear accumulation of MKL1/2 accompanied by the constitutive activation of target gene expression is directly linked to tumor progression.

7.1.5 MKL1/2 depletion induces alterations in the actin cytoskeleton of DLC1-deficient cancer cells

Our group showed that downregulation of MKL1/2 expression reverted the pro-migratory effect caused by DLC1 loss (Muehlich et al, 2012). The involvement of DLC1 signaling in the migratory behavior of human cancer cells has already been reported before (Holeiter et al, 2008; Kim et al, 2008; Ullmannova & Popescu, 2007). As changes in the cell motility are tightly associated with cytoskeletal reorganization, the effect of MKL1/2 expression on the actin cytoskeleton of DLC1-deficient HuH7 and MDA-MB-468 cells was analyzed. Stress fibers are required as contractile forces for cell migration and the decrease in the amount of stress fibers upon MKL1/2 depletion might reflect the observed anti-migratory effect of MKL1/2 depletion in DLC1-deficient HuH7 and MDA-MB-468 cells. The protrusive structures at the edges of the cells, named filopodia, were strongly diminished in DLC1-deficient HuH7 and MDA-MB-468 cells depleted of MKL1/2. Filopodia are considered as typical features of invasive tumor cells (Mattila & Lappalainen, 2008). Since loss of DLC1 expression stimulates tumor cell invasion, we assumed that MKL1/2 depletion might revert the invasive behavior of DLC1-deficient carcinoma cells (Tripathi et al, 2013; Wong et al, 2005). Our assumption is supported by a previously reported study by Medjkane and colleagues who demonstrated that MKL1/2 are required for cell adhesion, migration and experimental metastasis (Medjkane et al, 2009). The reduction of filopodia upon MKL1/2 depletion resembles to the phenotype for SRF knockout in endothelial cells where SRF depletion abolished filopodia formation, thereby disrupting angiogenesis (Franco et al, 2013). We assume that the effect of MKL1/2 depletion on the structure of the actin cytoskeleton is due to the involvement of MKL/SRF signaling in the transcription of genes involved in actin dynamics (Olson & Nordheim, 2010).

7.2 Influence of MKL1/2 expression on the tumor growth of hepatocellular carcinoma cells

7.2.1 Depletion of MKL1/2 in DLC1-deficient HCC cells inhibits tumor cell proliferation

Studies conducted by our group showed that loss of DLC1 expression correlated well with the nuclear accumulation of MKL1 in primary human hepatocellular carcinoma *in vivo,* accompanied by an increased expression of the proliferation marker Ki-67 (Muehlich et al,

2012). Expression of the human Ki-67 protein correlated directly with cell proliferation and progression of the disease. Its expression was detectable during all active phases of the cell cycle whereas it was lacking in resting cells (Scholzen & Gerdes, 2000). These data led to the assumption that MKL1/2 expression might affect the proliferation of hepatocellular carcinoma cells. The tumor suppressor DLC1 was initially identified to be frequently deleted in human hepatocellular carcinoma, the sixth most frequent type of cancer in the human population and the third highest cause of cancer-related death. We focused on the influence of MKL1/2 expression on the growth of hepatocellular carcinoma cells characterized by a DLC1-deficient background.

Our data highlighted, for the first time, that RNA-interference mediated downregulation of both MKL1 and MKL2 expression significantly suppressed the proliferation of the human HCC cells HuH6 and HuH7, both lacking endogenous DLC1 expression. As cell proliferation of endogenous DLC1-expressing HepG2 and HLF cells was not affected by MKL1/2 knockdown we hypothesized that DLC1 expression plays a crucial role in the MKL1/2 knockdown mediated growth arrest. Silencing of DLC1 expression in HepG2 cells increased the proliferation of the HCC cells which is in accordance with reported studies (Wong et al, 2005; Xue et al, 2008). However, depletion of MKL1/2 expression abolished the pro-proliferative effect caused by DLC1 loss. These data provided evidence that loss of DLC1 expression was a prerequisite to render HCC cells responsive to the effect of MKL1/2 knockdown on cell proliferation. Additional analysis revealed that expression of constitutively active RhoA in DLC1-expressing HepG2 cells not responding to the MKL1/2 knockdown, caused the nuclear translocation of MKL1 and enabled inhibition of cell proliferation upon MKL1/2 knockdown. As increased RhoA activity and the concomitant nuclear localization of MKL1/2 are direct consequences of DLC1 loss, it was evident why especially DLC1-deficient HCC cells responded to the MKL1/2 knockdown. Investigations by Medjkane and colleagues demonstrated that MKL1/2 depletion reduces the invasiveness and motility but does not affect the proliferative capacity of tumor cells (Medjkane et al, 2009). We presume that this discrepancy arises from the fact that Medjkane and colleagues analyzed DLC1-expressing tumor cells characterized by low RhoA activity and inactive, cytoplasmic sequestered MKL1/2. Their observations are in agreement with ours on endogenous DLC1-expressing HepG2 and HLF cells where MKL1/2 knockdown did not change their cell proliferation rate. These findings substantiated our data and document that the depletion of transcriptionally active, nuclear MKL1/2 provokes an anti-proliferative effect corresponding to our previous suggestion that nuclear targeted MKL1/2 feature oncogenic properties. On the other hand, our findings are contradictory to the study conducted by Descot and colleagues reporting that the overexpression of nuclear targeted MKL1 exerted a strong anti-proliferative effect on human fibroblasts by addressing target genes with a proven anti-proliferative function (Descot et al, 2009). A similar inverse effect of MKL1/2 expression has

been reported for cell migration, as MKL1/2 knockdown in fibroblasts enhanced cell migration, whereas it was blocked in tumor cells upon MKL1/2 depletion (Leitner et al, 2011; Medjkane et al, 2009; Muehlich et al, 2012). Consequently, we postulate that these effects of MKL1/2 expression constitute a cell type specific feature and argue that genes are differentially targeted by MKL1/2 depending on the cellular context. We were able to exclude apoptosis accounting for the observed anti-proliferative effect, as MKL1/2 have been described to be implicated in apoptotic signaling via their proapoptotic target genes Bok and Noxa (Shaposhnikov et al, 2012). At the cellular level, we identified cellular senescence as the underlying mechanism of the MKL1/2 depletion mediated growth arrest in DLC1-deficient HuH7 and HuH6 cells. The phenotype of cellular senescence was associated with morphological and structural alterations of MKL1/2 depleted HCC cells characterized by the induction of an enlarged, flat and vacuole-rich morphology which was devoid of actin stress fibers. Increased senescence-associated ß-galactosidase activity was detected in DLC1-deficient HuH7 and HuH6 cells depleted of MKL1/2, a well-established biomarker of senescent cells in vitro and *in vivo* (Debacq-Chainiaux et al, 2009). Silencing of DLC1 expression in HepG2 cells enabled the induction of cellular senescence upon MKL1/2 knockdown thereby verifying that the DLC1 expression status is critical for the MKL1/2 knockdown mediated senescence response. Furthermore, DLC1-deficient HuH7 cells accumulated upon MKL1/2 depletion in the G1-phase of the cell cycle, a prominent characteristic of cells undergoing the senescence response (Afshari et al, 1993; Gorman & Cristofalo, 1986; Sherwood et al, 1988). Cellular senescence is defined as a stable cycle arrest where cells are incapable to regain the proliferative capacity. Thus our data describe cellular senescence as the underlying mechanism of the obtained anti-proliferative effect of MKL1/2 knockdown in DLC1-deficient HCC cells. One of the classical definitions of senescence is that senescent cells are incapable of triggering the expression of genes required for proliferation (Seshadri & Campisi, 1990). As MKL1 and MKL2 function as transcriptional coactivators of SRF thereby controlling processes such as proliferation by transducing growth factor signaling into gene expression, we assumed that MKL1/2 depletion may affect the expression of genes which are involved in the cell cycle machinery. This assumption is substantiated by the findings reported by Shaposhnikov and colleagues showing that MKL1/2 expression is required for proper cell cycle progression (Shaposhnikov et al, 2013). Consequently these data led to the conclusion that MKL1/2 constitute novel, hitherto unnoticed modulators of the cellular senescence response in human HCC cells characterized by a DLC1-deficient background. In agreement with this, it has already been reported that homozygous inactivation of SRF in murine colon-derived SMCs led to a senescent phenotype (Angstenberger et al, 2007).

So far, MKL1/2 depletion provokes the phenotype of cellular senescence constituting a multifaceted process. We were thus interested in the exact underlying molecular mechanism of the senescence response.

We demonstrated that MKL1/2 depletion in DLC1-deficient HCC cells contributed to the activation of oncogenic Ras, indicated by the increased amount of GTP-bound Ras levels. Activated Ras signaling resulted in increased phosphorylation of ERK1/2 thereby reflecting the activation state of ERK1/2 (Crews et al, 1992; Zheng & Guan, 1993). Interestingly, Descot and colleagues reported a similar negative crosstalk between actin-MKL1 and the MAPK kinase pathway via the MKL1 target gene mig6 (Descot et al, 2009). We hypothesized that mig6 could mediate the effect upon MKL1/2 depletion on Ras activation, but experiments showing that mig6 expression was transcriptionally regulated by MKL1/2 expression in DLC1-deficient HuH7 cells were negative. According to reports from Morin and colleagues there exists an inverse correlation between RhoA and ERK activity like reduced ERK activity in cells expressing active RhoA (Morin et al, 2009). Therefore we tested whether MKL1/2 depletion can modify the constitutive RhoA activity in DLC1-deficient HuH7 cells but no influence of MKL1/2 expression on the RhoA activation status was detected. Consequently, we argued that a hitherto unknown gene might modulate the activation of MAPK signaling upon MKL1/2 depletion in DLC1-deficient HCC cells. We found that the Ras-activated ERK1/2 pathway was responsible for the growth arrest upon MKL1/2 depletion in DLC1-deficient HuH7 cells, because the MEK1 inhibitor UO126 abolished the anti-proliferative effect of MKL1/2 knockdown. According to a recent study, UO126 might also suppress senescence by inhibiting the MEK/mTOR pathway (Demidenko et al, 2009). It is conceivable that mTOR might also contribute to the pro-proliferative effect of UO126 in MKL1/2 depleted HuH7 cells. Initially, Serrano and colleagues demonstrated that the aberrant activation of the Ras/MAPK pathway by oncogenic Ras triggers a senescence response referred to as “oncogene-induced senescence” (Serrano et al, 1997). In response, it has been become a central issue that the overactivation of oncogenes can trigger the oncogene-induced senescence response that is supposed to act as a failsafe mechanism (Lin et al, 1998; Michaloglou et al, 2005; Serrano et al, 1997; Zhu et al, 1998). Our data demonstrate for the first time that oncogenic Ras signaling upon MKL1/2 depletion drives human DLC1-deficient HCC cells into the oncogene-induced senescence response. Studies by Serrano and colleagues showed that oncogenic Ras can induce premature senescence via activation of the tumor suppressors $p16^{Ink4a}$ and p53 (Serrano et al, 1997). $P16^{Ink4a}$ expression was significantly elevated in DLC1-deficient HuH7 and HuH6 cells upon MKL1/2 knockdown, but remained unchanged in endogenous DLC1-expressing HepG2 cells. The used HCC cells displayed very low endogenous expression levels of $p16^{Ink4a}$ corresponding to the assumption that $p16^{Ink4a}$ is commonly underexpressed in human cancer cell lines due to promoter methylation, mutation or homozygous deletion (Kim

& Sharpless, 2006; Nobori et al, 1994; Okamoto et al, 1994). In agreement with our findings, $p16^{Ink4a}$ expression is mostly induced in senescent cells and plays a key role in the establishment of the stable cell cycle arrest by activating the downstream tumor suppressor retinoblastoma protein (Rb) lying at the core of the senescence response (Alcorta et al, 1996; Hara et al, 1996; Lowe et al, 2004; Serrano & Blasco, 2001). Rb is considered as a master regulator of cell cycle progression because it represses the transcription of genes required for G1-S phase transition and DNA replication mediated by members of the E2F transcription factor family (Burkhart & Sage, 2008; Chicas et al, 2010). Our data demonstrated that downregulation of MKL1/2 expression in DLC1-deficient HuH7 and HuH6 cells provoked a hypophosphorylated form of the Rb protein which is consistent with the observations from other research groups reporting hypophosphorylation of Rb in cells undergoing the senescence response (Lin et al, 1998; Serrano et al, 1997; Stein et al, 1990). Hypophosphorylation of Rb reflects its activity and is linked to the inhibition of G1 progression (Yen & Sturgill, 1998). The observed G1-arrest in MKL1/2 depleted HuH7 cells is consistent with the hypophosphorylated form of the Rb protein. To demonstrate the importance of the $p16^{Ink4a}$-Rb tumor suppressor pathway in the MKL1/2 depletion mediated senescence response, $p16^{Ink4a}$ expression was silenced via RNA-interference and as a consequence hypophosphorylation of Rb was abrogated upon MKL1/2 knockdown. These data indicated that $p16^{Ink4a}$ constitutes a key effector protein of the MKL1/2 knockdown mediated senescence response corresponding to the previous notes that the lack of $p16^{Ink4a}$ expression can prevent the onset of the senescence response upon oncogenic signaling (Haferkamp et al, 2009; Lin et al, 1998). The establishment of the oncogene-induced senescence response was further substantiated by the findings that MKL1/2 depletion in DLC1-deficient HuH7 and HuH6 cells caused a DNA damage response documented by elevated phosphorylation of p53 on serine 15. In line with this observed effect, investigations by Di Micco and colleagues already demonstrated that oncogene-induced senescence arises from the induction of a robust DNA-damage response marked by increased phosphorylation of p53 on serine 15 (Di Micco et al, 2006). However, according to several reports, the induction of a DDR seems not to be obligatory for the establishment of oncogene-induced senescence (Efeyan et al, 2009; Olsen et al, 2002)

Oncogene-induced senescence is associated with chromatin remodeling resulting in the formation of heterochromatin structures termed senescence-associated heterochromatin foci (SAHF) which has been initially described by Narita and colleagues (Narita et al, 2003). SAHF plays a critical role in sequestering proliferation-promoting genes like E2F target genes thereby contributing to the cell cycle arrest. MKL1/2 depletion triggered the formation SAHFs in DLC1-negative HuH7 and HuH6 cells indicated by the accumulation of histone-3 trimethylated on lysine 9, specifically enriched in SAHFs (Narita et al, 2003). As SAHF formation upon

oncogene activation is well established, we conclude that the activation of oncogenic RAS signaling upon MKL1/2 depletion provokes SAHF formation thereby contributing to the irreversible cell cycle arrest (Michaloglou et al, 2005; Narita et al, 2003).

A further hallmark of cells undergoing the oncogene-induced senescence response are changes in their secretome collectively termed “senescence-messaging secretome” (SMS) (Kuilman & Peeper, 2009). The induction of the SMS is characterized by the upregulation of secretory factors like inflammatory cytokines, chemokines or growth factors that govern a variety of cellular responses (Coppe et al, 2010). Amongst the SMS factors, MKL1/2 depletion significantly upregulated the expression of the chemokine (C-S-C motif) ligand 10 (CXCL10) and tumor necrosis factor (ligand) superfamily member 10 (TNFSF10) in DLC1-deficient HuH7 and HuH6 cells which have been reported to be secreted by senescent cells (Braumuller et al, 2013; Cahu et al, 2012; Dabrowska et al, 2011). For both CXCL10 and TNFSF10 it has been shown that their expression push human cancers into the senescence response (Braumuller et al, 2013). Based on these findings we supposed that the enhanced CXCL10 and TNFSF10 expression in DLC1-deficient HCC cells depleted of MKL1/2 reinforce the senescence response and contribute to the maintenance of the stable cell cycle arrest.

7.2.2 Induction of cellular senescence upon reconstitution of DLC1 expression

We found that the oncogene-induced senescence response occurred exclusively in DLC1-negative HCC cells upon MKL1/2 depletion. After reports that MKL1/2 mediate the effects upon loss of the tumor suppressor DLC1, we addressed the question whether MKL1/2 downregulation may substitute for the tumor suppressive actions of DLC1. Reconstitution of DLC1 expression in the human hepatocellular carcinoma cells HuH7 reduced the cell proliferation due to the accumulation of DLC1-reconstituted HuH7 cells in the G1-phase of the cell cycle. The cell morphology of DLC1-reconstituted HuH7 cells adopted a senescence-like phenotype characterized by an enlarged morphology and vacuole enriched cytoplasm. Analysis of the oncogene-induced senescence markers demonstrated that the re-expression of DLC1 in HuH7 cells caused the induction of $p16^{Ink4a}$ expression and provoked the hypophosphorylation of the Rb protein accounting for the obtained G1-arrest. In addition, DLC1 reconstitution provoked an accumulation of the SAHF component histone 3 trimethylated on lysine 9 and induced a DDR indicated by elevated phosphorylation of p53 on serine 15. Based on the findings we concluded that the restoration of DLC1 expression in HCC cells induced cellular senescence that constitutes a novel hitherto unnoticed tumor suppressive property of DLC1. According to this note, restoration of the famous tumor suppressor p53 has already been reported to cause senescence (Ventura et al, 2007; Xue et al, 2007). It might be possible that senescence is a common feature of the restoration of tumor suppressors. As the expression of the senescence markers upon DLC1 reconstitution resembled to the effect of MKL1/2 depletion in DLC1-deficient HCC cells we suppose that MKL1/2 depletion mimics the

effects of DLC1 reconstitution. Zhang and colleagues observed a cell cycle arrest in the G1-phase upon DLC1 re-expression but proposed apoptosis as the underlying mechanism (Zhang et al, 2009). We speculate that this discrepancy is due to the use of different tumor cell lines. The senescence response upon DLC1 reconstitution has not been noticed before, possibly due to the use of transient transfection methods which does not allow long-term analysis of cell proliferation and senescence induction (Qin et al, 2013; Yuan et al, 2004; Zhang et al, 2009; Zhou et al, 2004). Our notice of the senescence response upon DLC1 restoration is substantiated by the work of Qian and colleagues who reported a direct correlation between DLC1 and $p16^{Ink4a}$ expression, a crucial effector protein of the cellular senescence response (Qian et al, 2012).

7.2.3 Evaluation of MKL1/2 as novel anti-tumor target *in vivo*

Our in vitro data make MKL1/2 likely anti-tumor targets for the treatment of hepatocellular carcinoma cells characterized by loss of DLC1 expression. We studied the therapeutic efficacy of MKL1/2 knockdown by a therapeutic knockdown approach, using RNA-interference *in vivo* as a highly efficient tool for the exploration of novel targets. We employed polymer-based nanoparticles for siRNA delivery into established subcutaneous HCC xenografts derived from DLC1-deficient HuH7 cells. Due to a higher relevance in a therapeutic setting, we preferred the systemic application of siRNAs by intraperitoneal injection rather than the intratumoral application. SiRNA targeting both MKL1 and MKL2, a combination of MKL1 and MKL2 specific siRNAs and MKL1 siRNA alone were complexed with polyethylenimine for systemic delivery (Hobel et al, 2010). The systemic application of PEI complexed MKL1/2 siRNA for a treatment period of 22 days completely abolished tumor growth of HCC xenografts. The combination of MKL1+2 specific siRNAs also reduced tumor growth albeit somewhat less efficiently, compared to the siRNA targeting both MKL1 and 2. We assume that this may be due to the lower dose of MKL1 and MKL2 siRNAs: the combination of MKL1 and 2 consists of 7.5 µg MKL1 and 7.5 µg MKL2 siRNA, whereas 15 µg MKL1/2 siRNA targeting both MKL1 and 2 was used. We used comparably low siRNAs amounts that have been proven in this tumor model for inhibition of HCC xenograft growth. The systemic application of MKL1 siRNA alone was sufficient to completely abrogate HCC xenograft growth. These findings indicated that MKL1 and MKL2 may not act redundantly in the context of tumor growth. In addition, these data are substantiated by preliminary findings of our group which indicate that MKL1 depletion in HuH7 cells is sufficient to suppress tumor-relevant target gene expression. By contrast, in human fibroblasts MKL1 depletion was not sufficient to reduce target gene expression because MKL1 and MKL2 bind mainly in their heterodimerized form to SRF (Cen et al, 2003). At the moment we speculate whether in DLC1-deficient HuH7 cells MKL1 may bind in its homodimerized form to SRF that would argue for its unique role in HCC tumor growth. Nevertheless, the involvement of MKL2 expression in HCC xenograft growth remains to be clearly investigated.

Moreover it would be interesting to evaluate the consequences of either MKL1 or MKL2 depletion on the onset of the oncogene-induced senescence response in vitro. Remarkably, no adverse side effects were detected upon systemic therapy with PEI/complexed siRNAs targeting MKL1 and MKL2. It has been reported that MKL1 knockout mice are viable and fertile but fail to nurse their offspring (Li et al, 2006; Sun et al, 2006b). Moreover, it was recognized that MKL1 expression is required for the maturation of megakaryocytes and platelet formation whereas global MKL2 deletion contributes to embryonic lethality due to defects in the cardiac development (Cheng et al, 2009; Oh et al, 2005; Ragu et al, 2010). Long-term treatment may lead to unexpected adverse side effects, owing to other physiological functions of MKL1 and MKL2. It raised the question whether the regression of the tumors was due to a senescence response *in vivo*. Evaluation of oncogene-induced senescence markers in HCC xenografts treated with MKL1+2 siRNA revealed a significant induction of the tumor suppressor $p16^{Ink4a}$. Induction of $p16^{Ink4a}$ expression has been reported to occur in senescent mouse and human lesions *in vivo* (Collado et al, 2005; Michaloglou et al, 2005). An accumulation of the SAHF component histone H3 trimethylated on lysine 9 and increased phosphorylation of the DDR marker p53 on serine 15 was detected in HCC xenografts treated with the combination of MKL1 and MKL2 specific siRNAs. The regression of the tumors was associated with enhanced expression of the senescence-associated chemokine ligand CXCL10. Several groups reported that the secretion of SMS factors plays a critical role in the induction of an immune response against premalignant cells which triggers the clearance of pre-cancerous senescent cells *in vivo* and in vitro, thereby limiting the development of liver cancer (Kang et al, 2011; Krizhanovsky et al, 2008; Xue et al, 2007). We speculated whether the increase of CXCL10 expression in MKL1+2 treated tumors influences the clearance of senescent cells thereby accounting to the distinctive phenotype of HCC xenograft growth inhibition *in vivo*. Our data highlight for the first time that downregulation of MKL1/2 expression abolish tumor growth of DLC1-deficient hepatocellular carcinoma by inducing oncogene-induced senescence *in vivo*. In concert with this, induction of oncogene-induced senescence *in vivo* has already been reported to act as a failsafe mechanism limiting tumor progression (Braig et al, 2005; Michaloglou et al, 2005). We conclude that depletion of oncogenic MKL1/2 signaling provokes oncogene-induced senescence to counteract DLC1-loss driven hepatocarcinogenesis. A future goal might be to evaluate whether MKL1/2 depletion can trigger the oncogene-induced senescence response in vitro and *in vivo* in other tumor identities characterized by a DLC1-deficient background like breast or colon carcinoma cells. In agreement with this suggestion, our group could already show that silencing of MKL1/2 expression in human DLC1-deficient breast carcinoma cells reduced their cell proliferation (Muehlich et al, 2012). It might interesting to investigate whether cellular senescence is a common mechanism of the MKL1/2 depletion mediated proliferation arrest.

7.3 Analysis of MKL1/2 dependent target gene expression in human DLC1-deficient hepatocellular carcinoma cells

7.3.1 Transcriptome analysis of MKL1/2 depleted hepatocellular carcinoma cells with DLC1-deficiency

To date, our data illustrate that MKL1/2 expression is required for the tumor growth of DLC1-deficient hepatocellular carcinoma cells in vitro and *in vivo*. We aimed to identify which MKL1/2 dependent target genes are involved in regression of the tumor growth and induction of the oncogene-induced senescence response. The transcriptome of DLC1-deficient HuH7 cells stably depleted of MKL1/2 expression was analyzed. One key aspect of our gene expression analysis was the identification of transcriptionally regulated genes upon depletion of active nuclear MKL1/2. Comparison with the list of target genes regulated by MKL1/2 expression in human breast cancer cells from the microarray study conducted by Medjkane and colleagues suggested that there is only little consistency with our MKL1/2 regulated target genes (Medjkane et al, 2009). We assume that this effect is due to the fact that Medjkane and colleagues analyzed genes that were regulated upon depletion of cytoplasmic, quiescent MKL1/2 whereas we analyzed the consequences of nuclear, active MKL1/2. Some genes described to be regulated by G-actin-MKL1 signaling like transgelin/ smooth muscle protein alpha 22 (SM22) and calponin also appeared in our gene list (Descot et al, 2009). Our microarray approach was validated to be selective for MKL1/2 regulated genes because known TCF-dependent target genes like c-fos or egr-1 did not appear in the list. Our differentially regulated genes were nicely validated in HCC xenografts treated with MKL1+2 siRNA. SM22, which is aberrantly expressed in smooth muscle cells, was found to be downregulated upon MKL1/2 depletion in vitro. SM22 is known to have both pro-neoplastic and anti-neoplastic functions (Assinder et al, 2009; Lee et al, 2010a). Contradictory to our findings in vitro, we observed a significant upregulation of SM22 expression upon MKL1/2 downregulation *in vivo*. With regard to the increased SM22 expression in senescent cells, we assumed that the augmented expression of SM22 in HCC xenografts was due to the observed senescence response (Thompson et al, 2012). Our microarray approach revealed that the Glioma-pathogenesis related 1 gene (GLIPR1) was transcriptionally downregulated by MKL1/2 depletion in vitro and *in vivo*. GLIPR1 has been initially reported to act as a tumor suppressor which is frequently downregulated in prostate cancer and seems to be a target gene of p53 (Ren et al, 2002; Ren et al, 2004; Ren et al, 2006). Conversely, GLIPR1 was found to be specifically expressed in glioma and Wilm`s tumor, where its expression featured oncogenic properties (Chilukamarri et al, 2007; Murphy et al, 1995; Rich et al, 1996). It seems to be a cell-type specific feature whether GLIPR1 exerts oncogenic or tumor suppressive functions. In the context of hepatocarcinogenesis, GLIPR1 has not been noticed before and its functional implication remains to be addressed. Nevertheless, we assume that the suppressed GLIPR1

expression levels upon MKL1/2 depletion contributed to the tumor regression of DLC1-deficient HuH7 cells. In addition, non-muscle heavy chain 9 (MYH9) was transcriptionally suppressed upon MKL1/2 depletion in vitro and *in vivo*. These findings are in agreement with the study from Medjkane and colleagues describing MYH9 as a MKL1/2 controlled gene the expression of which is implicated in tumor cell invasion of breast carcinoma cells (Betapudi et al, 2006; Medjkane et al, 2009). We conclude that MYH9 expression is involved in the invasive behavior of DLC1-deficient HuH7 cells. A hereto unnoticed MKL1/2 regulated target gene constitutes the transforming growth factor beta 1 (TGFß1) the expression of which was reduced upon MKL1/2 depletion in vitro and *in vivo.* Whether increased TGFß1 expression is associated with the induction of a senescence response is controversial because we found decreased TGFß1 expression in senescent HuH7 cells depleted of MKL1/2 (Acosta et al, 2013; Senturk et al, 2010). In our setting of DLC1-deficient HuH7 cells, TGFß1 is unlikely to participate directly in the senescence response. Another aspect of TGFß1 expression is its implication in the mechanism of epithelial to mesenchymal transition (EMT), a fundamental step in the process of cancer progression where epithelial cells are converted to migratory and invasive cells (Thiery, 2002). Consistent with the observation that MKL1/2 are required for TGFß1-induced EMT reported by Morita and colleagues, we supposed that decreased TGFß1 expression in vitro and *in vivo* upon MKL1/2 downregulation accounted for the limitation of the malignant progression of DLC1-deficient HuH7 cells (Morita et al, 2007). In agreement with Medjkane and colleagues, we found decreased expression of the vestigial-like protein 3 (VGLL3) in MKL1/2 depleted HuH7 cells. However, its expression was not regulated by MKL1/2 in HCC xenografts *in vivo* (Medjkane et al, 2009). VGLL3 was described as a cofactor of the TEAD transcription factors and there is some evidence for their role in tumor progression (Pobbati & Hong, 2013). It might be possible that the transcriptional downregulation of VGLL3 expression upon MKL1/2 depletion contributes to the limitation of the malignant phenotype of DLC1-deficient HuH7 cells. Our data showed that the microtubule-associated protein 1B (MAP1B), encoding a structural microtubule-associated protein, constitutes a new member of the group of cytoskeletal proteins the expression of which is regulated by MKL1/2 signaling in vitro and *in vivo.* MAP1B is described to have a special role in the stability of the cytoskeleton of neuronal cells and its expression influenced neuronal migration and growth (Lu et al, 2004; Tymanskyj et al, 2012). This raises the important question whether its expression affects the growth and migratory behavior of DLC1-deficient HCC cells. MAP1B appeared for the first time in our microarray study and we speculate that it has a special relevance in our setting of DLC1-deficient HuH7 cells. In addition, another interesting aspect of our microarray analysis was the identification of myoferlin, encoding a transmembrane protein the expression of which was transcriptionally downregulated in DLC1-deficient HuH7 cells depleted of MKL1/2 and in HCC xenografts treated with MKL1+2 siRNA. The influence of myoferlin expression on tumor growth

in our setting of DLC1-deficient HuH7 cells will be discussed below in detail. We postulate that each target gene whose expression was transcriptionally suppressed upon MKL1/2 depletion, was functionally implicated in the process of tumor regression of DLC1-deficient HCC cells. Evaluation of the functional role of each MKL1/2 regulated target gene provide mechanistic insights into MKL1/2 promoted tumor growth and onset of the oncogene-induced senescence response.

7.3.2 Functional characterization of Myoferlin

Of particular interest to us was myoferlin, a member of the conserved family of ferlin proteins which reportedly has a role in variety of membrane processes like endocytosis, membrane repair and vesicular transport (Bernatchez et al, 2009; Cipta & Patel, 2009; Sharma et al, 2010). We were able to demonstrate that loss of the tumor suppressor DLC1 directly activated the expression of myoferlin, which was proven to be transcriptionally regulated by the MKL1/2 and SRF signaling axis. Thus one major aspect of our study was the analysis of the functional role of myoferlin expression in relation to hepatocellular carcinoma cells characterized by a DLC1-deficient background. Interestingly, silencing of myoferlin expression strongly reduced the invasiveness of human DLC1-deficient HuH7 cells. Similar findings were reported by Li and colleagues and by Eisenberg and colleagues both showing that myoferlin depletion impairs the invasion of breast cancer cells (Eisenberg et al, 2011; Li et al, 2012a). Based on our findings, we suppose that besides MYH9, which has already been described to be required for MKL1/2 promoted tumor cell invasion, myoferlin constitutes a new MKL1/2 dependent target gene whose expression is functionally implicated in the invasive behavior of DLC1-deficient HuH7 cells. Moreover short-hairpin mediated myoferlin depletion significantly inhibited the tumor cell proliferation of HuH7 cells. These results are in close agreement with those obtained by Leung and colleagues, who demonstrated that myoferlin downregulation reduced the cell proliferation of mouse Lewis lung carcinoma cells (Leung et al, 2013). Depletion of myoferlin exhibited a similar anti-proliferative effect on the tumor growth of DLC1-deficient HuH7 cells like MKL1/2 knockdown. The reduction of MYOF expression enhanced the senescence-associated ß-galactosidase activity and contributed to the activation of MAPK signaling as indicated by increased ERK1/2 phosphorylation. Analysis of oncogene-induced senescence markers demonstrated that MYOF depletion caused the activation of the DNA-damage response documented by increased phosphorylation of p53 on serine 15 and led to the induction of $p16^{Ink4a}$ expression, a key inducer of the senescence response. Hence, the expression of the MKL1/2 dependent target gene myoferlin is functionally involved in the oncogene-induced senescence response of human hepatocellular carcinoma cells marked by loss of DLC1 expression. We found that myoferlin depletion led to sustained EGFR activation as documented by prominent phosphorylation of tyrosine 1173 residue. Myoferlin was specified as the target gene mediating the effects of MKL1/2 expression on EGF receptor

signaling. Preliminary data provided evidence that myoferlin depletion not only affects the EGFR phosphorylation status but even the overall expression levels of the EGF receptor. Silencing of MKL1/2 expression suppressed myoferlin expression and, as a consequence, alleviation of EGFR signaling occurred. Our observations are consistent with a previously reported study by Turtoi and colleagues, who highlighted myoferlin as a key regulator of EGFR activity in breast cancer cells (Turtoi et al, 2013). Turtoi and colleagues found that increased EGFR activity was due to impaired degradation of phosphorylated EGF receptors upon myoferlin depletion (Turtoi et al, 2013). A similar effect was reported by Bernatchez and colleagues, demonstrating that myoferlin expression stabilized VEGF receptor expression in endothelial cells (Bernatchez et al, 2007). Myoferlin expression blocked the polyubiquitination of activated VEGF receptors which is mediated by the E3-ubiquitin ligase CBL, thereby labeling the receptors for their subsequent proteasomal degradation. It was supposed that myoferlin is functionally implicated in the mechanism of receptor dependent endocytosis, part of the process of receptor internalization which functions as a negative feedback mechanism controlling the intensity and duration of receptor signaling (Wells et al, 1990). Receptor dependent endocytosis is characterized by the fission of endocytotic vesicles which require the coat proteins clathrin and caveolin and plasma membrane fission is facilitated by the family of dynamin proteins. Bernatchez and colleagues found that in endothelial cells myoferlin colocalized with caveolin and dynamin 2 and assumed a functional role of myoferlin in the receptor dependent endocytosis (Bernatchez et al, 2009). Mechanistically, we speculate whether in our setting of DLC1-deficient HuH7 cells, downregulation of myoferlin expression may interfere with the activity of the CBL ubiquitin ligase, thereby preventing the ubiquitination of active EGF receptors and inhibiting their degradation. Along with the study of Turtoi and colleagues, there is given evidence for another scenario, where myoferlin depletion may disrupt the formation of plasma membrane caveolae which is required for proper endocytosis. It might be interesting to investigate the mechanism of increased EGFR signaling upon myoferlin depletion in DLC1-deficient human hepatocellular carcinoma cells. So, the functional characterization of myoferlin links MKL1/2 depletion to the onset of the oncogene-induced senescence response. Based on our data we established the following model for MKL1/2 as novel modulators of the oncogene-induced senescence response in human DLC1-deficient HCC cells in vitro and *in vivo*.

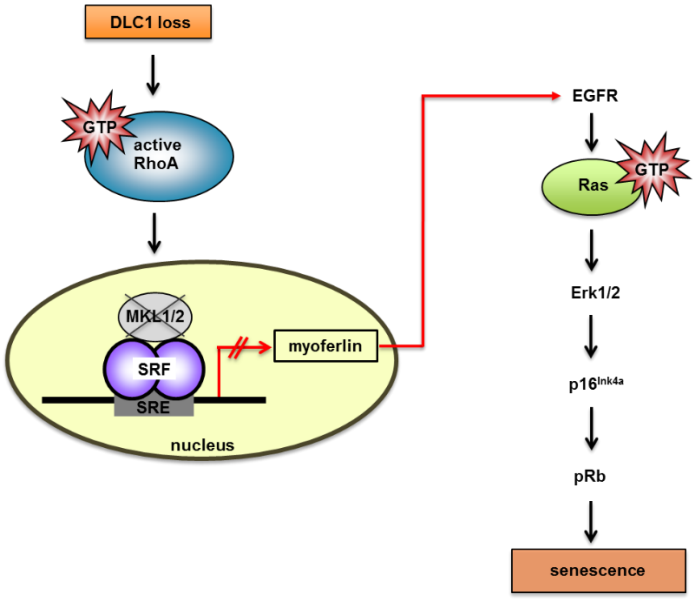

Figure 67: Proposed model for the induction of the oncogene-induced senescence response upon MKL1/2 depletion in human DLC1-deficient HCC cells.

We found that loss of the tumor suppressor DLC1 in human HCC cells provokes constitutive RhoA activation, thereby causing the nuclear accumulation of MKL1/2 and the concomitant activation of target gene expression. Depletion of nuclear, active MKL1/2 expression induces the transcriptional suppression of myoferlin expression that causes elevated EGFR signaling thereby activating downstream oncogenic Ras signaling. Oncogenic Ras activation provokes the activation of MAPK signaling and triggers via the $p16^{Ink4a}$/Rb tumor suppressor pathway the senescence response, characterized by an irreversible growth arrest. This model provides a mechanistic explanation for the observed oncogene-induced senescence response upon DLC1 reconstitution. As we have already demonstrated that restoration of DLC1 expression targets MKL1/2 into the cytoplasm and diminishes the expression of MKL/SRF dependent target genes, we suggest that restoration of DLC1 expression in HCC cells suppresses the expression of myoferlin, comparable to the effect of MKL1/2 silencing and enables thereby activation of EGFR signaling and the subsequent oncogene-induced senescence response.

7.4 Novel pharmacological targets for the treatment of DLC1-deficient HCC cells

The proposed model provides several novel options for the pharmacological treatment of HCC characterized by loss of DLC1 expression. One approach is the pharmacological reactivation of the tumor suppressive functions of DLC1, but this is conceptually and technically difficult. Tumor suppressors like DLC1 are not directly accessible for therapeutic intervention. Blocking of RhoA by geranylgeranyltransferase inhibition appears to be less desirable due to the ubiquitous cellular distribution of geranylgeranylation of proteins. Nuclear MKL1/2 constitute

potent anti-tumor targets as their depletion causes the tumor suppressive oncogene-induced senescence response. Inhibition of nuclear MKL1/2 signaling simultaneously suppresses the expression of multiple tumor-promoting target genes involved in growth, migration and invasion of DLC1-deficient HCC cells. Their inhibition would have multiple beneficial therapeutic effects. Recently, Bell and colleagues established a new chemical compound, named CCG-1423, together with its related structural analogues as a new class of inhibitors of Rho/MKL1/SRF dependent gene transcription (Bell et al, 2013a; Bell et al, 2013b). So far the exact molecular target of these compounds remains to be investigated, but it was shown that treatment with CCG-1423 block the nuclear localization of MKL1 (Jin et al, 2011). Given that depletion of nuclear MKL1 is sufficient to abrogate HCC tumor growth *in vivo*, it might be attractive to evaluate the therapeutic efficacy of the new compounds to inhibit the tumor growth of DLC1-deficient HCC cells. The pharmacological blocking of myoferlin expression might be another attractive candidate as its suppression initiates the oncogene-induced senescence response and the concomitant reduction of the invasiveness of DLC1-deficient HCC cells would have a beneficial therapeutic effect. In DLC1-deficient HCC cells, we found that activation of sustained EGFR-Ras-MEK-ERK signaling modulates the tumor suppressive oncogene-induced senescence response. Aberrant activation of EGFR-Ras-Raf-MEK-ERK signaling is a consistent finding in numerous cancers but, in contrast, there it is tightly linked to the promotion of cell proliferation, cell survival and metastasis (Roberts & Der, 2007). Therefore, the molecular components of the EGFR-Ras-Raf-MEK-ERK signaling pathway are subjects of intensive scientific investigations to find new inhibitors that provide an efficient treatment of human malignancies. It is documented that EGFR signaling is involved in hepatocarcinogenesis and pharmacologically targeting the EGFR system for HCC treatment is clinically proven. One approach relies on the small molecules gefitinib and erlotinib, both inhibiting the tyrosine kinase activity of the EGF receptor. Another approach is the application of EGFR targeted antibodies like cetuximab. However, only a subset of HCC patients responded to the therapy. At the moment, the multikinase inhibitor sorafenib is used for the therapy of advanced HCC but exerted only modest clinical benefit. A reasonable explanation of the limited responsiveness of HCC to targeting EGFR-MAPK signaling is given by our evidence that inhibition of EGFR-Ras-MEK-ERK signaling blocks the onset of the oncogene-induced senescence response. We found that activation of EGFR-MAPK signaling results exclusively in the oncogene-induced senescence response in human HCC cells lacking endogenous expression of the tumor suppressor DLC1 accounting for approximately 50 % of HCC cases. Consequently we argue that the molecular heterogeneity of HCC may account for suboptimal therapeutic outcomes. Genomic profiling of HCC allows an appropriate therapeutic strategy for optimal medical outcomes and our data emphasize the necessity of personalized health care approaches. Our studies provide mechanistic insights into the underlying

pathomechanism that drives hepatocarcinogenesis upon loss of the tumor suppressor DLC1. Silencing of MKL1/2 expression was evaluated as an efficient approach to antagonize the growth of HCC lacking DLC1 by inducing the oncogene-induced senescence response. A future challenge will be to discover novel senescence inducing drugs, as some DNA-damaging agents have already been reported to cause oncogene-induced senescence (Chang et al, 1999; Schmitt et al, 2002; te Poele et al, 2002). It is conceivable that the pharmacological induction of oncogene-induced senescence in a therapeutic setting reverts malignant cells into resting, senescent cells thereby limiting tumor progression.

8 Figures

9 Tables

10 Abbreviation index

µg	micro gram
µL	micro liter
µM	micro molar
aa	amino acids
APS	ammoniumperoxodisulfate
bp	base pairs
BSA	bovine serum albumin
DAPI	4`,6-diamindino-2-phenylindole
DLC	Deleted in Liver Cancer
DMEM	Dulbecco's Modified Eagle medium
DNA	deoxyribonucleic acid
E.*coli*	*Escherichia coli*
ECL	enhanced chemiluminescence kit
ECM	extracellular matrix
EDTA	ehtylendiaminetetracetic acid
EGFR	epidermal growth factor receptor
ERK	extracellular signal-regulated kinase
ES	embryonic stem cells
FCS	fetal calf serum
h	hour(s)
HA	hemagglutine
HRP	horseradish peroxidase
IEG	immediate early gene
IF	immunofluorescence
IP	immunoprecipitation
KCl	potassium chloride
kDa	kilo Dalton
KH_2PO_4	potassium dehydrogen phosphatase
LPA	lysophosphatidic acid
LSB	Laemmli sample buffer
M	molar
mA	milli ampere
mg	milli gramm
min	minute (s)
MKL1	megakaryoblastic leukemia protein1

MKL2	megakaryoblastic leukemia protein2
mL	milliliter
mm	millimeter
MRTF-A	myocardin-related transcription factor A
MRTF-B	myocardin-related transcription factor B
MYOF	myoferlin
NaCl	sodium chloride
nm	nano meter
o/n	over night
OIS	oncogene-induced senescence response
Opti-MEM	reduced serum medium
PAGE	polyacrylamide gel electrophoresis
PBS	phosphate buffered saline
PBST	phosphate buffered saline Tween 20
PCR	polymerase chain reaction
PI	complete protease inhibitor cocktail
pmol	pico mol
PVDF	polyvinylidene fluoride
RNA	ribonucleic acid
rpm	rounds per minute
RT	room temperature
RT-PCR	Real-time polymerase chain reaction
s	seconds
SDS	sodium dodecyl sulfate
siRNA	small-interfering ribonucleic acid
SMS	senescence-messaging secretome
SRE	serum response element
SRF	serum response factor
TA	transactivator
TBST	tris-buffered saline Tween 20
TCF	ternary complex factors
TEMED	tetramethylethylenediamine
TRIS	Tris(hydroxymethyl)aminomethane
U	Units (of enzymatic activity)
VEGFR	vascular endothelial growth factor receptor

11 References

Acosta JC, Banito A, Wuestefeld T, Georgilis A, Janich P, Morton JP, Athineos D, Kang TW, Lasitschka F, Andrulis M et al (2013) A complex secretory program orchestrated by the inflammasome controls paracrine senescence. Nature cell biology 15**:** 978-990

Acosta JC, O'Loghlen A, Banito A, Guijarro MV, Augert A, Raguz S, Fumagalli M, Da Costa M, Brown C, Popov N et al (2008a) Chemokine signaling via the CXCR2 receptor reinforces senescence. Cell 133**:** 1006-1018

Acosta JC, O'Loghlen A, Banito A, Raguz S, Gil J (2008b) Control of senescence by CXCR2 and its ligands. Cell cycle 7**:** 2956-2959

Adams PD (2007) Remodeling chromatin for senescence. Aging cell 6**:** 425-427

Adamson P, Etienne S, Couraud PO, Calder V, Greenwood J (1999) Lymphocyte migration through brain endothelial cell monolayers involves signaling through endothelial ICAM-1 via a rho-dependent pathway. Journal of immunology 162**:** 2964-2973

Afshari CA, Vojta PJ, Annab LA, Futreal PA, Willard TB, Barrett JC (1993) Investigation of the role of G1/S cell cycle mediators in cellular senescence. Experimental cell research 209**:** 231-237

Alberti S, Krause SM, Kretz O, Philippar U, Lemberger T, Casanova E, Wiebel FF, Schwarz H, Frotscher M, Schutz G et al (2005) Neuronal migration in the murine rostral migratory stream requires serum response factor. Proceedings of the National Academy of Sciences of the United States of America 102**:** 6148-6153

Alcorta DA, Xiong Y, Phelps D, Hannon G, Beach D, Barrett JC (1996) Involvement of the cyclin-dependent kinase inhibitor p16 (INK4a) in replicative senescence of normal human fibroblasts. Proceedings of the National Academy of Sciences of the United States of America 93**:** 13742-13747

Alpy F, Tomasetto C (2005) Give lipids a START: the StAR-related lipid transfer (START) domain in mammals. Journal of cell science 118**:** 2791-2801

Angello JC, Pendergrass WR, Norwood TH, Prothero J (1989) Cell enlargement: one possible mechanism underlying cellular senescence. Journal of cellular physiology 140**:** 288-294

Angstenberger M, Wegener JW, Pichler BJ, Judenhofer MS, Feil S, Alberti S, Feil R, Nordheim A (2007) Severe intestinal obstruction on induced smooth muscle-specific ablation of the transcription factor SRF in adult mice. Gastroenterology 133**:** 1948-1959

Aravind L, Koonin EV (2000) SAP - a putative DNA-binding motif involved in chromosomal organization. Trends in biochemical sciences 25**:** 112-114

Arbieva ZH, Banerjee K, Kim SY, Edassery SL, Maniatis VS, Horrigan SK, Westbrook CA (2000) High-resolution physical map and transcript identification of a prostate cancer deletion interval on 8p22. Genome research 10**:** 244-257

Arsenian S, Weinhold B, Oelgeschlager M, Ruther U, Nordheim A (1998) Serum response factor is essential for mesoderm formation during mouse embryogenesis. The EMBO journal 17**:** 6289-6299

Assinder SJ, Stanton JA, Prasad PD (2009) Transgelin: an actin-binding protein and tumour suppressor. The international journal of biochemistry & cell biology 41**:** 482-486

Ayadi A, Zheng H, Sobieszczuk P, Buchwalter G, Moerman P, Alitalo K, Wasylyk B (2001) Net-targeted mutant mice develop a vascular phenotype and up-regulate egr-1. The EMBO journal 20**:** 5139-5152

Baarlink C, Wang H, Grosse R (2013) Nuclear actin network assembly by formins regulates the SRF coactivator MAL. Science 340**:** 864-867

Bansal D, Campbell KP (2004) Dysferlin and the plasma membrane repair in muscular dystrophy. Trends in cell biology 14**:** 206-213

Bartkova J, Rezaei N, Liontos M, Karakaidos P, Kletsas D, Issaeva N, Vassiliou LV, Kolettas E, Niforou K, Zoumpourlis VC et al (2006) Oncogene-induced senescence is part of the tumorigenesis barrier imposed by DNA damage checkpoints. Nature 444**:** 633-637

Basu TN, Gutmann DH, Fletcher JA, Glover TW, Collins FS, Downward J (1992) Aberrant regulation of ras proteins in malignant tumour cells from type 1 neurofibromatosis patients. Nature 356**:** 713-715

Bell JL, Haak AJ, Wade SM, Kirchhoff PD, Neubig RR, Larsen SD (2013a) Optimization of novel nipecotic bis(amide) inhibitors of the Rho/MKL1/SRF transcriptional pathway as potential anti-metastasis agents. Bioorganic & medicinal chemistry letters 23**:** 3826-3832

Bell JL, Haak AJ, Wade SM, Sun Y, Neubig RR, Larsen SD (2013b) Design and synthesis of tag-free photoprobes for the identification of the molecular target for CCG-1423, a novel inhibitor of the Rho/MKL1/SRF signaling pathway. Beilstein journal of organic chemistry 9**:** 966-973

Bernatchez PN, Acevedo L, Fernandez-Hernando C, Murata T, Chalouni C, Kim J, Erdjument-Bromage H, Shah V, Gratton JP, McNally EM et al (2007) Myoferlin regulates vascular endothelial growth factor receptor-2 stability and function. The Journal of biological chemistry 282**:** 30745-30753

Bernatchez PN, Sharma A, Kodaman P, Sessa WC (2009) Myoferlin is critical for endocytosis in endothelial cells. American journal of physiology Cell physiology 297**:** C484-492

Betapudi V, Licate LS, Egelhoff TT (2006) Distinct roles of nonmuscle myosin II isoforms in the regulation of MDA-MB-231 breast cancer cell spreading and migration. Cancer research 66**:** 4725-4733

Bollag G, Clapp DW, Shih S, Adler F, Zhang YY, Thompson P, Lange BJ, Freedman MH, McCormick F, Jacks T et al (1996) Loss of NF1 results in activation of the Ras signaling pathway and leads to aberrant growth in haematopoietic cells. Nature genetics 12**:** 144-148

Bos JL, Rehmann H, Wittinghofer A (2007) GEFs and GAPs: critical elements in the control of small G proteins. Cell 129**:** 865-877

Braig M, Lee S, Loddenkemper C, Rudolph C, Peters AH, Schlegelberger B, Stein H, Dorken B, Jenuwein T, Schmitt CA (2005) Oncogene-induced senescence as an initial barrier in lymphoma development. Nature 436**:** 660-665

Braig M, Schmitt CA (2006) Oncogene-induced senescence: putting the brakes on tumor development. Cancer research 66**:** 2881-2884

Brandt DT, Baarlink C, Kitzing TM, Kremmer E, Ivaska J, Nollau P, Grosse R (2009) SCAI acts as a suppressor of cancer cell invasion through the transcriptional control of beta1-integrin. Nature cell biology 11**:** 557-568

Braumuller H, Wieder T, Brenner E, Assmann S, Hahn M, Alkhaled M, Schilbach K, Essmann F, Kneilling M, Griessinger C et al (2013) T-helper-1-cell cytokines drive cancer into senescence. Nature 494**:** 361-365

Brown JP, Wei W, Sedivy JM (1997) Bypass of senescence after disruption of p21CIP1/WAF1 gene in normal diploid human fibroblasts. Science 277**:** 831-834

Buchwalter G, Gross C, Wasylyk B (2004) Ets ternary complex transcription factors. Gene 324**:** 1-14

Burkhart DL, Sage J (2008) Cellular mechanisms of tumour suppression by the retinoblastoma gene. Nature reviews Cancer 8**:** 671-682

Cahu J, Bustany S, Sola B (2012) Senescence-associated secretory phenotype favors the emergence of cancer stem-like cells. Cell death & disease 3**:** e446

Campisi J, d'Adda di Fagagna F (2007) Cellular senescence: when bad things happen to good cells. Nature reviews Molecular cell biology 8**:** 729-740

Cen B, Selvaraj A, Burgess RC, Hitzler JK, Ma Z, Morris SW, Prywes R (2003) Megakaryoblastic leukemia 1, a potent transcriptional coactivator for serum response factor (SRF), is required for serum induction of SRF target genes. Molecular and cellular biology 23**:** 6597-6608

Chan LK, Ko FC, Ng IO, Yam JW (2009) Deleted in liver cancer 1 (DLC1) utilizes a novel binding site for Tensin2 PTB domain interaction and is required for tumor-suppressive function. PloS one 4**:** e5572

Chan LK, Ko FC, Sze KM, Ng IO, Yam JW (2011) Nuclear-targeted deleted in liver cancer 1 (DLC1) is less efficient in exerting its tumor suppressive activity both in vitro and in vivo. PloS one 6**:** e25547

Chang BD, Broude EV, Dokmanovic M, Zhu H, Ruth A, Xuan Y, Kandel ES, Lausch E, Christov K, Roninson IB (1999) A senescence-like phenotype distinguishes tumor cells that undergo terminal proliferation arrest after exposure to anticancer agents. Cancer research 59**:** 3761-3767

Chen L, Liu C, Ko FC, Xu N, Ng IO, Yam JW, Zhu G (2012) Solution structure of the phosphotyrosine binding (PTB) domain of human tensin2 protein in complex with deleted in liver cancer 1 (DLC1) peptide reveals a novel peptide binding mode. The Journal of biological chemistry 287**:** 26104-26114

Chen Z, Trotman LC, Shaffer D, Lin HK, Dotan ZA, Niki M, Koutcher JA, Scher HI, Ludwig T, Gerald W et al (2005) Crucial role of p53-dependent cellular senescence in suppression of Pten-deficient tumorigenesis. Nature 436**:** 725-730

Cheng EC, Luo Q, Bruscia EM, Renda MJ, Troy JA, Massaro SA, Tuck D, Schulz V, Mane SM, Berliner N et al (2009) Role for MKL1 in megakaryocytic maturation. Blood 113**:** 2826-2834

Chicas A, Wang X, Zhang C, McCurrach M, Zhao Z, Mert O, Dickins RA, Narita M, Zhang M, Lowe SW (2010) Dissecting the unique role of the retinoblastoma tumor suppressor during cellular senescence. Cancer cell 17**:** 376-387

Chilukamarri L, Hancock AL, Malik S, Zabkiewicz J, Baker JA, Greenhough A, Dallosso AR, Huang TH, Royer-Pokora B, Brown KW et al (2007) Hypomethylation and aberrant expression of the glioma pathogenesis-related 1 gene in Wilms tumors. Neoplasia 9**:** 970-978

Ching YP, Wong CM, Chan SF, Leung TH, Ng DC, Jin DY, Ng IO (2003) Deleted in liver cancer (DLC) 2 encodes a RhoGAP protein with growth suppressor function and is underexpressed in hepatocellular carcinoma. The Journal of biological chemistry 278**:** 10824-10830

Chow KL, Schwartz RJ (1990) A combination of closely associated positive and negative cis-acting promoter elements regulates transcription of the skeletal alpha-actin gene. Molecular and cellular biology 10**:** 528-538

Cipta S, Patel HH (2009) Molecular bandages: inside-out, outside-in repair of cellular membranes. Focus on "Myoferlin is critical for endocytosis in endothelial cells". American journal of physiology Cell physiology 297**:** C481-483

Collado M, Gil J, Efeyan A, Guerra C, Schuhmacher AJ, Barradas M, Benguria A, Zaballos A, Flores JM, Barbacid M et al (2005) Tumour biology: senescence in premalignant tumours. Nature 436**:** 642

Collado M, Serrano M (2006) The power and the promise of oncogene-induced senescence markers. Nature reviews Cancer 6**:** 472-476

Connell-Crowley L, Harper JW, Goodrich DW (1997) Cyclin D1/Cdk4 regulates retinoblastoma protein-mediated cell cycle arrest by site-specific phosphorylation. Molecular biology of the cell 8**:** 287-301

Copeland JW, Treisman R (2002) The diaphanous-related formin mDia1 controls serum response factor activity through its effects on actin polymerization. Molecular biology of the cell 13**:** 4088-4099

Coppe JP, Desprez PY, Krtolica A, Campisi J (2010) The senescence-associated secretory phenotype: the dark side of tumor suppression. Annual review of pathology 5**:** 99-118

Crews CM, Alessandrini A, Erikson RL (1992) The primary structure of MEK, a protein kinase that phosphorylates the ERK gene product. Science 258**:** 478-480

Crews CM, Erikson RL (1993) Extracellular signals and reversible protein phosphorylation: what to Mek of it all. Cell 74**:** 215-217

d'Adda di Fagagna F (2008) Living on a break: cellular senescence as a DNA-damage response. Nature reviews Cancer 8**:** 512-522

Dabrowska M, Skoneczny M, Rode W (2011) Functional gene expression profile underlying methotrexate-induced senescence in human colon cancer cells. Tumour biology : the

journal of the International Society for Oncodevelopmental Biology and Medicine 32**:** 965-976

Dancker P, Low I, Hasselbach W, Wieland T (1975) Interaction of actin with phalloidin: polymerization and stabilization of F-actin. Biochimica et biophysica acta 400**:** 407-414

Davis M, Johnston SR, DiMicco W, Findlay MP, Taylor JA (1996) The case for a student honor code and beyond. Journal of professional nursing : official journal of the American Association of Colleges of Nursing 12**:** 24-30

Debacq-Chainiaux F, Erusalimsky JD, Campisi J, Toussaint O (2009) Protocols to detect senescence-associated beta-galactosidase (SA-betagal) activity, a biomarker of senescent cells in culture and in vivo. Nature protocols 4**:** 1798-1806

Demidenko ZN, Shtutman M, Blagosklonny MV (2009) Pharmacologic inhibition of MEK and PI-3K converges on the mTOR/S6 pathway to decelerate cellular senescence. Cell cycle 8**:** 1896-1900

Demonbreun AR, Posey AD, Heretis K, Swaggart KA, Earley JU, Pytel P, McNally EM (2010) Myoferlin is required for insulin-like growth factor response and muscle growth. FASEB journal : official publication of the Federation of American Societies for Experimental Biology 24**:** 1284-1295

Descot A, Hoffmann R, Shaposhnikov D, Reschke M, Ullrich A, Posern G (2009) Negative regulation of the EGFR-MAPK cascade by actin-MAL-mediated Mig6/Errfi-1 induction. Molecular cell 35**:** 291-304

Descot A, Rex-Haffner M, Courtois G, Bluteau D, Menssen A, Mercher T, Bernard OA, Treisman R, Posern G (2008) OTT-MAL is a deregulated activator of serum response factor-dependent gene expression. Molecular and cellular biology 28**:** 6171-6181

Di Micco R, Fumagalli M, Cicalese A, Piccinin S, Gasparini P, Luise C, Schurra C, Garre M, Nuciforo PG, Bensimon A et al (2006) Oncogene-induced senescence is a DNA damage response triggered by DNA hyper-replication. Nature 444**:** 638-642

Di Micco R, Sulli G, Dobreva M, Liontos M, Botrugno OA, Gargiulo G, dal Zuffo R, Matti V, d'Ario G, Montani E et al (2011) Interplay between oncogene-induced DNA damage response and heterochromatin in senescence and cancer. Nature cell biology 13**:** 292-302

Dimri GP, Itahana K, Acosta M, Campisi J (2000) Regulation of a senescence checkpoint response by the E2F1 transcription factor and p14(ARF) tumor suppressor. Molecular and cellular biology 20**:** 273-285

Dimri GP, Lee X, Basile G, Acosta M, Scott G, Roskelley C, Medrano EE, Linskens M, Rubelj I, Pereira-Smith O et al (1995) A biomarker that identifies senescent human cells in culture and in aging skin in vivo. Proceedings of the National Academy of Sciences of the United States of America 92**:** 9363-9367

Dransart E, Olofsson B, Cherfils J (2005) RhoGDIs revisited: novel roles in Rho regulation. Traffic 6**:** 957-966

Du KL, Chen M, Li J, Lepore JJ, Mericko P, Parmacek MS (2004) Megakaryoblastic leukemia factor-1 transduces cytoskeletal signals and induces smooth muscle cell differentiation from undifferentiated embryonic stem cells. The Journal of biological chemistry 279**:** 17578-17586

Du X, Qian X, Papageorge A, Schetter AJ, Vass WC, Liu X, Braverman R, Robles AI, Lowy DR (2012) Functional interaction of tumor suppressor DLC1 and caveolin-1 in cancer cells. Cancer research 72**:** 4405-4416

Durkin ME, Avner MR, Huh CG, Yuan BZ, Thorgeirsson SS, Popescu NC (2005) DLC-1, a Rho GTPase-activating protein with tumor suppressor function, is essential for embryonic development. FEBS letters 579**:** 1191-1196

Durkin ME, Ullmannova V, Guan M, Popescu NC (2007a) Deleted in liver cancer 3 (DLC-3), a novel Rho GTPase-activating protein, is downregulated in cancer and inhibits tumor cell growth. Oncogene 26**:** 4580-4589

Durkin ME, Yuan BZ, Thorgeirsson SS, Popescu NC (2002) Gene structure, tissue expression, and linkage mapping of the mouse DLC-1 gene (Arhgap7). Gene 288**:** 119-127

Durkin ME, Yuan BZ, Zhou X, Zimonjic DB, Lowy DR, Thorgeirsson SS, Popescu NC (2007b) DLC-1:a Rho GTPase-activating protein and tumour suppressor. Journal of cellular and molecular medicine 11**:** 1185-1207

Efeyan A, Murga M, Martinez-Pastor B, Ortega-Molina A, Soria R, Collado M, Fernandez-Capetillo O, Serrano M (2009) Limited role of murine ATM in oncogene-induced senescence and p53-dependent tumor suppression. PloS one 4**:** e5475

Eisenberg MC, Kim Y, Li R, Ackerman WE, Kniss DA, Friedman A (2011) Mechanistic modeling of the effects of myoferlin on tumor cell invasion. Proceedings of the National Academy of Sciences of the United States of America 108**:** 20078-20083

Ferbeyre G, de Stanchina E, Querido E, Baptiste N, Prives C, Lowe SW (2000) PML is induced by oncogenic ras and promotes premature senescence. Genes & development 14**:** 2015-2027

Fernandes-Alnemri T, Litwack G, Alnemri ES (1994) CPP32, a novel human apoptotic protein with homology to Caenorhabditis elegans cell death protein Ced-3 and mammalian interleukin-1 beta-converting enzyme. The Journal of biological chemistry 269**:** 30761-30764

Fidyk NJ, Cerione RA (2002) Understanding the catalytic mechanism of GTPase-activating proteins: demonstration of the importance of switch domain stabilization in the stimulation of GTP hydrolysis. Biochemistry 41**:** 15644-15653

Franco CA, Blanc J, Parlakian A, Blanco R, Aspalter IM, Kazakova N, Diguet N, Mylonas E, Gao-Li J, Vaahtokari A et al (2013) SRF selectively controls tip cell invasive behavior in angiogenesis. Development 140**:** 2321-2333

Gale NW, Kaplan S, Lowenstein EJ, Schlessinger J, Bar-Sagi D (1993) Grb2 mediates the EGF-dependent activation of guanine nucleotide exchange on Ras. Nature 363**:** 88-92

Geneste O, Copeland JW, Treisman R (2002) LIM kinase and Diaphanous cooperate to regulate serum response factor and actin dynamics. The Journal of cell biology 157**:** 831-838

Gerdes J, Schwab U, Lemke H, Stein H (1983) Production of a mouse monoclonal antibody reactive with a human nuclear antigen associated with cell proliferation. International journal of cancer Journal international du cancer 31**:** 13-20

Gohring F, Schwab BL, Nicotera P, Leist M, Fackelmayer FO (1997) The novel SAR-binding domain of scaffold attachment factor A (SAF-A) is a target in apoptotic nuclear breakdown. The EMBO journal 16**:** 7361-7371

Goldstein S (1990) Replicative senescence: the human fibroblast comes of age. Science 249**:** 1129-1133

Gomez del Pulgar T, Benitah SA, Valeron PF, Espina C, Lacal JC (2005) Rho GTPase expression in tumourigenesis: evidence for a significant link. BioEssays : news and reviews in molecular, cellular and developmental biology 27**:** 602-613

Goodison S, Yuan J, Sloan D, Kim R, Li C, Popescu NC, Urquidi V (2005) The RhoGAP protein DLC-1 functions as a metastasis suppressor in breast cancer cells. Cancer research 65**:** 6042-6053

Gorman SD, Cristofalo VJ (1986) Analysis of the G1 arrest position of senescent WI38 cells by quinacrine dihydrochloride nuclear fluorescence. Evidence for a late G1 arrest. Experimental cell research 167**:** 87-94

Guan M, Zhou X, Soulitzis N, Spandidos DA, Popescu NC (2006) Aberrant methylation and deacetylation of deleted in liver cancer-1 gene in prostate cancer: potential clinical applications. Clinical cancer research : an official journal of the American Association for Cancer Research 12**:** 1412-1419

Guettler S, Vartiainen MK, Miralles F, Larijani B, Treisman R (2008) RPEL motifs link the serum response factor cofactor MAL but not myocardin to Rho signaling via actin binding. Molecular and cellular biology 28**:** 732-742

Haferkamp S, Tran SL, Becker TM, Scurr LL, Kefford RF, Rizos H (2009) The relative contributions of the p53 and pRb pathways in oncogene-induced melanocyte senescence. Aging 1**:** 542-556

Hampel B, Malisan F, Niederegger H, Testi R, Jansen-Durr P (2004) Differential regulation of apoptotic cell death in senescent human cells. Experimental gerontology 39**:** 1713-1721

Hanahan D, Weinberg RA (2000) The hallmarks of cancer. Cell 100**:** 57-70

Hara E, Smith R, Parry D, Tahara H, Stone S, Peters G (1996) Regulation of p16CDKN2 expression and its implications for cell immortalization and senescence. Molecular and cellular biology 16**:** 859-867

Harley CB, Futcher AB, Greider CW (1990) Telomeres shorten during ageing of human fibroblasts. Nature 345**:** 458-460

Hayflick L, Moorhead PS (1961) The serial cultivation of human diploid cell strains. Experimental cell research 25**:** 585-621

Healy KD, Hodgson L, Kim TY, Shutes A, Maddileti S, Juliano RL, Hahn KM, Harden TK, Bang YJ, Der CJ (2008) DLC-1 suppresses non-small cell lung cancer growth and invasion by RhoGAP-dependent and independent mechanisms. Molecular carcinogenesis 47**:** 326-337

Hellwinkel OJ, Rogmann JP, Asong LE, Luebke AM, Eichelberg C, Ahyai S, Isbarn H, Graefen M, Huland H, Schlomm T (2008) A comprehensive analysis of transcript signatures of the phosphatidylinositol-3 kinase/protein kinase B signal-transduction pathway in prostate cancer. BJU international 101**:** 1454-1460

Herbig U, Ferreira M, Condel L, Carey D, Sedivy JM (2006) Cellular senescence in aging primates. Science 311**:** 1257

Herold T, Jurinovic V, Mulaw M, Seiler T, Dufour A, Schneider S, Kakadia PM, Feuring-Buske M, Braess J, Spiekermann K et al (2011) Expression analysis of genes located in the minimally deleted regions of 13q14 and 11q22-23 in chronic lymphocytic leukemia-unexpected expression pattern of the RHO GTPase activator ARHGAP20. Genes, chromosomes & cancer 50**:** 546-558

Hill CS, Treisman R (1995) Differential activation of c-fos promoter elements by serum, lysophosphatidic acid, G proteins and polypeptide growth factors. The EMBO journal 14**:** 5037-5047

Hill CS, Wynne J, Treisman R (1995) The Rho family GTPases RhoA, Rac1, and CDC42Hs regulate transcriptional activation by SRF. Cell 81**:** 1159-1170

Hipskind RA, Buscher D, Nordheim A, Baccarini M (1994) Ras/MAP kinase-dependent and -independent signaling pathways target distinct ternary complex factors. Genes & development 8**:** 1803-1816

Hipskind RA, Rao VN, Mueller CG, Reddy ES, Nordheim A (1991) Ets-related protein Elk-1 is homologous to the c-fos regulatory factor p62TCF. Nature 354**:** 531-534

Hobel S, Aigner A (2010) Polyethylenimine (PEI)/siRNA-mediated gene knockdown in vitro and in vivo. Methods in molecular biology 623**:** 283-297

Hobel S, Aigner A (2013) Polyethylenimines for siRNA and miRNA delivery in vivo. Wiley interdisciplinary reviews Nanomedicine and nanobiotechnology 5**:** 484-501

Hobel S, Koburger I, John M, Czubayko F, Hadwiger P, Vornlocher HP, Aigner A (2010) Polyethylenimine/small interfering RNA-mediated knockdown of vascular endothelial growth factor in vivo exerts anti-tumor effects synergistically with Bevacizumab. The journal of gene medicine 12**:** 287-300

Holeiter G, Heering J, Erlmann P, Schmid S, Jahne R, Olayioye MA (2008) Deleted in liver cancer 1 controls cell migration through a Dia1-dependent signaling pathway. Cancer research 68**:** 8743-8751

Hsu JM, Chen CT, Chou CK, Kuo HP, Li LY, Lin CY, Lee HJ, Wang YN, Liu M, Liao HW et al (2011) Crosstalk between Arg 1175 methylation and Tyr 1173 phosphorylation negatively modulates EGFR-mediated ERK activation. Nature cell biology 13**:** 174-181

Iyer LM, Koonin EV, Aravind L (2001) Adaptations of the helix-grip fold for ligand binding and catalysis in the START domain superfamily. Proteins 43**:** 134-144

Jaffe AB, Hall A (2005) Rho GTPases: biochemistry and biology. Annual review of cell and developmental biology 21**:** 247-269

Jin W, Goldfine AB, Boes T, Henry RR, Ciaraldi TP, Kim EY, Emecan M, Fitzpatrick C, Sen A, Shah A et al (2011) Increased SRF transcriptional activity in human and mouse skeletal muscle is a signature of insulin resistance. The Journal of clinical investigation 121**:** 918-929

Johansen FE, Prywes R (1995) Serum response factor: transcriptional regulation of genes induced by growth factors and differentiation. Biochimica et biophysica acta 1242**:** 1-10

Johnstone CN, Castellvi-Bel S, Chang LM, Bessa X, Nakagawa H, Harada H, Sung RK, Pique JM, Castells A, Rustgi AK (2004) ARHGAP8 is a novel member of the RHOGAP family related to ARHGAP1/CDC42GAP/p50RHOGAP: mutation and expression analyses in colorectal and breast cancers. Gene 336**:** 59-71

Kalita K, Kharebava G, Zheng JJ, Hetman M (2006) Role of megakaryoblastic acute leukemia-1 in ERK1/2-dependent stimulation of serum response factor-driven transcription by BDNF or increased synaptic activity. The Journal of neuroscience : the official journal of the Society for Neuroscience 26**:** 10020-10032

Kamijo T, Zindy F, Roussel MF, Quelle DE, Downing JR, Ashmun RA, Grosveld G, Sherr CJ (1997) Tumor suppression at the mouse INK4a locus mediated by the alternative reading frame product p19ARF. Cell 91**:** 649-659

Kang TW, Yevsa T, Woller N, Hoenicke L, Wuestefeld T, Dauch D, Hohmeyer A, Gereke M, Rudalska R, Potapova A et al (2011) Senescence surveillance of pre-malignant hepatocytes limits liver cancer development. Nature 479**:** 547-551

Kaplan-Albuquerque N, Van Putten V, Weiser-Evans MC, Nemenoff RA (2005) Depletion of serum response factor by RNA interference mimics the mitogenic effects of platelet derived growth factor-BB in vascular smooth muscle cells. Circulation research 97**:** 427-433

Kawai K, Kitamura SY, Maehira K, Seike J, Yagisawa H (2010) START-GAP1/DLC1 is localized in focal adhesions through interaction with the PTB domain of tensin2. Advances in enzyme regulation 50**:** 202-215

Kawai K, Seike J, Iino T, Kiyota M, Iwamae Y, Nishitani H, Yagisawa H (2009) START-GAP2/DLC2 is localized in focal adhesions via its N-terminal region. Biochemical and biophysical research communications 380**:** 736-741

Kerr JF, Winterford CM, Harmon BV (1994) Apoptosis. Its significance in cancer and cancer therapy. Cancer 73**:** 2013-2026

Kim CA, Bowie JU (2003) SAM domains: uniform structure, diversity of function. Trends in biochemical sciences 28**:** 625-628

Kim TY, Healy KD, Der CJ, Sciaky N, Bang YJ, Juliano RL (2008) Effects of structure of Rho GTPase-activating protein DLC-1 on cell morphology and migration. The Journal of biological chemistry 283**:** 32762-32770

Kim TY, Jong HS, Song SH, Dimtchev A, Jeong SJ, Lee JW, Kim TY, Kim NK, Jung M, Bang YJ (2003) Transcriptional silencing of the DLC-1 tumor suppressor gene by epigenetic mechanism in gastric cancer cells. Oncogene 22**:** 3943-3951

Kim TY, Lee JW, Kim HP, Jong HS, Kim TY, Jung M, Bang YJ (2007) DLC-1, a GTPase-activating protein for Rho, is associated with cell proliferation, morphology, and migration in human hepatocellular carcinoma. Biochemical and biophysical research communications 355**:** 72-77

Kim WY, Sharpless NE (2006) The regulation of INK4/ARF in cancer and aging. Cell 127**:** 265-275

King KL, Hwang JJ, Chau GY, Tsay SH, Chi CW, Lee TG, Wu LH, Wu CW, Lui WY (1998) Ki-67 expression as a prognostic marker in patients with hepatocellular carcinoma. Journal of gastroenterology and hepatology 13**:** 273-279

Kipp M, Gohring F, Ostendorp T, van Drunen CM, van Driel R, Przybylski M, Fackelmayer FO (2000) SAF-Box, a conserved protein domain that specifically recognizes scaffold attachment region DNA. Molecular and cellular biology 20**:** 7480-7489

Kourlas PJ, Strout MP, Becknell B, Veronese ML, Croce CM, Theil KS, Krahe R, Ruutu T, Knuutila S, Bloomfield CD et al (2000) Identification of a gene at 11q23 encoding a guanine nucleotide exchange factor: evidence for its fusion with MLL in acute myeloid

leukemia. Proceedings of the National Academy of Sciences of the United States of America 97**:** 2145-2150

Kranenburg O, Poland M, van Horck FP, Drechsel D, Hall A, Moolenaar WH (1999) Activation of RhoA by lysophosphatidic acid and Galpha12/13 subunits in neuronal cells: induction of neurite retraction. Molecular biology of the cell 10**:** 1851-1857

Krizhanovsky V, Yon M, Dickins RA, Hearn S, Simon J, Miething C, Yee H, Zender L, Lowe SW (2008) Senescence of activated stellate cells limits liver fibrosis. Cell 134**:** 657-667

Krtolica A, Parrinello S, Lockett S, Desprez PY, Campisi J (2001) Senescent fibroblasts promote epithelial cell growth and tumorigenesis: a link between cancer and aging. Proceedings of the National Academy of Sciences of the United States of America 98**:** 12072-12077

Kuilman T, Michaloglou C, Vredeveld LC, Douma S, van Doorn R, Desmet CJ, Aarden LA, Mooi WJ, Peeper DS (2008) Oncogene-induced senescence relayed by an interleukin-dependent inflammatory network. Cell 133**:** 1019-1031

Kuilman T, Peeper DS (2009) Senescence-messaging secretome: SMS-ing cellular stress. Nature reviews Cancer 9**:** 81-94

Kuwahara K, Teg Pipes GC, McAnally J, Richardson JA, Hill JA, Bassel-Duby R, Olson EN (2007) Modulation of adverse cardiac remodeling by STARS, a mediator of MEF2 signaling and SRF activity. The Journal of clinical investigation 117**:** 1324-1334

Kwan JJ, Donaldson LW (2007) The NMR structure of the murine DLC2 SAM domain reveals a variant fold that is similar to a four-helix bundle. BMC structural biology 7**:** 34

Laemmli UK (1970) Cleavage of structural proteins during the assembly of the head of bacteriophage T4. Nature 227**:** 680-685

Lazer G, Katzav S (2011) Guanine nucleotide exchange factors for RhoGTPases: good therapeutic targets for cancer therapy? Cellular signalling 23**:** 969-979

Leask A, Abraham DJ (2006) All in the CCN family: essential matricellular signaling modulators emerge from the bunker. Journal of cell science 119**:** 4803-4810

Lee BY, Han JA, Im JS, Morrone A, Johung K, Goodwin EC, Kleijer WJ, DiMaio D, Hwang ES (2006) Senescence-associated beta-galactosidase is lysosomal beta-galactosidase. Aging cell 5**:** 187-195

Lee EK, Han GY, Park HW, Song YJ, Kim CW (2010a) Transgelin promotes migration and invasion of cancer stem cells. Journal of proteome research 9**:** 5108-5117

Lee SM, Vasishtha M, Prywes R (2010b) Activation and repression of cellular immediate early genes by serum response factor cofactors. The Journal of biological chemistry 285**:** 22036-22049

Leitner L, Shaposhnikov D, Descot A, Hoffmann R, Posern G (2010) Epithelial Protein Lost in Neoplasm alpha (Eplin-alpha) is transcriptionally regulated by G-actin and MAL/MRTF coactivators. Molecular cancer 9**:** 60

Leitner L, Shaposhnikov D, Mengel A, Descot A, Julien S, Hoffmann R, Posern G (2011) MAL/MRTF-A controls migration of non-invasive cells by upregulation of cytoskeleton-associated proteins. Journal of cell science 124**:** 4318-4331

Leung C, Yu C, Lin MI, Tognon C, Bernatchez P (2013) Expression of myoferlin in human and murine carcinoma tumors: role in membrane repair, cell proliferation, and tumorigenesis. The American journal of pathology 182**:** 1900-1909

Levine AJ, Oren M (2009) The first 30 years of p53: growing ever more complex. Nature reviews Cancer 9**:** 749-758

Li H, Fung KL, Jin DY, Chung SS, Ching YP, Ng IO, Sze KH, Ko BC, Sun H (2007) Solution structures, dynamics, and lipid-binding of the sterile alpha-motif domain of the deleted in liver cancer 2. Proteins 67**:** 1154-1166

Li J, Zhu X, Chen M, Cheng L, Zhou D, Lu MM, Du K, Epstein JA, Parmacek MS (2005a) Myocardin-related transcription factor B is required in cardiac neural crest for smooth muscle differentiation and cardiovascular development. Proceedings of the National Academy of Sciences of the United States of America 102**:** 8916-8921

Li R, Ackerman WEt, Mihai C, Volakis LI, Ghadiali S, Kniss DA (2012a) Myoferlin depletion in breast cancer cells promotes mesenchymal to epithelial shape change and stalls invasion. PloS one 7**:** e39766

Li S, Chang S, Qi X, Richardson JA, Olson EN (2006) Requirement of a myocardin-related transcription factor for development of mammary myoepithelial cells. Molecular and cellular biology 26**:** 5797-5808

Li S, Czubryt MP, McAnally J, Bassel-Duby R, Richardson JA, Wiebel FF, Nordheim A, Olson EN (2005b) Requirement for serum response factor for skeletal muscle growth and maturation revealed by tissue-specific gene deletion in mice. Proceedings of the National Academy of Sciences of the United States of America 102**:** 1082-1087

Li ZQ, Ding W, Sun SJ, Li J, Pan J, Zhao C, Wu WR, Si WK (2012b) Cyr61/CCN1 is regulated by Wnt/beta-catenin signaling and plays an important role in the progression of hepatocellular carcinoma. PloS one 7**:** e35754

Liao YC, Shih YP, Lo SH (2008) Mutations in the focal adhesion targeting region of deleted in liver cancer-1 attenuate their expression and function. Cancer research 68**:** 7718-7722

Liao YC, Si L, deVere White RW, Lo SH (2007) The phosphotyrosine-independent interaction of DLC-1 and the SH2 domain of cten regulates focal adhesion localization and growth suppression activity of DLC-1. The Journal of cell biology 176**:** 43-49

Lin AW, Barradas M, Stone JC, van Aelst L, Serrano M, Lowe SW (1998) Premature senescence involving p53 and p16 is activated in response to constitutive MEK/MAPK mitogenic signaling. Genes & development 12**:** 3008-3019

Low JS, Tao Q, Ng KM, Goh HK, Shu XS, Woo WL, Ambinder RF, Srivastava G, Shamay M, Chan AT et al (2011) A novel isoform of the 8p22 tumor suppressor gene DLC1 suppresses tumor growth and is frequently silenced in multiple common tumors. Oncogene 30**:** 1923-1935

Lowe SW, Cepero E, Evan G (2004) Intrinsic tumour suppression. Nature 432**:** 307-315

Lowe SW, Lin AW (2000) Apoptosis in cancer. Carcinogenesis 21**:** 485-495

Lu R, Wang H, Liang Z, Ku L, O'Donnell W T, Li W, Warren ST, Feng Y (2004) The fragile X protein controls microtubule-associated protein 1B translation and microtubule stability in brain neuron development. Proceedings of the National Academy of Sciences of the United States of America 101**:** 15201-15206

Lukasik D, Wilczek E, Wasiutynski A, Gornicka B (2011) Deleted in liver cancer protein family in human malignancies (Review). Oncology letters 2**:** 763-768

Ma Z, Morris SW, Valentine V, Li M, Herbrick JA, Cui X, Bouman D, Li Y, Mehta PK, Nizetic D et al (2001) Fusion of two novel genes, RBM15 and MKL1, in the t(1;22)(p13;q13) of acute megakaryoblastic leukemia. Nature genetics 28**:** 220-221

Marks P, Rifkind RA, Richon VM, Breslow R, Miller T, Kelly WK (2001) Histone deacetylases and cancer: causes and therapies. Nature reviews Cancer 1**:** 194-202

Martin C, Chen S, Heilos D, Sauer G, Hunt J, Shaw AG, Sims PF, Jackson DA, Lovric J (2010) Changed genome heterochromatinization upon prolonged activation of the Raf/ERK signaling pathway. PloS one 5**:** e13322

Mattila PK, Lappalainen P (2008) Filopodia: molecular architecture and cellular functions. Nature reviews Molecular cell biology 9**:** 446-454

Mazzocca A, Fransvea E, Dituri F, Lupo L, Antonaci S, Giannelli G (2010) Down-regulation of connective tissue growth factor by inhibition of transforming growth factor beta blocks the tumor-stroma cross-talk and tumor progression in hepatocellular carcinoma. Hepatology 51**:** 523-534

McNeil PL, Kirchhausen T (2005) An emergency response team for membrane repair. Nature reviews Molecular cell biology 6**:** 499-505

Medjkane S, Perez-Sanchez C, Gaggioli C, Sahai E, Treisman R (2009) Myocardin-related transcription factors and SRF are required for cytoskeletal dynamics and experimental metastasis. Nature cell biology 11**:** 257-268

Mercher T, Raffel GD, Moore SA, Cornejo MG, Baudry-Bluteau D, Cagnard N, Jesneck JL, Pikman Y, Cullen D, Williams IR et al (2009) The OTT-MAL fusion oncogene activates

RBPJ-mediated transcription and induces acute megakaryoblastic leukemia in a knockin mouse model. The Journal of clinical investigation 119**:** 852-864

Miano JM, Long X, Fujiwara K (2007) Serum response factor: master regulator of the actin cytoskeleton and contractile apparatus. American journal of physiology Cell physiology 292**:** C70-81

Michaloglou C, Vredeveld LC, Soengas MS, Denoyelle C, Kuilman T, van der Horst CM, Majoor DM, Shay JW, Mooi WJ, Peeper DS (2005) BRAFE600-associated senescence-like cell cycle arrest of human naevi. Nature 436**:** 720-724

Miralles F, Posern G, Zaromytidou AI, Treisman R (2003) Actin dynamics control SRF activity by regulation of its coactivator MAL. Cell 113**:** 329-342

Mishima K, Handa JT, Aotaki-Keen A, Lutty GA, Morse LS, Hjelmeland LM (1999) Senescence-associated beta-galactosidase histochemistry for the primate eye. Investigative ophthalmology & visual science 40**:** 1590-1593

Miwa T, Kedes L (1987) Duplicated CArG box domains have positive and mutually dependent regulatory roles in expression of the human alpha-cardiac actin gene. Molecular and cellular biology 7**:** 2803-2813

Mokalled MH, Johnson A, Kim Y, Oh J, Olson EN (2010) Myocardin-related transcription factors regulate the Cdk5/Pctaire1 kinase cascade to control neurite outgrowth, neuronal migration and brain development. Development 137**:** 2365-2374

Monje P, Marinissen MJ, Gutkind JS (2003) Phosphorylation of the carboxyl-terminal transactivation domain of c-Fos by extracellular signal-regulated kinase mediates the transcriptional activation of AP-1 and cellular transformation induced by platelet-derived growth factor. Molecular and cellular biology 23**:** 7030-7043

Morin P, Flors C, Olson MF (2009) Constitutively active RhoA inhibits proliferation by retarding G(1) to S phase cell cycle progression and impairing cytokinesis. European journal of cell biology 88**:** 495-507

Morita T, Mayanagi T, Sobue K (2007) Dual roles of myocardin-related transcription factors in epithelial mesenchymal transition via slug induction and actin remodeling. The Journal of cell biology 179**:** 1027-1042

Mouilleron S, Guettler S, Langer CA, Treisman R, McDonald NQ (2008) Molecular basis for G-actin binding to RPEL motifs from the serum response factor coactivator MAL. The EMBO journal 27**:** 3198-3208

Muehlich S, Cicha I, Garlichs CD, Krueger B, Posern G, Goppelt-Struebe M (2007) Actin-dependent regulation of connective tissue growth factor. American journal of physiology Cell physiology 292**:** C1732-1738

Muehlich S, Hampl V, Khalid S, Singer S, Frank N, Breuhahn K, Gudermann T, Prywes R (2012) The transcriptional coactivators megakaryoblastic leukemia 1/2 mediate the effects of loss of the tumor suppressor deleted in liver cancer 1. Oncogene 31**:** 3913-3923

Muehlich S, Wang R, Lee SM, Lewis TC, Dai C, Prywes R (2008) Serum-induced phosphorylation of the serum response factor coactivator MKL1 by the extracellular signal-regulated kinase 1/2 pathway inhibits its nuclear localization. Molecular and cellular biology 28**:** 6302-6313

Murphy EV, Zhang Y, Zhu W, Biggs J (1995) The human glioma pathogenesis-related protein is structurally related to plant pathogenesis-related proteins and its gene is expressed specifically in brain tumors. Gene 159**:** 131-135

Nalefski EA, Falke JJ (1996) The C2 domain calcium-binding motif: structural and functional diversity. Protein science : a publication of the Protein Society 5**:** 2375-2390

Narita M, Narita M, Krizhanovsky V, Nunez S, Chicas A, Hearn SA, Myers MP, Lowe SW (2006) A novel role for high-mobility group a proteins in cellular senescence and heterochromatin formation. Cell 126**:** 503-514

Narita M, Nunez S, Heard E, Narita M, Lin AW, Hearn SA, Spector DL, Hannon GJ, Lowe SW (2003) Rb-mediated heterochromatin formation and silencing of E2F target genes during cellular senescence. Cell 113**:** 703-716

Ng DC, Chan SF, Kok KH, Yam JW, Ching YP, Ng IO, Jin DY (2006) Mitochondrial targeting of growth suppressor protein DLC2 through the START domain. FEBS letters 580**:** 191-198

Ng IO, Liang ZD, Cao L, Lee TK (2000) DLC-1 is deleted in primary hepatocellular carcinoma and exerts inhibitory effects on the proliferation of hepatoma cell lines with deleted DLC-1. Cancer research 60**:** 6581-6584

Nicholson DW, Ali A, Thornberry NA, Vaillancourt JP, Ding CK, Gallant M, Gareau Y, Griffin PR, Labelle M, Lazebnik YA et al (1995) Identification and inhibition of the ICE/CED-3 protease necessary for mammalian apoptosis. Nature 376**:** 37-43

Nicoletti I, Migliorati G, Pagliacci MC, Grignani F, Riccardi C (1991) A rapid and simple method for measuring thymocyte apoptosis by propidium iodide staining and flow cytometry. Journal of immunological methods 139**:** 271-279

Nobori T, Miura K, Wu DJ, Lois A, Takabayashi K, Carson DA (1994) Deletions of the cyclin-dependent kinase-4 inhibitor gene in multiple human cancers. Nature 368**:** 753-756

Norman C, Runswick M, Pollock R, Treisman R (1988) Isolation and properties of cDNA clones encoding SRF, a transcription factor that binds to the c-fos serum response element. Cell 55**:** 989-1003

Oh J, Richardson JA, Olson EN (2005) Requirement of myocardin-related transcription factor-B for remodeling of branchial arch arteries and smooth muscle differentiation. Proceedings of the National Academy of Sciences of the United States of America 102**:** 15122-15127

Okamoto A, Demetrick DJ, Spillare EA, Hagiwara K, Hussain SP, Bennett WP, Forrester K, Gerwin B, Serrano M, Beach DH et al (1994) Mutations and altered expression of p16INK4 in human cancer. Proceedings of the National Academy of Sciences of the United States of America 91**:** 11045-11049

Olsen CL, Gardie B, Yaswen P, Stampfer MR (2002) Raf-1-induced growth arrest in human mammary epithelial cells is p16-independent and is overcome in immortal cells during conversion. Oncogene 21**:** 6328-6339

Olson EN, Nordheim A (2010) Linking actin dynamics and gene transcription to drive cellular motile functions. Nature reviews Molecular cell biology 11**:** 353-365

Paradis V, Youssef N, Dargere D, Ba N, Bonvoust F, Deschatrette J, Bedossa P (2001) Replicative senescence in normal liver, chronic hepatitis C, and hepatocellular carcinomas. Human pathology 32**:** 327-332

Parlakian A, Tuil D, Hamard G, Tavernier G, Hentzen D, Concordet JP, Paulin D, Li Z, Daegelen D (2004) Targeted inactivation of serum response factor in the developing heart results in myocardial defects and embryonic lethality. Molecular and cellular biology 24**:** 5281-5289

Pawlikowski JS, Adams PD, Nelson DM (2013) Senescence at a glance. Journal of cell science 126**:** 4061-4067

Pawlowski R, Rajakyla EK, Vartiainen MK, Treisman R (2010) An actin-regulated importin alpha/beta-dependent extended bipartite NLS directs nuclear import of MRTF-A. The EMBO journal 29**:** 3448-3458

Pearson M, Carbone R, Sebastiani C, Cioce M, Fagioli M, Saito S, Higashimoto Y, Appella E, Minucci S, Pandolfi PP et al (2000) PML regulates p53 acetylation and premature senescence induced by oncogenic Ras. Nature 406**:** 207-210

Pellegrini L, Tan S, Richmond TJ (1995) Structure of serum response factor core bound to DNA. Nature 376**:** 490-498

Plaumann M, Seitz S, Frege R, Estevez-Schwarz L, Scherneck S (2003) Analysis of DLC-1 expression in human breast cancer. Journal of cancer research and clinical oncology 129**:** 349-354

Pobbati AV, Hong W (2013) Emerging roles of TEAD transcription factors and its coactivators in cancers. Cancer biology & therapy 14**:** 390-398

Ponting CP, Aravind L (1999) START: a lipid-binding domain in StAR, HD-ZIP and signalling proteins. Trends in biochemical sciences 24**:** 130-132

Posern G, Miralles F, Guettler S, Treisman R (2004) Mutant actins that stabilise F-actin use distinct mechanisms to activate the SRF coactivator MAL. The EMBO journal 23**:** 3973-3983

Posern G, Sotiropoulos A, Treisman R (2002) Mutant actins demonstrate a role for unpolymerized actin in control of transcription by serum response factor. Molecular biology of the cell 13**:** 4167-4178

Posern G, Treisman R (2006) Actin' together: serum response factor, its cofactors and the link to signal transduction. Trends in cell biology 16**:** 588-596

Qian X, Durkin ME, Wang D, Tripathi BK, Olson L, Yang XY, Vass WC, Popescu NC, Lowy DR (2012) Inactivation of the Dlc1 gene cooperates with downregulation of p15INK4b and p16Ink4a, leading to neoplastic transformation and poor prognosis in human cancer. Cancer research 72**:** 5900-5911

Qian X, Li G, Asmussen HK, Asnaghi L, Vass WC, Braverman R, Yamada KM, Popescu NC, Papageorge AG, Lowy DR (2007) Oncogenic inhibition by a deleted in liver cancer gene requires cooperation between tensin binding and Rho-specific GTPase-activating protein activities. Proceedings of the National Academy of Sciences of the United States of America 104**:** 9012-9017

Qiao F, Bowie JU (2005) The many faces of SAM. Science's STKE : signal transduction knowledge environment 2005**:** re7

Qin Y, Chu B, Gong W, Wang J, Tang Z, Shen J, Quan Z (2013) Restoration of deleted in liver cancer 1 gene expression inhibits gallbladder cancer growth through induction of cell cycle arrest and apoptosis. Journal of gastroenterology and hepatology

Ragu C, Boukour S, Elain G, Wagner-Ballon O, Raslova H, Debili N, Olson EN, Daegelen D, Vainchenker W, Bernard OA et al (2010) The serum response factor (SRF)/megakaryocytic acute leukemia (MAL) network participates in megakaryocyte development. Leukemia 24**:** 1227-1230

Ren C, Li L, Goltsov AA, Timme TL, Tahir SA, Wang J, Garza L, Chinault AC, Thompson TC (2002) mRTVP-1, a novel p53 target gene with proapoptotic activities. Molecular and cellular biology 22**:** 3345-3357

Ren C, Li L, Yang G, Timme TL, Goltsov A, Ren C, Ji X, Addai J, Luo H, Ittmann MM et al (2004) RTVP-1, a tumor suppressor inactivated by methylation in prostate cancer. Cancer research 64**:** 969-976

Ren C, Ren CH, Li L, Goltsov AA, Thompson TC (2006) Identification and characterization of RTVP1/GLIPR1-like genes, a novel p53 target gene cluster. Genomics 88**:** 163-172

Reuther GW, Lambert QT, Booden MA, Wennerberg K, Becknell B, Marcucci G, Sondek J, Caligiuri MA, Der CJ (2001) Leukemia-associated Rho guanine nucleotide exchange factor, a Dbl family protein found mutated in leukemia, causes transformation by activation of RhoA. The Journal of biological chemistry 276**:** 27145-27151

Rich T, Chen P, Furman F, Huynh N, Israel MA (1996) RTVP-1, a novel human gene with sequence similarity to genes of diverse species, is expressed in tumor cell lines of glial but not neuronal origin. Gene 180**:** 125-130

Ridley AJ, Hall A (1992) The small GTP-binding protein rho regulates the assembly of focal adhesions and actin stress fibers in response to growth factors. Cell 70**:** 389-399

Rittling SR, Brooks KM, Cristofalo VJ, Baserga R (1986) Expression of cell cycle-dependent genes in young and senescent WI-38 fibroblasts. Proceedings of the National Academy of Sciences of the United States of America 83**:** 3316-3320

Roberts PJ, Der CJ (2007) Targeting the Raf-MEK-ERK mitogen-activated protein kinase cascade for the treatment of cancer. Oncogene 26**:** 3291-3310

Rodier F, Coppe JP, Patil CK, Hoeijmakers WA, Munoz DP, Raza SR, Freund A, Campeau E, Davalos AR, Campisi J (2009) Persistent DNA damage signalling triggers senescence-associated inflammatory cytokine secretion. Nature cell biology 11**:** 973-979

Rossman KL, Der CJ, Sondek J (2005) GEF means go: turning on RHO GTPases with guanine nucleotide-exchange factors. Nature reviews Molecular cell biology 6**:** 167-180

Sahai E, Marshall CJ (2002) RHO-GTPases and cancer. Nature reviews Cancer 2**:** 133-142

Schmitt CA (2003) Senescence, apoptosis and therapy--cutting the lifelines of cancer. Nature reviews Cancer 3**:** 286-295

Schmitt CA, Fridman JS, Yang M, Lee S, Baranov E, Hoffman RM, Lowe SW (2002) A senescence program controlled by p53 and p16INK4a contributes to the outcome of cancer therapy. Cell 109**:** 335-346

Scholz RP, Regner J, Theil A, Erlmann P, Holeiter G, Jahne R, Schmid S, Hausser A, Olayioye MA (2009) DLC1 interacts with 14-3-3 proteins to inhibit RhoGAP activity and block nucleocytoplasmic shuttling. Journal of cell science 122**:** 92-102

Scholzen T, Gerdes J (2000) The Ki-67 protein: from the known and the unknown. Journal of cellular physiology 182**:** 311-322

Schratt G, Philippar U, Berger J, Schwarz H, Heidenreich O, Nordheim A (2002) Serum response factor is crucial for actin cytoskeletal organization and focal adhesion assembly in embryonic stem cells. The Journal of cell biology 156**:** 737-750

Sekimata M, Kabuyama Y, Emori Y, Homma Y (1999) Morphological changes and detachment of adherent cells induced by p122, a GTPase-activating protein for Rho. The Journal of biological chemistry 274**:** 17757-17762

Selvaraj A, Prywes R (2003) Megakaryoblastic leukemia-1/2, a transcriptional co-activator of serum response factor, is required for skeletal myogenic differentiation. The Journal of biological chemistry 278**:** 41977-41987

Selvaraj A, Prywes R (2004) Expression profiling of serum inducible genes identifies a subset of SRF target genes that are MKL dependent. BMC molecular biology 5**:** 13

Seng TJ, Low JS, Li H, Cui Y, Goh HK, Wong ML, Srivastava G, Sidransky D, Califano J, Steenbergen RD et al (2007) The major 8p22 tumor suppressor DLC1 is frequently silenced by methylation in both endemic and sporadic nasopharyngeal, esophageal, and cervical carcinomas, and inhibits tumor cell colony formation. Oncogene 26**:** 934-944

Senturk S, Mumcuoglu M, Gursoy-Yuzugullu O, Cingoz B, Akcali KC, Ozturk M (2010) Transforming growth factor-beta induces senescence in hepatocellular carcinoma cells and inhibits tumor growth. Hepatology 52**:** 966-974

Serrano M, Blasco MA (2001) Putting the stress on senescence. Current opinion in cell biology 13**:** 748-753

Serrano M, Lin AW, McCurrach ME, Beach D, Lowe SW (1997) Oncogenic ras provokes premature cell senescence associated with accumulation of p53 and p16INK4a. Cell 88**:** 593-602

Seshadri T, Campisi J (1990) Repression of c-fos transcription and an altered genetic program in senescent human fibroblasts. Science 247**:** 205-209

Shaposhnikov D, Descot A, Schilling J, Posern G (2012) Myocardin-related transcription factor A regulates expression of Bok and Noxa and is involved in apoptotic signalling. Cell cycle 11**:** 141-150

Shaposhnikov D, Kuffer C, Storchova Z, Posern G (2013) Myocardin related transcription factors are required for coordinated cell cycle progression. Cell cycle 12**:** 1762-1772

Sharma A, Yu C, Leung C, Trane A, Lau M, Utokaparch S, Shaheen F, Sheibani N, Bernatchez P (2010) A new role for the muscle repair protein dysferlin in endothelial cell adhesion and angiogenesis. Arteriosclerosis, thrombosis, and vascular biology 30**:** 2196-2204

Sharrocks AD (2001) The ETS-domain transcription factor family. Nature reviews Molecular cell biology 2**:** 827-837

Shaw PE, Schroter H, Nordheim A (1989) The ability of a ternary complex to form over the serum response element correlates with serum inducibility of the human c-fos promoter. Cell 56**:** 563-572

Shelton DN, Chang E, Whittier PS, Choi D, Funk WD (1999) Microarray analysis of replicative senescence. Current biology : CB 9**:** 939-945

Sherr CJ, Roberts JM (1999) CDK inhibitors: positive and negative regulators of G1-phase progression. Genes & development 13**:** 1501-1512

Sherwood SW, Rush D, Ellsworth JL, Schimke RT (1988) Defining cellular senescence in IMR-90 cells: a flow cytometric analysis. Proceedings of the National Academy of Sciences of the United States of America 85**:** 9086-9090

Shore P, Sharrocks AD (1995) The MADS-box family of transcription factors. European journal of biochemistry / FEBS 229**:** 1-13

Smith EC, Thon JN, Devine MT, Lin S, Schulz VP, Guo Y, Massaro SA, Halene S, Gallagher P, Italiano JE, Jr. et al (2012) MKL1 and MKL2 play redundant and crucial roles in megakaryocyte maturation and platelet formation. Blood 120**:** 2317-2329

Sotiropoulos A, Gineitis D, Copeland J, Treisman R (1999) Signal-regulated activation of serum response factor is mediated by changes in actin dynamics. Cell 98**:** 159-169

Soulez M, Rouviere CG, Chafey P, Hentzen D, Vandromme M, Lautredou N, Lamb N, Kahn A, Tuil D (1996) Growth and differentiation of C2 myogenic cells are dependent on serum response factor. Molecular and cellular biology 16**:** 6065-6074

Spiegelman BM, Heinrich R (2004) Biological control through regulated transcriptional coactivators. Cell 119**:** 157-167

Stein GH, Beeson M, Gordon L (1990) Failure to phosphorylate the retinoblastoma gene product in senescent human fibroblasts. Science 249**:** 666-669

Stern S, Debre E, Stritt C, Berger J, Posern G, Knoll B (2009) A nuclear actin function regulates neuronal motility by serum response factor-dependent gene transcription. The Journal of neuroscience : the official journal of the Society for Neuroscience 29**:** 4512-4518

Sun D, Nassal M (2006) Stable HepG2- and Huh7-based human hepatoma cell lines for efficient regulated expression of infectious hepatitis B virus. Journal of hepatology 45**:** 636-645

Sun K, Battle MA, Misra RP, Duncan SA (2009) Hepatocyte expression of serum response factor is essential for liver function, hepatocyte proliferation and survival, and postnatal body growth in mice. Hepatology 49**:** 1645-1654

Sun Q, Chen G, Streb JW, Long X, Yang Y, Stoeckert CJ, Jr., Miano JM (2006a) Defining the mammalian CArGome. Genome research 16**:** 197-207

Sun Y, Boyd K, Xu W, Ma J, Jackson CW, Fu A, Shillingford JM, Robinson GW, Hennighausen L, Hitzler JK et al (2006b) Acute myeloid leukemia-associated Mkl1 (Mrtf-a) is a key regulator of mammary gland function. Molecular and cellular biology 26**:** 5809-5826

Syed V, Mukherjee K, Lyons-Weiler J, Lau KM, Mashima T, Tsuruo T, Ho SM (2005) Identification of ATF-3, caveolin-1, DLC-1, and NM23-H2 as putative antitumorigenic, progesterone-regulated genes for ovarian cancer cells by gene profiling. Oncogene 24**:** 1774-1787

Takeda S, North DL, Lakich MM, Russell SD, Whalen RG (1992) A possible regulatory role for conserved promoter motifs in an adult-specific muscle myosin gene from mouse. The Journal of biological chemistry 267**:** 16957-16967

Tcherkezian J, Lamarche-Vane N (2007) Current knowledge of the large RhoGAP family of proteins. Biology of the cell / under the auspices of the European Cell Biology Organization 99**:** 67-86

te Poele RH, Okorokov AL, Jardine L, Cummings J, Joel SP (2002) DNA damage is able to induce senescence in tumor cells in vitro and in vivo. Cancer research 62**:** 1876-1883

Thiery JP (2002) Epithelial-mesenchymal transitions in tumour progression. Nature reviews Cancer 2**:** 442-454

Thompson O, Moghraby JS, Ayscough KR, Winder SJ (2012) Depletion of the actin bundling protein SM22/transgelin increases actin dynamics and enhances the tumourigenic phenotypes of cells. BMC cell biology 13**:** 1

Tompa P (2003) Intrinsically unstructured proteins evolve by repeat expansion. BioEssays : news and reviews in molecular, cellular and developmental biology 25**:** 847-855

Towbin H, Staehelin T, Gordon J (1979) Electrophoretic transfer of proteins from polyacrylamide gels to nitrocellulose sheets: procedure and some applications. Proceedings of the National Academy of Sciences of the United States of America 76**:** 4350-4354

Treisman R (1986) Identification of a protein-binding site that mediates transcriptional response of the c-fos gene to serum factors. Cell 46**:** 567-574

Treisman R (1990) The SRE: a growth factor responsive transcriptional regulator. Seminars in cancer biology 1**:** 47-58

Treisman R (1992) The serum response element. Trends in biochemical sciences 17**:** 423-426

Treisman R (1994) Ternary complex factors: growth factor regulated transcriptional activators. Current opinion in genetics & development 4**:** 96-101

Treisman R (1995a) DNA-binding proteins. Inside the MADS box. Nature 376**:** 468-469

Treisman R (1995b) Journey to the surface of the cell: Fos regulation and the SRE. The EMBO journal 14**:** 4905-4913

Tripathi V, Popescu NC, Zimonjic DB (2013) DLC1 induces expression of E-cadherin in prostate cancer cells through Rho pathway and suppresses invasion. Oncogene

Tsai MS, Bogart DF, Castaneda JM, Li P, Lupu R (2002) Cyr61 promotes breast tumorigenesis and cancer progression. Oncogene 21**:** 8178-8185

Turcotte S, Desrosiers RR, Beliveau R (2003) HIF-1alpha mRNA and protein upregulation involves Rho GTPase expression during hypoxia in renal cell carcinoma. Journal of cell science 116**:** 2247-2260

Turtoi A, Blomme A, Bellahcene A, Gilles C, Hennequiere V, Peixoto P, Bianchi E, Noel A, De Pauw E, Lifrange E et al (2013) Myoferlin is a key regulator of EGFR activity in breast cancer. Cancer research 73**:** 5438-5448

Tymanskyj SR, Scales TM, Gordon-Weeks PR (2012) MAP1B enhances microtubule assembly rates and axon extension rates in developing neurons. Molecular and cellular neurosciences 49**:** 110-119

Ullmannova V, Popescu NC (2006) Expression profile of the tumor suppressor genes DLC-1 and DLC-2 in solid tumors. International journal of oncology 29**:** 1127-1132

Ullmannova V, Popescu NC (2007) Inhibition of cell proliferation, induction of apoptosis, reactivation of DLC1, and modulation of other gene expression by dietary flavone in breast cancer cell lines. Cancer detection and prevention 31**:** 110-118

Urban-Klein B, Werth S, Abuharbeid S, Czubayko F, Aigner A (2005) RNAi-mediated gene-targeting through systemic application of polyethylenimine (PEI)-complexed siRNA in vivo. Gene therapy 12**:** 461-466

van Golen KL, Wu ZF, Qiao XT, Bao L, Merajver SD (2000) RhoC GTPase overexpression modulates induction of angiogenic factors in breast cells. Neoplasia 2**:** 418-425

Vartiainen MK, Guettler S, Larijani B, Treisman R (2007) Nuclear actin regulates dynamic subcellular localization and activity of the SRF cofactor MAL. Science 316**:** 1749-1752

Vega FM, Ridley AJ (2008) Rho GTPases in cancer cell biology. FEBS letters 582**:** 2093-2101

Ventura A, Kirsch DG, McLaughlin ME, Tuveson DA, Grimm J, Lintault L, Newman J, Reczek EE, Weissleder R, Jacks T (2007) Restoration of p53 function leads to tumour regression in vivo. Nature 445**:** 661-665

Verdoni AM, Ikeda S, Ikeda A (2010) Serum response factor is essential for the proper development of skin epithelium. Mammalian genome : official journal of the International Mammalian Genome Society 21**:** 64-76

Vousden KH, Lane DP (2007) p53 in health and disease. Nature reviews Molecular cell biology 8**:** 275-283

Wang D, Chang PS, Wang Z, Sutherland L, Richardson JA, Small E, Krieg PA, Olson EN (2001) Activation of cardiac gene expression by myocardin, a transcriptional cofactor for serum response factor. Cell 105**:** 851-862

Wang DZ, Li S, Hockemeyer D, Sutherland L, Wang Z, Schratt G, Richardson JA, Nordheim A, Olson EN (2002) Potentiation of serum response factor activity by a family of myocardin-related transcription factors. Proceedings of the National Academy of Sciences of the United States of America 99**:** 14855-14860

Wei L, Zhou W, Croissant JD, Johansen FE, Prywes R, Balasubramanyam A, Schwartz RJ (1998) RhoA signaling via serum response factor plays an obligatory role in myogenic differentiation. The Journal of biological chemistry 273**:** 30287-30294

Weinberg RA (1995) The retinoblastoma protein and cell cycle control. Cell 81**:** 323-330

Wells A, Welsh JB, Lazar CS, Wiley HS, Gill GN, Rosenfeld MG (1990) Ligand-induced transformation by a noninternalizing epidermal growth factor receptor. Science 247**:** 962-964

Williams GT (1991) Programmed cell death: apoptosis and oncogenesis. Cell 65**:** 1097-1098

Wong CC, Wong CM, Ko FC, Chan LK, Ching YP, Yam JW, Ng IO (2008) Deleted in liver cancer 1 (DLC1) negatively regulates Rho/ROCK/MLC pathway in hepatocellular carcinoma. PloS one 3**:** e2779

Wong CM, Lee JM, Ching YP, Jin DY, Ng IO (2003) Genetic and epigenetic alterations of DLC-1 gene in hepatocellular carcinoma. Cancer research 63**:** 7646-7651

Wong CM, Yam JW, Ching YP, Yau TO, Leung TH, Jin DY, Ng IO (2005) Rho GTPase-activating protein deleted in liver cancer suppresses cell proliferation and invasion in hepatocellular carcinoma. Cancer research 65**:** 8861-8868

Worthylake RA, Lemoine S, Watson JM, Burridge K (2001) RhoA is required for monocyte tail retraction during transendothelial migration. The Journal of cell biology 154**:** 147-160

Xie D, Nakachi K, Wang H, Elashoff R, Koeffler HP (2001) Elevated levels of connective tissue growth factor, WISP-1, and CYR61 in primary breast cancers associated with more advanced features. Cancer research 61**:** 8917-8923

Xiu M, Liu YH, Brigstock DR, He FH, Zhang RJ, Gao RP (2012) Connective tissue growth factor is overexpressed in human hepatocellular carcinoma and promotes cell invasion and growth. World journal of gastroenterology : WJG 18**:** 7070-7078

Xue W, Krasnitz A, Lucito R, Sordella R, Vanaelst L, Cordon-Cardo C, Singer S, Kuehnel F, Wigler M, Powers S et al (2008) DLC1 is a chromosome 8p tumor suppressor whose loss promotes hepatocellular carcinoma. Genes & development 22**:** 1439-1444

Xue W, Zender L, Miething C, Dickins RA, Hernando E, Krizhanovsky V, Cordon-Cardo C, Lowe SW (2007) Senescence and tumour clearance is triggered by p53 restoration in murine liver carcinomas. Nature 445**:** 656-660

Yam JW, Ko FC, Chan CY, Jin DY, Ng IO (2006) Interaction of deleted in liver cancer 1 with tensin2 in caveolae and implications in tumor suppression. Cancer research 66**:** 8367-8372

Yen A, Sturgill R (1998) Hypophosphorylation of the RB protein in S and G2 as well as G1 during growth arrest. Experimental cell research 241**:** 324-331

Yu C, Sharma A, Trane A, Utokaparch S, Leung C, Bernatchez P (2011) Myoferlin gene silencing decreases Tie-2 expression in vitro and angiogenesis in vivo. Vascular pharmacology 55**:** 26-33

Yuan BZ, Durkin ME, Popescu NC (2003a) Promoter hypermethylation of DLC-1, a candidate tumor suppressor gene, in several common human cancers. Cancer genetics and cytogenetics 140**:** 113-117

Yuan BZ, Jefferson AM, Baldwin KT, Thorgeirsson SS, Popescu NC, Reynolds SH (2004) DLC-1 operates as a tumor suppressor gene in human non-small cell lung carcinomas. Oncogene 23**:** 1405-1411

Yuan BZ, Jefferson AM, Millecchia L, Popescu NC, Reynolds SH (2007) Morphological changes and nuclear translocation of DLC1 tumor suppressor protein precede apoptosis in human non-small cell lung carcinoma cells. Experimental cell research 313**:** 3868-3880

Yuan BZ, Miller MJ, Keck CL, Zimonjic DB, Thorgeirsson SS, Popescu NC (1998) Cloning, characterization, and chromosomal localization of a gene frequently deleted in human liver cancer (DLC-1) homologous to rat RhoGAP. Cancer research 58**:** 2196-2199

Yuan BZ, Zhou X, Durkin ME, Zimonjic DB, Gumundsdottir K, Eyfjord JE, Thorgeirsson SS, Popescu NC (2003b) DLC-1 gene inhibits human breast cancer cell growth and in vivo tumorigenicity. Oncogene 22**:** 445-450

Zender L, Spector MS, Xue W, Flemming P, Cordon-Cardo C, Silke J, Fan ST, Luk JM, Wigler M, Hannon GJ et al (2006) Identification and validation of oncogenes in liver cancer using an integrative oncogenomic approach. Cell 125**:** 1253-1267

Zhang R, Chen W, Adams PD (2007) Molecular dissection of formation of senescence-associated heterochromatin foci. Molecular and cellular biology 27**:** 2343-2358

Zhang T, Zheng J, Jiang N, Wang G, Shi Q, Liu C, Lu Y (2009) Overexpression of DLC-1 induces cell apoptosis and proliferation inhibition in the renal cell carcinoma. Cancer letters 283**:** 59-67

Zhang X, Chai J, Azhar G, Sheridan P, Borras AM, Furr MC, Khrapko K, Lawitts J, Misra RP, Wei JY (2001) Early postnatal cardiac changes and premature death in transgenic

mice overexpressing a mutant form of serum response factor. The Journal of biological chemistry 276**:** 40033-40040

Zheng CF, Guan KL (1993) Properties of MEKs, the kinases that phosphorylate and activate the extracellular signal-regulated kinases. The Journal of biological chemistry 268**:** 23933-23939

Zheng H, Wasylyk C, Ayadi A, Abecassis J, Schalken JA, Rogatsch H, Wernert N, Maira SM, Multon MC, Wasylyk B (2003) The transcription factor Net regulates the angiogenic switch. Genes & development 17**:** 2283-2297

Zhong D, Zhang J, Yang S, Soh UJ, Buschdorf JP, Zhou YT, Yang D, Low BC (2009) The SAM domain of the RhoGAP DLC1 binds EF1A1 to regulate cell migration. Journal of cell science 122**:** 414-424

Zhou X, Thorgeirsson SS, Popescu NC (2004) Restoration of DLC-1 gene expression induces apoptosis and inhibits both cell growth and tumorigenicity in human hepatocellular carcinoma cells. Oncogene 23**:** 1308-1313

Zhu J, Woods D, McMahon M, Bishop JM (1998) Senescence of human fibroblasts induced by oncogenic Raf. Genes & development 12**:** 2997-3007

12 Publications

Parts of the results of this thesis have been submitted for publication or have already been published in peer-reviewed journals.

- Kirchner P, Nossek M, Drexler M, **Hampl V**, Grosse R, Lewis T, Prywes R, Gudermann T, Muehlich S.
  Filamin A interacts with Megakaryoblastic Leukemia 1 (MKL1) to regulate transcriptional activity of the Serum Response Factor (SRF)
  submitted

- **Hampl V,** Martin C, Aigner A, Hoebel S, Singer S, Frank N, Sarikas A, Ebert O, Prywes R, Gudermann T, Muehlich S.
  Depletion of the transcriptional coactivators megakaryoblastic leukemia 1 and 2 abolishes hepatocellular carcinoma xenograft growth by inducing oncogene-induced senescence.
  EMBO Mol Med., 2013 Sep; 5 (9):1367-82.

- Muehlich S, **Hampl V**, Khalid S, Singer S, Frank N, Breuhahn K, Gudermann T, Prywes R.
  The transcriptional coactivators megakaryoblastic leukemia 1/2 mediate the effects of loss of the tumor suppressor deleted in liver cancer 1.
  Oncogene, 2012; Aug 30, 31 (35): 3913-23

- **Hampl V**, Wetzel I, Bracher F, Krauss J.
  New substituted isocoumarins and Dihydroisocoumarins and their cytotoxic activities.
  Sci Pharm. 2011 Mar; 79 (1):21-30

Posters

- **Hampl V**, Martin C, Aigner A, Singer S, Frank N, Prywes R, Gudermann T, Muehlich S.
  Depletion of the transcriptional coactivators Megakaryoblastic Leukemia 1 and 2 (MKL1/2) abolishes hepatocellular carcinoma growth by inducing oncogene-induced senescence.
  Interact Symposium, Munich 2013

- **Hampl V**, Martin C, Aigner A, Singer S, Frank N, Prywes R, Gudermann T, Muehlich S.
  Depletion of the transcriptional coactivators Megakaryoblastic Leukemia 1 and 2 (MKL1/2) abolishes hepatocellular carcinoma growth by inducing oncogene-induced senescence.
  79. Annual Meeting of the German Society of Pharmacology and Toxicology, Halle 2013

- **Hampl V**, Khalid S, Singer S, Frank N, Prywes R, Gudermann T, Muehlich S., The Transcripitional coactivators Megakaryoblastic Leukemia 1/2 (MKL1/2) mediate tumorigenesis upon loss of the tumor suppressor Deleted in Liver Cancer 1. 78. Annual Meeting of the German Society of Pharmacology and Toxicology, Dresden 2012

- Muehlich S, **Hampl V**, Khalid S, Frank N, Dahm C, Gudermann T. Role of the transcripitional coactivators MKL1 and 2 in tumorigenesis. 77. Annual Meeting of the German Society of Pharmacology and Toxicology, Mainz 2011

13 Acknowledgements

I would like thank Prof. Dr. Angelika Vollmar for reviewing my thesis as first referee and for the external representation of this work at the faculty of chemistry and pharmacy.
Moreover, I would like deeply thank Prof. Dr. Thomas Gudermann for giving me the opportunity to perform my PhD thesis in his laboratories. I always appreciated his great mentoring and scientific support and that he trusted in me and my work.
I would like to thank Dr. Susanne Mühlich for providing this very interesting topic and her support in all matters concerning this project.
Thanks to Prof. Dr. Franz Bracher, Prof. Dr. Stefan Zahler, Prof. Dr. Christian Wahl-Schott and PD. Dr. Dietmar Martin for the time and interest in this work and being part of the examiner committee.
Special thanks go to the cooperation partners Prof. Dr. Achim Aigner for the support and advices with the xenograft mouse model and to PD Dr. Dietmar Martin and Kerstin Maier for the help with the DNA-microarray analysis.
I also want to deeply thank Clara-Mae Beer for the great technical help and for always being there whenever I needed an open ear. I am grateful to her for the tireless support and motivation during all ups and downs of this work.
Many thanks go to Renate Heilmaier for their help with the in vivo models and support and motivation during my work.
Thanks to Jutta Schreier for her help in organizational matters.
Special thanks to PD Dr. Harald Mückter for taking the time to proofread my thesis.
I also thank all past and present members of the Mühlich lab for being nice colleagues and for keeping up a good lab spirit.
Thanks to my master students Claudia, Christine and Jasmin for their support of my project.
Especially I want to thank Steffi, Maria and Annika for the wonderful time inside and outside the lab.
Thanks to Andrea, Dorke, Nele, Ellen, Jürgen, Heike, Vroni, Sebastian, Sarah, Valentina and Sheila for being excellent colleagues and for the nice time at the WSI.
Thanks to Susanna and Vladimir for scientific discussions and their good advices whenever needed.
Thanks to all the members of the mouse house for their great support with the in vivo models.
Last but not least, I thank my parents and my brother Sebastian for their great support and constant encouragement and Julian for being there for me every step of the way.